

Transcriptional regulation by sigma  
factor phosphorylation controls  
polymyxin resistance and swarming  
behavior in *Vibrio parahaemolyticus*

**DISSERTATION**

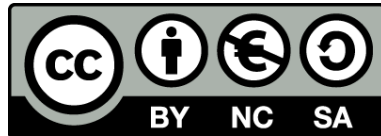
zur  
Erlangung des Doktorgrades  
der Naturwissenschaften  
(Dr. rer. nat.)

dem Fachbereich Biologie  
der Philipps-Universität Marburg  
vorgelegt

von  
SHANKAR CHANDRASHEKAR IYER  
aus Chennai, India

Marburg/Lahn im Juni 2019

Originaldokument gespeichert auf dem Publikationsserver der  
Philipps-Universität Marburg  
<http://archiv.ub.uni-marburg.de>



Dieses Werk bzw. Inhalt steht unter einer  
Creative Commons  
Namensnennung  
Keine kommerzielle Nutzung  
Weitergabe unter gleichen Bedingungen  
3.0 Deutschland Lizenz.

Die vollständige Lizenz finden Sie unter:  
<http://creativecommons.org/licenses/by-nc-sa/3.0/de/>

Die Untersuchungen zur vorliegenden Arbeit wurden von Oktober 2015 bis Juli 2019 am Max-Planck-Institut für Terrestrische Mikrobiologie unter der Leitung von Dr. Simon Ringgaard durchgeführt.

Vom Fachbereich Biologie der Philipps-Universität Marburg als Dissertation angenommen am:

Erstgutachter: Dr. Simon Ringgaard

Zweitgutachter: Prof. Dr. Anke Becker

Weitere Mitglieder der Prüfungskommission:

Prof. Dr. Gert Bange

Prof. Dr. Hans-Ulrich Mösch

Tag der mündlichen Prüfung am: 06.09.2019



Die während der Promotion erzielten Ergebnisse wurden zum Teil in folgenden  
Originalpublikationen veröffentlicht:

Shankar Chandrashekar Iyer, Delia Casas-Pastor, David Kraus, Petra Mann, Kathrin Schirner,  
Timo Glatter, Georg Fritz, and Simon Ringgaard

Transcriptional regulation by  $\sigma$  factor phosphorylation in bacteria. Nature Microbiology. In  
revision.



To Amma, Appa and my dear Kat





---

## Table of Contents

ABBREVIATIONS .....	11
ABSTRACT .....	13
ZUSAMMENFASSUNG .....	14
1. CHAPTER 1: INTRODUCTION .....	15
1.1. Post-translational modifications .....	16
1.1.1. Phosphorylation as a post-translational modification .....	17
1.2. Protein kinases .....	18
1.2.1. Discovery of protein kinases in eukaryotes .....	18
1.2.2. Discovery of protein kinases in bacteria .....	19
1.2.3. Classification of kinases: Chemical nature of the side chains .....	19
1.2.4. The high energy phosphate donor .....	20
1.2.5. Protein kinases as drug targets .....	20
1.2.6. Structure of eukaryotic protein kinases .....	20
1.2.6.1. cAPK has a bi-lobed structure .....	21
1.2.6.2. Distinct features of cAPK that are required for its activity .....	22
1.2.6.2.1. The catalytic domain .....	22
1.2.6.2.2. The activation loop .....	22
1.2.7. Kinases in bacteria .....	24
1.2.7.1. Two component systems (TCS) .....	24
1.2.7.2. Phosphotransferases .....	24
1.2.7.3. Serine/threonine kinases (STKs) .....	25
1.2.7.3.1. Comparison of STKs to TCS .....	25
1.2.7.3.2. Structure of bacterial STKs .....	25
1.2.7.3.3. A model for allosteric activation within STKs in bacteria .....	26
1.2.7.3.3.1. Ligand-based dimerization .....	26
1.2.7.3.3.2. Activation through transphosphorylation .....	27
1.2.7.3.4. C-terminal domains of STKs .....	27
1.2.7.3.5. Evolution of STKs .....	28
1.2.7.3.6. Biological roles for Ser/Thr kinases .....	28
1.2.7.3.6.1. Interaction with two component systems .....	29
1.2.7.3.6.2. Regulation of transcriptional factors .....	30
1.2.7.3.6.3. Regulation of protein synthesis .....	31
1.2.7.3.6.4. Roles in cell wall synthesis .....	31
1.2.7.3.6.5. Roles in cell morphology, division and development .....	32
1.2.7.3.6.6. Roles in central metabolism .....	34
1.2.7.3.6.7. Roles in virulence and pathogenicity .....	35
1.2.7.4. Dual specificity protein kinases .....	36

## Table of Contents

---

1.3.	Transcription in bacteria .....	38
1.3.1.	Components of the RNA polymerase .....	38
1.3.2.	Structural studies on the RNA polymerase .....	39
1.4.	Sigma factors .....	40
1.4.1.	Discovery and key features of $\sigma$ factors .....	40
1.4.2.	Sigma factors are important for promoter recognition .....	41
1.4.3.	$\sigma^{54}$ family of $\sigma$ factors .....	41
1.4.4.	$\sigma^{70}$ family of $\sigma$ factors .....	42
1.4.4.1.	Classification of the $\sigma^{70}$ family .....	42
1.4.5.	The different regions of $\sigma$ factors .....	43
1.4.6.	Interaction of the $\sigma$ factor with the RNA polymerase .....	44
1.4.7.	Molecular dynamics enabling promoter recognition and melting by $\sigma$ factors .....	46
1.4.8.	ECF sigma factors .....	47
1.4.8.1.	Identification of ECF $\sigma$ factors .....	47
1.4.8.2.	Principle roles of ECF $\sigma$ factors .....	48
1.4.8.3.	Interactions of the ECF $\sigma$ factor with the promoter DNA and the RNA polymerase .....	49
1.4.8.4.	Regulation of ECF $\sigma$ factors .....	49
1.4.8.4.1.	Regulated proteolysis .....	50
1.4.8.4.2.	Conformational changes within the anti- $\sigma$ factor .....	52
1.4.8.4.2.1.	Mechanism of inhibition of ECF $\sigma$ factors by anti- $\sigma$ factors .....	53
1.4.8.4.3.	Regulation by interactions with other proteins .....	54
1.4.8.4.4.	Regulation by partner switching mechanism .....	55
1.4.8.4.5.	C-terminal extensions within the $\sigma$ factor .....	57
1.4.8.4.6.	Through transcriptional activation .....	57
1.4.8.5.	Classification of ECF $\sigma$ factors .....	58
1.4.8.6.	Functions of ECF $\sigma$ factors .....	60
1.4.8.6.1.	Pathogenicity .....	60
1.4.8.6.2.	Developmental processes .....	60
1.4.8.6.3.	Responses to different extracellular stresses .....	61
1.4.8.6.3.1.	Heat shock .....	61
1.4.8.6.3.2.	Iron starvation .....	61
1.4.8.6.3.3.	Antibiotic stress .....	61
1.4.8.6.3.4.	ECF $\sigma$ factors often sense multiple external stresses .....	62
1.5.	<i>Vibrio parahaemolyticus</i> as a model organism .....	63
2.	Chapter 2: Aim and Scope .....	65
3.	Chapter 3: Regulation of ECF $\sigma$ factor through phosphorylation in bacteria .....	71
3.1.	Introduction .....	73
3.2.	Results .....	75
3.2.1.	ECF $\sigma$ factor phosphorylation in bacteria .....	75

3.2.2.	EcfP is phosphorylated on residue Thr63 by threonine kinase PknT .....	76
3.2.3.	The PknT/EcfP system is required for resistance of polymyxin antibiotics 80	
3.2.4.	PknT/EcfP confer polymyxin resistance by regulating the expression of the essential polymyxin resistance determinant <i>vpa0879</i> .....	84
3.2.5.	Phosphorylation of EcfP by PknT on residue Thr63 is required for EcfP activity 87	
3.2.6.	Polymyxin stress induces PknT kinase activity and EcfP phosphorylation, resulting in expression of a polymyxin resistance determinant.....	92
3.2.7.	EcfP Thr63 is part of a deviant non-charged motif that has replaced a usually negatively charged motif mediating interaction with RNAP .....	94
3.2.8.	Phosphorylation of EcfP at Thr63 enables its interaction with $\beta/\beta'$ of RNAP 98	
3.2.9.	$\sigma$ factor phosphorylation occurs in distantly related bacteria .....	102
3.3.	Discussion .....	107
3.3.1.	Overview of ECF $\sigma$ factor phosphorylation regulation transcription .....	107
3.3.2.	Importance of the highly conserved Thr63 residue of EcfP .....	108
3.3.3.	Reception of the external polymyxin stimulus by the PknT/EcfP system 109	
3.3.4.	Genes downregulated by the PknT/EcfP system.....	110
3.3.5.	Genes upregulated by the PknT/EcfP system .....	112
3.3.6.	PknT possesses basal activity in the absence of polymyxin .....	112
4.	Chapter 4. Regulation of swarming behavior by the PknT/EcfP system in <i>V.</i> <i>parahaemolyticus</i> .....	115
4.1.	Introduction .....	117
4.1.1.	Swarming motility in bacteria .....	117
4.1.2.	Characteristics of swarming behavior.....	117
4.1.3.	Factors that regulate swarming behavior .....	118
4.1.4.	Swarming in <i>V. parahaemolyticus</i> .....	118
4.1.4.1.	Dual flagellar systems of <i>V. parahaemolyticus</i> .....	119
4.1.4.2.	Regulation of swarming behavior of <i>V. parahaemolyticus</i> .....	120
4.2.	Results .....	122
4.2.1.	PknT is important for swarming behavior .....	123
4.2.2.	VP0054, VP0056 and EcfP also regulate swarming behavior .....	125
4.2.3.	The catalytic activity of PknT and the conserved Thr63 residue of EcfP are indispensable for swarming behavior .....	127
4.2.4.	Swarming-specific proteins that are regulated by PknT.....	129
4.2.5.	Swarming-specific proteins that are regulated by VP0054, EcfP and VP0056 132	
4.3.	Discussion .....	135
5.	Chapter 5: Conclusions and future prospects .....	139
6.	Chapter 6: Materials and Methods .....	145
6.1.	Chemicals, equipments and software.....	147

## Table of Contents

6.2.	Media, buffers and solutions .....	151
6.3.	Microbiological methods.....	152
6.3.1.	Bacterial growth conditions .....	152
6.3.2.	Bacterial strains .....	153
6.3.3.	Swimming assays.....	155
6.3.4.	Growth curves .....	155
6.3.5.	Swarming assays .....	155
6.3.6.	Submerged biofilm formation assay.....	156
6.3.7.	Bacterial two hybrid assays.....	156
6.3.8.	Stressor sensitivity assay .....	157
6.3.9.	Membrane orientation assay .....	158
6.4.	Molecular cloning .....	158
6.4.1.	Isolation of genomic DNA from <i>V. parahaemolyticus</i> .....	158
6.4.2.	Isolation of plasmid DNA from <i>E. coli</i> .....	158
6.4.3.	Polymerase chain reaction (PCR).....	159
6.4.4.	Separation and detection of DNA using agarose gel electrophoresis ....	159
6.4.5.	Site-directed mutagenesis.....	160
6.4.6.	Restriction digestion of DNA .....	160
6.4.7.	Ligation of DNA .....	160
6.4.8.	Preparation of chemically competent <i>E. coli</i> cells .....	161
6.4.9.	Transformation of chemically competent <i>E. coli</i> cells.....	161
6.4.10.	Preparation of electro-competent <i>Vibrio parahaemolyticus</i> cells.....	162
6.4.11.	Transformation of electro-competent <i>V. parahaemolyticus</i> cells.....	162
6.4.12.	Plasmids.....	162
6.4.12.1.	Construction of plasmids .....	164
6.4.13.	Primers .....	170
6.5.	Biochemical methods .....	173
6.5.1.	Separation and detection of proteins by SDS PAGE .....	173
6.5.2.	Immunoblot analysis.....	173
6.5.3.	Immunoprecipitation and co-immunoprecipitation assays followed by LC-MS analysis .....	174
6.5.3.1.	<i>Vibrio parahaemolyticus</i> .....	174
6.5.3.2.	<i>Escherichia coli</i> .....	177
6.5.4.	Co-immunoprecipitation upon Polymyxin treatment .....	177
6.5.5.	Detection of phosphorylation by Phostag gels .....	178
6.5.5.1.	Detection of phosphorylation by Phostag gels upon polymyxin treatment	178
6.6.	Label-free quantification of total cell lysates using LC-MS-based proteomics	179
6.6.1.	Proteomics upon polymyxin treatment.....	180
6.7.	RNA sequencing/ Transcriptomics.....	181

## Table of Contents

---

6.7.1.	Isolation of total RNA .....	181
6.7.2.	Data analysis .....	182
6.8.	Stereo microscopy .....	182
6.9.	Bioinformatic analysis .....	182
6.9.1.	Identification of targets for analysis .....	182
6.9.2.	Generation of the phylogenetic tree .....	183
6.9.3.	Analysis of the phylogenetic tree .....	183
6.9.4.	Homology structural modeling .....	184
6.9.5.	Identification of domains of kinases similar to PknT .....	184
6.9.6.	Frequency of essential regions of EcfP within other species.....	184
7.	Chapter 7: Supplementary Materials .....	185
8.	Chapter 8: References .....	203
	Acknowledgments .....	231
	CURRICULUM VITAE .....	235
	ERKLÄRUNG .....	237
	EINVERSTÄNDNISERKLÄRUNG.....	239



## List of Figures

Figure 1. General scheme of the action of protein kinases .....	18
Figure 2. Overview of the regulation of cAPK .....	21
Figure 3. Three-dimensional structure of cAPK and the essential features of the catalytic cleft.....	23
Figure 4. Conservation of key residues within the catalytic cleft of PknB .....	26
Figure 5. Activation model for STKs in bacteria with PknB of <i>M. tuberculosis</i> as an example.....	27
Figure 6. The <i>B. subtilis</i> PrkC plays a role in sporulation and germination .....	33
Figure 7. Model depicting the assembly of the RNA polymerase holozyeme .....	39
Figure 8. Schematic overview of the roles of different $\sigma$ regions.....	45
Figure 9. Promoter recognition by primary $\sigma$ factors in complex with the RNAP .....	47
Figure 10. Regulation of ECF $\sigma$ factors by proteolysis .....	50
Figure 11. Regulated proteolysis of RseA releases $\sigma^E$ of <i>E. coli</i> .....	51
Figure 12. Regulation of ECF $\sigma$ factors by conformational changes within the anti- $\sigma$ factor .....	53
Figure 13. Regulation of ECF $\sigma$ factors by partner switching .....	56
Figure 14. Possible regulation of ECF $\sigma$ factors by Ser/Thr kinases (STKs) .....	59
Figure 15. Phosphorylation of ECF $\sigma$ factor occurs in <i>V. parahaemolyticus</i> .....	75
Figure 16. Domain architecture and inner membrane orientation of PknT.....	76
Figure 17. EcfP is phosphorylated by the Serine/Threonine kinase, PknT.....	77
Figure 18. PknT and EcfP form an interaction complex.....	78
Figure 19. PknT is a genuine and the sole kinase responsible for the phosphorylation of EcfP .....	79
Figure 20. EcfP phosphorylation occurs at a specific threonine residue, Thr63 .....	80
Figure 21. Results of miscellaneous stresses on $\Delta ecfP$ and $\Delta pknT$ mutants .....	81
Figure 22. Both PknT and EcfP are essential for conferring resistance to polymyxin antibiotics.....	83
Figure 23. EcfP and PknT function in the same signaling pathway.....	84
Figure 24. The PknT/EcfP system regulate the expression of the putative UDP-glucose-4-epimerase encoding gene, <i>vpa0879</i> .....	85
Figure 25. Overview of the number of targets regulated by the PknT/EcfP system.....	86
Figure 26. VPA0879 is extremely sensitive to polymyxin B.....	87
Figure 27. The Thr63 residue of EcfP is essential for conferring polymyxin resistance to <i>V. parahaemolyticus</i> .....	88
Figure 28. EcfPT63A prevents phosphorylation of EcfP at residue 63 (T63).....	89
Figure 29. A strain expressing EcfPT63E is less sensitive to polymyxin stress than an <i>ecfP</i> deletion .....	90
Figure 30. The catalytic D202 residue of PknT is important for its interaction with EcfP and response to polymyxin .....	91
Figure 31. The catalytic D202 residue of PknT is indispensable for phosphorylation of EcfP.....	92
Figure 32. Polymyxin induces phosphorylation of EcfP .....	93
Figure 33. Induction of VPA0879 upon polymyxin treatment is dependent on the Thr63 residue of EcfP .....	94
Figure 34. Phylogenetic tree depicting the salient features of ECF $\sigma$ factors associated with STKs .....	95
Figure 35. Different members of ECF43 are associated to a distinct protein kinase domain architecture .....	96
Figure 36. Multiple sequence alignment of distinct regions of $\sigma^{2.1}$ and $\sigma^{2.2}$ with associated sequence logo .....	97

## List of Figures

Figure 37. Conservation of key negatively charged residues within $\sigma_{2.2}$ in different ECF groups .....	98
Figure 38. Overview of the predicted structure of $\sigma_2$ domain of EcfP overlaid with SigH from <i>M. tuberculosis</i> in the RNAP open complex .....	99
Figure 39. Phosphorylation of EcfP enables its interaction with $\beta/\beta'$ of RNAP .....	100
Figure 40. Interaction of EcfP with the RNAP is dependent on phosphorylation of the Thr63 residue .....	101
Figure 41. Polymyxin enhances the interaction of EcfP with the RNAP .....	102
Figure 42. Phylogenetic tree of species encoding EcfP homologs in their genomes ...	104
Figure 43. ECF $\sigma$ factor phosphorylation in <i>Hyphomonas neptunium</i> .....	105
Figure 44. Identification of the phosphorylated residue in the ECF $\sigma$ factor of <i>H. neptunium</i> .....	106
Figure 45. Transcriptional regulation by $\sigma$ factor phosphorylation .....	108
Figure 46. Swimmer and swarmer cells of <i>V. parahaemolyticus</i> .....	119
Figure 47. Distinct layers within the swarm colony of <i>V. parahaemolyticus</i> .....	122
Figure 48. Phenotypic characterization of PknT .....	123
Figure 49. PknT is required for swarming behavior .....	124
Figure 50. The swarm colony of $\Delta pknT$ appears to be morphologically different than wild type .....	124
Figure 51. Swarming phenotypes of $\Delta vp0054$ , $\Delta ecfP$ and $\Delta vp0056$ mutant strains ...	125
Figure 52. Colony morphologies of $\Delta vp0054$ , $\Delta ecfP$ and $\Delta vp0056$ mutants .....	126
Figure 53. Swarming behavior of combinatorial deletions of genes within the operon	127
Figure 54. Swarming behavior of the catalytically inactive <i>pknTD202A</i> and the phosphoablative <i>ecfPT63A</i> mutants .....	128
Figure 55. Morphological differences in the swarm colonies of the <i>pknTD202A</i> and <i>ecfPT63A</i> mutants .....	128
Figure 56. Global LC-MS proteomics on $\Delta pknT$ mutant compared to wild type .....	130
Figure 57. An overview of the targets that are significantly regulated by PknT swarms .....	130
Figure 58. Functional groups of the proteins significantly regulated by PknT swarms .....	131
Figure 59. Global LC-MS proteomics studies on $\Delta vp0054$ , $\Delta ecfP$ and $\Delta vp0056$ mutant strains compared to wild type .....	134



## List of Tables

Table 1. List of reagents .....	147
Table 2. List of commercial kits and assays .....	149
Table 3. List of software and online resources .....	149
Table 4. List of essential equipments .....	150
Table 5. List of media, buffer and solutions .....	151
Table 6. List of strains .....	154
Table 7. Components of the Q5 PCR reaction mix .....	159
Table 8. Components of the Phusion PCR reaction mix .....	159
Table 9. List of plasmids .....	162
Table 10. List of primers .....	170
Table 11. List of SDS PAGE gels .....	173
Table 12. Genes significantly downregulated in both $\Delta ecfP$ and $\Delta pknT$ mutants with respect to wild type .....	187
Table 13. Genes significantly upregulated in both $\Delta ecfP$ and $\Delta pknT$ mutants with respect to wild type .....	187
Table 14. List of genes that are significantly downregulated in the $\Delta ecfP$ mutant when compared to wild type .....	188
Table 15. List of genes that are significantly upregulated in the $\Delta ecfP$ mutant when compared to wild type .....	190
Table 16. List of genes that are significantly downregulated in the $\Delta pknT$ mutant when compared to wild type .....	191
Table 17. List of genes that are significantly upregulated in the $\Delta pknT$ mutant when compared to wild type .....	192
Table 18. Targets that were significantly downregulated in $\Delta pknT$ swimmers when compared to wild type swimmers .....	195
Table 19. Targets that were significantly upregulated in $\Delta pknT$ swimmers when compared to wild type swimmers .....	196
Table 20. List of strains used to calculate the frequency of Ser or Thr at the same position as T63 of EcfP .....	197



## ABBREVIATIONS

---

μ-	Micro
aa	Amino acid
BACTH	Bacterial Adenylate Cyclase-based Two Hybrid
bp	Base pair
h	Hour
IPTG	Isopropyl β-D-1-thiogalactopyranoside
LB	Luria-Bertani medium
LC-MS	Liquid chromatography mass spectrometry
min	Minutes
NA	Not applicable
pH	Negative decimal logarithmic of the hydrogen ion activity
SEM	Standard Error of the Mean
Xgal	5-Bromo-4-chlor-3-indoxyl-β-D-galactopyranosid
DNA	Deoxyribonucleic acid
RNA	Ribonucleic acid
RNAP	RNA polymerase
ECF	Extracytoplasmic function
PTM	Post-translational modification
ATP	Adenosine triphosphate
GTP	Guanosine triphosphate
PKA	Protein kinase A
TCS	Two component system
STK	Serine/Threonine kinase
Pbp	Penicillin binding protein
PASTA	Pbp and STK associated domain
SDS	Sodium dodecyl sulfate
PAGE	Polyacrylamide gel electrophoresis
PknT	Protein Kinase of ECF Threonine
EcfP	ECF σ factor activated by Phosphorylation
co-IP	Co-immunoprecipitation
Thr	Threonine
Ser	Serine
Glu	Glutamate
LPS	Lipopolysaccharide
TTSS	Type III secretion system

## Abbreviations

---

QS	Quorum signal
FDR	False discovery rate
GO	Gene ontology
OP	Opaque
TR	Translucent
UDP	Uridine diphosphate
OD	Optical density
FC	Fold change
w/v	Weight/ volume
Amp	Ampicillin
Cm	Chloramphenicol
nm	Nanometer
ND	Not detected
AU	Arbitrary unit
CFU	Colony forming unit
BME	$\beta$ -mercaptoethanol
mL	Milliliter
RPKM	Reads Per Kilobase Million
GFP	Green fluorescent protein
sfGFP	Superfolded GFP

---

## ABSTRACT

A major form of bacterial transcriptional regulation occurs by the exchange of the primary  $\sigma$  factor of the RNA polymerase with alternative ECF  $\sigma$  factors, which generally are retained in an inactive state by sequestration into  $\sigma$ /anti- $\sigma$  factor complexes (until they are needed). Using *Vibrio parahaemolyticus* as a model organism, we report a novel mechanism of transcriptional regulation, which instead relies on intrinsically inactive ECF  $\sigma$  factors that in turn rely on  $\sigma$  factor phosphorylation for interaction with the RNA polymerase. Particularly, we show that upon polymyxin stress, the threonine kinase PknT phosphorylates the  $\sigma$  factor EcfP, resulting in EcfP activation and expression of an essential polymyxin resistance regulon. EcfP phosphorylation occurs at a highly conserved threonine residue, Thr63, positioned within a divergent region in the  $\sigma$ 2.2 helix. EcfP is intrinsically inactive and unable to bind RNA polymerase due to the absence of a negatively charged DAED motif in this region. Our results indicate that phosphorylation at residue Thr63 mimics this negative charge and licenses EcfP for interaction with RNA polymerase and activation of target gene expression. Regulation of gene expression by phosphorylation of ECF  $\sigma$  factor is likely a widespread mechanism in bacteria, presenting a new paradigm in transcriptional regulation.

One of the unique features of *V. parahaemolyticus* is that it exhibits a dual lifestyle. In liquid environments, where the bacteria are free-living, they exist as short swimmer cells with a single polar flagellum. However, upon encountering solid surfaces, the bacteria differentiate into highly elongated swarmer cells that are characterized by the presence of numerous peritrichous lateral flagella. Here, we report the involvement of the aforementioned threonine kinase/ECF  $\sigma$  factor system, namely PknT/EcfP, in regulation of swarming behavior. Strikingly, our findings indicate that this regulatory role depends on a phosphorylation-driven mechanism. We also provide evidence for the role of two other proteins encoded by genes present within the same operon as that of *pknT* and *ecfP*, namely VP0054 and VP0056, in regulation of swarming behavior. Our findings also reveal several key targets such as transporters and proteins involved in certain biosynthetic processes that are regulated by PknT. This is the first time that STKs have been implicated in swarming behavior in bacteria.

# ZUSAMMENFASSUNG

Eine wichtige Form der bakteriellen Transkriptionsregulation ist der Austausch des primären  $\sigma$ -Faktors der RNA-Polymerase mit alternativen ECF  $\sigma$ -Faktoren. Diese werden in der Regel durch Sequestrierung in  $\sigma$ /anti- $\sigma$ -Faktorkomplexe in einem inaktiven Zustand gehalten (bis sie gebraucht werden). Wir berichten hier über einen neuartigen Mechanismus der transkriptionellen Regulation in unserem Modellorganismus *V. parahaemolyticus*, bei dem stattdessen intrinsisch inaktive ECF  $\sigma$  Faktoren, die durch  $\sigma$  Faktor Phosphorylierung für die Interaktion mit der RNA-Polymerase aktiviert werden. Insbesondere zeigen wir, dass die Threoninkinase PknT bei Polymyxinstress den  $\sigma$ -Faktor EcfP phosphoryliert, was zu einer EcfP-Aktivierung und im Folgenden zur Expression eines Polymyxin-Resistenzregulons führt. Die EcfP-Phosphorylierung erfolgt an einem hochkonservierten Threoninrest, Thr63, der in einer divergierenden Region in der Helix  $\sigma 2.2$  positioniert ist. EcfP ist an sich inaktiv und kann keine RNA-Polymerase binden, da in dieser Region kein negativ geladenes DAED-Motiv vorhanden ist. Die Phosphorylierung an Thr63 imitiert diese negative Ladung und lizenziert EcfP für die Interaktion mit RNA-Polymerase und die Aktivierung der Zielgenexpression. Expressionsregulation durch Phosphorylierung des ECF  $\sigma$  Faktors ist wahrscheinlich ein weit verbreiteter Mechanismus in Bakterien, der ein neues Paradigma in der transkriptionellen Regulation darstellt.

Eines der einzigartigen Merkmale von *V. parahaemolyticus* ist, dass es einen dualen Lebensstil aufweist. In flüssigen Umgebungen existieren die freilebenden Bakterien als kurze Schwimmerzellen mit einem einzigen polaren Flagellum. Bei Auftreffen auf feste Oberflächen differenzieren sich die Bakterien jedoch zu stark verlängerten Schwärmerzellen, die sich durch das Vorhandensein zahlreicher peritricher Seitenflagellen auszeichnen. Hier berichten wir über die Beteiligung des oben genannten Threoninkinase/ECF  $\sigma$ -Faktorsystems PknT/EcfP an der Regulierung des Schwarmverhaltens. Interessanterweise zeigen unsere Ergebnisse, dass diese regulatorische Rolle von einem phosphorylierungsgetriebenen Mechanismus abhängt. Wir liefern auch Hinweise für die Rolle von zwei weiteren Proteinen, die im selben Operon wie *pknT* und *ecfP* codiert sind, nämlich VP0054 und VP0056, bei der Regulierung des Schwärmverhaltens. Unsere Ergebnisse offenbaren außerdem auch mehrere weitere Zielgene die durch PknT reguliert werden, wie z.B. Transporter und Proteine, die an bestimmten biosynthetischen Prozessen beteiligt sind. Dies ist das erste Mal, dass STKs in das Schwärmverhalten von Bakterien involviert sind.

## **CHAPTER 1: INTRODUCTION**

### 1.1. Post-translational modifications

The increasing complexity of the proteome, when compared to the genome can be attributed primarily to changes that occur at the transcriptional level, for instance, mRNA splicing and those that occur at the protein level, namely post-translational modifications (PTMs). As suggested by the name, the latter involve chemical and covalent modifications of proteins upon being translated. Despite the fact that PTMs do occur extensively in prokaryotes, their prevalence is much higher in eukaryotes. These modifications can usually be divided into two groups: one involving the addition of a chemical group to the nucleophilic side chain of the protein and the other involving the cleavage of the peptide bonds of proteins. There are several different types of PTMs and all of them, with the exception of alkylation reactions, are catalyzed by enzymes (C. T. Walsh, Garneau-Tsodikova, & Gatto, 2005). Based on the nature of the chemical modification, PTMs are generally reversible in nature. The directed nature of PTMs has made the enzymes catalyzing these modifications attractive models for drug targeting (Santos & Lindner, 2017).

PTMs have been shown to exert their action by inducing structural changes within the protein that results in a change in activity (Eichmann et al., 2016). The effect of these modifications can be seen in a wide variety of responses including transcription (Seth, Hausladen, Wang, & Stamler, 2012), pathogenicity (Dubrana et al., 2017) and carbon metabolism (Wang et al., 2010), to name a few. The occurrence of a single PTM on multiple sites within a protein and the co-occurrence of multiple PTMs within a protein have been now well documented and shown to be implicated in protein-protein interaction networks (Beltrao, Bork, Krogan, & Van Noort, 2013; Duan & Walther, 2015; Pawson & Scott, 2005). Crosstalk between PTMs is also quite common, in that some of these modifications affect the activity of certain enzymes. An example of this is the role of ubiquitination in regulating kinase activity (Hunter, 2007). With more sensitive ways to detect these modifications (Forbes et al., 2004; Jensen, 2004), there now exist a few databases with an exhaustive list of PTMs recorded among several eukaryotes and prokaryotes within their proteome. These databases help shed light on distinct PTM motifs within a protein and could also be used for identifying substrate specificity for specifically modified sites (Gnad, Gunawardena, & Mann, 2011; Lu et al., 2013).



---

### 1.1.1. Phosphorylation as a post-translational modification

Protein phosphorylation is one of the most well-studied PTMs. It is a reversible mechanism that involves the addition of a phosphate group to certain critical residues (usually polar) in the side chain of the protein. The phosphorus within the phosphate group has high water solubility and is able to form up to five covalent bonds, thus rendering the formation of alkyl esters by interactions with the polar residues in the side chain of proteins feasible. A vast majority of phosphorylation events occur on serine, threonine or tyrosine residues and among these, modification of the -OH group of serine is the most prevalent (Ardito, Giuliani, Perrone, Troiano, & Muzio, 2017; Ubersax & Ferrell, 2007).

The first evidence of protein phosphorylation came in the early 1900s when modification of vitellin, which was significant due to its association with haemoglobin, was recorded (Levene & Alsberg, 1906). However, it was not until the early 1930s that the modified residue in this phosphorylation event was found to be serine. In prokaryotes, however, the first evidences of phosphorylation came much later. The stability of the chemical bond was exploited to assess which residues were modified. Phosphorylation events were recorded in the mid to late 1970s among bacterial proteins on serine, threonine and tyrosine residues (Garnak & Reeves, 1979; Hunter, Sefton, & Holley, 1980; Yin, Wang, & Koshland, 1978). Shortly thereafter, phosphorylation of several proteins in the stationary phase was reported in the archaea, *Sulfolobus acidocaldarius* on serine or threonine residues (SKÓRKO, 1984).

Phosphorylation modifications result in a change in the protein structure and eventually, its function. Phosphorylation of certain residues also enables interactions with other proteins consisting of distinct domains. For example, in eukaryotes, the 14-3-3 family of proteins, which are involved in cell cycle regulation, bind to phosphorylated serine residues with a very high affinity (Muslin, Tanner, Allen, & Shaw, 1996). This interaction combines the role of distinct structural motifs within the protein (Yaffe et al., 1997). Another example is the forkhead associated (FHA) domains that are found in both prokaryotes and eukaryotes. These have been shown to possess high binding affinities to the phosphorylated peptides of several proteins, many of which are involved in a wide range of biological functions (Durocher, Henckel, Fersht, & Jackson, 1999). Phosphorylated tyrosine residues have also been shown to have a role in this regard: proteins comprising of SH2 domains bind to phosphotyrosine residues and partake in signaling mechanisms (Hunter & Cooper, 1985; Sadowski, Stone, & Pawson, 1986).

### 1.2. Protein kinases

#### 1.2.1. Discovery of protein kinases in eukaryotes

It was not until 1954 that a certain enzyme present in the mitochondria of rat liver was found to exhibit phosphorylation activity upon incubation with a protein substrate and a high energy donor molecule, ATP, in this case (Burnett & Kennedy, 1954). Soon after, Fischer and Krebs showed that conversion of the inactive phosphorylase b to the active phosphorylase a within muscle extracts required the presence of both a divalent metal ion and a high energy phosphate containing molecule acting as a nucleotide (FISCHER & KREBS, 1955). It was also shown that this activation resulted by phosphorylation of a specific serine residue, mediated by an enzyme, subsequently named phosphorylase b kinase. This enzyme's activity is in turn controlled by the action of another enzyme, cAMP-dependent protein kinase through phosphorylation (D. A. Walsh, Perkins, & Krebs, 1968), thereby resulting in the establishment of a signal cascade.

Kinases are enzymes that catalyze the covalent addition of a phosphate group to mostly polar groups in the side chains of proteins (Figure 1). These enzymes are among the largest class of enzymes involved in PTMs. There are three distinct mechanisms that are key to the activity of protein kinases. These are proper orientation and binding of the donor molecule (either ATP or GTP), proper binding and orientation of the substrate protein and eventually, chemical transfer of the gamma-phosphate from the donor molecule to the substrate (Hanks & Hunter, 1995).

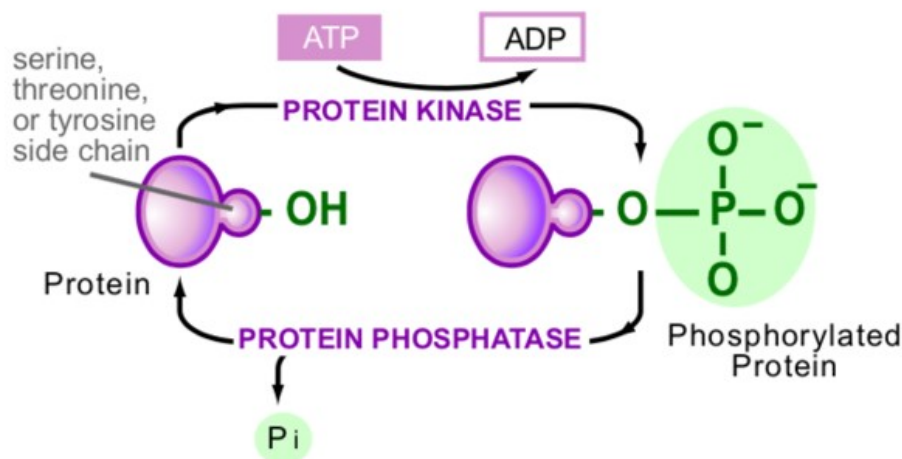


**Figure 1. General scheme of the action of protein kinases.** By using the gamma-phosphate of a high-energy donor molecule such as ATP, in this case, protein kinases modify the side chains of amino acids, thereby resulting in the release of an ADP molecule and the phosphorylated protein. This phosphorylated protein can then be subject to dephosphorylation by protein

phosphatases, resulting in the release of inorganic phosphate. Figure adapted from The Science Creative Quarterly (SCQ).

### 1.2.2. Discovery of protein kinases in bacteria

Like in the case of phosphorylation, the discovery of protein kinases in bacteria came much later. In 1982, LaPorte and Koshland Jr. reported that the key tricarboxylic acid (TCA) cycle enzyme, namely isocitrate dehydrogenase (IDH), which was shown to be phosphorylated just a couple of years earlier (Garnak & Reeves, 1979) was modified by a protein that comprises both kinase and phosphatase activities (Laporte & Koshland, 1982). This protein, alongside the Histidine-containing phosphocarrier protein (HPr) kinase/phosphorylase protein is part of a special family of kinases that do not bear much sequence similarity with their eukaryotic counterparts. One of the key differences between bacterial and eukaryotic protein kinases is that the former is known for its substrate specificity, in that bacterial kinases do not possess the ability to phosphorylate exogenous substrates, such as casein for instance (Pereira, Goss, & Dworkin, 2011b).

### 1.2.3. Classification of kinases: Chemical nature of the side chains

Protein kinases can be divided based on the chemical nature of the side group that they modify. Modifications can occur at the hydroxyl groups of serine, threonine or tyrosine residues leading to the formation of esters, the acyl groups of aspartic and glutamic acid residues or the side chains of histidine and arginine resulting in the formation of stable phosphoramidate bonds. There are also examples of other residues being modified by protein kinases. In *Staphylococcus aureus*, phosphorylation on cysteine residues regulates the levels of certain global transcriptional regulators that have a role in virulence (F. Sun et al., 2012). Additionally, phosphorylation on arginine has been shown to mediate heat shock responses by keeping the transcriptional repressor, CtsR in check (Fuhrmann et al., 2009). An upcoming group of kinases, namely proline directed kinases, which are characterized by the presence of a distinct motif next to the phosphorylated serine or threonine residues have been found to have major roles in host-pathogen interactions (M. Miller et al., 2010). Interestingly, there are also instances wherein phosphorylation has been shown to occur independently of the kinase under question. For example, the response regulators involved in chemotaxis, namely, CheY and CheB were shown to be phosphorylated in the absence of their histidine kinase, CheA. However this phosphorylation event required the presence of acetate,

which could undergo chemical modification resulting in acetylphosphate that can then serve as a donor molecule for the phosphorylation reaction (Lukat, McCleary, Stockt, & Stock, 1992).

### **1.2.4. The high energy phosphate donor**

The phosphate group within a typical kinase reaction (Figure 1) usually comes from a high energy molecule. This molecule is usually ATP, which donates its gamma-phosphate group for the phosphotransfer reaction. However, there have been studies wherein other molecules such as phosphoenolpyruvate have been utilized as a donor instead (Cozzone, 1993). Some kinases have also been shown to use GTP as their phosphate donor. This is evident in the case of AlgR1, a response regulator that regulates the production of the critical peptidoglycan component alginate in *Pseudomonas aeruginosa*, which was found to be phosphorylated by the protein kinase, AlgR2 (Roychoudhury, Sakai, & Chakrabarty, 2006).

### **1.2.5. Protein kinases as drug targets**

Due to the wide range of biological functions that protein kinases are involved in, they have been used extensively as drug targets. The first breakthrough in this regard was the discovery of Imatinib by Novartis. This drug acts as an inhibitor and competes with ATP to bind to Bcr-Abl, a protein that is implicated in tumor formation. It is now commonly used in the treatment of chronic myelogenous leukemia (CML) (Jiao et al., 2018). Another example is the drug Gefitinib, which interferes with the phosphorylation of several receptor tyrosine kinases, especially those involved in Epidermal growth factor receptor (EGFR) signaling pathways. Its use in the reduction of posterior capsule opacification (PCO), which is a common occurrence post cataract surgery, has been tested in the laboratory (Wertheimer et al., 2015). Apart from the above, certain proteins can also be used as inhibitors, an example of this being the use of Ankyrin repeat (AR) proteins against a phosphotransferase enzyme that confers resistance to aminoglycoside antibiotics such as streptomycin and kanamycin in bacteria (Amstutz et al., 2005).

### **1.2.6. Structure of eukaryotic protein kinases**

Prior to the structural resolution of the first eukaryotic protein kinase, Hanks and colleagues performed an alignment of 65 members of the protein kinase superfamily within eukaryotes in an attempt to search for conserved residues and domains (Hanks, Quinn, & Hunter, 1988). This alignment revealed several highly conserved regions and residues. These include a glycine rich region and an invariant lysine residue close to the amino terminus. The central region of the catalytic domain was found to be particularly highly conserved than any other region. It was found to contain an invariant aspartic acid residue, which likely participates in the phosphotransfer activity by the formation of salt bridges with the gamma phosphate of the donor ATP molecule (Hanks et al., 1988).

The first kinase structure to be resolved was that of the cAMP dependent protein kinase (cAPK) (Knighton, Xuong, Taylor, & Sowadski, 1991). This was a landmark discovery in the field as studies till date use it as a template for alignment and examination of sequence homology, especially among key regions involved in catalysis. In its inactive state, cAPK was found to form a heterotetramer composed of two regulatory and two catalytic subunits. As a result of binding of cAMP to the regulatory subunits, the catalytic subunits are released and they in turn proceed from the cytoplasm into the nucleus, resulting in the subsequent activation of other proteins (Figure 2) (C. Kim, Xuong, & Taylor, 2005; Su et al., 1995).

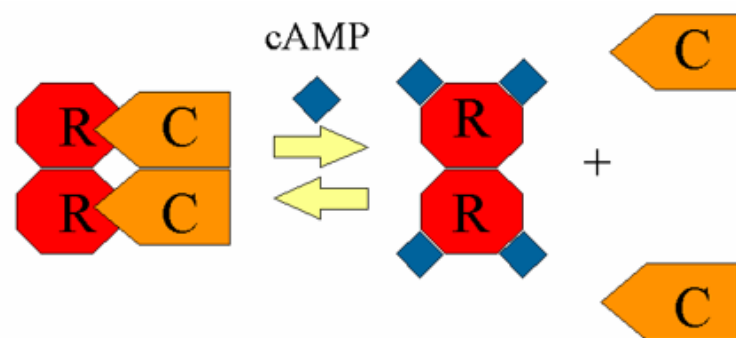


**Figure 2. Overview of the regulation of cAPK.** The structure of cAPK comprises of two regulatory (red, R) and two catalytic (orange, C) subunits. Upon the binding of cAMP molecules on distinct sites on the regulatory subunits, the catalytic subunits are released, thereby resulting in activation of the kinase's catalytic subunits, which then proceed to the nucleus. Adapted from (Skalhegg & Tasken, 1997).

### 1.2.6.1. cAPK has a bi-lobed structure

The catalytic subunit of cAPK was found to contain two lobes: the smaller N terminal one, which comprises of the ATP binding and phosphoacceptor sites and the larger C terminal lobe which is involved in peptide recognition of the substrate. The cleft

between these two lobes was identified as the site for catalysis. The smaller lobe was found to consist of 5 beta strands and one alpha helix, whereas the larger lobe was composed of seven alpha helices. Upon comparison to the sequence alignment studies by Hanks and colleagues, the existence and position of several key residues, especially those within the catalytic core, were confirmed (Knighton et al., 1991). The invariant lysine residue found at the bottom of the N terminal lobe, close to the catalytic cleft was found to have a role in Mg-ATP binding. The glycine rich element, Gly-Thr-Gly-Ser-Phe-Gly was also implicated in Mg-ATP binding. Given the aforementioned conservation of key residues as described by Hanks and colleagues (Hanks et al., 1988), the term “Hanks-type kinases” arose to the fore. Furthermore, due to the presence of the highly conserved aspartate and arginine residues within the catalytic loop, these kinases are also referred to as RD kinases.

### **1.2.6.2. Distinct features of cAPK that are required for its activity**

#### **1.2.6.2.1. The catalytic domain**

Alignment studies were performed to better understand the distinct domains within the site of catalysis. The catalytic domain was found to comprise of twelve subdomains (Shi, Potts, & Kennelly, 1998). Of these, subdomains I-IV consist of the nucleotide-binding region, with subdomain I being characterized by the glycine rich region interspersed with highly hydrophobic residues and subdomain II hosting the lysine residue (Hanks et al., 1988; Knighton et al., 1991), which has been shown to interact with the gamma-phosphate of ATP (Carrera, Alexandrov, & Roberts, 1993). Subdomain VI and VII comprise of key residues that partake in catalysis, with the latter being the site for the highly conserved aspartate and arginine residues (constituting the RD box). Subdomain VIII is house to the invariant glutamate residue which plays a role in stabilizing interactions with the substrate peptide through the formation of a salt bridge with an arginine residue in subdomain XI (Shi et al., 1998; Jie Yang et al., 2012).

#### **1.2.6.2.2. The activation loop**

A key feature of cAPK, that is essential to its kinase activity, is the activation segment. This segment comprises of three regions: the magnesium binding loop, the activation loop and the P+1 loop (L. N. Johnson, Noble, & Owen, 1996; Nolen, Taylor, & Ghosh, 2004). The P+1 loop is a very important region that governs binding of the substrate peptide and also dictates substrate specificity of the kinase. The activation

loop, which is in close proximity to the catalytic loop comprises the threonine residue that is known to be autophosphorylated. Interestingly, phosphorylation of this threonine was observed much earlier (Shoji, Titani, Demaille, & Fischer, 1979) but it was not until 1993 that its role in activation of the kinase was shown (Steinberg, Cauthron, Symcox, & Shuntoh, 2015). Autophosphorylation of the residue within the activation loop results in activation of the kinase by inducing a conformational change bringing the N and C lobes into a closed conformation. This autophosphorylation event also appears to be crucial to establish a successful hydrogen bond between the phosphothreonine and the conserved arginine residue in the catalytic site (Steichen et al., 2010).

Autophosphorylation can also occur in residues other than those present in the activation loop. However, these modifications do not contribute to the catalytic activity of the kinase (Romano et al., 1998). Most importantly, only the inactive form of the kinase has the ability to transfer the gamma phosphate from the donor molecule to the activation loop (Beenstock, Mooshayef, & Engelberg, 2016). An overview of the essential regions, described above, is shown in Figure 3.

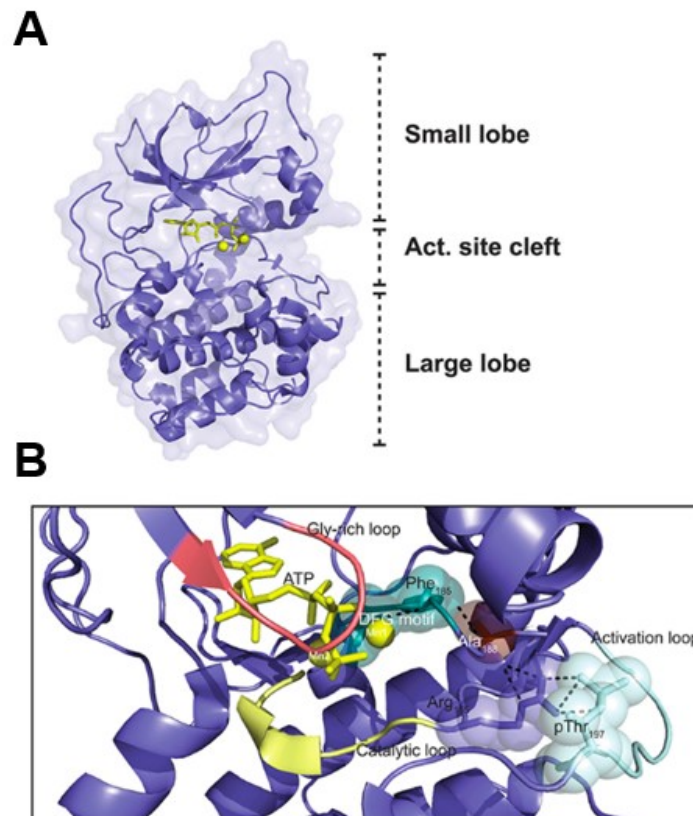


**Figure 3. Three-dimensional structure of cAPK and the essential features of the catalytic cleft.** (A) The catalytic (or C) subunit of cAPK comprises of a smaller N terminal lobe and a larger C terminal lobe. The active site cleft where catalysis occurs is found between these two lobes. This cleft also consists of a binding site for ATP (shown in yellow) (B) The catalytic cleft comprises of several essential features that are required for the kinase's activity, namely the catalytic loop,

activation loop and the glycine rich region (Gly-rich loop), which is essential for Mg-ATP binding. Figure adapted from (Søberg & Skålhegg, 2018).

### **1.2.7. Kinases in bacteria**

#### **1.2.7.1. Two component systems (TCS)**

In prokaryotes, initial research studies in phosphorylation were focused on two-component systems (TCS), a term that was first coined by Nixon, Ronson, and Ausubel (Nixon, Ronson, & Ausubel, 2006). A classical TCS was found to comprise of a sensor histidine kinase and a response regulator. Upon sensing the external stimulus through its N-terminal, autophosphorylation of the catalytic C terminal domain of the sensor histidine kinase ensues. This activated sensor then transphosphorylates the response regulator on an aspartate residue present within its N-terminal receiver domain (Zschiedrich, Keidel, & Szurmant, 2016).

Some of the key residues within the sensor kinase include the H box consisting of the conserved histidine residue and two glycine rich boxes, G1 and G2 which serve as the site for nucleotide binding (Alex & Simon, 1994). The response regulators are characterized by the presence of a minimum of two aspartic acid residues and one lysine residue, all of which are invariant. The aspartate residues usually form an acidic pocket and this serves as the site of phosphorylation (Lukat et al., 1992).

#### **1.2.7.2. Phosphotransferases**

The phosphoenolpyruate:sugar phosphotransferase system (PTS) is a system, which is responsible for both the phosphorylation and also the translocation of several sugars. It is a prevalent system in several bacterial species. One of the key enzymes in this reaction is the Histidine-containing Phosphocarrier protein (HPr), which plays a major role in catabolite repression. Phosphorylation of this protein was found to occur on two residues, namely serine and histidine (Deutscher, Saier, & Jr, 1983). Phosphorylation on the serine residue was found to be an ATP-driven process whereas that on the histidine residue was found to be dependent on phosphoenolpyruvate (PEP). In addition, these two phosphorylation events have distinct fates in the cell, with the serine phosphorylation playing a critical role in catabolite repression while the histidine phosphorylation is involved in the regulation of the key metabolic enzyme, glycerol kinase (Reizer, Romano, & Deutscher, 1993). The enzyme capable of the ATP-driven serine phosphorylation was found to be bifunctional possessing both kinase and



phosphorylase activities (Kravanja et al., 1999). The bifunctional Hpr kinase/phosphorylase (HPrK/P) protein was found to be structurally dissimilar to eukaryotic protein kinases. The C terminal domain of the protein comprises of the well-studied Walker A motif, also referred to as P-loop, typically associated with ATP-binding proteins. Crystallographic studies have revealed that this loop functions by interacting with inorganic phosphate (Fieulaine et al., 2001). In addition to HPrK/P, other kinases have also been found to contain Walker A motifs in their structure, key of these being the tyrosine kinases (Grangeasse, Nessler, & Mijakovic, 2012).

### 1.2.7.3. Serine/threonine kinases (STKs)

In 1992, Zhang and colleagues reported evidence for the first Hanks type serine/threonine kinase (STK) in bacteria. They found that the kinase, Pkn1 was essential for cell development in *Myxococcus xanthus* (W. Zhang, Munoz-Dorado, Inouye, & Inouye, 1992). Upon performing a genome screen using a fragment of *pkn1*, several other genes (approximately 26) were revealed to be putative kinases. More importantly, all of these had the highly conserved residues that were key for the activity of eukaryotic STKs (W. Zhang et al., 1992).

Further evidence came through experiments that looked at the proteins found in culture supernatants secreted by *Yersinia pseudotuberculosis*. A key component of these supernatants was a protein kinase, that was capable of autophosphorylation on a serine residue (Galyov, Håkansson, Forsberg, & Wolf-Watz, 1993). These studies led to the beginning of a new era of characterizing Hanks-type kinases in bacteria.

#### 1.2.7.3.1. Comparison of STKs to TCS

As opposed to the TCS, where rapid hydrolysis of the phosphoaspartate takes place, in the case of STKs, the phosphorylated substrate is usually stable at least until its acted on by protein phosphatases. Additionally, the list of substrates that are capable of being phosphorylated by STKs are more extensive, when compared to TCS. It needs to be noted here that while not very common, there are instances of several STKs phosphorylating a single substrate (Didier, Cozzone, & Duclos, 2010; Kobir et al., 2014). There is also significant crosstalk between the two methods of signaling, as described later in detail (Section 1.2.7.3.6.1).

#### 1.2.7.3.2. Structure of bacterial STKs

## Introduction

The first crystallographic studies on STKs in bacteria came only in the early 2000s. The structure of the catalytic domain of the STK, PknB of *Mycobacterium tuberculosis* showed substantial similarity to that of Hanks-type protein kinases. The ATP-bound form was designated the active or the “on” conformation. As many as six residues were found to be phosphorylated and of these, four were present within the activation loop. The extracellular domain was found to comprise of PASTA (Pbp1 and Ser/Thr kinase attached) domains, suggesting a possible role for the kinase in the cell wall biosynthesis machinery. Upon superimposing the structure of PknB atop that of cAPK, the key residues responsible for catalytic activity were found to be highly conserved (Ortiz-Lombardía, Pompeo, Boitel, & Alzari, 2003; T. A. Young, Delagoutte, Endrizzi, Falick, & Alber, 2003) (Figure 4).

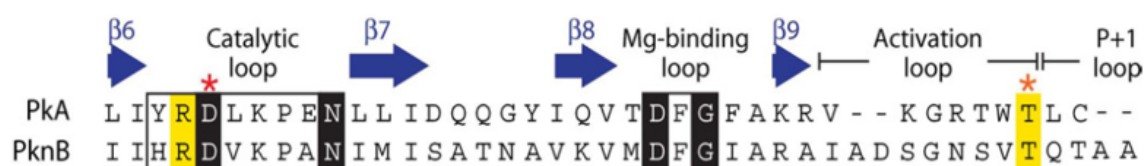


**Figure 4. Conservation of key residues within the catalytic cleft of PknB.** Upon aligning the residues within the catalytic cleft between the N- and C- terminal lobes of PknB with those of cAPK, several key features were found to be conserved. These include the essential aspartate residue (D) within the catalytic loop, the DFG stretch of residues within the Mg-binding loop and the phosphorylatable threonine residue (T) within the activation loop. Adapted from (Pereira et al., 2011b).

### 1.2.7.3.3. A model for allosteric activation within STKs in bacteria

#### 1.2.7.3.3.1. Ligand-based dimerization

The signal or ligand that activates these STKs is poorly understood. In the case of PknG, a nitroalkane was found to bind to the cysteine residues within the rubredoxin-like domain Rbx, thereby inhibiting the activity of the kinase (Gil et al., 2013). Ligand binding results in dimerization and this has been shown to be important for substrate binding and eventual phosphorylation (Greenstein, Echols, Lombana, King, & Alber, 2007). As a result of ligand binding, dimerization of the extracellular domains ensues, which in turn results in dimerization of the kinase domains in a symmetric “back-to-back” fashion and eventual activation by autophosphorylation (Figure 5A). Crystal structure of the extracellular PASTA domain of the *M. tuberculosis* STK, PknB supports this theory of ligand-based dimerization and activation. Interestingly, dimerization of the PknB

PASTA domains was found to result only in the active closed conformation of the kinase (Barthe, Mukamolova, Roumestand, & Cohen-Gonsaud, 2010).

#### 1.2.7.3.3.2. Activation through transphosphorylation

In order to identify the mechanism by which auto-activation happens, the crystal structure of the PknB dimer with an inhibitor molecule was obtained (Mieczkowski, Iavarone, & Alber, 2008). The kinase domains of the two dimers revealed interesting features: only one monomer was found to be ordered whereas the other was positioned in a way that it extends to the activation loop of the former. This model supports the idea of a “front-to-front” association which mediates autoactivation of the kinase, in that one of the monomers acts as a substrate and the other an activator, thereby resulting in the formation of a transphosphorylation complex (Mieczkowski et al., 2008). This phenomenon of activation is very interesting, especially in those STKs that do not possess a ligand-binding domain, which can be transphosphorylated by allosterically activated kinases (Figure 5B).

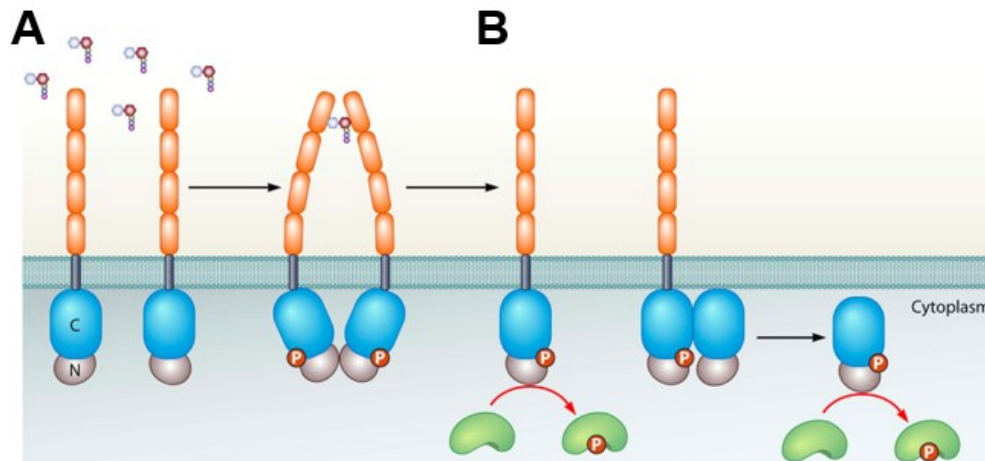


**Figure 5. Activation model for STKs in bacteria with PknB of *M. tuberculosis* as an example.** (A) In the presence of a ligand, the extracellular (PASTA) domains (orange) of PknB bind to it, consequently resulting in a symmetric “back-to-back” dimerization of the catalytic domains (blue, C) and activation through autophosphorylation. (B) Activated kinases can then induce direct phosphorylation of their targets. They can also be involved in activation of certain soluble kinases that lack an extracellular domain. This activation occurs with the formation of an asymmetric “front-to-front” dimer. This activated kinase can then directly phosphorylate its downstream targets. Adapted from (Pereira et al., 2011b).

#### 1.2.7.3.4. C-terminal domains of STKs

There exists huge diversity in the C terminal regions of bacterial STKs. In the case of *M. tuberculosis*, which comprises of 11 STKs, the C terminals of the kinases comprise of different signature repeats (Chakraborti et al., 2011). Nine out of the 11 STKs comprise of a kinase domain and an additional transmembrane domain and are found to be associated with the cell membrane. Some of these C terminal repeat motifs have marked roles in signaling. This is evidenced in the case of the kinase, PknB which serves as a very good target for beta-lactam antibiotics. Further, the presence of several genes responsible for cell wall biosynthesis found in the vicinity of PASTA-containing STKs also suggests a role for the domains in these highly regulated processes (Yeats, Finn, & Bateman, 2002).

### **1.2.7.3.5. Evolution of STKs**

The notion that STKs in the prokaryotic genome evolved from eukaryotes through lateral gene transfer is not accurate. Upon comparing the protein kinases of several bacterial and archaeal genomes, five novel subfamilies were found (C. J. Leonard, Arvind, & Koonin, 1998). These subfamilies share evolutionary ancestry with the eukaryotic protein kinases, thereby indicating the existence of a common ancestor for these proteins before their divergence among the three domains: eukaryotes, bacteria and archaea. Bioinformatics studies in the *Synechocystis spp.* of cyanobacteria revealed the presence of several STKs. These kinases were found to be true to the organism based on the remarkable similarity in codon usage and GC content that they exhibited with the other genes within the genome (Han, 2002). These results strongly indicate the existence of these STKs long before evolutionary divergence.

While most of the eukaryotic subfamilies of protein kinases have diverse occurrences, it is interesting to note that bacterial Ser/Thr kinases occur in distinct taxonomic specific subfamilies (Tyagi, Anamika, & Srinivasan, 2010). This sheds light on the role of these kinases in specialized functions that are specific to a limited group of prokaryotes. Given that STKs were found to go as far back as the last universal common ancestor, referring to the bacterial counterparts as “eukaryotic-like” protein kinases is clearly incorrect (Stancik et al., 2018).

### **1.2.7.3.6. Biological roles for Ser/Thr kinases**

Bacterial serine/threonine kinases have widespread roles in several important biological processes (Canova & Molle, 2014; Cousin et al., 2013; Dworkin, 2015a;

Pereira et al., 2011b; Wright & Ulijasz, 2014). Depending on the stimulus, a single STK can phosphorylate different substrates (reflecting the promiscuity of these kinases), thereby eliciting a range of cellular responses. Interestingly, in the case of the bacterial pathogen *M. tuberculosis*, cross-phosphorylation among kinases has been shown to occur (Baer, Iavarone, Alber, & Sassetti, 2014; C. M. Kang et al., 2005). This could result in the simultaneous activation of several signaling networks. The following paragraphs will aim to provide a detailed overview about the different physiological roles of bacterial STKs.

### 1.2.7.3.6.1. Interaction with two component systems

STKs help mediate several transcriptional effects by direct interaction with two component systems. Despite certain sensor histidine kinases being affected by STKs, this section will focus exclusively on the effects of STKs on response regulators (Jers, Kobir, Søndergaard, Jensen, & Mijakovic, 2011). The *M. tuberculosis* response regulator, DosR plays a key role in hypoxic response. It does so by binding specific hypoxic genes through the winged helix-turn-helix (HTH) motif on its C terminal (H.-D. Park et al., 2003). The transcription of several DosR regulons was found to be improved upon phosphorylation by its sensor histidine kinase, DosK. Studies have shown that DosR is also capable of being phosphorylated by the STK, PknH on a specific threonine residue. The above two phosphorylation events both cumulatively increase the binding of DosR to the promoter region of a DosR regulon, *hspX* (Chao et al., 2010). The aforementioned type of cumulative effect is not always the case. In *Streptococcus agalactiae*, phosphorylation of the response regulator, CovR by the serine/threonine kinase, Stk1 significantly reduces phosphorylation on the aspartate residue by its sensor histidine kinase, CovS and vice versa (W. J. Lin et al., 2009).

The VraR/VraS TCS in *Staphylococcus aureus* is responsible for conferring resistance to vancomycin. Phosphorylation of the response regulator, VraR by VraS results in a marked increase in expression of certain genes involved in cell wall synthesis. This phosphorylation mechanism results in several conformational changes in the structure of VraR including the opening of a hydrophobic pocket which promotes dimerization of the DNA binding domain (P. G. Leonard, Golemi-Kotra, & Stock, 2013). VraR has also been shown to be phosphorylated by the serine/threonine kinase, Stk1 on four threonine residues, which negatively regulates DNA binding to its target promoters (Canova et al., 2014). On the flip side, phosphorylation of the response regulator, GraR, which is responsible for resistance to cationic antimicrobial peptides, on threonine

## Introduction

---

residues significantly increases binding to its targets, for instance, the *vraFG* operon (Fridman et al., 2013).

STKs have also been shown to compete with other proteins that bind to response regulators, thereby influencing their activity. For instance, the *Streptococcus pneumoniae* response regulator, RitR forms a complex with the phosphatase, PhpP, which enables interaction of the former with its target promoters. The serine/threonine kinase, Stk1 competes with the formation of this complex by phosphorylating RitR, thereby negatively regulating its activity (Ulijasz, Falk, & Weisblum, 2009).

### 1.2.7.3.6.2. Regulation of transcriptional factors

STKs can also directly phosphorylate transcriptional factors, thereby controlling their activity. For instance, the *M. tuberculosis* STK, PknL phosphorylates EthR, which, in turn transcriptionally represses the enzyme, EthA (Leiba et al., 2014). This enzyme is required for the formation of the active metabolite of the anti-tubercular drug, ethionamide (ETH) and is thereby involved in mediating resistance. This phosphorylation event on EthR occurs on both serine and threonine residues and reduces its DNA binding activity, thus impacting resistance to ETH. Phosphorylation of transcriptional regulators can have different effects on different promoters. This can be seen in the case of the *S. aureus* global transcriptional factor, MgrA, which controls the expression of a wide variety of genes involved in virulence and multidrug efflux pumps. The serine/threonine kinase, Stk1 has been found to phosphorylate MgrA on serine residues and this phosphorylation has opposing roles in the transcriptional activities of two genes, namely *norA* and *norB*, which are involved in multidrug resistance (Truong-Bolduc & Hooper, 2010).

The effects of STKs on transcriptional regulators are extremely specific to the kinase under question. For instance, the *S. aureus* transcriptional regulator SarA, which influences the expression of virulence factors has been shown to be phosphorylated by two different kinases, Stk1 and Stk2, the former phosphorylating primarily on threonine residues while the latter on serine residues. The two phosphorylation events have different effects on the activity of SarA in that phosphorylation by Stk1 increases its DNA binding ability whereas that by Stk2 markedly reduces the same (Didier et al., 2010).

STKs are also known to exert their effects on different components within the transcriptional machinery. One example is the *M. tuberculosis* alternative  $\sigma$  factor, SigH, which is known to regulate the expression of several genes involved in stress response.

The activity of SigH is controlled by the anti- $\sigma$  factor, RshA, which in turn was found to be phosphorylated by the STK, PknB on a specific threonine residue. This phosphorylation reaction results in a marked reduction of its interaction with SigH, thereby resulting in increased resistance to stress conditions (S. T. Park, Kang, & Husson, 2008). Another instance is the STK, PknD, which phosphorylates the anti-anti- $\sigma$  factor, Rv0516 (Hatzios et al., 2013).

### 1.2.7.3.6.3. Regulation of protein synthesis

In 1993, the first evidence of phosphorylation within the translational machinery was shown. The elongation factor, EF-Tu, which is responsible for the binding of an aminoacyl tRNA on to the ribosome was found to be phosphorylated in *Escherichia coli* both *in vivo* and *in vitro* (Lippmann et al., 1993). In *Thermus thermophilus*, where once again EF-Tu was found to exist in a phosphorylated state, the modified residue was found to be threonine. Ever since, several phosphoproteomics studies have reported phosphorylated EF-Tu across a broad spectrum of bacterial species (Holub, Bezoušková, Kalachová, & Weiser, 2007; Sajid et al., 2011). In *M. tuberculosis*, the phosphorylation of EF-Tu by the STK, PknB on both serine and threonine residues was found to abrogate its interaction with GTP. Another example of the effect of STKs on protein synthesis is the phosphorylation of the *Bacillus subtilis* GTPase CpgA, which plays a key role in the final stage of assembly of the smaller ribosomal subunit. (Absalon et al., 2009). This phosphorylation event, enabled by the STK PrkC, primarily occurs on threonine residues and significantly increases the GTPase activity of the protein (Pompeo et al., 2012).

### 1.2.7.3.6.4. Roles in cell wall synthesis

STKs play key roles in regulation of cell wall metabolism and synthesis. An example of this is the *Streptococcus pneumoniae* kinase, StkP, which was found to phosphorylate the phosphoglucosamine mutase, GlmM. This is essential for the formation of UDP-N-acetylglucosamine, an important precursor for the formation of components of the cell envelope (Nováková et al., 2005).

One way through which mycobacteria evade host anti-inflammatory responses is through arabinosylation of one of their cell wall glycolipids, lipomannan. In *M. tuberculosis*, this reaction is catalyzed by an enzyme, encoded by the gene *embC*, which in turn exists in an operon with two other genes, *embA* and *embB*. These three genes

## Introduction

---

are in turn regulated by the regulator, EmbR, which is phosphorylated by the STK, PknH. This phosphorylation reaction increases the binding of EmbR to the promoter of the aforementioned *embCAB* operon, thereby positively regulating the expression of the three genes (K. Sharma et al., 2006).

Another example is the C terminal PASTA domains of the *M. tuberculosis* STK, PknB, which is capable of binding to muropeptides. This binding event was found to depend on the residue at the third position of the stem peptide (Mir et al., 2011) and was responsible for the localization of PknB to areas of high peptidoglycan hydrolysis, namely the mid-cell position and to a certain extent, the poles. A more recent example is that of the *S. aureus* kinase/phosphatase pair Stk/Stp. Deletion of the phosphatase resulted in a significantly thicker cell wall with a reduced susceptibility to the endopeptidase, lysostaphin. More significantly, the kinase, Stk was found to phosphorylate FemX that, alongside proteins FemA and FemB, is responsible for the formation of the critical pentaglycine interpeptide bridge within the lipid II molecule, thus contributing to cell wall integrity (Jarick et al., 2018).

### **1.2.7.3.6.5. Roles in cell morphology, division and development**

Serine/threonine kinases have very important roles in cell morphogenesis and developmental processes. An example is the *M. xanthus* kinase, Pkn14 which was found to phosphorylate the transcription factor, MrpC that in turn controls expression of the fruiting body formation gene, *fruA*. Phosphorylation of MrpC was found to greatly reduce binding to its target promoters (Nariya & Inouye, 2006). Some STKs play a role in cell division by directly phosphorylating the essential protein, FtsZ. For instance, the *M. tuberculosis* STK, PknA was found to phosphorylate FtsZ on threonine residues (M. Thakur & Chakraborti, 2006). This reaction affected both the GTPase and polymerization activities of FtsZ. Furthermore, overexpression of PknA resulted in the formation of elongated cells, pointing towards a defect in septum formation. Another example is the *S. pneumoniae* kinase, StkP which was found to localize to the septum. Deletion of the kinase resulted in marked chaining of cells and this effect was dependent on the catalytic N terminal as well as the C terminal PASTA domains. The cell morphology and chromosome segregation determinant, DivIVA was found to be one of the substrates of Stk1 (Fleurie et al., 2012). Interestingly, more recent phosphoproteomics studies have revealed phosphorylation of the essential cell division proteins, DivIVA and MinD by the kinase, PtkA in *B. subtilis* (Garcia-Garcia et al., 2016).



The role of STKs in germination and sporulation has been well investigated, especially in *B. subtilis*. In this gram-positive bacterium, the peptidoglycan from vegetative cells was found to induce germination of spores in a PrkC-dependent manner. As in the case of the protein, PknB of *M. tuberculosis*, the *B. subtilis* kinase PrkC consists of PASTA domains within its C terminal that were required for binding to peptidoglycan and its hydrolysis products (muropeptides), in a site-specific manner (Shah, Laaberki, Popham, & Dworkin, 2008). Upon binding to these peptidoglycan fragments, PrkC becomes activated and stimulates the expression of both EF-G and the peptidoglycan hydrolase, YocH which probably induce germination and the production of more muropeptides, respectively (Shah & Dworkin, 2010) (Figure 6).

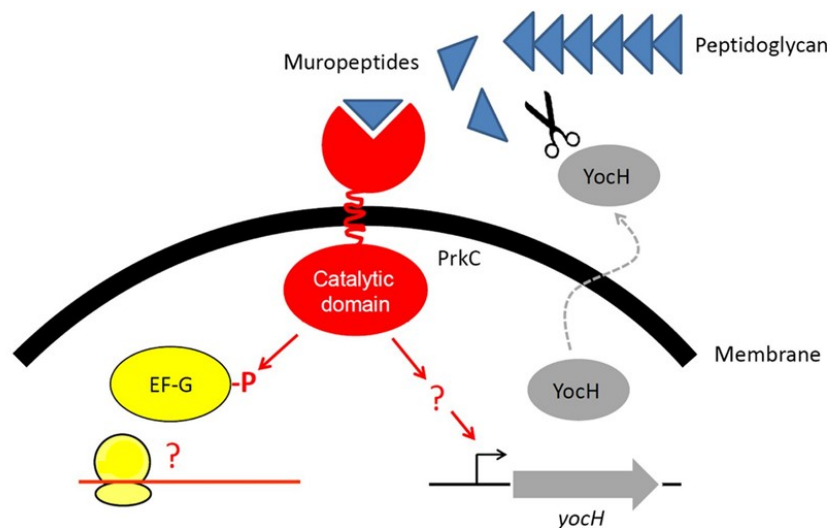


**Figure 6. The *B. subtilis* PrkC plays a role in sporulation and germination.** Peptidoglycan fragments (muropeptides, blue) resulting from a growing cell bind to the PASTA domain of PrkC (red). This results in activation of the kinase, which then phosphorylates several substrates including EF-G (yellow) and YocH (grey). Adapted from (Cousin et al., 2013).

STKs have also been implicated in cell repair. For instance, autophosphorylation of the *B. subtilis* kinase YabT was strongest in the presence of ssDNA (single stranded DNA). Activated YabT could in turn phosphorylate the DNA repair protein, RecA, resulting in its activation and the subsequent formation of multiple RecA foci to counter DNA damage (Bidnenko et al., 2013).

The effect of STKs on cell morphology is evident from the *M. tuberculosis* kinase, PknE. Deletion of this kinase results in a severe reduction in growth of the bacterium and also induces a change in colony morphology. Alongside these effects, other phenotypes were observed including increased resistance to the cell wall solubilizing detergent, SDS

(sodium dodecyl sulphate) and increased pathogenicity in guinea pigs (Kumar, Palaniyandi, Challu, Kumar, & Narayanan, 2013).

### 1.2.7.3.6.6. Roles in central metabolism

Just as in the case of eukaryotes such as yeast (Oliveira et al., 2012), bacterial STKs have significant roles in carbon metabolism. In fact, a range of phosphoproteomics studies have now been performed in several bacterial species and among the vast number of phosphorylated peptides detected, majority are predicted to be implicated in carbon metabolism (Bendt et al., 2003; Lima et al., 2011; Macek, Gnad, et al., 2007; Macek, Mijakovic, et al., 2007; Schmidl et al., 2010). An example of this is the *M. tuberculosis* kinase PknG, the deletion of which results in significantly lower *de novo* synthesis of glutamine (Cowley et al., 2004). Yet another instance is regulation of the catabolite repression regulator, CcpA in *S. aureus*. This protein was found to be phosphorylated by the kinase, Stk1 on threonine residues (Leiba et al., 2012). This phosphorylation event inactivates the protein and results in severe impairment in DNA binding. Phosphorylation of certain metabolic enzymes has also been reported. The *M. tuberculosis* kinase, PknF was found to efficiently phosphorylate the cyclopropane synthase, PcaA at two threonine residues (Corrales et al., 2012). This phosphorylation resulted in a defective cell wall, due largely to the altered production of mycolic acid. It also caused a marked reduction in the phagosome maturation block response, which involves binding of mycobacteria to phagosomes, thereby preventing their maturation into lysosomes.

The Gram-positive bacterium, *Streptomyces coelicolor* has been known to produce several secondary metabolites, including the pH-sensitive blue pigmented antibiotic namely actinorhodin. One of the key regulatory proteins which controls secondary metabolism, namely, AfsR has been shown to be phosphorylated by the kinase, AfsK (Atsushi, Soon-Kwang, Hiroshi, Sueharu, & Teruhiko, 1994). AfsR comprises of DNA-binding and nucleotide-binding domains and phosphorylation by AfsK increases its DNA binding ability, in a manner that is independent of its ATPase activity (Lee, Umeyama, & Horinouchi, 2002). Intriguingly, the gene upstream of *afsK* encodes the protein, KbpA that represses actinorhodin production. KbpA exerts this inhibitory action by interacting with the unphosphorylated form of AfsK and thereby preventing its

autophosphorylation and eventual phosphorylation of AfsR (Umeyama & Horinouchi, 2001).

### 1.2.7.3.6.7. Roles in virulence and pathogenicity

STKs play important roles in virulence among several bacterial species. For instance, the *M. tuberculosis* kinase, PknG is required for pathogenicity, as its deletion resulted in significantly reduced survival of the bacterium in mice (Cowley et al., 2004). Further instances come from studies on *S. agalactiae* or Group B Streptococcus (GBS), which are one of the leading causes of invasive bacterial infections, especially in infants. One of the key determinants for the virulence of GBS is the surface-associated toxin,  $\beta$ -haemolysin/cytolysin ( $\beta$ H/C). The kinase, Stk1 has been shown to be important for the survival of the pathogen and in the absence of Stk1,  $\beta$ H/C activity was found to be considerably reduced. This occurs through Stk1-mediated phosphorylation of CovR, a negative regulator of *cylE*, the gene encoding  $\beta$ H/C (Rajagopal, Vo, Silvestroni, & Rubens, 2006). It is interesting to note that CovR exists as part of a TCS and is phosphorylated by its sensor kinase, CovS. However, this activity is greatly reduced in the presence of Stk1-mediated threonine phosphorylation of CovR (W. J. Lin et al., 2009).

One of the main routes through which bacteria exert their pathogenicity is by interfering with host immune responses. Several studies have now implicated STKs in host-pathogen interactions. A widely studied example comes from the *Yersinia* kinase, YpkA (or YopO) which is secreted into host cells and is an essential virulence determinant (Cornelis et al., 1998). YopO was found to interact with two Rho GTPases, namely RhoA and Rac1 without any preference for the GTP bound or the GDP bound forms negating the possibility that it acts as a guanine exchange factor (GEF). These two proteins function as molecular switches that are required for several cellular signaling functions within the host (Barz, Abahji, Trülsch, & Heesemann, 2000). Furthermore, YpkA has been shown to be activated by the host protein, actin and it exerts its activity by disrupting the formation of the cytoskeleton. This could happen through the YpkA-mediated phosphorylation of the deubiquitinating enzyme, namely otubain 1, which in turn has been found to interact with actin (Juris, Shah, Shokat, Dixon, & Vacratsis, 2006).

STKs have also been found to interfere with the signaling pathways of the host system, resulting in an attenuation of the inflammatory response. This is once again evident from YpkA, which was found to phosphorylate a G-protein subunit namely,  $G_{\alpha q}$ , which is involved in the activation of the Rho GTPase, RhoA. This phosphorylation event, which happens on a single serine residue, inhibits the activity of the G-protein subunit (Navarro et al., 2007). As a result of this, the entire GPCR signaling cascade that is stimulated by this subunit is also severely affected. This can be seen through the loss of nuclear localization of the transcription factor, *tubby* in host cells. Yet another widely used signaling mechanism within the host involves the NF- $\kappa$ B family of transcription factors that activate several genes. NF- $\kappa$ B is usually kept in check within the cytoplasm by association with the I $\kappa$ B family of inhibitors and this inhibition is lifted by phosphorylation, followed by ubiquitination and eventual degradation of the proteins. This results in the release of NF- $\kappa$ B whereby it translocates to the nucleus and results in the activation of its downstream targets. STKs have been found to interfere with the aforementioned NF- $\kappa$ B signaling pathway. This can be seen in the case of the pathogenic bacterium *Shigella flexneri* that causes shigellosis, which results in destruction of the colonic epithelium. Among the effectors released into the host upon infection is the kinase, OspG, which was found to bind to a family of ubiquitin-conjugating enzymes that are responsible for the ubiquitination and degradation process of the NF- $\kappa$ B inhibitors, as mentioned above (D. W. Kim et al., 2005). Accordingly, deletion of the kinase resulted in a significantly higher inflammatory response, as a result of higher rates of degradation of I $\kappa$ B $\alpha$  (which is part of the I $\kappa$ B family of inhibitory proteins).

There are also instances of STKs that induce host signaling pathways and could therefore be used as potential targets for drug therapy. This can be seen from studies on the pathogenic organism, *Legionella pneumophila*, the main cause of Legionnaire's disease. Among the effectors that are secreted by this bacterium into the host, the putative kinase LegK1 was found. This effector stimulated phosphorylation of the inhibitor, I $\kappa$ B $\alpha$  on serine residues, thereby resulting in induction of the NF- $\kappa$ B signaling pathway (Ge et al., 2009). Interestingly, this phosphorylation event did not require prior phosphorylation of the residues present within the activation loop.

### 1.2.7.4. Dual specificity protein kinases

Several eukaryotic protein kinases were found to autophosphorylate on serine/threonine and tyrosine residues (Ben-David, Letwin, Tannock, Bernstein, & Pawson,

1991; Howell et al., 1991). This dual specificity of protein kinases was first discovered in the *S. coelicolor* kinase, AfsK, which was able to autophosphorylate on both serine and tyrosine residues (Atsushi et al., 1994). Another instance is the *Chlamydophila pneumoniae* kinase, PknD whose kinase domain was found to autophosphorylate on both threonine and tyrosine residues (D. L. Johnson & Mahony, 2007). However, in these examples, the kinases are still regulated through phosphorylation on serine or threonine residues within the activation loop. A breakthrough came in 2012 when the first novel tyrosine phosphorylation-regulated dual specificity protein kinase came into the fore. Two *Bacillus anthracis* kinases, PrkD and PrkG were characterized and their activities were regulated by phosphorylation on tyrosine residues. While both kinases were able to autophosphorylate on serine, threonine and tyrosine residues, only PrkG exhibited dual specificity with regards to substrate phosphorylation as well (Arora et al., 2012).

Given the widespread biological implications of protein kinases in bacteria and the advent of several advancements in phosphoproteomics applications, one can expect that these enzymes, particularly STKs, will soon be at the crux of several important signaling systems and protein-protein interaction networks. With the unraveling of several of these enzymes involved in pathogenicity, their attractiveness as drug targets has become more evident than before.

### 1.3. Transcription in bacteria

Transcription in bacteria occurs in three steps, namely initiation, elongation and termination. The main enzyme involved in the process of transcription is the RNA polymerase (RNAP). Of the three steps mentioned above, the most highly regulated one is transcription initiation. Initiation can in turn be viewed as a reaction that takes place in multiple steps. The first step involves binding of the RNAP to the promoter DNA resulting in a “closed” complex. This is followed by isomerization of this complex, aided by melting of the DNA at the transcription site giving rise to an “open” complex. Subsequently, RNA chain initiation ensues resulting in the formation of a dinucleoside tetraphosphate which is attached to the RNA polymerase-DNA complex. Elongation enables the addition of nucleoside monophosphate moieties to this complex at the 3' OH terminus (Walter, Zillig, Palm, & Fuchs, 1967).

#### 1.3.1. Components of the RNA polymerase

The RNA polymerase (minimal) core enzyme comprises of two  $\alpha$  subunits and one each of  $\beta$ ,  $\beta'$  and  $\omega$  subunits. Association of the  $\sigma$  subunit with the minimal enzyme results in the formation of the active holoenzyme. Among the above components of the enzyme, the smallest and the least well characterized is the omega ( $\omega$ ) subunit. In fact, even its identification as a subunit of the RNA polymerase was of much debate. However, once this was confirmed, it was found to be surface exposed and was hypothesized to have a role in interactions with transcriptional activators. It was also found to interact simultaneously with both the N and C terminals of the  $\beta'$  subunit and aid in maintaining its structure by facilitating proper folding. The  $\omega$  subunit also aids in formation of the active holoenzyme by enabling recruitment of the  $\beta'$  subunit to the intermediary  $\alpha_2\beta$  structure (Mathew & Chatterji, 2006) (Figure 7).

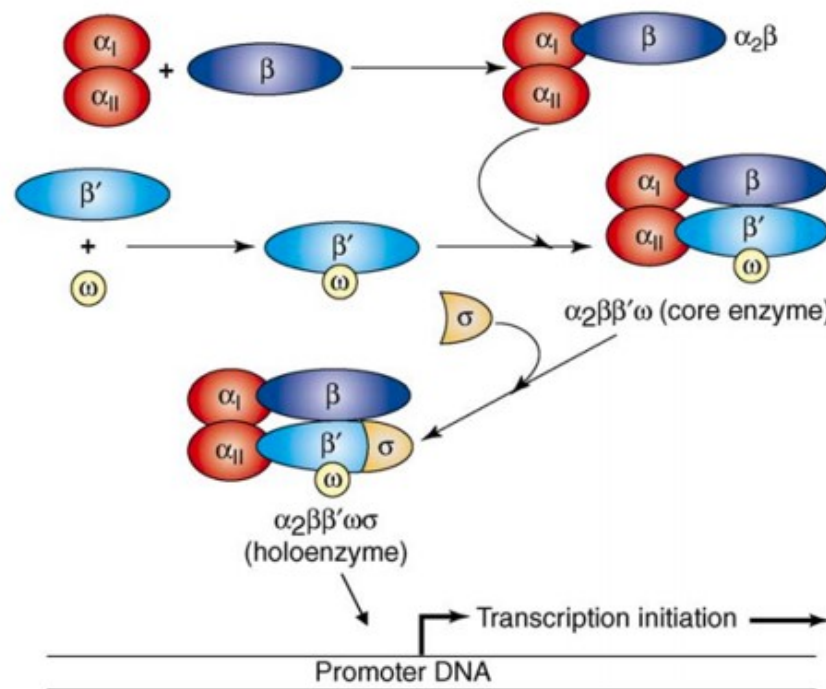


**Figure 7. Model depicting the assembly of the RNA polymerase holoenzyme.** Initiation of the assembly of RNAP occurs with the dimerization of two  $\alpha$  subunits. This dimer then interacts with the  $\beta$  subunit. This is followed by binding of both the  $\beta'$  and  $\omega$  subunits with the  $\alpha_2\beta$  complex, resulting in the formation of the core enzyme. Formation of the active holoenzyme requires association of the  $\sigma$  subunit ( $\sigma$  factor) with the core enzyme. Adapted from (Mathew & Chatterji, 2006).

### 1.3.2. Structural studies on the RNA polymerase

The very first study attempting to highlight the structural features of the RNAP shed light on the N-terminal dimeric  $\alpha$  subunit of *E. coli* (G. Zhang & Darst, 1998) and found that it was composed of two domains. Both these domains consist of a well conserved hydrophobic core. The part between the two domains was found to be composed of an extremely flexible linker rich in glycine and proline residues. A highly exposed loop containing conserved acidic residues enables interaction of the  $\alpha$  with the  $\beta$  subunit.

Crystallization of the RNAP of *Thermus aquaticus* revealed several details about some of the other subunits (ZHANG et al., 1999). The crab claw like structure of the enzyme was found to consist of two distinct arms with one containing the  $\beta$  and the other the  $\beta'$  subunit. Interactions between the different subunits occurs through their respective solvent exposed surfaces. Interactions between the  $\beta$  and  $\beta'$  subunit takes place at a cleft like region found at the base of the channel where the divalent  $Mg^{2+}$  ion is chelated.

## Introduction

---

This cleft was found to be the active site for catalysis and comprises of three highly conserved aspartate residues (ZHANG et al., 1999).

The  $\beta$  subunit was shown to be involved in several significant interactions: the N terminal region aiding in the formation of the intermediary  $\alpha_2\beta$ , the central region enabling the formation of the catalytic center by interacting with the  $\beta'$  component and the C terminal region, with help from the  $\omega$  subunit, in recruitment of  $\beta'$  into the intermediary  $\alpha_2\beta$  structure. In addition, other key features of these subunits were also revealed, namely the flexible flap like domain of the  $\beta$  component and the coiled coil structure of the  $\beta'$  subunit. The  $\beta'$  subunit was found to be composed of a zinc binding motif with highly conserved cysteine residues and a trigger loop/ helix which is essential for the addition of incoming nucleotides. These incoming nucleotides induce a structural transition, altering the tip of the helix from a flexible to a highly rigid structure. Additionally, the helical motif also divides the deep groove of the enzyme into two distinct channels namely the (primary) DNA-binding and the NTP (nucleoside triphosphate) entry channels (Murakami, 2015).

## 1.4. Sigma factors

### 1.4.1. Discovery and key features of $\sigma$ factors

For quite a while, it was assumed that no individual components could be separated from the RNA polymerase complex without altering its enzymatic activity. This assumption was challenged by a landmark study wherein researchers found a component, namely  $\sigma$  (referred to as the “sigma factor” or “ $\sigma$  factor” henceforth) that was found to associate with the RNA polymerase (Burgess, Travers, Dunn, & Bautz, 1969). Only the presence of this stimulating component could result in transcription of T7 DNA.

The  $\sigma$  subunit of the RNA polymerase was required during the initiation step of transcription. Once RNA synthesis begins, the  $\sigma$  subunit is released from the RNA polymerase holozyme and thereby is free to be bound by another minimal enzyme to perform transcription initiation elsewhere (Travers & Burgess, 1969). Sigma factors generally contain 4 regions, among which Regions 2 and 4 are highly conserved. These regions are further subdivided and are implicated in promoter recognition, DNA melting and binding to the RNA polymerase. The individual functions of the different subregions will be discussed elsewhere within this chapter (Section 1.4.5). Even though  $\sigma$  factors



interact with both the  $\beta$  and  $\beta'$  subunit of the RNA polymerase, they have a significantly higher affinity to the latter (Arthur & Burgess, 1998).

### 1.4.2. Sigma factors are important for promoter recognition

Upon comparison of several promoters from *E. coli*, a consensus sequence was identified based on homology. The main components of this consensus sequence were found to be the -10, -35 regions and the spacer in between them (positions relative to the transcription start site). It was also interesting that this obtained consensus sequence exhibited maximal promoter strength (McClure, 1985).

The characterization of  $\sigma$  factors in *E. coli* quickly revealed the presence of two distinct families, namely  $\sigma^{70}$  and  $\sigma^{54}$ . The primary or housekeeping  $\sigma$  factor i.e.,  $\sigma^{70}$  (whereby the number refers to the molecular weight of the  $\sigma$  factor) is encoded by the gene, *rpoD* (Harris, Heilig, Martinez, Calendar, & Isaksson, 1978). Surprisingly, several promoters in *E. coli*, which are recognized by this  $\sigma$  factor comprise of the highly conserved residues found within the -10 and -35 consensus sequence. This led to the discovery of one of the most important roles for  $\sigma$  factors namely, promoter recognition (Reznikoff, Siegele, Deborah, & Gros, 1985). In addition to  $\sigma$  factors, other components of the transcription machinery could also recognize these promoter regions. An example of this is transcriptional repressors; in this case, the RNA polymerase was found to be unable to bind to the promoter region unless the repressor was removed from its own recognition site on the promoter (Payankulam, Li, & Arnosti, 2010).

### 1.4.3. $\sigma^{54}$ family of $\sigma$ factors

The alternative  $\sigma$  factor that is largely responsible for the control of genes involved in nitrogen regulation was identified as  $\sigma^{54}$  or  $\sigma^N$  (Buck & Cannon, 1992). These  $\sigma$  factors are not essential for growth and can bind to the promoter even in the absence of the RNA polymerase enzyme (Cannon, Claverie-Martin, Austin, & Buck, 1993). It has to be noted that their affinity to the promoter is significantly enhanced in the presence of RNAP (Merrick, 1993). The most essential promoter elements for the  $\sigma^N$  family of  $\sigma$  factors are found in the -12 and the -24 elements of the promoter. One of the most important aspects of the  $\sigma^{54}$  family of  $\sigma$  factors that sets them apart from the  $\sigma^{70}$  family is that in the former, the formation of an open complex can only take place in the presence of an activator protein, which binds roughly 100 bp upstream of the transcription start site (Wösten, 1998). However, once this complex is formed, it can be maintained even

in the absence of activators (Bush & Dixon, 2012). As opposed to the  $\sigma^{70}$  family of  $\sigma$  factors,  $\sigma^N$  proteins comprise only three regions that are involved in both binding to the RNA polymerase and promoter recognition (Cannon, Gallegos, Casaz, & Buck, 1999).

### 1.4.4. $\sigma^{70}$ family of $\sigma$ factors

The discovery of the primary  $\sigma$  factor in *E. coli* ( $\sigma^{70}$ ) provided significant momentum in the field. It led to the discovery of additional  $\sigma$  factors in both *E. coli* and other organisms and these factors were found to have significant roles (Galibert et al., 2001; Green & Donohue, 2006; Gruber & Gross, 2003; Narberhaus, Krummenacher, Fischer, & Hennecke, 1997). For instance, the heat shock response in *E. coli* was conferred by the action of  $\sigma^{32}$  and this was found to show considerable homology with the C terminus of  $\sigma^{70}$  (Kourennaia, Tsujikawa, & DeHaseth, 2005). Studies in *B. subtilis* resulted in the identification of several  $\sigma$  factors (Haldenwang, 1995). The most abundant of these was found to be  $\sigma^{43}$ , which was encoded by the gene, *rpoD* and was responsible for the transcription of several genes during vegetative growth (Gitt, Wang, & Doi, 1985). The consensus promoter sequence that is identified by this  $\sigma$  factor-RNA polymerase holozyne (hereon, referred to as  $E\sigma$ ) was similar to that observed for  $\sigma^{70}$  in *E. coli* (Moran, Johnson, & Losick, 1982). Minor  $\sigma$  factors were also revealed including  $\sigma^{29}$ , which was the first of its kind to have a role in sporulation (NAKAYAMA, WILLIAMSON, BURTIS, & DOI, 1978).

#### 1.4.4.1. Classification of the $\sigma^{70}$ family

Sigma factors of the  $\sigma^{70}$  family were initially classified into the following groups (M. Lonetto, Gribskov, & Gross, 1992). Group I  $\sigma$  factors or the primary  $\sigma$  factors were found to be indispensable for the organism's survival. The  $\sigma$  factors belonging to this group show significant homology in the promoter regions/ sequences that they identify. The Group II  $\sigma$  factors comprise of proteins that show significant homology to Group I but were not found to be essential for growth. An example of this is the stationary phase  $\sigma$  factor in *E. coli* namely  $\sigma^S$ . Group III comprise of alternative  $\sigma$  factors whose expression is required during several stress conditions. These  $\sigma$  factors are often shorter than the primary  $\sigma$  factors. Group III includes  $\sigma$  factors that govern flagellar synthesis both in *E. coli* and *B. subtilis* such as  $\sigma^F$  for instance (Arnosti & Chamberlin, 1989). Group IV comprises of the most abundant  $\sigma$  factors belonging to the extracytoplasmic function (ECF) subfamily. While initial classification by Lonetto and colleagues placed them in Group III, it is now clear that these  $\sigma$  factors are divergent in sequence when compared

to the members of Group III and thereby, it is fitting that they be classified separately (Helmann, 2002). One of the principle differences between primary and alternative  $\sigma$  factors is that the latter are usually smaller in size and are recruited for specialized functions (Kazmierczak, Wiedmann, & Boor, 2005). The alternative  $\sigma$  factors can in turn be divided into several categories, key among these being the extracytoplasmic function (ECF)  $\sigma$  factors, which will be reviewed separately later.

### 1.4.5. The different regions of $\sigma$ factors

As mentioned previously, the different regions within  $\sigma$  factors can in turn be divided into subregions. Region 1, which is located at the N terminus is found in all primary  $\sigma$  factors can in turn be divided into 1.1 and 1.2. While subregion 1.1 is only found in primary  $\sigma$  factors, 1.2 has been shown to occur in both primary and alternative  $\sigma$  factors.  $\sigma_{1.1}$  was composed of four alpha helices and was surrounded by the following components: the  $\sigma_2$  subunit (Region 2), the  $\beta$  lobe, the  $\beta'$  clamp and the active site cleft (Murakami, 2013).  $\sigma_{1.1}$  has been shown to have an inhibitory effect on DNA binding, in that only interaction with the RNA polymerase exposes its DNA binding motifs (Dombroski, Walter, & Gross, 1993). This inhibitory effect is due largely to the association of subregion 1.1 with Region 4.  $\sigma_{1.2}$  has been implicated in interactions with the discriminator of the promoter. Instability in these interactions in turn destabilizes the open complex (Tare, Mallick, & Nagaraja, 2013).

Region 2 is usually divided into 4 subregions (Helmann & Chamberlin, 1988). This region was found to be composed entirely of alpha helices and its shape resembles that of a V and consists of two distinct motifs (Malhotra, Severinova, & Darst, 1996), one of which appears to be involved in promoter recognition and DNA melting to form the open complex and the other in interaction with the core enzyme (Lesley & Burgess, 1989). Subregions 2.1 and 2.3 have roles in DNA melting, while 2.4 is involved in recognition of the -10 promoter region. The existence of another region immediately after 2.4 but before 3 (the so-called subregion 2.5) has been shown and this contains a highly conserved histidine residue. It has been implicated in binding to regions near -10 especially in instances wherein the promoters are very large (Barne, Bown, Busby, & Minchin, 1997).

Region 3, which is in turn divided into subregions 3.1 and 3.2, constitutes one of the most weakly conserved regions and is only found in primary  $\sigma$  factors (Nagai, Shimamoto, & Ishihama, 1997). On the other hand, region 4 is very highly conserved

among  $\sigma$  factors and can in turn be divided into 4.1 and 4.2 (Nagai et al., 1997). It has been hypothesized that subregion 4.1 takes part in the transcription initiation process by binding to certain activators (M. Li, Moyle, & Susskind, 1994). The C terminal which comprises of subregion 4.2 recognizes the -35 region of the promoter through its helix-turn-helix (HTH) motif (Dove, Darst, & Hochschild, 2003).

### 1.4.6. Interaction of the $\sigma$ factor with the RNA polymerase

Both regions 2 and 4 were found to be responsible for interactions with the RNA polymerase enzyme. In fact, interactions with the enzyme is necessary for the  $\sigma$  factor to discern the spacing between the -10 and -35 promoter elements (Yeh et al., 2011). Interactions between  $\sigma_{2.3}$  and the minimal enzyme depend on a conserved stretch of 13 amino acid residues, termed as the RpoD box (Tanaka, Shiina, & Takahashi, 1988).

The coiled coil structure of the  $\beta'$  component interacts with the alpha helices of subregion 2.2 (Arthur & Burgess, 1998; Vassilyev et al., 2002). While the above interaction interface is surface exposed, the interactions between the zinc binding domain and residues within  $\sigma_{3.1}$ - $\sigma_{4.2}$  are masked by  $\sigma_{1.1}$  and only become exposed during initiation of transcription (Gruber et al., 2001). Interaction of  $\sigma_{2.2}$  with the coiled coil motif of  $\beta'$  is essential for the selective binding of the  $\sigma$  factor to the nontemplate DNA strand (B. A. Young et al., 2001). The polar residues within the amphipathic helix of  $\sigma_{2.2}$  that are involved in this above interaction are occluded by the loop between subregions 1.2 and 2.1. This occlusion is lifted and the corresponding binding motifs are exposed upon formation of a closed complex (B. A. Young et al., 2001). Additionally, subregions 2.1 and 2.2 exhibit extensive interactions with the clamp helices of the  $\beta'$  subunit and this interaction was found to be dependent on a stretch of conserved residues (DAEDLXQETF) within the proximal region of subregion 2.2 (Lane & Darst, 2010). Strikingly, a previous study had implicated a single amino acid within the subregion 2.2 of *E. coli*  $\sigma^{32}$  in interaction with the clamp helices of the  $\beta'$  subunit of the RNAP (Joo, Ng, & Calendar, 1997).

The flexible flap domain of the  $\beta$  subunit is required for appropriate positioning of  $\sigma_{4.2}$  within the RNA polymerase holozyeme. Unavailability of the flap domain of the RNAP causes subregions 2.4 and 4.2 to move away from one another, thereby preventing simultaneous recognition of both the -10 and -35 promoter elements (Kuznedelov et al., 2002). An additional allosteric switch is provided by interactions between region 4 and the flap tip helix domain of the  $\beta$  subunit, which in turn is dictated by the flexibility of the

helix. This contact with  $\beta$ , which was dependent on the residues within the hydrophobic core, is also required for engagement with the -35 region of the promoter (Geszvain, Gruber, Mooney, Gross, & Landick, 2004).

Subregion 1.1 positions itself initially within the active site cleft through its highly acidic residues. It is then duly displaced from this cleft upon the formation of the open complex. The part between regions 3 and 4 is composed of a flexible hairpin-like loop (or subregion 3.2), also known as the  $\sigma$  finger, which assists the enzyme in binding to its substrate (Feklístov, Sharon, Darst, & Gross, 2014). The C terminal domain of the  $\alpha$  subunit of the RNAP interacts with region 4 of the  $\sigma$  subunit. The orientation of this binding interface changes upon the binding of certain transcriptional activators such as the cAMP receptor protein (CAP) (Liu, Hong, Huang, & Yu, 2017). Figure 8 provides a brief schematic design of the different regions of  $\sigma$  factors and their broad roles in promoter recognition and interaction with the RNAP.

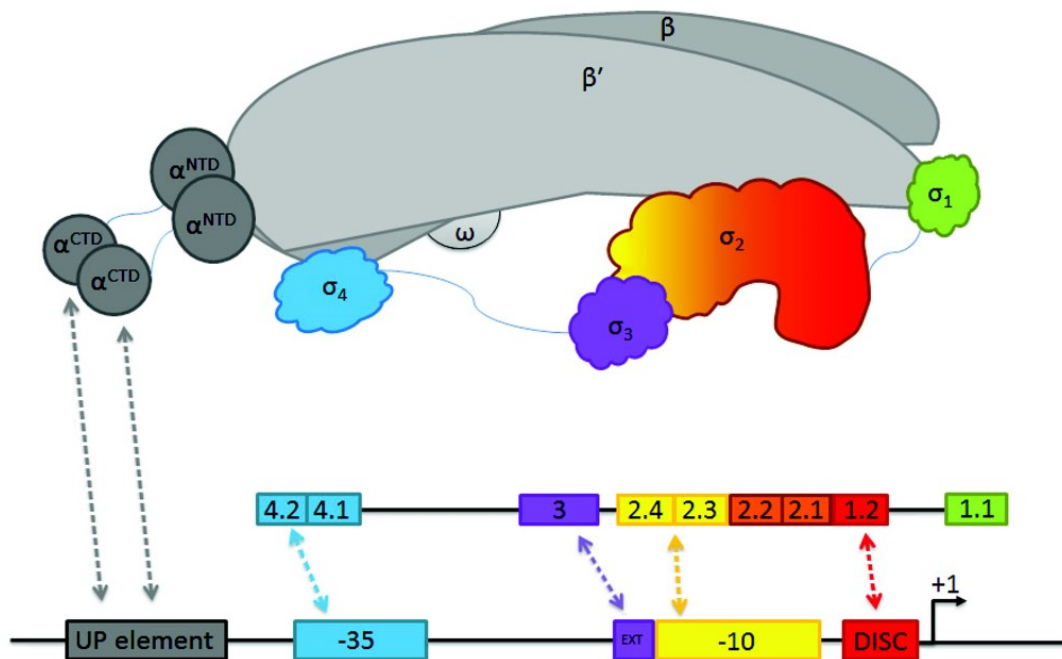


**Figure 8. Schematic overview of the roles of different  $\sigma$  regions.** Sigma factors have four regions, among which regions 2 and 4 are significantly involved in interactions with the  $\beta'$  and  $\beta$  subunits of the RNAP, respectively. The 4 regions of  $\sigma$  factors can in turn be divided into subregions and these are involved in recognition of distinct parts of the promoter, as shown by the dotted arrows. Adapted from (Davis, Kesthely, Franklin, & MacLellan, 2016).

### 1.4.7. Molecular dynamics enabling promoter recognition and melting by $\sigma$ factors

Studies on the primary  $\sigma$  factor,  $\sigma^A$  of *T. aquaticus* highlighted several key residues involved in promoter recognition (Campbell et al., 2002). A striking observation was that in the case of specialized extended promoters, transcription initiation could be induced with just regions 2 and 3 of the  $\sigma$  factor. In all other cases, interaction of the HTH motif of subregion 4.2 with the phosphate backbone requires bending of the DNA molecule. In the case of the template strand, this is facilitated by the presence of water molecules. This was dependent on a conserved arginine residue (R409) that binds the DNA at position -31 through hydrogen bonds. Interestingly, a previous study had revealed that mutation of this residue resulted in considerably decreased expression from the promoter (Siegele, Hut, & Walter, 1989). In addition, a conserved glutamine residue (Q414) was also found to interact with the -35 promoter element on the nontemplate strand through hydrogen bonds. The hydrophobic pocket of region 4, which participates in binding with RNAP is buried deep inside its concave structure.

In order to better understand the molecular mechanism behind promoter selectivity of the *T. aquaticus*  $\sigma$  factor,  $\sigma^A$ , crystallization studies were performed with an 11mer synthetic DNA fragment comprising the -10 region (Feklistov & Darst, 2011). A vast majority of the interactions between ssDNA and the  $\sigma$  factor take place in subregions 2.1 and 2.3. This occurs through the aromatic amino acids found within this region. In fact, mutations of some of these amino acids result in severe impairment in the ability of the  $\sigma$  factor to form closed complexes (Juang & Helmann, 2002). The nucleotide, T<sub>-12</sub> was found to make contacts with the highly conserved tryptophan dyad of  $\sigma_2$  through Van der Waal's interactions. While W256 interacts with the deoxyribose chain of the nucleotide, W257 interacts with the pyrimidine ring.

Region 2 has also been implicated in DNA melting with the nucleotide at position -11 (A<sub>-11</sub>) – also referred to as the “master nucleotide” – playing a major role in the process. The first tryptophan of the aforementioned dyad, W256 interacts with A<sub>-11</sub> and places itself in the region whereby this nucleotide would interact with the one downstream at position -12. The net effect of this placement of the tryptophan dyad is the flipping out of the A<sub>-11</sub> base and its subsequent burial within a hydrophobic protein pocket. This protein pocket is highly specific to the nucleotide under question. A second flipping mechanism ensues further upstream at the -7 (T<sub>-7</sub>) position. This occurs with the help of two residues, namely T255 and R259 which, just like the W256 residue, ensure

that the base stack does not continue downstream. This results in flipping out of the T<sub>-7</sub> base and eventually, accommodating it within yet another protein pocket that is formed by subregions 1.2, 2.1 and 2.3 of the  $\sigma$  factor. This protein pocket is quite different from the A<sub>-11</sub> protein pocket, in that it is significantly bigger and more importantly, is hydrophilic in nature and is thereby able to accommodate water molecules that aid in interaction with the nucleotide. An important observation here is that recognition of the -10 promoter region occurs only upon initiation of strand separation. The aforementioned results are simplified in the illustration presented in Figure 9.

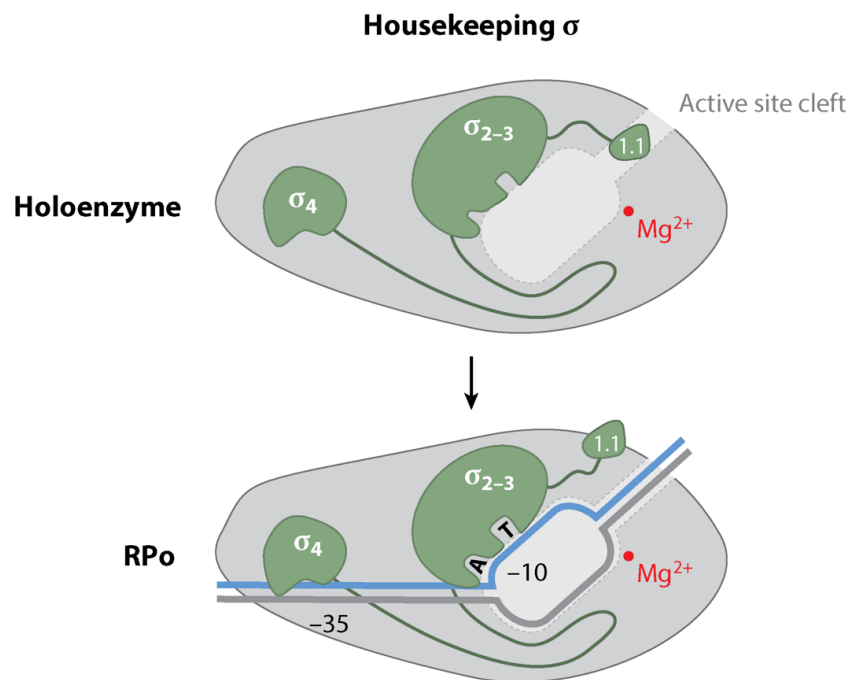


**Figure 9. Promoter recognition by primary  $\sigma$  factors in complex with the RNAP.** The above illustration is based on molecular details revealed for the *T. aquaticus* primary  $\sigma$  factor,  $\sigma^A$ . Promoter melting is established by the  $\sigma$  factor (green) through the flipping of two nucleotides within the -10 region of the promoter, namely A<sub>-11</sub> and T<sub>-7</sub> and inserting them into specific protein pockets. This occurs in the RPo conformation (bottom panel). Nonspecific base interactions are prevented by subregion 1.1 (upper panel), which is displaced upon entry of the promoter DNA. Adapted from (Feklistov et al., 2014).

### 1.4.8. ECF sigma factors

#### 1.4.8.1. Identification of ECF $\sigma$ factors

Identification of ECF  $\sigma$  factors came forth through transcriptional studies on the *dagA* gene in *Streptomyces coelicolor*. This bacterium was capable of using agar as its sole carbon source and the product of the *dagA* gene, namely extracellular agarase, was essential for hydrolysis of agar. Transcription initiation of this gene was found to happen at four distinct promoter sequences (Buttner, Fearnley, Bibb, Lane, & Nr, 1987). Different RNA polymerase holozyne complexes were involved in transcription from the

aforementioned promoters. The transcription of one of these promoters, namely p2, was dependent on association of a novel  $\sigma$  factor with the RNA polymerase (Buttner, Smith, & Bibb, 1988). This  $\sigma$  factor was designated as  $\sigma^E$  and was found to belong to an entirely new family referred to as extracytoplasmic function (ECF)  $\sigma$  factors (M. A. Lonetto, Brown, Rudd, & Buttner, 1994). These sigma factors were considerably smaller than primary  $\sigma$  factors, in that they only contained regions 2 and 4, thereby keeping the -10 and -35 promoter recognition elements intact. As the name implies, these proteins were found to regulate genes involved in extracytoplasmic functions (Brooks & Buchanan, 2009; Helmann, 2002; Missiakas & Raina, 1998).

The aforementioned identification spurred the discovery of several ECF  $\sigma$  factors in many different organisms. For example,  $\sigma^X$  of *B. subtilis* was required for peroxide stress and also transcription of genes that govern survival of the bacteria at higher temperatures (Xuejun Huang, Decatur, Sorokin, & Helmann, 1997). So far, seven ECF  $\sigma$  factors have been found in the genome of *B. subtilis* (Helmann, 2016). Another example is the bacterium *S. aureus*, which encodes four  $\sigma$  factors, out of which one of them, namely  $\sigma^S$  was found to belong to the ECF family (Arbade, 2017). Inactivation of this  $\sigma$  factor was found to significantly reduce viability of the bacteria (Shaw et al., 2008). While certain ECF  $\sigma$  factors have basal expression even in the absence of stresses, some others are not expressed under standard growth conditions and are recruited only upon encountering certain stresses. This can be seen in the cases of the *B. subtilis* factor,  $\sigma^Z$  and also the *S. aureus* factor mentioned above,  $\sigma^S$  (Arbade, 2017; Horsburgh, Thackray, & Moir, 2001).

### 1.4.8.2. Principle roles of ECF $\sigma$ factors

Just like primary  $\sigma$  factors, one of the principle roles of ECF  $\sigma$  factors includes promoter recognition and this occurs only upon the formation of the RNAP holozyme. Several studies have been carried out in an attempt to predict promoter elements that are recognized by ECF  $\sigma$  factors. An example is  $\sigma^E$  of *E. coli*, which was found to recognize an extended regulon that is highly conserved in nine different genomes and was found to contain key players in the assembly of the lipopolysaccharide (LPS) layer (Rhodius, Suh, Nonaka, West, & Gross, 2006). There are also several cases wherein the  $\sigma$  factors show considerable overlap in promoter selectivity. This can be seen in the case of the *B. subtilis*  $\sigma$  factors,  $\sigma^W$  and  $\sigma^X$  (Xuejun Huang, Fredrick, & Helmann, 1998). This results in overlapping stress responses and thereby, makes it difficult to distinguish the exact roles of each individual factor (Raivio & Silhavy, 2002). ECF  $\sigma$  factors exhibit



two distinct features: positive autoregulation and regulation by anti- $\sigma$  factors, which are usually co-transcribed alongside the  $\sigma$  factor (Helmann, 2002). However, it is now known that this is not the only means by which their activity can be regulated and this will be discussed in greater length elsewhere in this chapter (Section 1.4.8.4).

### **1.4.8.3. Interactions of the ECF $\sigma$ factor with the promoter DNA and the RNA polymerase**

The interaction interfaces between the RNA polymerase and ECF  $\sigma$  factors are essentially homologous to the ones that were discussed previously for primary  $\sigma$  factors. This could be attributed to the significant conservation of RNAP subunits and the interacting interface of  $\sigma$  factors that are involved in RNAP core binding (Sharp et al., 1999; Werner & Grohmann, 2011a). Recent structural studies on the *M. tuberculosis*  $\sigma$  factor,  $\sigma^L$  show that just as in the case of primary  $\sigma$  factors, the linker between regions 2 and 4 of the  $\sigma$  factor enters the active site cleft of the RNA polymerase wherein it encounters the ssDNA and exits through the RNA-exit channel. Upon the nascent RNA reaching a length beyond 5 nucleotides, displacement of this linker is essential for transcription to continue (W. Lin et al., 2019). Interestingly, as opposed to the mechanism found for primary  $\sigma$  factors,  $\sigma^L$  plays a role in recognition of the -10 promoter region by the flipping of nucleotides at three different positions and eventually, inserting them in different protein pockets. As supported by earlier observations (Sébastien Campagne, Marsh, Capitani, Vorholt, & Allain, 2014), the loop within region 2 – loop L3 – was found to be the one that was primarily involved in creation of the protein pocket into which the “master nucleotide” was inserted (W. Lin et al., 2019). Interaction between the RNA polymerase and the linker between regions 2 and 4 was also shown in the case of the ECF  $\sigma$  factor,  $\sigma^H$  of *M. tuberculosis* (L. Li, Fang, Zhuang, Wang, & Zhang, 2019). This study also showed that subregion 2.1 – more specifically, the distal end of its alpha helix – interacts with the discriminator of the promoter.

### **1.4.8.4. Regulation of ECF $\sigma$ factors**

ECF  $\sigma$  factors are usually retained in an inactive state until the bacteria encounter certain stresses/ external stimuli. The most common mechanism of regulation involves the sequestration of these  $\sigma$  factors into complexes with anti- $\sigma$  factors that in turn prevents their interaction with the RNAP and subsequently, transcriptional regulation of genes (M. S. Paget, 2015; Treviño-Quintanilla, Freyre-González, & Martínez-Flores, 2013). Upon sensing particular stimuli, this inhibitory effect is alleviated (through

## Introduction

mechanisms which will be explained in detail in the upcoming paragraphs) and the ECF  $\sigma$  factors proceed to regulate the transcription of specific stress response genes (Brooks & Buchanan, 2009). Regulation through the action of anti- $\sigma$  factors is not the only means by which ECF  $\sigma$  factors are controlled. There are several other mechanisms of regulation, which will be discussed in detail in this section.

### 1.4.8.4.1. Regulated proteolysis

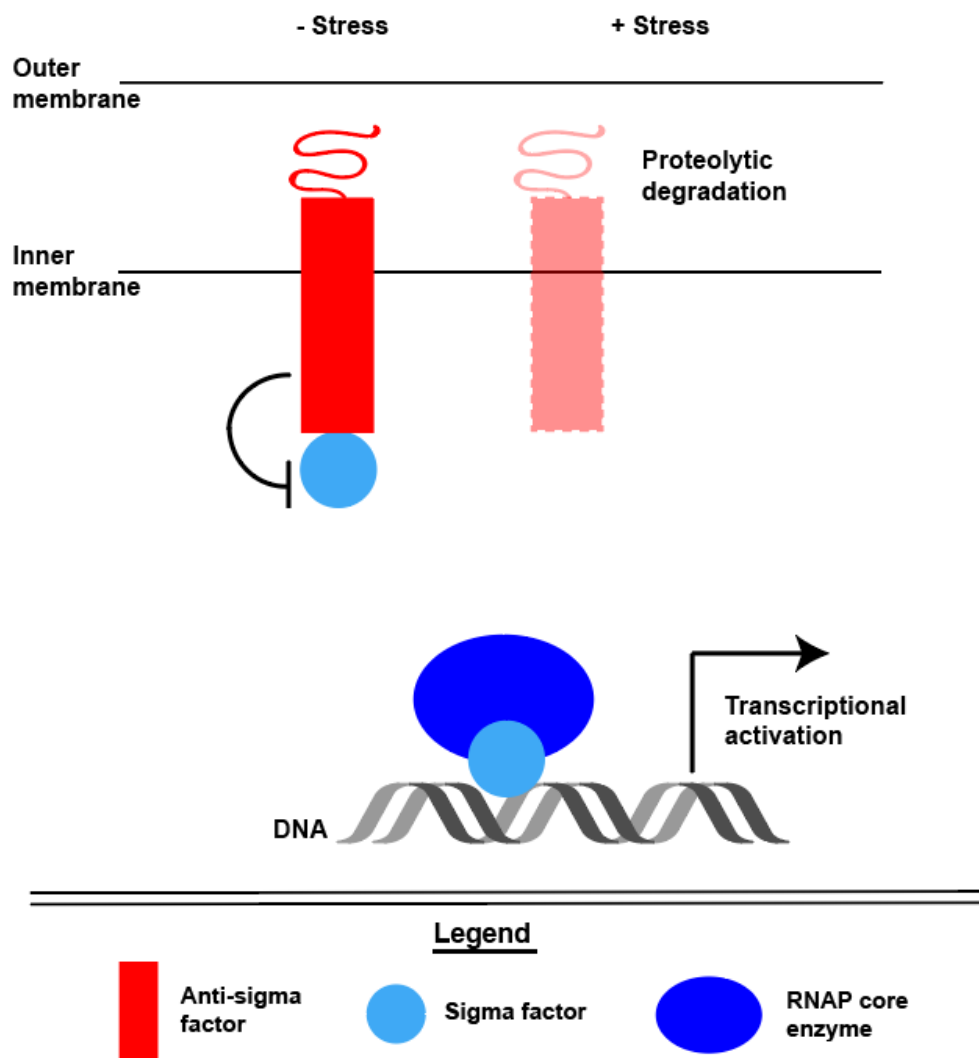


**Figure 10. Regulation of ECF  $\sigma$  factors by proteolysis.** As described in detail in the text, regulation of ECF  $\sigma$  factors occurs through a multitude of ways. One of the most common means is regulation through proteolysis of the anti- $\sigma$  factor, thereby alleviating the inhibitory effect of it on the  $\sigma$  factor.

One of the most common mechanisms of ECF  $\sigma$  factor regulation is proteolysis of the anti- $\sigma$  factor that is usually anchored to the membrane (Figure 10). This mechanism of regulation is exemplified by the *E. coli*  $\sigma$  factor,  $\sigma^E$  that is induced upon

the accumulation of several misfolded outer membrane proteins (OMPs). Immediately downstream of the gene that encodes this  $\sigma$  factor (*rpoE*), two other genes were found, namely *rseA* and *rseB*. Of these, the inner membrane protein, RseA was found to comprise of a transmembrane spanning region and a cytoplasmic region. Importantly, it functions as an anti- $\sigma$  factor and thereby negatively regulates the activity of  $\sigma^E$  by interacting with it through the cytoplasmic domain (De Las Peñas, Connolly, & Gross, 1997; Missiakas, Mayer, Lemaire, Georgopoulos, & Raina, 1997). RseB was found to exert its activity by stabilizing this interaction between RseA and the  $\sigma$  factor. Interestingly, upon encountering external stress (through induction of OmpC), RseA was found to be degraded rapidly. This was found to be accomplished by the extracytoplasmic protease, DegS whose proteolytic activity was in turn required for the activity of  $\sigma^E$  (Ades, Connolly, Alba, & Gross, 1999) (Figure 11).

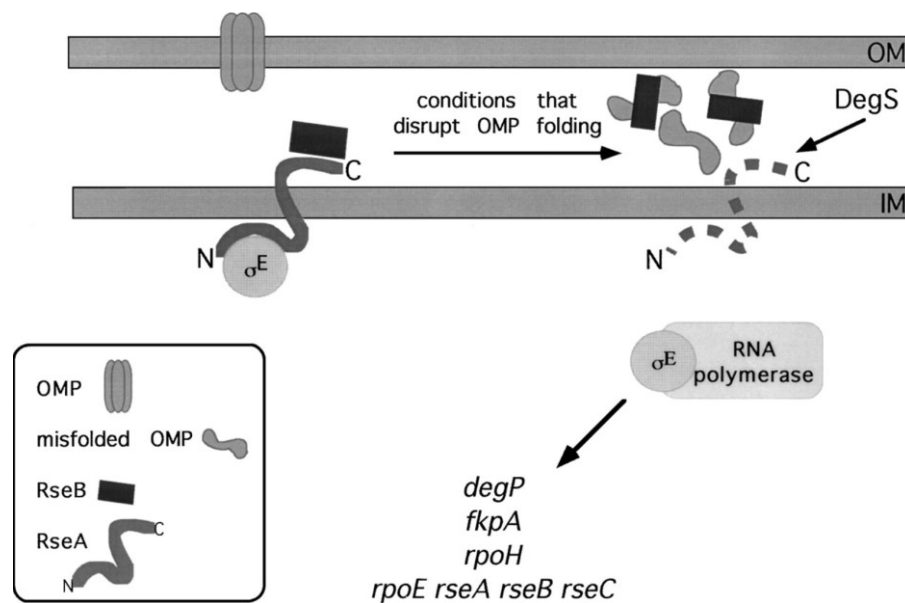


**Figure 11. Regulated proteolysis of RseA releases  $\sigma^E$  of *E. coli*.** In the absence of any external stimulus,  $\sigma^E$  of *E. coli* is kept under the control of the anti- $\sigma$  factor, RseA. The protein, RseB in turn stabilizes this interaction. Upon the accumulation of misfolded outer membrane proteins (OMPs), several events ensue, namely destabilization of the interaction between RseA and RseB, proteolytic degradation of RseA by the DegS protease and eventual release of  $\sigma^E$  into the cytoplasm, where it can form a complex with the RNA polymerase and result in transcription of genes that are required for OMP folding. Adapted from (Raivio & Silhavy, 2002).

Yet another instance of regulation through proteolysis can be seen for the *B. subtilis* ECF  $\sigma$  factor,  $\sigma^W$ . Its activity was found to be regulated by the anti- $\sigma$  factor, which is encoded by a gene within the same operon as that of  $\sigma^W$ . However, unlike RseA, the activity of the  $\sigma$  factor is regulated by both the extracytoplasmic and cytoplasmic portions of RsiW. Alkaline stresses induce a truncation within the extracytoplasmic domain and

this makes it accessible to the protease YluC, which then degrades the anti- $\sigma$  factor and eventually releases  $\sigma^W$  (Schöbel, Zellmeier, Schumann, & Wiegert, 2004).

### 1.4.8.4.2. Conformational changes within the anti- $\sigma$ factor

This mechanism of regulation involves direct sensing of an external signal by anti- $\sigma$  factors, which results in a conformational change in the protein structure, thereby resulting in the ECF  $\sigma$  factor being released (Figure 12). An example of this is the  $\sigma$  factor,  $\sigma^R$  which is responsible for sensing oxidative stress in *S. coelicolor*. The activity of  $\sigma^R$  is negatively regulated by the anti- $\sigma$  factor, RsrA as follows: under conditions of no stress, RsrA exists in a reduced form and this facilitates its binding to  $\sigma^S$ . Upon encountering oxidative stress, disulfide bonds are formed within the anti- $\sigma$  factor's structure, which causes it to have a reduced affinity to the  $\sigma$  factor, thereby releasing it and allowing transcription of the *trxB* operon of oxidative stress response encoding genes (J. G. Kang et al., 1999). The binding of RsrA in its reduced state to the  $\sigma$  factor was found to be dependent on a zinc metal ion within the anti- $\sigma$  factor's structure (W. Li et al., 2003). Oxidative stress results in displacement of this metal ion that results in a conformational change, thereby releasing  $\sigma^S$ . A similar mechanism can be observed in the case of the *Bradyrhizobium jaboricum* ECF  $\sigma$  factor, EcfF which responds to oxidative stress. It is negatively regulated by the anti- $\sigma$  factor, OsrA and the interaction between these two was dependent on two highly conserved cysteine residues (Masloboeva et al., 2012).

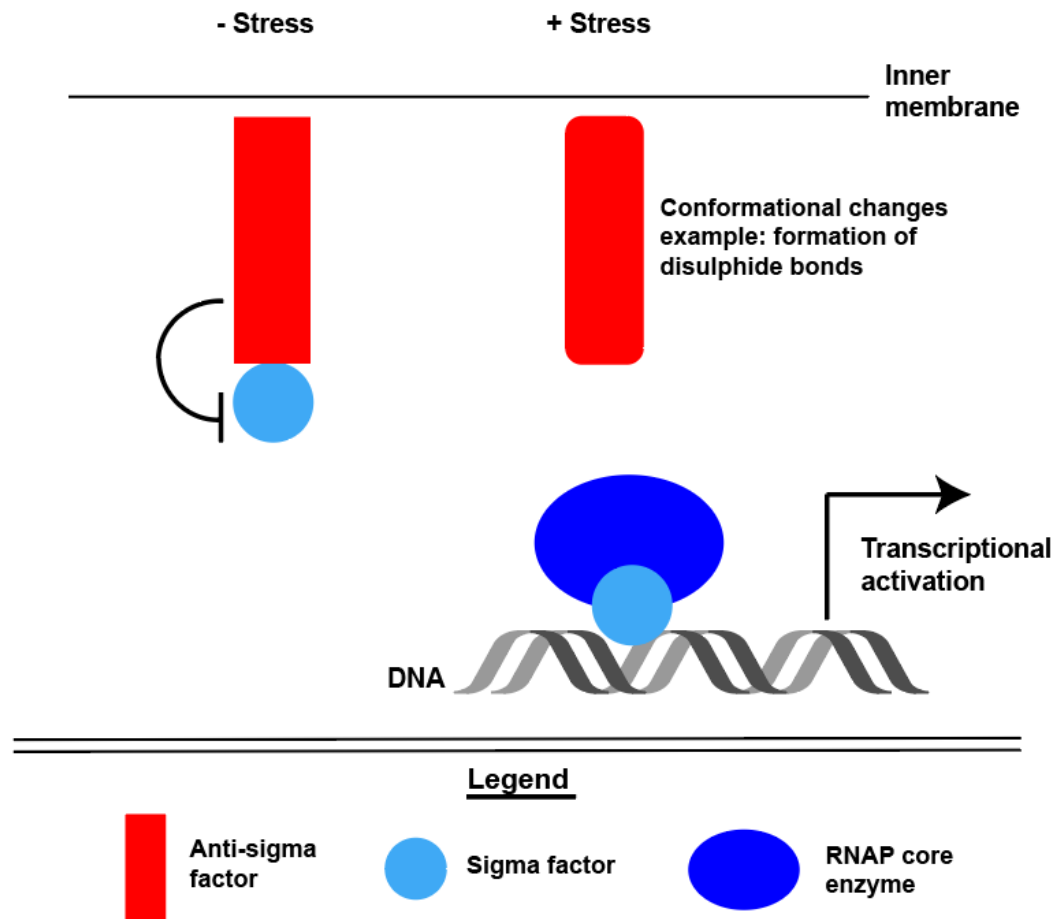


**Figure 12. Regulation of ECF  $\sigma$  factors by conformational changes within the anti- $\sigma$  factor.** Upon sensing external stimuli, conformational changes such as the formation of disulphide bonds ensue within the structure of the anti- $\sigma$  factor, thereby alleviating its inhibitory effect on the  $\sigma$  factor, allowing the latter to regulate transcription of appropriate genes.

#### 1.4.8.4.2.1. Mechanism of inhibition of ECF $\sigma$ factors by anti- $\sigma$ factors

Structural studies have shed light on distinct molecular mechanisms through which anti- $\sigma$  factors are found to inactivate ECF  $\sigma$  factors. Investigation of the  $\sigma$ /anti- $\sigma$  complex,  $\sigma^E$ /RseA of *E. coli* revealed that the N terminal cytoplasmic part of RseA which interacts with the  $\sigma$  factor comprises of a distinct helical domain fold with four alpha helices ( $\alpha_1$ - $\alpha_4$ ). The anti- $\sigma$  factor was found to be sandwiched within regions 2 and 4 of  $\sigma^E$ . This interaction was dependent on a conserved arginine residue within  $\sigma^E_4$  and serine and aspartate residues within  $\alpha_1$ . Furthermore, two kinds of sterical clashes work hand-in-hand to occlude the  $\sigma$  factor from interacting with the RNAP: residues within  $\alpha_3$  with the flap-tip helix of the  $\beta$  subunit and residues within  $\alpha_4$  with the coiled coil region of the  $\beta'$  subunit (Campbell et al., 2003). A similar mechanism can also be observed for the

*Rhodobacter sphaeroides*  $\sigma$  factor,  $\sigma^E$  whose activity is inhibited by the anti- $\sigma$  factor, ChrR. Provided that mutations of many of the residues that were involved in interaction of  $\sigma^E$  with the RNA polymerase also affected its interaction with ChrR, it was hypothesized that, as in the case of  $\sigma^E$ /RseA, ChrR possibly sterically occludes the  $\sigma$  factor, preventing its association with RNAP (Anthony, Newman, & Donohue, 2004). In fact, ChrR was found to consist of an N terminal anti- $\sigma$  domain (ASD) which was found to be essential for its inhibitory effect. This domain was stabilized by interactions with a zinc metal ion and was buried between regions 2 and 4 of the  $\sigma$  factor (Campbell et al., 2007). Eventually, this ASD domain was found to be characteristic of several anti- $\sigma$  factors that inhibit the activity of ECF  $\sigma$  factors.

A second mechanism by which anti- $\sigma$  factors exert their effect is by wrapping themselves around free ECF  $\sigma$  factors, thereby stabilizing this structure and preventing interactions of the latter with RNAP. This can be best described by the *Cupriavidus metallidurans*  $\sigma$  factor, CnrH which is involved in conferring cobalt and nickel resistance to the bacterium, as part of the CnrYXH complex. Upon binding of a metal ion, CnrX undergoes a conformational change and communicates the corresponding signal to the anti- $\sigma$  factor, CnrY causing the release of CnrH (Trepreau, Girard, et al., 2011). However, rather than sandwiching itself within the  $\sigma$  subunits, CnrY exerts its action by ensuring that the subunits are retained in a stable closed conformation and also masking the determinants that enable interaction with the  $\beta$  and  $\beta'$  subunits of the RNA polymerase (Maillard et al., 2014).

### 1.4.8.4.3. Regulation by interactions with other proteins

ECF  $\sigma$  factors can also be activated through contact with other proteins within the cytoplasm that, instead of functioning as an anti- $\sigma$  factor, facilitate its interaction with the RNA polymerase (Figure 13A). This is exemplified by the *E. coli* iron transport dependent  $\sigma$  factor, FecI. Due to the insolubility of iron in the aerobic environment, bacteria employ complex signaling systems in order to obtain these metal ions, as exemplified by the iron citrate transport system (Brooks & Buchanan, 2009). One of the main components that is involved in sensing ferric citrate is the protein, FecA and this is in turn dependent on TonB which recognizes the former at a specific sequence designated as the TonB box. Upon binding ferric citrate at the cell surface, FecA transduces the corresponding signal through its N terminal to the cytoplasmic regulatory protein, FecR, which induces the binding of the  $\sigma$  factor, FecI to the RNA polymerase (Braun, Mahren, & Ogierman, 2003).

#### **1.4.8.4.4. Regulation by partner switching mechanism**

This type of mechanism of  $\sigma$  factor regulation by mimicry/ partner switching is particularly common among Gram positive bacteria (Figure 13). An example of this can be seen in the case of the *B. subtilis* heat response  $\sigma$  factor,  $\sigma^B$ . This  $\sigma$  factor is inactivated by the anti- $\sigma$  factor, RsbW which also functions as a protein kinase. Under conditions of no stress, RsbW phosphorylates the anti-anti- $\sigma$  factor RsbV, which prevents their association (Dufour & Haldenwang, 1994). However, upon encountering stress (heat, in this case), dephosphorylation of RsbV ensues, accomplished by the RsbTU complex, eventually enabling its interaction with RsbW and thereby releasing the  $\sigma$  factor (C. M. Kang, Brody, Akbar, Yang, & Price, 1996; Voelker, Voelker, & Haldenwang, 1996).

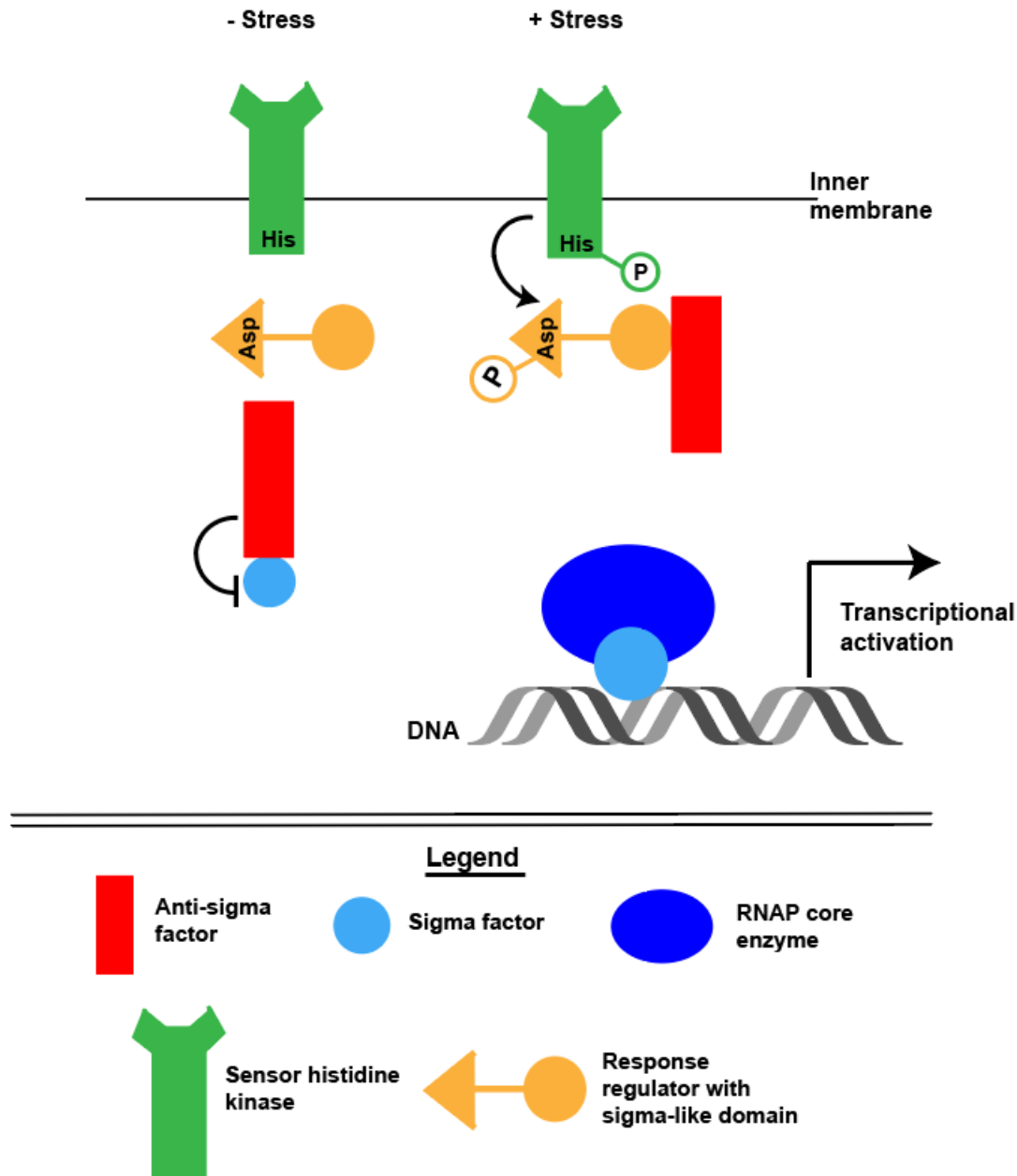


**Figure 13. Regulation of ECF  $\sigma$  factors by partner switching.** In certain instances, the anti- $\sigma$  factor shares a greater affinity with certain proteins that possess a  $\sigma$  factor like domain, thereby alleviating its effect on the ECF  $\sigma$  factor and allowing it to regulate transcription of appropriate genes.

Partner switching has also been shown to provide a bridge between ECF  $\sigma$  factors and two component systems. An example is the  $\sigma$  factor,  $\sigma^{\text{EcfG1}}$  of the alphaproteobacterium, *Methylobacterium extorquens* that is controlled by the anti- $\sigma$  factor NepR. This mechanism of regulation involves the response regulator, PhyR which comprises of an ECF  $\sigma$  factor like domain in its N terminal and a receiver domain in its C terminal. During conditions of external stress, PhyR gets phosphorylated on an aspartate residue by its cognate sensor histidine kinase. This phosphorylation event



results in a conformational change, resulting in the binding of its N-terminal domain with NepR. This causes release of the  $\sigma$  factor and subsequent transcription of the corresponding stress response genes (Francez-Charlot et al., 2009).

Upon looking at the crystal structure of the Phy<sub>SL</sub> ( $\sigma$  factor-like domain) – NepR complex from *Sphingomonas spp.*, several key molecular traits of the above mechanism were revealed (S. Campagne et al., 2012a). Phosphorylation of PhyR destabilizes the receiver domain, making it possible for the  $\sigma$  factor-like domain to interact with NepR. A stretch of hydrophobic amino acids within NepR were responsible for this interaction and these were highly conserved among several members of alphaproteobacteria. Interestingly, these residues were also the ones that were found to participate in the interaction between NepR and the ECF  $\sigma$  factor. A key observation, upon which the partner switching mechanism hinges, is that NepR was found to have a much higher affinity to Phy<sub>SL</sub> than to the  $\sigma$  factor (Herrou, Rotskoff, Luo, Roux, & Crosson, 2012).

#### 1.4.8.4.5. C-terminal extensions within the $\sigma$ factor

While not very common, regulation of ECF  $\sigma$  factors through their C terminal extensions has been hypothesized to occur, especially during instances wherein a conserved anti- $\sigma$  factor is absent (Wecke et al., 2012). A striking example of this is the ECF  $\sigma$  factor, CorE of *M. xanthus*, which was found to have a role in copper homeostasis (Gómez-Santos, Pérez, Sánchez-Sutil, Moraleda-Muñoz, & Muñoz-Dorado, 2011). While monovalent copper ions prevent the  $\sigma$  factor from binding to the DNA, divalent ions induce this association, resulting in the regulation of genes such as the multicopper peroxidase, *cuoB* and the P1B-type ATPase, *copB*. While no anti- $\sigma$  factor was found to be co-transcribed alongside CorE, its activation/ inactivation state seems to be dependent on a cysteine-rich region within its C terminal. Interestingly, the cysteine residues present in this region were highly conserved among several other  $\sigma$  factors within the bacterial kingdom, possibly referencing to this being a widespread mechanism (Mascher, 2013; M. S. Paget, 2015; Sineva, Savkina, & Ades, 2017).

#### 1.4.8.4.6. Through transcriptional activation

In cases where ECF  $\sigma$  factors lack an obvious anti- $\sigma$  factor, regulation also occurs by direct transcriptional control. This mechanism of regulation can be seen in the case of the *S. coelicolor*  $\sigma$  factor,  $\sigma^E$  which controls transcription of the *cwg* (cell wall glycan) operon of genes. The  $\sigma$  factor is regulated by a the CseB/CseC two component system

as follows: upon sensing extracellular stresses, the sensor histidine kinase, CseC gets autophosphorylated, eventually transferring its phosphate group to the response regulator, CseB, which in turn positively regulates  $\sigma^E$  (Hong, Paget, & Buttner, 2002). A wide range of compounds such as lysozyme and antibiotics including vancomycin have been shown to induce the aforementioned system.

### 1.4.8.5. Classification of ECF $\sigma$ factors

ECF  $\sigma$  factors constitute the third most abundant family of signal transduction proteins, following one component and two component systems (Staroń et al., 2009). Currently the highest number of ECF  $\sigma$  factors is found in the deltaproteobacterium, *Plesiocystis pacifica* (118 ECF  $\sigma$  factors) (Jogler et al., 2012).

Classification of ECF  $\sigma$  factors resulted in the discovery of 43 phylogenetically distinct groups (Staroń et al., 2009). Despite the fact that majority of the proteins belonged to either RpoE-type or Fecl-type  $\sigma$  factors, further classification was performed based on sequence conservation. Subgroups with interesting features were identified: for instance, members of the ECF43 group were found to show homology to not just the ECF family of proteins but also to other  $\sigma^{70}$  proteins (Staroń et al., 2009). More importantly, the  $\sigma$  factors of the ECF43 group were found to comprise serine/threonine kinases (STKs) in their vicinity (Jogler et al., 2012; Marcos-Torres, Perez, Gomez-Santos, Moraleda-Munoz, & Munoz-Dorado, 2016). As a consequence of this observation, it has been proposed that the activity of these  $\sigma$  factors could in turn be controlled by phosphorylation (Mascher, 2013) (Figure 14).

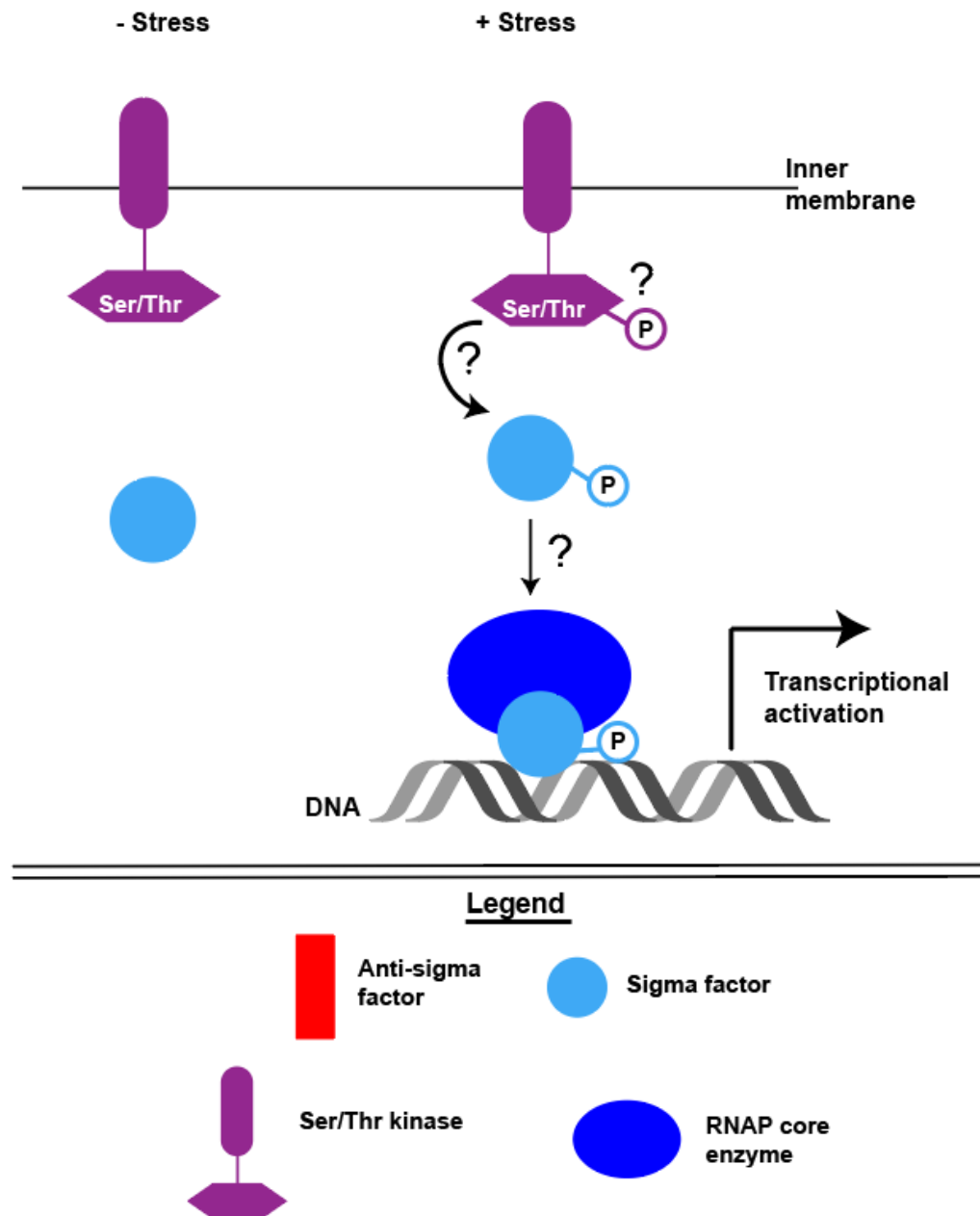


**Figure 14. Possible regulation of ECF  $\sigma$  factors by Ser/Thr kinases (STKs).** Upon characterization of a new group of ECF  $\sigma$  factors (ECF43) that possess a Ser/Thr kinase in their genetic neighborhood, it has been proposed that these  $\sigma$  factors could be regulated by phosphorylation.

Many of the identified subgroups of ECF  $\sigma$  factors had an anti- $\sigma$  factor with a well-conserved ASD in their genetic neighborhood. However, ECF41, for instance was found to not contain an anti- $\sigma$  factor in its vicinity. Instead, these  $\sigma$  factors had genes that encoded a carboxymyconolactone decarboxylase, an oxidoreductase or an epimerase (COE) in its neighborhood (Wecke et al., 2012). These COE encoding genes were often found to be the targets of these  $\sigma$  factors. Intriguingly, the ECF41 subfamily of  $\sigma$  factors were also found to comprise of an extended C terminal region that is essential for both

recognition of promoter elements and binding to the RNA polymerase, in a mechanism that is not yet fully understood (Wecke et al., 2012).

Several additional classifications were carried out on distinct populations and yielded more novel groups. For example, in Planctomycetes, eight additional groups of ECFs were found (Jogler et al., 2012). In Actinobacteria, classification of ECF  $\sigma$  factors led to the identification of eighteen additional groups (Huang et al., 2015).

### **1.4.8.6. Functions of ECF $\sigma$ factors**

As the name implies, these proteins are involved in sensing several extracellular stresses and accordingly, regulating the transcription of said stress response genes. This section will explore some of the functions of ECF  $\sigma$  factors and in doing so, attempt to highlight the stress response pathways that they are involved in.

#### **1.4.8.6.1. Pathogenecity**

Several studies have highlighted the importance of ECF  $\sigma$  factors in pathogenic bacteria. For instance, inactivation of the *M. tuberculosis*  $\sigma$  factor, *sigC* resulted in delayed lethality as a result of significant differences in the immunopathology that the mutant elicits (R. Sun et al., 2004). The role of these proteins in virulence is further exemplified from the *P. aeruginosa*  $\sigma$  factor, PvdS. This  $\sigma$  factor was found to regulate expression of genes involved in the synthesis of several virulence factors that were secreted into the host (Wilson & Lamont, 2006). Additionally, the ability of the bacterium, *Enterococcus faecalis* to colonize host tissues was dramatically reduced upon mutation of the ECF  $\sigma$  factor, *sigV* (Le Jeune et al., 2010).

#### **1.4.8.6.2. Developmental processes**

ECF  $\sigma$  factors are also implicated in developmental processes. For instance, deletion of the  $\sigma$  factor, *whiN* of *S. coelicolor* results in a bald appearance, as opposed to the fuzzy formation that results in differentiation into exospores (Bibb, Molle, & Buttner, 2000). This  $\sigma$  factor was eventually renamed *bldN* and while it was not active during vegetative growth, it dramatically increased during formation of the aerial mycelium, retaining very high levels through sporulation. Of the five Fecl type ECF  $\sigma$  factors identified in *P. syringae*, one of them was shown to have a profound effect on swarming,

the coordinated motility exhibited by bacteria on solid surfaces (P. B. Thakur, Vaughn-Diaz, Greenwald, & Gross, 2013). This is covered in detail in Chapter 3.

### **1.4.8.6.3. Responses to different extracellular stresses**

#### **1.4.8.6.3.1. Heat shock**

A key role for ECF  $\sigma$  factors is regulation of genes that are involved in heat shock response. For instance, levels of the *M. tuberculosis*  $\sigma$  factor,  $\sigma^B$  increased significantly upon exposure to heat shock and this was found to be dependent on  $\sigma^H$ , deletion of which also made the cells more sensitive to high temperatures (Manganelli et al., 2002). Yet another example is the *B. subtilis*  $\sigma$  factor, *sigI* whose inactivation resulted in reduced survival of the bacteria at temperatures as high as 55 °C (Zuber, Drzewiecki, & Hecker, 2001).

#### **1.4.8.6.3.2. Iron starvation**

One of the first studies that implicated ECF  $\sigma$  factors in iron starvation came from the *P. aeruginosa*  $\sigma$  factor PvdS, which was found to positively regulate expression of the siderophore, pyoverdine that the bacterium secretes during iron limiting conditions (Miyazaki, Kato, Nakazawa, & Tsuda, 1995). The  $\sigma$  factor was found to accomplish this by positively regulating the expression of the *pvcABCD* operon of genes (Stintzi et al., 1999). Comparison of the genes regulated by PvdS revealed a key element designated as the IS (iron starvation) box to which the  $\sigma$  factor binds, thereby enabling transcription (Ochsner, Wilderman, Vasil, & Vasil, 2002). The following mechanism of  $\sigma$  factor regulation has now been duly proposed: upon binding of iron by pyoverdine, the resulting compound binds to FpvA, a cell surface receptor which enables its transportation to the cell. Once inside the cell, the signal is communicated to the anti- $\sigma$  factor, FpvR which accordingly releases PvdS, enabling transcription of the *pvd* genes (Kazmierczak et al., 2005).

#### **1.4.8.6.3.3. Antibiotic stress**

One of the key stresses that is regulated by ECF  $\sigma$  factor signaling is response to antibiotics. This is exemplified by ECF  $\sigma$  factors of the Gram-positive bacterium, *B. subtilis*. One of the key determinants of fosfomycin resistance in the bacterium is FosB, which was found to be regulated by  $\sigma^W$ . Deletion of the gene encoding either of these proteins results in increased sensitivity to the antibiotic (M. Cao, Bernat, Wang,

Armstrong, & Helmann, 2001). Resistance to the antibiotic, bacitracin occurs via the BcrABC transport system, which comprises of proteins BcrB and BcrC that aid in the formation of a transmembrane channel, whereas BcrA acts as an ATPase. *bcrC* is in turn regulated by ECF  $\sigma$  factors,  $\sigma^X$  and  $\sigma^M$  (Min Cao & Helmann, 2002). However, in the presence of the antibiotic, induction was found to be solely dependent on  $\sigma^M$ . Transcriptomics studies on the deletion mutants of all the above mentioned ECF  $\sigma$  factors showed the regulation of several genes within the *eps* operon by these proteins (Luo, Asai, Sadaie, & Helmann, 2010). Another example is the *S. coelicolor*  $\sigma$  factor,  $\sigma^E$  that was found to induce certain genes involved in cell envelope functions. Some of these genes were induced in the presence of vancomycin (M. S. B. Paget, Hong, Bibb, & Buttner, 2002).

#### **1.4.8.6.3.4. ECF $\sigma$ factors often sense multiple external stresses**

While the above examples show that ECF  $\sigma$  factors govern specific stress response pathways, more often than not, these proteins sense a wide range of stresses. The *S. typhimurium*  $\sigma$  factor,  $\sigma^E$  regulates responses to both oxidative and polymyxin stresses (Humphreys, Stevenson, Bacon, Weinhardt, & Roberts, 1999). Similarly, inactivation of  $\sigma^E$  of *M. tuberculosis* renders the cells significantly more sensitive to SDS, heat shock and oxidative stresses (Manganelli, Voskuil, Schoolnik, & Smith, 2001). Activation of the *B. subtilis*  $\sigma$  factor,  $\sigma^M$  occurs through several stresses including high salt, alkalinity, ethanol, heat and antibiotics (Thackray & Moir, 2003). Another example is the *S. aureus* ECF  $\sigma$  factor,  $\sigma^S$  which was found to regulate both intra- and extracellular stress response pathways (H. K. Miller et al., 2012).

The invariant nature of  $\sigma$  factors in transcriptional regulation has certainly made them one of the most important cornerstones in molecular biology. Among these proteins, ECF  $\sigma$  factors have evidently been shown to regulate multiple stress response pathways. Given the increasing number of stresses that bacterial species are exposed to, study of ECF  $\sigma$  factors could certainly pave way to understanding how they combat certain external stimulus and possibly implicate these proteins in drug targeting strategies.

## 1.5. *Vibrio parahaemolyticus* as a model organism

In order to study a possible role for STKs in the regulation of ECF  $\sigma$  factors, we employed *Vibrio parahaemolyticus* as our model organism.

*Vibrio parahaemolyticus* is a gram-negative gammaproteobacterium that exists in marine and estuarine habitats and is the major causative agent of seafood borne gastroenteritis (Letchumanan, Chan, & Lee, 2014). It is caused as a result of consumption of both raw and undercooked seafood. The bacterium can readily colonize many hosts including salmon, shrimps, crabs, pomfrets and humans (M. A. Miller et al., 2010). It was initially isolated from an outbreak of food poisoning caused as a result of consumption of shirasu (whitebait) in Japan (Fujino et al., 1953). There are seasonal variations as to where it is usually present, in that during the summer months, the bacteria are present on planktons while in the winter months, they are detected in sediments. It is assumed that the sediments offer protection to the bacteria against low temperatures (T. Kaneko & Colwell, 1973). Despite being prevalent in marine environments and in estuaries such as those in Chesapeake Bay, *V. parahaemolyticus* has also been found in environments of no salinity such as ponds in Calcutta, India (De et al., 1977).

Interestingly, a few patients who suffered from *V. parahaemolyticus* induced gastroenteritis in Calcutta, India reported no seafood consumption in the week prior to infection, suggesting that cross-contamination is also another means through which infection could occur (Sircar, Deb, De, Ghosh, & Pal, 1976). The clinical infection that is caused by the bacterium is similar in pathology to that caused by certain *Salmonella* species and enteropathogenic *E. coli*. In addition to Japan and India, incidences of infection caused by *V. parahaemolyticus* have also been reported in Thailand, Philippines, Mexico and the United States of America (Barker H & Gangarosa J, 1974; de Hernández-Díaz et al., 2015; Maluping, Ravelo, Lavilla-Pitogo, Krovacek, & Romalde, 2005; Thongjun et al., 2013). The chitinoclastic nature of the bacterium enables it to attach to chitin and copepods (small crustaceans). Different factors including pH, metal ions and salinity were found to affect the adsorption of the bacteria to chitin particles tested in the laboratory. Interestingly, attachment of the bacteria to chitin was significantly greater than to copepods, possibly due to the slimy nature of the latter (Tatsuo Kaneko & Colwell, 1975).

## Introduction

---

One of the most unique characteristics of *V. parahaemolyticus* is that upon encountering solid surfaces, the bacteria differentiate into swarmer cells, which are morphologically different than the (free-living) swimmer cells found in liquid environments (Sar, McCarter, Simon, & Silverman, 1990). This will be reviewed in detail in Chapter 4.



## **Chapter 2: Aim and Scope**

In addition to being the third most abundant member of signal transduction proteins in bacteria, ECF  $\sigma$  factors also make up the largest fraction of  $\sigma^{70}$  proteins. ECF  $\sigma$  factors are regulated by several different mechanisms. The most well-characterized of these involves their control by an anti- $\sigma$  factor that is usually co-transcribed along with the  $\sigma$  factor. Upon encountering certain external stresses, the inhibitory effect of the anti- $\sigma$  factor is alleviated either by regulated proteolysis, partner switching or conformational changes within the protein, to name a few.

However, there are instances where a cognate anti- $\sigma$  factor is absent from the genetic neighborhood of the  $\sigma$  factor. In these cases, other mechanisms such as regulation by C-terminal extensions take over in certain  $\sigma$  factors. Classification of ECF  $\sigma$  factors into phylogenetically distinct groups led to the identification of the ECF43 family, wherein  $\sigma$  factors were found to contain putative serine/threonine kinases (STKs) in their vicinity. Given the abundant roles and targets of STKs and their widespread functions in signaling pathways, it was proposed that they could potentially also regulate the activity of ECF  $\sigma$  factors.

The principle aim of this thesis was to identify whether ECF  $\sigma$  factors can indeed be regulated by phosphorylation – more specifically, by STKs. In order to address this, we employed the Gram-negative marine pathogen, *Vibrio parahaemolyticus*, which is the leading cause of seafood-borne gastroenteritis as our model organism. Importantly, upon scanning the genome of the organism, we found an ECF  $\sigma$  factor within its first chromosome that was found to be co-transcribed alongside an STK. Given that ECF  $\sigma$  factors generally respond to certain external stresses, we also aimed to phenotypically characterize these two proteins and evaluate whether they participate in the same stress response pathway. Since the presence of external stresses usually results in association of the free (upon dissociation from the anti- $\sigma$  factor, for instance) ECF  $\sigma$  factor with the RNA polymerase core enzyme and eventual transcriptional regulation, we assessed whether this association is aided by phosphorylation in the case of the  $\sigma$  factor found in *V. parahaemolyticus*. Altogether, the principle aim of this thesis was to characterize a new mode of regulation of ECF  $\sigma$  factors – one that involves phosphorylation by their cognate STKs. Finally, given the vast abundance of both these proteins (ECF  $\sigma$  factors and STKs), we used a bioinformatics approach to explore whether this kind of regulation was also common among other bacterial species. We then used the results obtained

from this analysis to perform *in vivo* experiments and obtain further proof of the widespread implications of this novel mechanism in a distantly related bacterial species.

One of the key features that sets *V. parahaemolyticus* apart is that upon encountering solid surfaces or viscous environments, the bacteria elongate into highly peritrichously flagellated swarmer cells. Apart from being morphologically different, these swarmer cells are also metabolically distinct from the free-living swimmer cells (in liquid medium). In order to evaluate the possibility of signal transduction by STKs playing a role in this second motility system, we tested if the aforementioned STK and ECF  $\sigma$  factor have an effect on swarming behavior. We also performed proteomics experiments to better understand the molecular targets and the different processes that are regulated by the STK/ECF  $\sigma$  factor system. Finally, in order to examine whether phosphorylation could likely be implicated in this functionality, we designed respective point mutants within both the ECF  $\sigma$  factor and the STK and examined whether they affect swarming behavior.



# RESULTS



## **Chapter 3: Regulation of ECF $\sigma$ factor through phosphorylation in bacteria**





### 3.1. Introduction

In order to survive in changing environments, it is essential for cells to be able to sense their surroundings, respond to extracellular stresses, and adapt gene expression accordingly. A major form of transcriptional regulation in bacteria is through the exchange of the primary  $\sigma$  factor of RNA polymerase (RNAP) with an alternative  $\sigma$  factor. Upon stimulus detection, alternative  $\sigma$  factors recruit RNAP to promoter sequences distinct from the promoters recognized by the housekeeping  $\sigma$  factors, thereby activating condition-specific regulons. This allows for a rapid modification of cellular gene expression profiles and consequently a fast adaptation to changing environments. Of particular importance are extracytoplasmic function  $\sigma$  factors (ECF  $\sigma$  factors), which are among the most abundant signal transduction mechanisms in bacteria (Mascher, 2013). ECF  $\sigma$  factors are generally intrinsically active and only upon inhibition of their activity is their effect on gene regulation controlled.

Indeed, ECF  $\sigma$  factor is regulated by several distinct mechanisms, which serve to retain the  $\sigma$  factor in an inactive state – thus, preventing  $\sigma$  factor action on regulating gene expression (S. Campagne et al., 2012b; Campbell et al., 2007; Chaba et al., 2011; Chaba, Grigorova, Flynn, Baker, & Gross, 2007; Francez-Charlot et al., 2009; Heinrich & Wiegert, 2009; Herrou et al., 2012; Sohn, Grant, & Sauer, 2007; Trepreau, De Rosny, et al., 2011; Trepreau, Girard, et al., 2011; Wilken, Kitzing, Kurzbauer, Ehrmann, & Clausen, 2004; Zdanowski et al., 2006). Upon sensing a specific stimulus, the inhibitory effect on the  $\sigma$  factor is alleviated, enabling its interaction with the core RNAP enzyme, and ultimately modulating the cellular transcription profile by directing transcription initiation to its specific target promoters. A major mechanism of  $\sigma$  factor regulation is through the action of an anti- $\sigma$  factor, which specifically binds and sequesters the  $\sigma$  factor, resulting in inactivation of the  $\sigma$  factor. One mechanism by which ECF  $\sigma$  factor activity is regulated is by proteolysis of membrane anchored anti- $\sigma$  factors. In this model, the inhibitory effect of the anti- $\sigma$  factor is relieved by the sensing of an external cue, which triggers the regulated cleavage of the anti- $\sigma$  factor and the subsequent activation and release of the  $\sigma$  factor into the cytoplasm (Chaba et al., 2011, 2007; Heinrich & Wiegert, 2009; Sohn et al., 2007; Wilken et al., 2004). Soluble anti- $\sigma$  factors are similar in structure to the regulatory domain of membrane-associated anti- $\sigma$  factors, but differ in their mechanism of regulating the release of the  $\sigma$  factors – e.g. as a response to intracellular redox or oxidative stress, a conformational change occurs in the anti- $\sigma$

factor, resulting in the release and activation of its cognate  $\sigma$  factor (Campbell et al., 2007; Trepreau, De Rosny, et al., 2011; Trepreau, Girard, et al., 2011; Zdanowski et al., 2006).

Yet another mechanism involves partner switching of the anti- $\sigma$  factor by  $\sigma$  factor mimicry (S. Campagne et al., 2012b; Francez-Charlot et al., 2009; Herrou et al., 2012). Here, a  $\sigma$  factor-like domain is fused and tightly bound to a response regulator domain. Upon sensing a specific stimulus, the response regulator is phosphorylated by a histidine kinase. As a result, the tight binding to the  $\sigma$  factor-like domain is relieved, and can now be recognized and bound by the anti- $\sigma$  factor, which so far has been in complex with its cognate  $\sigma$  factor – this ultimately frees and activates the  $\sigma$  factor (S. Campagne et al., 2012b; Francez-Charlot et al., 2009; Herrou et al., 2012). Certain  $\sigma$  factors have also been shown to possess C-terminal extensions that have a regulatory function on  $\sigma$  factor activity (Gómez-Santos et al., 2011; Wecke et al., 2012; Wu et al., 2019). There are also several interesting instances of anti- $\sigma$  factors possessing a dual role, where in addition to keeping their cognate  $\sigma$  factor inactive, they also function as “ $\sigma$  activators” (Mettrick & Lamont, 2009; Ochs et al., 1995). Finally, the activity of some  $\sigma$  factors is regulated on the transcriptional level where a specific input induces expression of the  $\sigma$  factor (Hong et al., 2002; M. S. B. Paget, Chamberlin, Atrih, Foster, & Buttner, 1999).

Some subgroups of the ECF  $\sigma$  factor family show highly conserved microsynteny between genes encoding ECF  $\sigma$  factors and STKs (Serine/Threonine Kinases) (Jogler et al., 2012; Staroń et al., 2009). The absence of a conserved anti- $\sigma$  factor suggested that STKs might have a role in controlling  $\sigma$  factor activity (see e.g. (Mascher, 2013)) and recent *in vivo* data has further implied that  $\sigma$  factors might be regulated by phosphorylation in bacteria (Bayer-Santos et al., 2018). However, to date there exists no clear evidence that  $\sigma$  factors in bacteria can be phosphorylated and that transcription can be regulated in a  $\sigma$  factor phosphorylation-dependent manner. Here we report a new mechanism of transcriptional regulation in bacteria. Particularly we report a mechanism of  $\sigma$  regulation that relies on intrinsically inactive  $\sigma$  factors that are only active and able to interact with core RNAP upon phosphorylation at a highly conserved threonine residue. Our data indicate that this mechanism constitutes a new paradigm in ECF  $\sigma$  factor regulation that is widespread in bacteria.

## 3.2. Results

### 3.2.1. ECF $\sigma$ factor phosphorylation in bacteria

We set out to test if ECF  $\sigma$  factor phosphorylation occurs in bacteria, using the Gram-negative human pathogen *Vibrio parahaemolyticus*, which is the major cause of seafood-borne gastroenteritis in humans worldwide (Letchumanan et al., 2014), as a model organism. *V. parahaemolyticus* encodes one predicted STK, VP0057, upstream of a predicted ECF  $\sigma$  factor, VP0055 (Figure 15) – hereafter named i) VP0057, PknT (Protein Kinase of ECF Threonine) and ii) VP0055, EcfP (ECF  $\sigma$  factor activated by Phosphorylation).

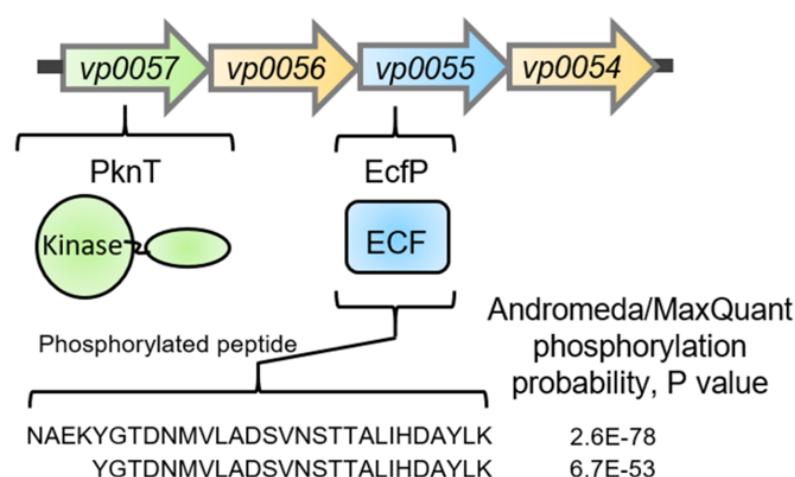


**Figure 15. Phosphorylation of ECF  $\sigma$  factor occurs in *V. parahaemolyticus*.** Schematic showing the genetic context of *vp0055* (*ecfP*) and *vp0057* (*pknT*) and the sequences of detected phosphorylated EcfP peptides with their corresponding phosphorylation probability as calculated by Andromeda embedded in MaxQuant.

The genes *pknT* and *ecfP* are in a putative operon with two other genes (*vp0054* and *vp0056*) encoding proteins of unknown function. *In silico* analysis predicted PknT to consist of an N-terminal STK domain (amino acids (aa) 1-336) and a C-terminal domain of unknown function (aa 358-450), separated by a single transmembrane region (aa 337-357) (Figure 15, Figure 16A). Furthermore, membrane topology mapping indicated that the N-terminal STK domain is positioned in the cytoplasm, while the C-terminal domain is in the periplasm (Figure 16B-C). Strikingly, by using affinity purification of sfGFP-tagged EcfP (sfGFP-EcfP) ectopically expressed in wild-type cells, followed by MS/MS analysis, we detected phosphorylated versions of two overlapping EcfP-specific peptides

## Results – Part I

(Figure 15). This shows that phosphorylation of ECF  $\sigma$  factors does indeed occur in bacteria.

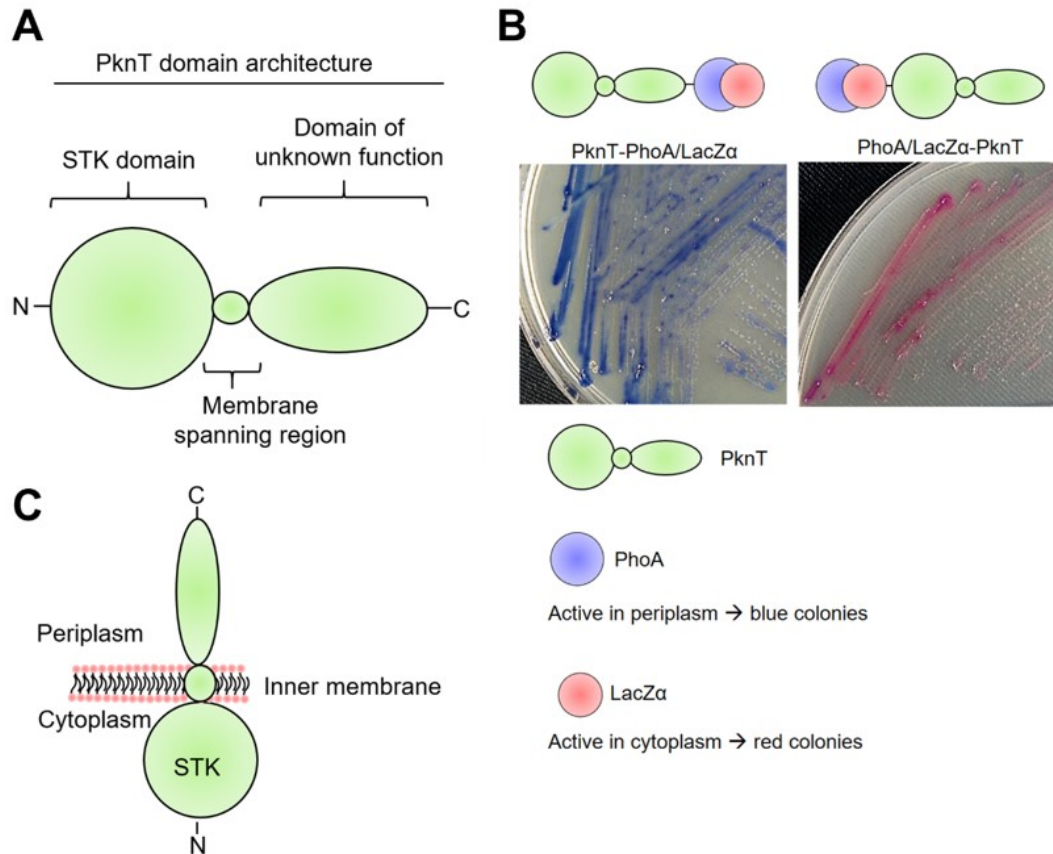


**Figure 16. Domain architecture and inner membrane orientation of PknT.** (A) Schematic showing the domain architecture of PknT. (B) Membrane topology assay of PknT. *E. coli* cells expressing PknT N- and C-terminally translationally fused to PhoA-LacZα. The position of the fusion is indicated in the figure. Cells were propagated on indicator medium including the two chromogenic substrates, Red-Gal (indicating LacZ galactosidase activity) and X-Pho (indicating phosphatase activity). Blue coloration of the colonies is the result of high phosphatase activity, indicating a periplasmic location of the fusion point. Red coloration of the colonies shows a high galactosidase activity, indicating cytosolic location of the fusion point. (C) Schematic showing the orientation of PknT in the inner membrane.

### 3.2.2. EcfP is phosphorylated on residue Thr63 by threonine kinase PknT

While under standard laboratory growth conditions only a very small fraction (~0.5%) of EcfP was phosphorylated (Figure 17A orange bars, Figure 17B), overexpression of PknT resulted in almost 50% of EcfP being in a phosphorylated state, a 10<sup>3</sup>-fold increase in EcfP phosphorylation (Figure 17A green bars, Figure 17B). This indicates that in wild-type cells, phosphorylation of EcfP does occur, however, only at a very low basal level and that PknT mediates EcfP phosphorylation.

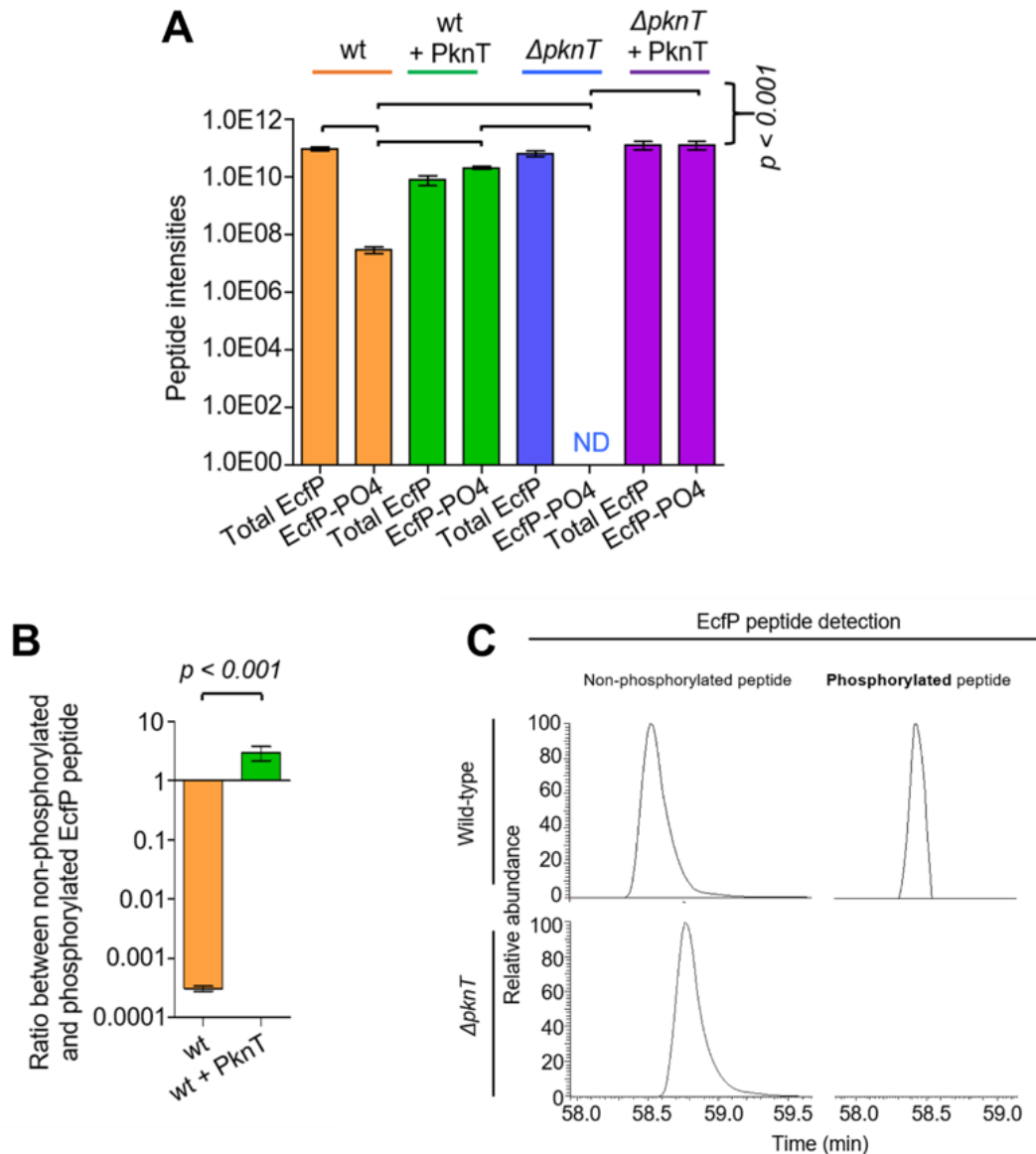


**Figure 17. EcfP is phosphorylated by the Serine/Threonine kinase, PknT.** (A) Upon co-IP-MS experiments of strains expressing sfGFP-EcfP, label-free quantification was performed. Bar graphs show summed peptide intensities of total EcfP and phosphorylated EcfP peptides in wild-type (orange), wild-type with ectopic overexpression of PknT (green), in a  $\Delta pknT$  background (blue), and in a  $\Delta pknT$  background with ectopic expression of PknT to test for complementation of the phenotype (purple). “ND”: non-detected. (B) Bar graph showing the ratio between non-phosphorylated and phosphorylated VP0055 peptide in wild-type cells and cells overexpressing PknT (wt + PknT). (C) Extracted ion chromatogram of a non-phosphorylated EcfP peptide and detected EcfP phosphopeptide in wild-type and  $\Delta pknT$  strain backgrounds. Three biological replicates were performed and analyzed for all the above experiments. Error bars indicate SEM and p-values were calculated by Students t-test.

Importantly, phosphorylated EcfP was not detected in a strain deleted for *pknT* ( $\Delta pknT$ ), while the total amount of detected EcfP peptide was identical for wild-type and  $\Delta pknT$  (Figure 17A blue bars, Figure 17C). Furthermore, phosphorylation of EcfP could be complemented in  $\Delta pknT$  by ectopic expression of PknT (Figure 17A purple bars).

## Results – Part I

Altogether these results indicate that PknT is a true kinase responsible for the phosphorylation of EcfP.

To analyze if PknT and EcfP directly interact, we performed a co-immunoprecipitation assay using anti-GFP beads followed by LC-MS (co-IP LC-MS) analysis on wild-type *V. parahaemolyticus* cells expressing sfGFP alone or sfGFP-EcfP, respectively. The assay showed that PknT specifically co-purified with sfGFP-EcfP but not with sfGFP alone (Figure 18A). Furthermore, a bacterial-two-hybrid-assay result suggested that both PknT and EcfP self-interact (dimerize) and that a direct protein interaction between PknT and EcfP occurs (Figure 18B) – thus supporting the results of the co-IP LC-MS experiment (Figure 18A) and altogether indicating that PknT and EcfP form an interaction complex.

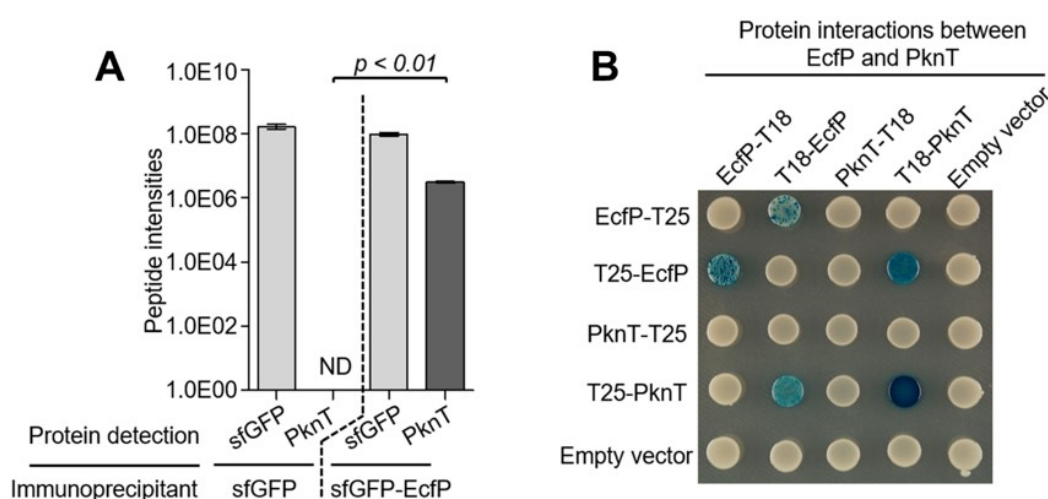


**Figure 18. PknT and EcfP form an interaction complex.** (A) Bar graph showing summed protein peptide intensities of a co-immunoprecipitation LC-MS experiment using beads with attached  $\alpha$ -GFP antibodies on wild-type *V. parahaemolyticus* cells expressing sfGFP (negative control) or sfGFP-EcfP, respectively. The assay shows that PknT is significantly co-immunoprecipitated with sfGFP-EcfP but not sfGFP alone. “ND”: non-detected. (B) Bacterial-two-hybrid assay (BACTH), testing for protein-protein interaction between EcfP and PknT. Blue colony formation suggests that a direct interaction occurs. Three biological replicates were performed and analyzed for all the above experiments. Error bars indicate SEM and p-values were calculated by Students t-test.

Importantly, reconstitution of the PknT/EcfP system in *E. coli* also showed that phosphorylation of EcfP in *E. coli* was strictly dependent on co-expression with PknT (Figure 19A-B), strongly supporting that PknT is a genuine kinase for direct EcfP phosphorylation.

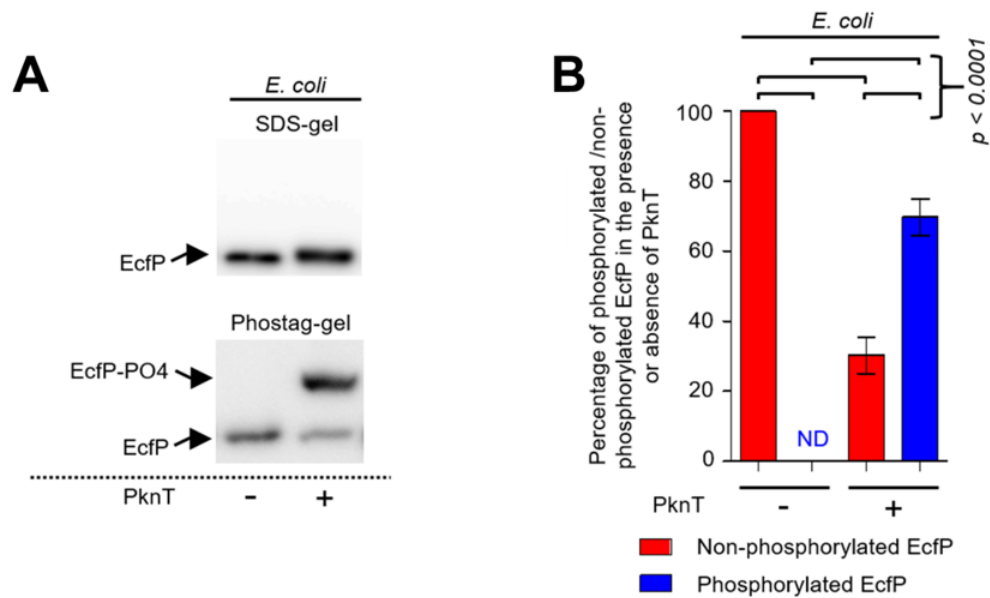


**Figure 19. PknT is a genuine and the sole kinase responsible for the phosphorylation of EcfP.** (A) Western-blot using anti-GFP antibodies on *E. coli* cells ectopically expressing sfGFP-EcfP in the presence or absence of ectopic expression of PknT. Cells were analyzed on phostag-gel to assay for EcfP phosphorylation. Samples were additionally analyzed on a standard SDS gel acting as a loading control. (B) Bar graphs showing the percentage of phosphorylated and non-phosphorylated EcfP in *E. coli* cells in the presence or absence of ectopic expression of PknT – quantification of experiments depicted in panel “A”. “ND”: non-detected. Three biological replicates were performed and analyzed for all the above experiments. Error bars indicate SEM and p-values were calculated by Student's t-test.

To further identify at which residue EcfP is phosphorylated, we expanded on our MS/MS analysis of immuno-purified sfGFP-EcfP, which clearly showed that the detected phosphopeptides were phosphorylated on one specific threonine (Thr) residue, namely Thr63 of EcfP (Figure 20). Thus, altogether, these experiments indicate that PknT and EcfP form an interaction complex and that the ECF  $\sigma$  factor EcfP is directly phosphorylated at Thr63 by the threonine kinase PknT.

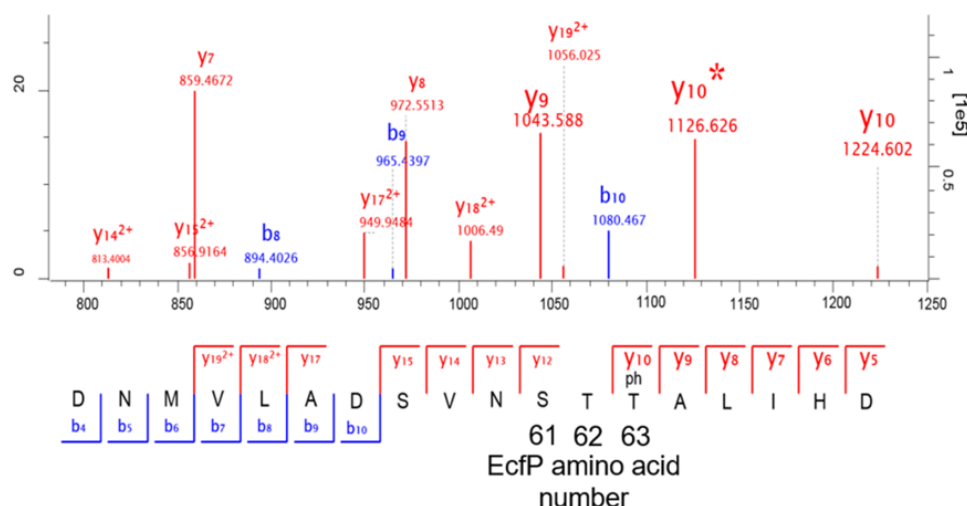


**Figure 20. EcfP phosphorylation occurs at a specific threonine residue, Thr63.** MS/MS spectrum of the mapped phosphorylation site in the phosphopeptide of ECF  $\sigma$  factor EcfP. The identified b- and y-fragment ions are shown in blue and red, respectively. The y-ion series allowed identification of the phosphorylation modification. For the y10 ion, a neutral loss of the phosphate (H3PO4-98Da) was detected showing that Thr63 if EcfP is phosphorylated. The neutral loss peak is marked with an asterisk, y10\*.

### 3.2.3. The PknT/EcfP system is required for resistance of polymyxin antibiotics

To explore cellular function and the importance of EcfP phosphorylation, we tested the effect of several cellular stresses on strains individually deleted for *ecfP* and *pknT*. Several conditions, such as heat stress, translational stress (streptomycin), cell wall stress (Penicillin G), salt stress, and cell envelope stress (SDS, polymyxin B and E (colistin)) were tested. Strikingly, many of these stresses had no effect (Figure 21) and only treatment with polymyxin antibiotics had an effect on strains lacking the PknT/EcfP system (Figure 22A-C).



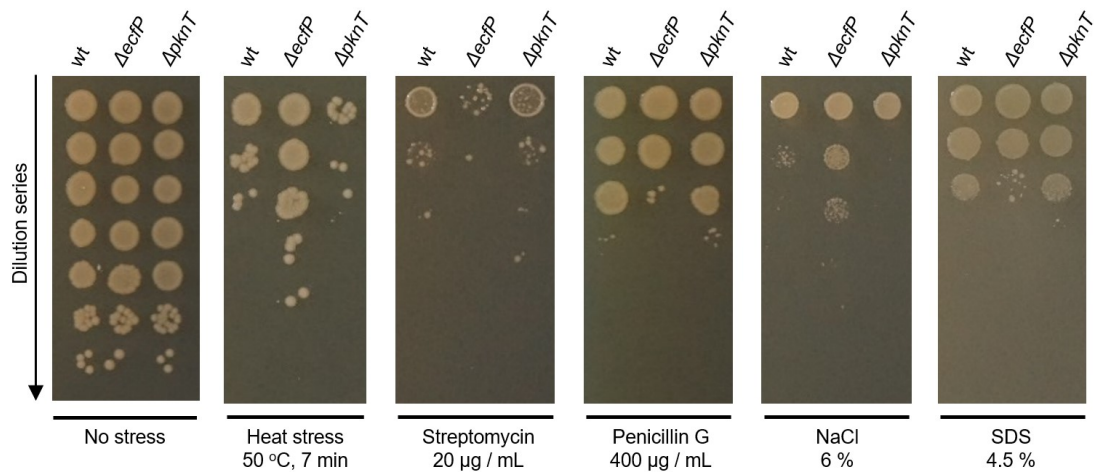


**Figure 21. Results of miscellaneous stresses on  $\Delta ecfP$  and  $\Delta pknT$  mutants.** Spot dilution assay of *V. parahaemolyticus* wild-type and mutant variants on LB growth medium in the presence and absence of indicated stress compounds, or after spotted on LB agar subsequent to heat stress.

In fact, a strain lacking either EcfP or PknT was highly sensitive to both polymyxin B and E antibiotics and resulted in an up to  $10^7$ -fold decrease in CFUs subsequent to polymyxin treatment compared to wild-type (Figure 22A-C).

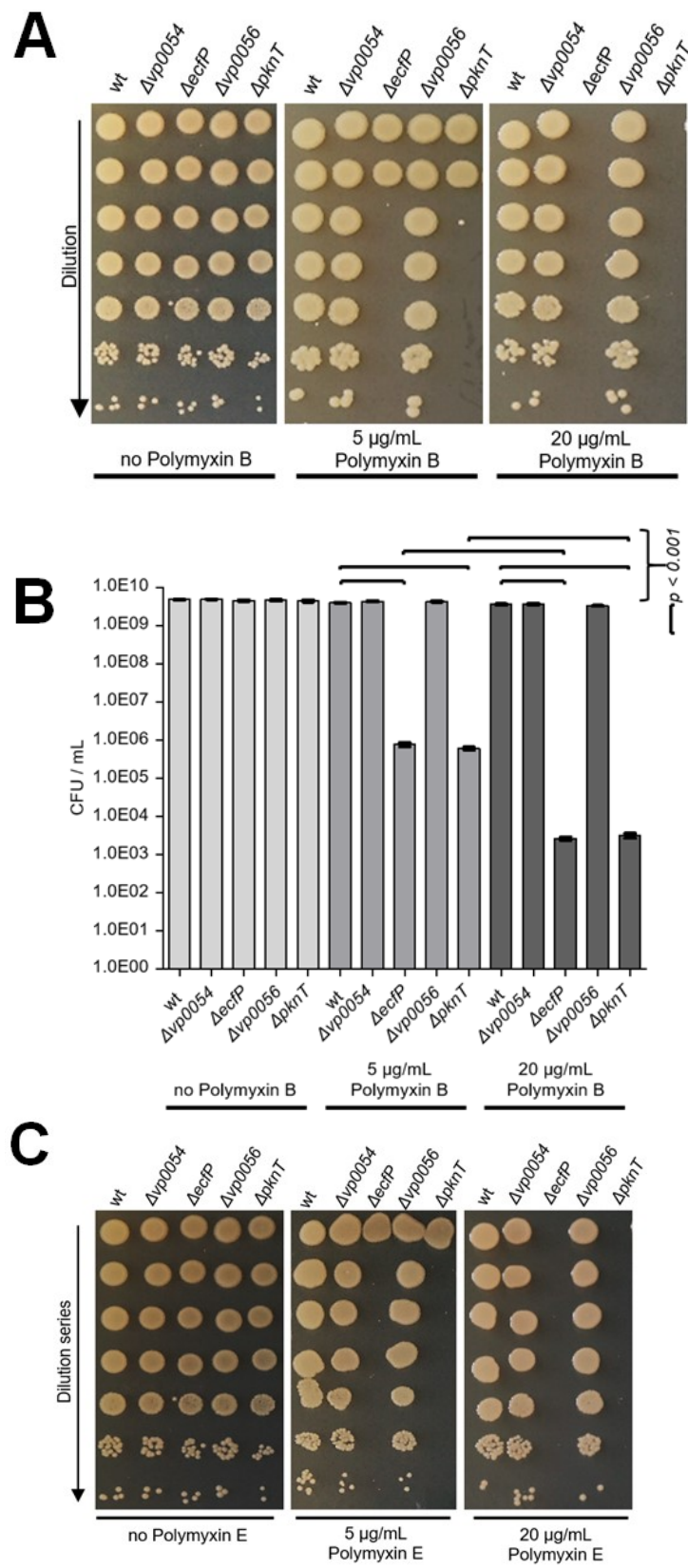


**Figure 22. Both PknT and EcfP are essential for conferring resistance to polymyxin antibiotics.** (A) Spot dilution assay of wild-type and mutant variants on LB growth medium in the presence and absence of Polymyxin B. (B) Bar graph showing the number of colony-forming-units (CFU) per mL of bacterial culture in the presence or absence of Polymyxin B for *V. parahaemolyticus* wild-type and mutant variants. Three biological replicates were performed and analyzed for this experiment. Error bars indicate SEM and p-values were calculated by Students t-test. (C) Spot dilution assay of wild-type and mutant variants on LB growth medium in the presence and absence of Polymyxin E.

Thus, the PknT/EcfP system is required for resistance towards polymyxin antibiotics. Polymyxins are cationic antimicrobial peptides generally used in the treatment of Gram-negative bacterial infections. They function primarily by targeting lipopolysaccharides (LPS) and breaking up the bacterial cell membrane causing cell envelope stress. Polymyxins are usually used only as a last resort if more traditional antibiotics are non-functional (Anaya-López, López-Meza, & Ochoa-Zarzosa, 2013; Olaitan, Morand, & Rolain, 2014).

Absence of VP0054 or VP0056 did not influence polymyxin sensitivity of *V. parahaemolyticus* (Figure 22A-C) and a combinatorial deletion of *ecfP* and *pknT* did not result in increased polymyxin sensitivity compared to individual deletions, indicating that EcfP and PknT function in the same signaling pathway, consistent with a regulatory role of PknT on EcfP activity (Figure 23).

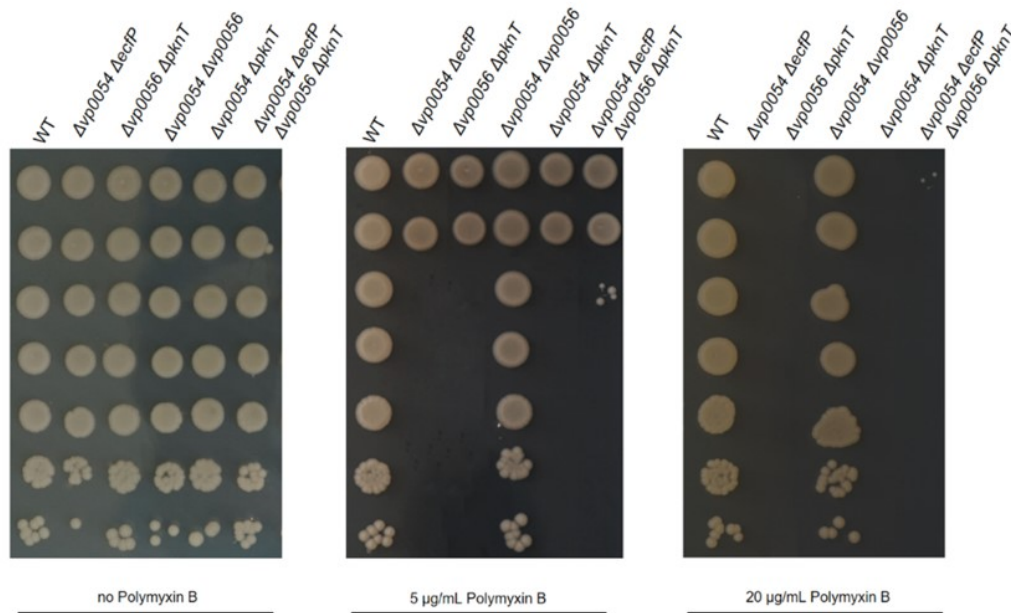


**Figure 23. EcfP and PknT function in the same signaling pathway.** Spot dilution assay of *V. parahaemolyticus* wild-type and mutant variants on LB growth medium in the presence and absence of Polymyxin B.

### 3.2.4. PknT/EcfP confer polymyxin resistance by regulating the expression of the essential polymyxin resistance determinant *vpa0879*

To further understand the cellular output of the PknT/EcfP system, we performed transcriptomics analyses in the absence of polymyxin B on exponentially grown wild-type,  $\Delta pknT$  and  $\Delta ecfP$  cells, respectively. We identified 18 genes to be significantly ( $p < 0.0001$ ) up- or down-regulated ( $>4$ -fold) in the absence of either EcfP or PknT (Figure 25). Among these targets, 10 were commonly upregulated and 8 were commonly downregulated in both mutant strains (Table 12 and Table 13).

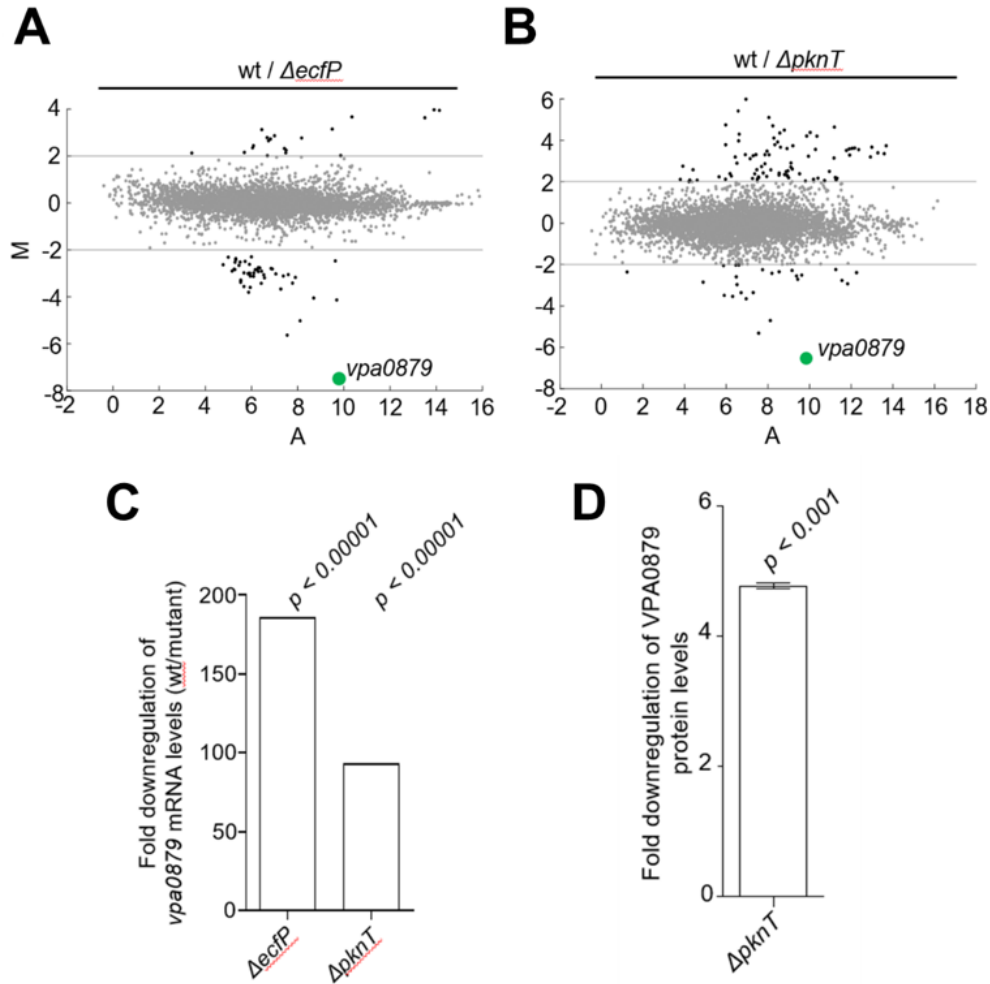


**Figure 24. The PknT/EcfP system regulates expression of the putative UDP-glucose-4-epimerase encoding gene, *vpa0879*.** (A) MA plots for *V. parahaemolyticus* gene expression in wild-type versus  $\Delta ecfP$ . (B) MA plots for *V. parahaemolyticus* gene expression in wild-type versus  $\Delta pknT$ . For the above two figures,  $M = \log_2(R/G)$  and  $A = 0.5 \cdot \log_2(RG)$ . R and G values are calculated as the mean RPKM of the biological replicates of the mutant and wild type respectively. Genes highlighted in black are significantly up- or downregulated. Gene highlighted in green represents *vpa0879*. (C) Bar-graph showing the fold down-regulation of *vpa0879* in transcriptomics experiments. The values represent RPKM mean of the biological replicates of the wild type with respect to the mutants (WT/mutant). Two biological replicates were performed and analyzed for all the above experiments. p-values were calculated by Students t-test. (D) Bar graph showing the fold downregulation of VPA0879 protein levels in the absence of PknT. Three biological replicates were performed and analyzed for this experiment. Error bars indicate SEM and p-values were calculated by Students t-test.

In both  $\Delta ecfP$  and  $\Delta pknT$  strains, the most significantly down-regulated gene (down-regulated by 185- and 95-fold in  $\Delta ecfP$  and  $\Delta pknT$ , respectively) was *vpa0879* (Figure 24A-C), which encodes for a predicted UDP-glucose 4-epimerase with an unknown function. The complete list of genes that were significantly downregulated or upregulated in a  $\Delta ecfP$  background when compared to wild type can be found in Table 14 and Table 15, respectively. Similarly, the complete list of genes that were significantly

## Results – Part I

downregulated or upregulated in a  $\Delta pknT$  background when compared to wild type can be found in Table 16 and Table 17, respectively.

This result was further substantiated by LC-MS global proteomic analysis, confirming that VPA0879 protein levels were significantly down-regulated in  $\Delta pknT$  compared to wild-type (Figure 24D).

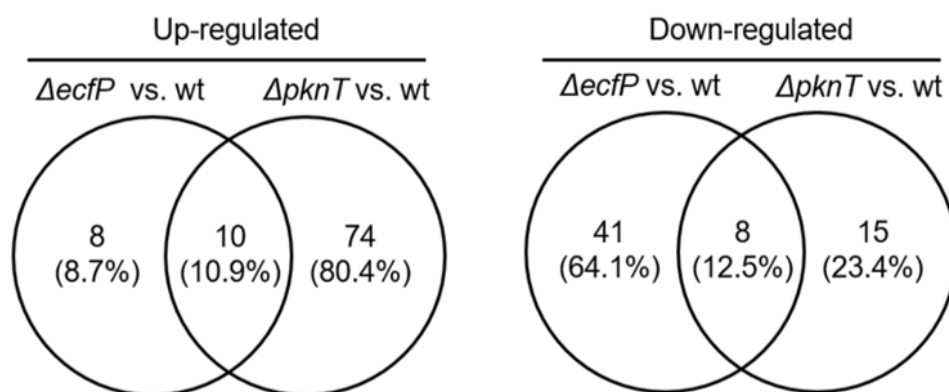


**Figure 25. Overview of the number of targets regulated by the PknT/EcfP system.** Venn diagrams showing overlaps among genes with up-regulated or down-regulated transcript abundance in response to deletion of *ecfP* or *pknT* relative to wild-type.

Importantly, a  $\Delta vpa0879$  strain was highly sensitive to polymyxins, to a level similar to strains  $\Delta ecfP$  and  $\Delta pknT$  (Figure 26), indicating that the PknT/EcfP system confers polymyxin resistance by regulating the expression of the essential polymyxin resistance determinant *vpa0879*.

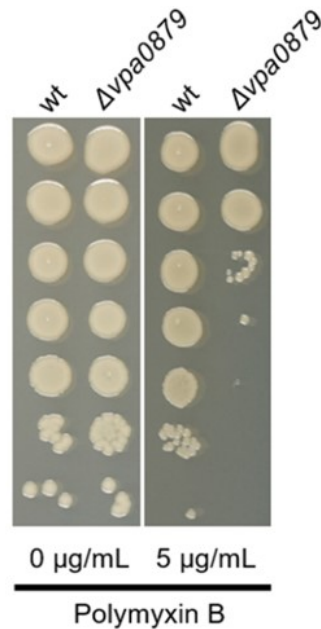


**Figure 26. VPA0879 is extremely sensitive to polymyxin B.** Spot dilution growth-assay of wild-type and  $\Delta vpa0879$  *V. parahaemolyticus* in the presence and absence of Polymyxin B.

### 3.2.5. Phosphorylation of EcfP by PknT on residue Thr63 is required for EcfP activity

Subsequently, we used polymyxin sensitivity and VPA0879 expression as reporters for PknT/EcfP activity. To test the importance of residue Thr63 and EcfP phosphorylation on its activity, we replaced the native *ecfP* locus with *ecfPT63A*, which encodes the EcfP variant EcfPT63A carrying an amino acid substitution of Thr63 with alanine. The resulting *V. parahaemolyticus* strain, *ecfPT63A*, was highly sensitive to polymyxin stress similar to  $\Delta ecfP$  (Figure 27A). Furthermore, proteomics analysis showed that in contrast to wild-type cells where VPA0879 is expressed, no VPA0879 was detected in the strain, *ecfPT63A* (Figure 27B).

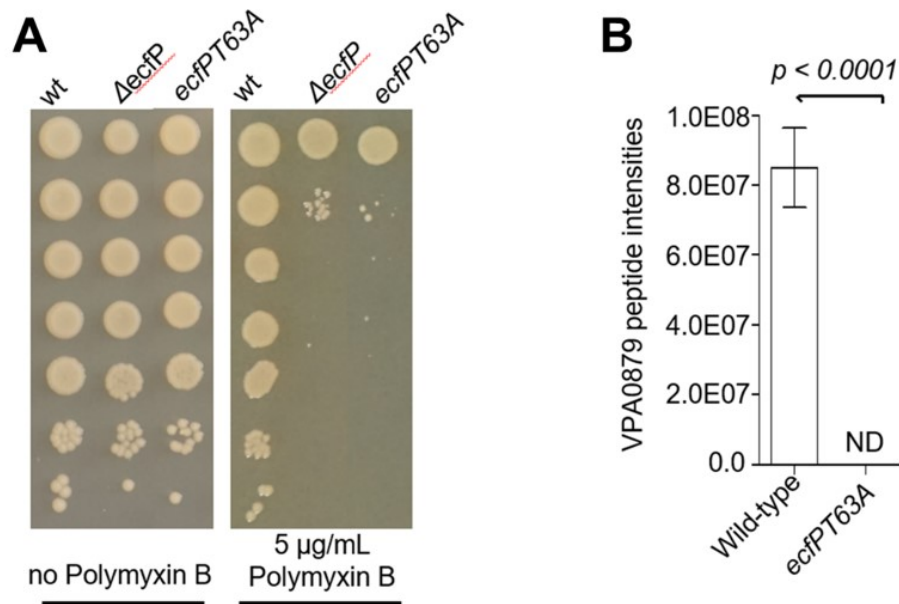


**Figure 27. The Thr63 residue of EcfP is essential for conferring polymyxin resistance to *V. parahaemolyticus*.** (A) Spot dilution assay of *V. parahaemolyticus* wild-type and strain *ecfPT63A* in the presence and absence of polymyxin B. (B) Bar-graph showing expression of protein VPA0879 detected by LC/MS global proteomics. “ND”: non-detected. Three biological replicates were performed and analyzed for this experiment. Error bars indicate SEM and p-values were calculated by Students t-test.

This is consistent with the finding that *ecfPT63A* has lost polymyxin resistance. To test if the T63A substitution indeed does prevent phosphorylation, sfGFP-EcfPT63A was immunoprecipitated and analyzed by MS/MS to detect for phosphorylation (Figure 28A) in a manner identical to that for wild-type sfGFP-EcfP (Figure 15, Figure 17A). Importantly, no phosphorylation was detected of the EcfPT63A derived peptide that corresponds to the phosphorylated peptide in wild-type EcfP (Figure 28A, Figure 15, Figure 17A). Furthermore, the EcfPT63A variant still interacted with PknT (Figure 28B), thus suggesting that EcfPT63A loss-of-function is not due to a defective interaction with PknT, but due to the absence of phosphorylation of residue Thr63.



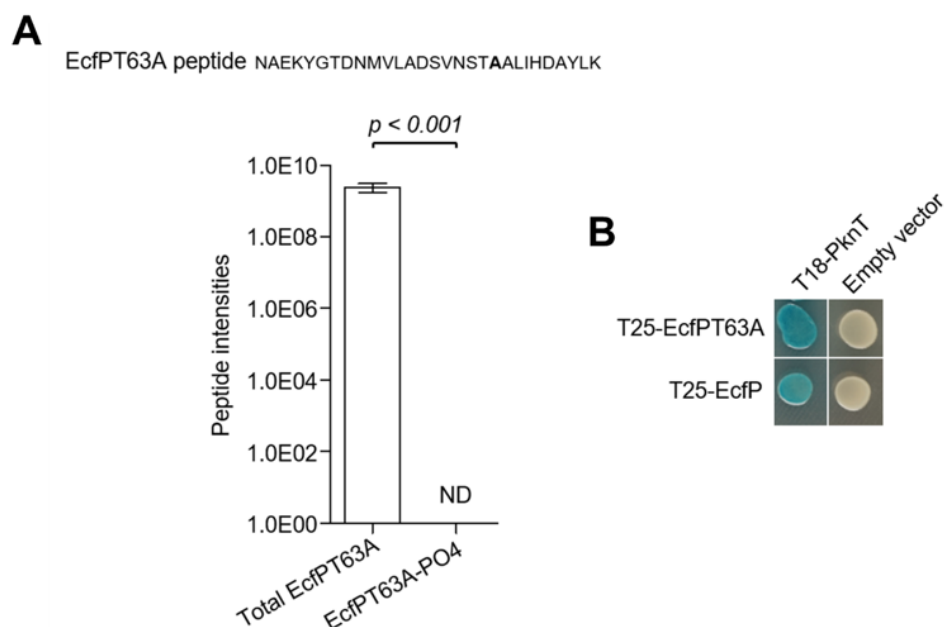


**Figure 28. EcfPT63A prevents phosphorylation of EcfP at residue 63 (T63).** (A) Upon IP-MS experiments of cells expressing sfGFP-EcfPT63A, label-free quantification was performed. Bar graph shows summed peptide intensities of total EcfPT63A and phosphorylated EcfPT63A peptides. . “ND”: non-detected. Three biological replicates were performed and analyzed for this experiment. Error bars indicate SEM and p-values were calculated by Students t-test. (B) BACTH assay testing for interaction between EcfP variant EcfPT63A and PknT.

Next, we substituted T63 for Glutamic acid, which is often used as a phosphomimetic residue, resulting in the variant EcfPT63E. We then constructed a *V. parahaemolyticus* strain where the native *ecfP* locus was replaced by *ecfPT63E*, encoding the protein variant EcfPT63E. When analyzing the susceptibility of this strain to polymyxin B, we observed a 100-fold increase in survival of the strain *ecfPT63E* in the presence of polymyxin compared to a  $\Delta ecfP$  strain (Figure 29), suggesting that the T63E substitution is phosphomimetic to some extent.

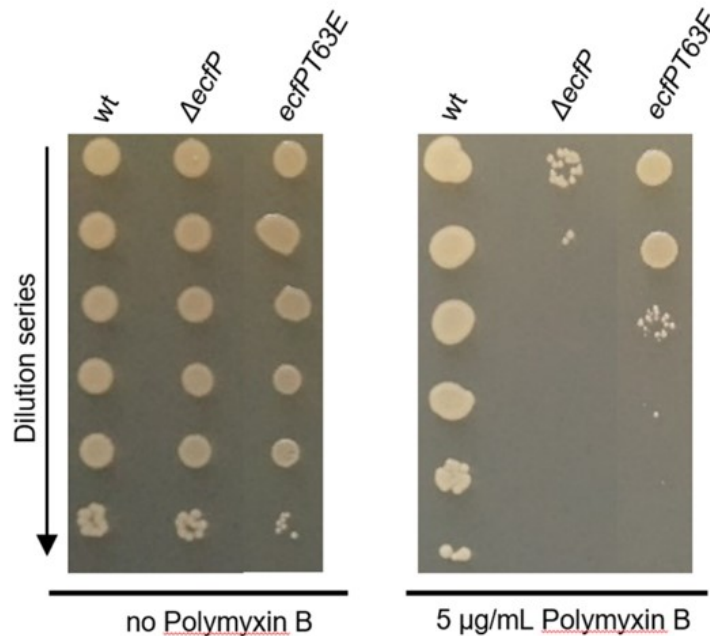


**Figure 29. A strain expressing EcfPT63E is less sensitive to polymyxin stress than an *ecfP* deletion.** Spot dilution assay of *V. parahaemolyticus* wild-type and mutant variants on LB growth medium in the presence and absence of Polymyxin B.

Altogether, these results indicate that PknT-mediated phosphorylation of EcfP at Thr63 positively regulates EcfP activity and is essential for EcfP function in regulating the cellular gene expression profile – ultimately mediating the *V. parahaemolyticus* polymyxin stress response and resulting in resistance to polymyxin antibiotics.

To test the importance of PknT kinase activity in regulating EcfP activity, we substituted the catalytically significant residue D202 in PknT for alanine. PknTD202A was defective for interaction with EcfP but retained its ability for self-interaction (Figure 30A). When replacing the native *pknT* locus with *pknTD202A*, the resulting strain became hypersensitive to polymyxins, similar to  $\Delta pknT$  (Figure 30B).

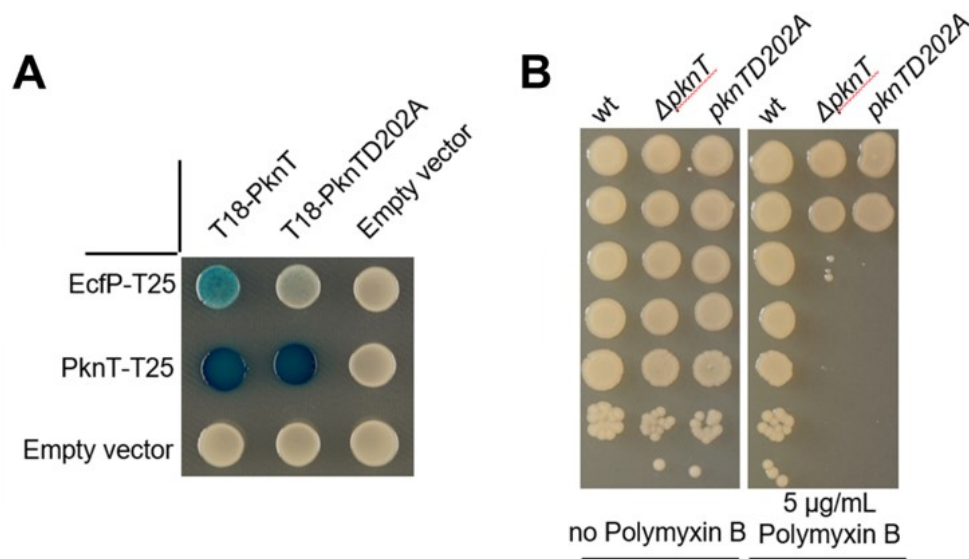


**Figure 30. The catalytic D202 residue of PknT is important for its interaction with EcfP and response to polymyxin.** (A) BACTH assay testing for interaction between EcfP and PknT variant PknTD202A. (B) Spot dilution assay of *V. parahaemolyticus* wild-type and strain *pknTD202A* in the presence and absence of Polymyxin B.

Importantly, EcfP was not phosphorylated in *pknTD202A* while the total level of EcfP was unchanged (Figure 31A-B) – a phenotype identical to a strain lacking *pknT* (Figure 17A, Figure 17C). This indicates the importance of the catalytic activity of PknT in EcfP phosphorylation, once again reiterating the role of the former as a true kinase regulating the activity and function of EcfP.

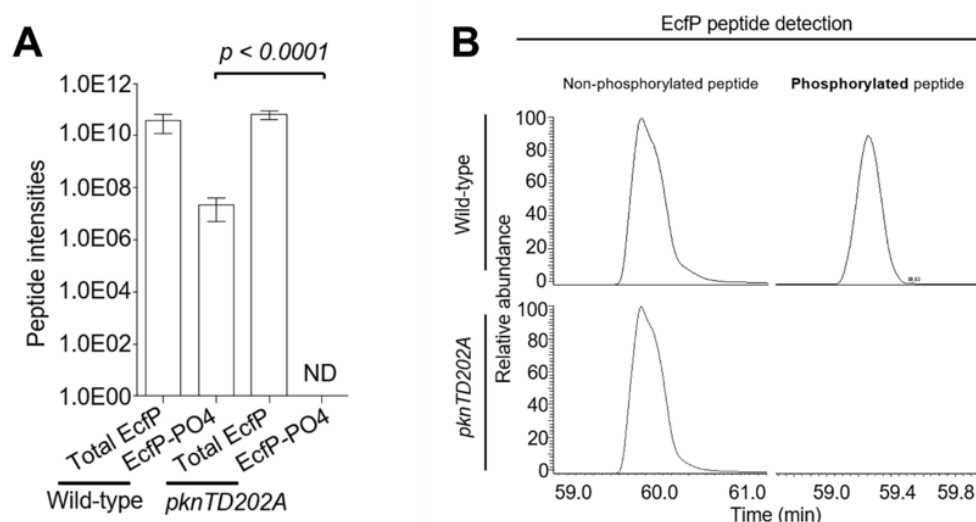


**Figure 31. The catalytic D202 residue of PknT is indispensable for phosphorylation of EcfP.** Bar graph showing summed detected peptide intensities of total EcfP and phosphorylated Thr63 EcfP peptide in wild-type and *pknTD202A* strain backgrounds upon co-IP-MS experiments of sfGFP-EcfP. “ND”: non-detected. Error bars indicate SEM and p-values were calculated by Students t-test. (B) Extracted ion chromatograms of a non-phosphorylated EcfP peptide and detected EcfP phosphopeptide in wild-type and *pknTD202A* strain backgrounds. Three biological replicates were performed and analyzed for all the above experiments.

### 3.2.6. Polymyxin stress induces PknT kinase activity and EcfP phosphorylation, resulting in expression of a polymyxin resistance determinant

Since the PknT/EcfP system is required for mediating the cellular response upon polymyxin stress, we hypothesized that addition of polymyxin to *V. parahaemolyticus* would induce the PknT/EcfP system. We tested EcfP phosphorylation levels by phostag gel analysis in wild-type cells ectopically expressing PknT in the presence and absence of polymyxin. In the absence of polymyxin, we observed that ~50% of EcfP was phosphorylated (Figure 32A-B) – a result very similar to that observed by MS/MS analysis (Figure 17A, green bars). Notably, in the presence of polymyxin there was a significant increase in the amount of phosphorylated EcfP (Figure 32A-B), indicating that addition of polymyxin to *V. parahaemolyticus* induced phosphorylation of EcfP.

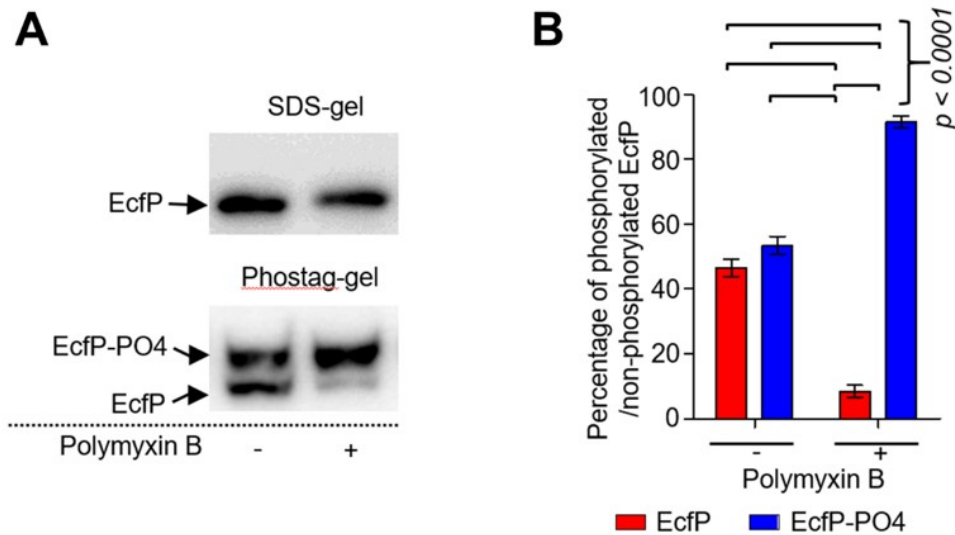


**Figure 32. Polymyxin induces phosphorylation of EcfP.** (A) Western-blot using anti-GFP antibodies on *V. parahaemolyticus* cells expressing sfGFP-EcfP after treatment or no treatment with polymyxin B. Cells were analyzed on phostag-gel to assay for EcfP phosphorylation. Samples were additionally analyzed on a standard SDS gel acting as a loading control. (B) Bar graph showing the percentage of phosphorylated and non-phosphorylated EcfP in cell treated with or not treated with polymyxin B antibiotic – quantification of experiments depicted in panel “A”. Three biological replicates were performed and analyzed for this experiment. Error bars indicate SEM and p-values were calculated by Student's t-test.

Using proteomics, we next analyzed the effect of polymyxin treatment on the expression of the EcfP-dependent polymyxin resistance determinant, VPA0879. Indeed, addition of polymyxin to *V. parahaemolyticus* cells also resulted in an  $\approx 8$ -fold increase in VPA0879 expression compared to non-treated cells (Figure 33). This indicates that *V. parahaemolyticus* responds to polymyxin treatment by activating kinase activity of PknT, resulting in phosphorylation-activation of EcfP and expression of the EcfP-dependent gene *vpa0789*, which is required for surviving polymyxin stress.

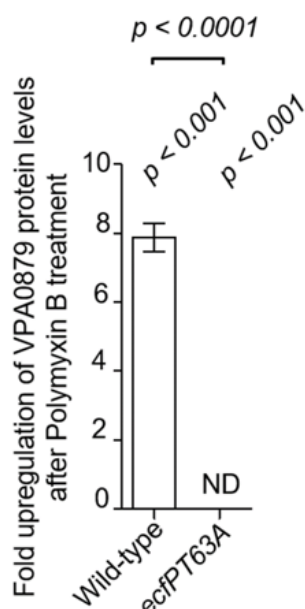


**Figure 33. Induction of VPA0879 upon polymyxin treatment is dependent on the Thr63 residue of EcfP.** Bar-graph showing the fold upregulation of VPA0879 protein levels after Polymyxin B treatment in *V. parahaemolyticus* wild-type and strain *ecfPT63A*. “ND”: non-detected. Three biological replicates were performed and analyzed for this experiment. Error bars indicate SEM and p-values were calculated by Students t-test.

### 3.2.7. EcfP Thr63 is part of a deviant non-charged motif that has replaced a usually negatively charged motif mediating interaction with RNAP

To further understand the mechanism by which phosphorylation regulates EcfP activity, we took a bioinformatics approach to determine what distinguishes ECF  $\sigma$  factors with an associated STK from non-STK associated  $\sigma$  factors. To this end we searched all genomes deposited in the NCBI database for proteins homologous to EcfP and filtered for sequences encoded in close genomic proximity (<5000bp) to a protein homologous to PknT. Interestingly, most of the resulting 1,603 non-redundant protein sequences were classified as members of three phylogenetically distinct ECF  $\sigma$  factor groups (Figure 34, ring #1): ECF43 (52 %, including EcfP), ECF59 (4.5 %) and ECF60 (4.5 %), all members of which share a conserved STK in the genomic neighborhood of the ECF, as noted earlier (Mascher, 2013; Staroń et al., 2009). The remaining ECF sequences (39 %) belonged to a diverse range of ECF  $\sigma$  factor groups known to be regulated by anti- $\sigma$  factors or other characterized mechanisms.

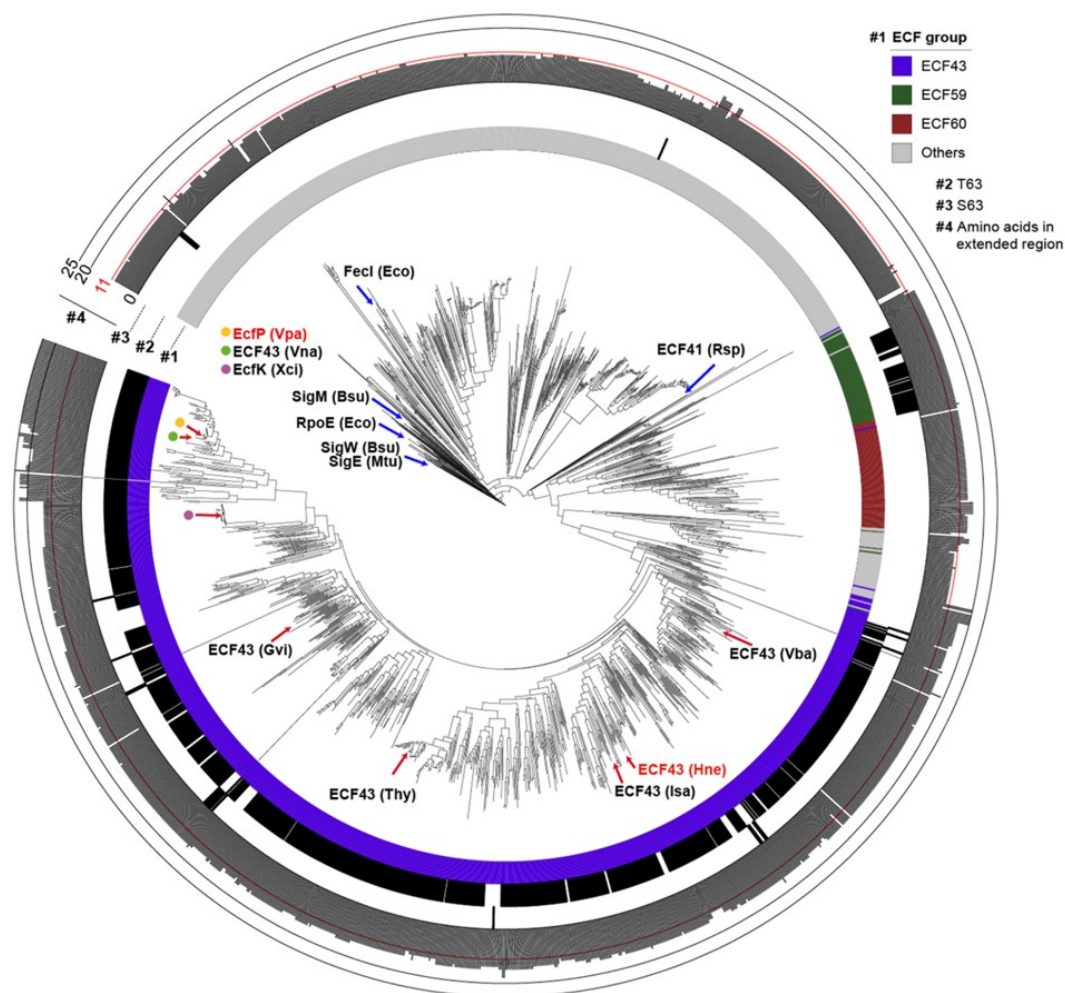


**Figure 34. Phylogenetic tree depicting the salient features of ECF  $\sigma$  factors associated with STKs.** Phylogenetic tree of homologs of EcfP. Ring #1 represents ECF  $\sigma$  factor groups. Ring #2 and #3 depict the presence of threonine or serine residues, respectively, in the position equivalent to Thr63 of EcfP. Ring #4 indicates the length of the region that connects  $\sigma$ 2.1 and  $\sigma$ 2.2, enclosed between dashed lines in the multiple-sequence alignment of Figure 36. Extended variants, present members of ECF43, ECF59 and ECF60, are those with length greater than 11. The closest homologs to EcfP contain longer extensions, of approx. 25 amino acids. Red arrows and dots indicate specific ECFs from ECF43. ECFs that are not regulated by STK are indicated by blue arrows. Throughout this figure (and Figure 36), the naming code for the species is as follows: Bsu = *Bacillus subtilis*, Eco = *Escherichia coli*, Fma = *Fuerstia marisgermanicae*, Gob = *Gemmata obscuriglobus*, Gvi = *Gloeobacter violaceus*, Hne = *Hyphomonas neptunium*, Isa = *Ideonella sakaiensis*, Mtu = *Mycobacterium tuberculosis*, Pbo = *Paludisphaera borealis*, Ppi = *Planctomicrobium piriforme*, Rba = *Rhodopirellula baltica*, Rsp = *Rhodobacter sphaeroides*, Sac = *Singulisphaera acidiphila*, Thy = *Thermomonas hydrothermalis*, Vba = *Verrucomicrobiaceae* bacterium, Vna = *Vibrio natriegens*, Vpa = *Vibrio parahaeomolyticus*, Wma = *Wenzhouxiangella marina* and Xci = *Xanthomonas citri*.

Further bioinformatics analysis revealed that, while the kinase domain was conserved, STKs associated with  $\sigma$  factors belonging to ECF43 are fused to a broad array of predicted sensing modules (Figure 35). This could indicate that STKs associated with ECF43  $\sigma$  factors are regulated by distinct inputs and involved in



## Results – Part I

mediating cellular responses to a diverse range of external signals – a result, which will be revisited in more detail in the “Discussion” section (Section 3.3).

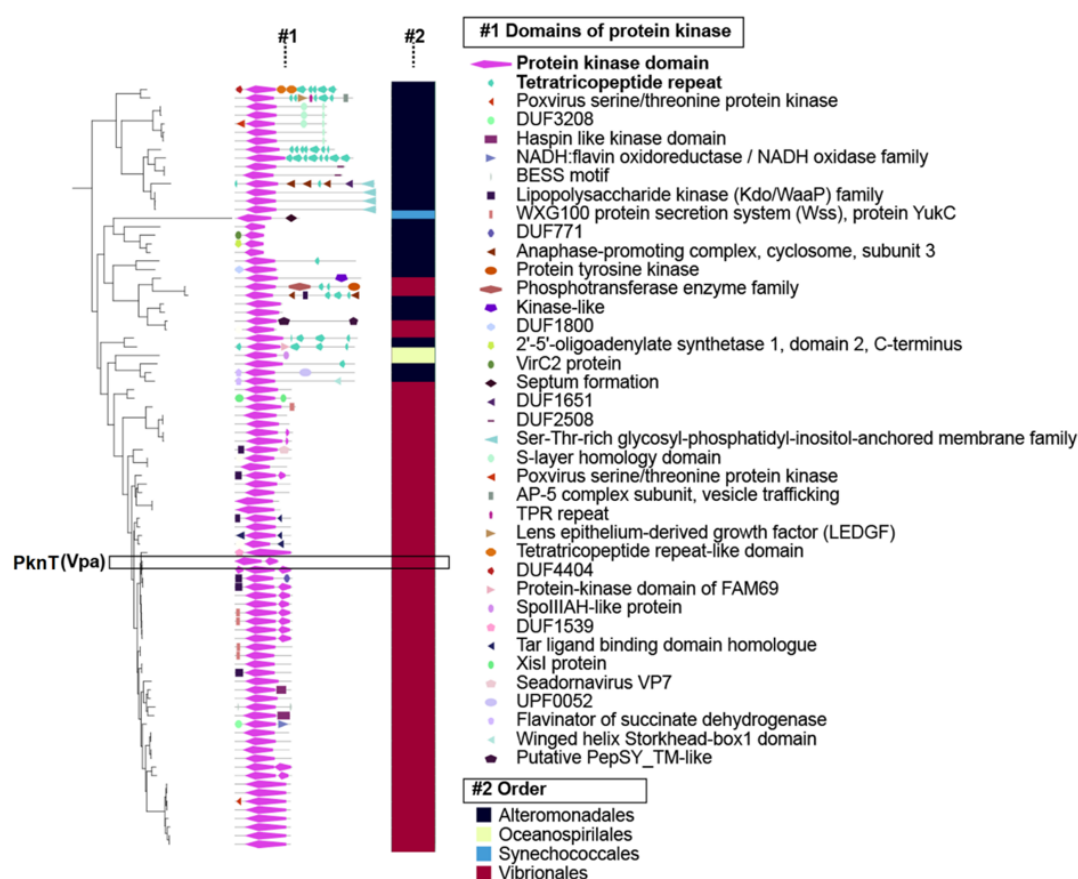


**Figure 35. Different members of ECF43 are associated to a distinct protein kinase domain architecture.** The phylogenetic tree on the left side is a fragment of the ECF tree of the homologs of EcfP show in Figure 34. For simplicity, only the closest variants to EcfP are shown. Group #1 depicts the position and the Pfam domains found in the STK associated to each ECF. Group #2 shows the order of the organisms of origin of the proteins. The extracytoplasmic input domains, located in C-termini from the protein kinase domain, vary across protein kinases, indicating a potential response to different stimuli or a different sensing mechanism.

ECF  $\sigma$  factors share a characteristic protein domain architecture consisting of two regions,  $\sigma 2$  and  $\sigma 4$ , that mediate interaction to the RNAP core enzyme and are responsible for promoter recognition. The  $\sigma 2$  domain consists of four regions ( $\sigma 2.1$  -  $\sigma 2.4$ ) of which  $\sigma 2.1$  and  $\sigma 2.2$  form two anti-parallel  $\alpha$ -helices that interact with the conserved clamp helices of the  $\beta'$  subunit of the RNA polymerase core complex (Lane & Darst, 2010). The first part of region  $\sigma 2.2$ , with the consensus sequence DAEDLXQETF (Figure 36) has been found to be essential for RNAP core binding in different  $\sigma$  factors (Joo et al., 1997; Sharp et al., 1999; Wilson & Lamont, 2006). This binding relies on the negative residues that interact with the positively charged ones of the  $\beta'$  clamp helices (Lane & Darst, 2010; L. Li et al., 2019). Our analysis revealed that in ECF43  $\sigma$  factors,





## Results – Part I

(Figure 36, Figure 37). Most strikingly, the STTA motif includes the phosphorylated Thr63 residue of EcfP (underlined T in STTA) and corresponds to a highly conserved (88.8%) Thr residue in an alignment of ECF43 proteins, while no Thr residue was found at this position in other ECF groups (Figure 34, ring #2, Figure 36, Figure 37). Indeed, this position typically encodes a negatively charged amino acid in canonical ECF  $\sigma$  factors (Figures 35, 36). Interestingly, our analysis showed that this residue is replaced by Ser in members of ECF59 (61.4%) (Figure 34, ring #3, Figure 36, Figure 37), while the other ECF group that shares microsynteny with STKs, ECF60, contains a conserved Ser (92%) in a position that typically contains a negative charge and corresponds to Glu60 in SigH from *Mycobacterium tuberculosis* (Figure 36, Figure 37), suggesting this Ser residue could be a potential target for phosphorylation in the ECF group, ECF60.]

	% conservation of the DAED motif amongst ECF groups										% conservation of E60					
	D53			A54	E55					D56			E60			
	%D	%E	Total	%A	%D	%E	%S	%T	Total	%D	%E	Total	%D	%E	%S	Total
ECF43	16.0	3.8	19.8	27.0	0.2	0.1	2.3	88.8	91.4	5.1	10.7	15.9	12.2	83.6	0.5	96.2
ECF59	54.3	20.0	74.3	8.6	8.6	4.3	61.4	0.0	74.3	98.6	0.0	98.6	14.3	64.3	1.4	80.0
ECF60	96.1	1.3	97.4	9.2	9.2	75.1	0.0	0.0	84.3	96.1	2.6	98.7	1.3	1.3	92.0	94.7
non-STK associated	33.8	10.3	44.1	74.6	16.0	62.0	0.0	0.0	78.2	66.8	31.1	98.2	16.7	83.3	0.0	100

**Figure 37. Conservation of key negatively charged residues within  $\sigma 2.2$  in different ECF groups.** Conservation of the DAED motif and other negatively charged residues of  $\sigma 2.2$ , responsible for mediating interaction to the  $\beta'$  subunit of the core RNAP enzyme. Amino acid coordinates refer to SigH from *M. tuberculosis*.

### 3.2.8. Phosphorylation of EcfP at Thr63 enables its interaction with $\beta/\beta'$ of RNAP

To better understand the interaction between EcfP and the RNA polymerase complex, we modeled the structure of EcfP using the already published data of SigH from *M. tuberculosis* in the RNA polymerase open complex as a template (PDB: 5ZX2, (L. Li et al., 2019)). The results of the modeling indicated that the residue Thr63 of EcfP lies in the same position as the residue Glu (E) residue of the DAED motif of SigH (Figure 38), suggesting that they may interact similarly with the RNA polymerase complex – that is, with the clamp helices of the  $\beta'$  subunit. However, the function of the extended region observed in members of ECF43 between  $\sigma 2.1$  and  $\sigma 2.2$  is unclear. SigH (in complex with the RNAP) contacts the promoter discriminator at base G(-4) with P51 (L. Li et al., 2019), located at the end of the alpha helix of  $\sigma 2.1$  and in close proximity to the loop that connects it to the  $\sigma 2.2$  helix. Whether the extended region between  $\sigma 2.1$  and  $\sigma 2.2$  in EcfP has a similar function is unclear. Given that this extended region is not present in SigH, the current model of EcfP lacks confidence in assigning a conformation or a secondary structure to this area.

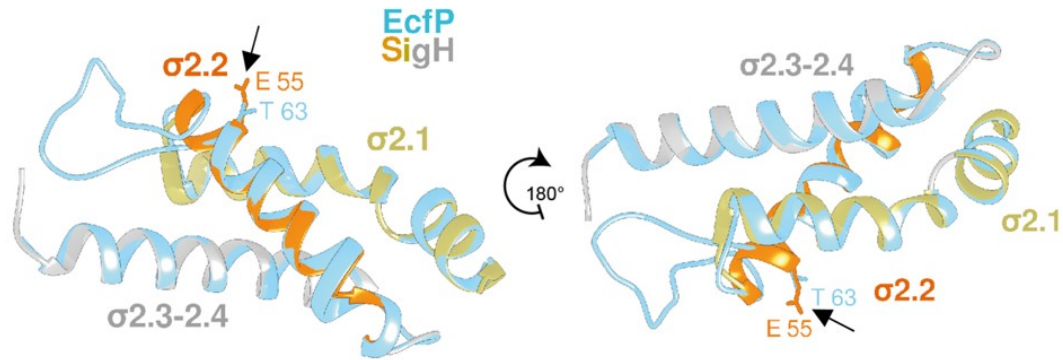


**Figure 38. Overview of the predicted structure of  $\sigma 2$  domain of EcfP overlaid with SigH from *M. tuberculosis* in the RNAP open complex.** EcfP structure was modelled with Swiss-model 46 using SigH from *M. tuberculosis* as a template (PDB: 5ZX2 31). Residue Thr63 (EcfP) and Glu55 (SigH) are in the same orientation, indicating that Thr63 is in close proximity to the positively charged surface of the clamp helices of the  $\beta'$  subunit.

Based on these results, we hypothesized that the non-phosphorylated EcfP should have a low affinity for RNAP, due to the absence of negative charges usually provided by the DAED motif. Particularly, we predicted that phosphorylation of EcfP on the highly conserved Thr63 restores and mimics the negative charge usually provided by the DAED motif, thereby allowing for interaction with the positively charged residues on the  $\beta'$  clamp helices of RNAP. The clamp helices of RNAP are conserved and  $\sigma$  factors from *B. subtilis* and *E. coli* are interchangeable to a large degree (Helmann & Chamberlin, 1988; Murakami, 2015; Sharp et al., 1999; Werner & Grohmann, 2011b). Thus, as antibodies against the *E. coli* RNAP  $\beta/\beta'$ -subunits are commercially available, we tested interaction of EcfP with *E. coli* RNAP  $\beta/\beta'$  by performing co-immunoprecipitation of *E. coli*  $\beta/\beta'$  with sfGFP-EcfP using anti-GFP beads (Figure 39A-D, Figure 40). Importantly, we know that no phosphorylation of EcfP occurs in *E. coli* in the absence of PknT, however, when co-expressed with PknT we found ~65% of EcfP to be in a phosphorylated state (Figure 19A-B).

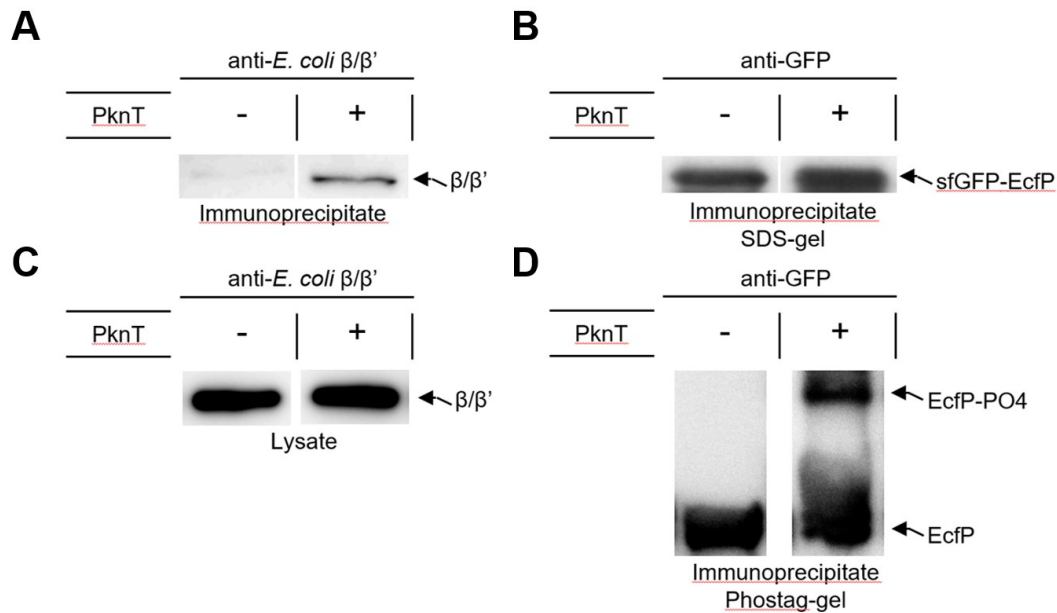


**Figure 39. Phosphorylation of EcfP enables its interaction with  $\beta/\beta'$  of RNAP.** Analysis for co-immunoprecipitation of *E. coli*  $\beta/\beta'$  with sfGFP-EcfP using anti-GFP beads in the absence and presence of PknT. (A) Westernblot of immunoprecipitate using anti-*E. coli*  $\beta/\beta'$  antibodies in the presence or absence of PknT. (B) Westernblot of immunoprecipitate analyzed in (A) on an SDS gel. (C) Westernblot of cleared lysates using anti-*E. coli*  $\beta/\beta'$  antibodies in the presence or absence of PknT. (D) A phostag-gel using anti-GFP antibodies in the presence or absence of PknT. Three biological replicates were performed and analyzed for the above experiments.

Thus, sfGFP-EcfP was expressed in *E. coli* in the presence or absence of PknT, followed by immunoprecipitation of sfGFP-EcfP. Subsequently, immunoprecipitated samples were tested for co-purification of *E. coli*  $\beta/\beta'$ -subunits by Western blot analysis using anti- $\beta/\beta'$  antibodies. As a control, samples were also analyzed by Western blot analysis using anti-GFP antibodies, which showed that equal amounts of sfGFP-EcfP was immunoprecipitated independently of the presence or absence of co-expression with PknT (Figure 39B). Furthermore, Western blot analysis showed that presence or absence of PknT did not influence  $\beta/\beta'$  levels, as equal amounts of  $\beta/\beta'$  was present in cleared *E. coli* lysates prior to the immunoprecipitation (Figure 39C). Phostag-gel analysis of immunoprecipitated samples showed that immunoprecipitated EcfP was phosphorylated only in the presence of PknT and not in its absence (Figure 39D). Importantly, ~20 fold more  $\beta/\beta'$  was co-immunoprecipitated with EcfP in the presence of PknT compared to its absence (Figure 39A, Figure 40).

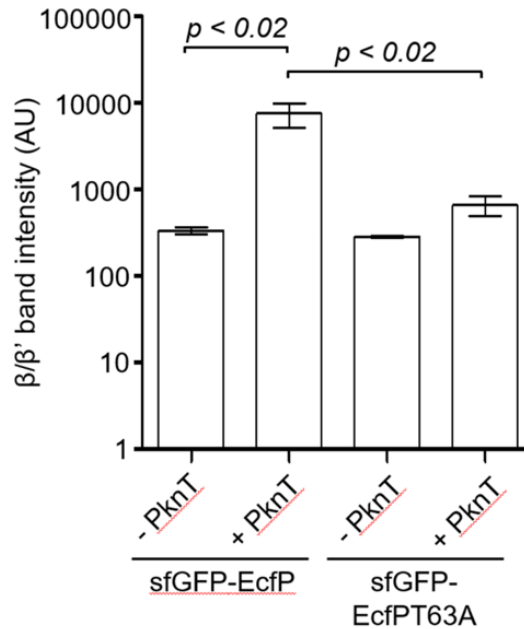


**Figure 40. Interaction of EcfP with the RNAP is dependent on phosphorylation of the Thr63 residue.** Bar graph showing the quantification of the amount of *E. coli*  $\beta/\beta'$  in immunoprecipitated samples of sfGFP-EcfP and sfGFP-EcfPT63A, respectively, in the absence or presence of PknT. Three biological replicates were performed and analyzed for this experiment. Error bars indicate SEM and p-values were calculated by Students t-test.

Furthermore, we performed an identical experiment using sfGFP-EcfPT63A, which is non-phosphorylated even when co-expressed with PknT (Figure 28A). The immunoprecipitation using sfGFP-EcfPT63A showed no significant difference in  $\beta/\beta'$  levels co-immunoprecipitated with EcfPT63A in the absence or presence of PknT (Figure 40). Thus,  $\beta/\beta'$  is only significantly enriched during co-immunoprecipitation with EcfP when EcfP is in a phosphorylated state. Altogether, these results indicate that EcfP directly interacts with the  $\beta/\beta'$  of RNAP and that EcfP phosphorylation by PknT stimulates and enhances this interaction.

This supports the notion that phosphorylation of EcfP at Thr63 by PknT activates EcfP and facilitates its interaction with the RNAP core-enzyme. In support of this mode of action, addition of polymyxin to *V. parahaemolyticus*, which induces EcfP phosphorylation (Figure 32A-B), led to significantly increased co-purification of  $\beta$  and  $\beta'$  subunits of RNAP with sfGFP-EcfP (Figure 41).

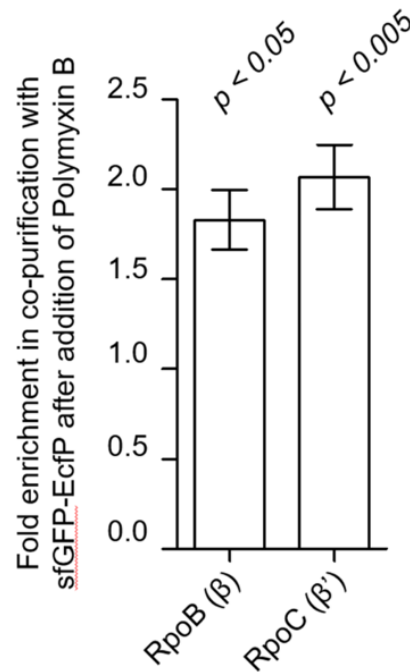
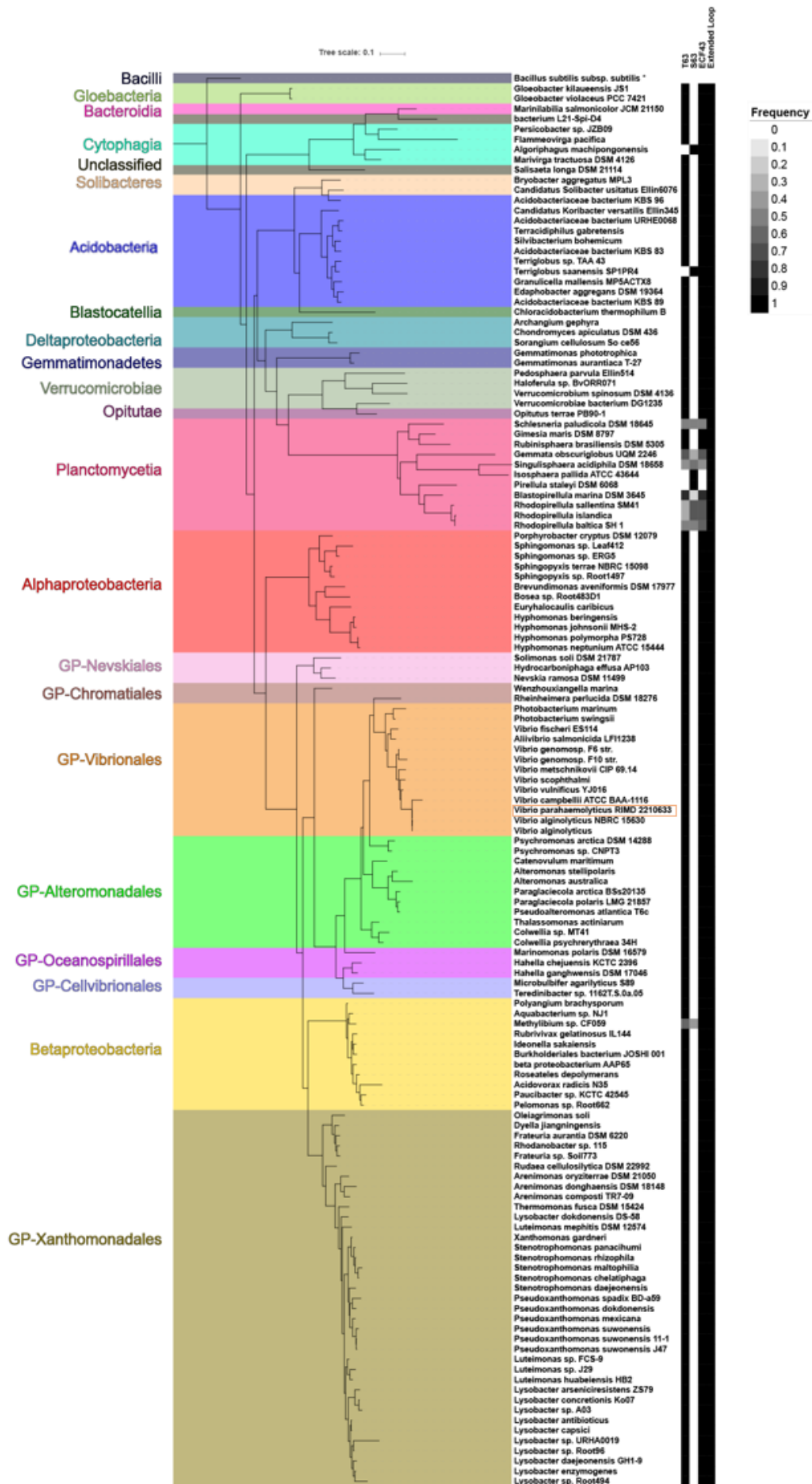


**Figure 41. Polymyxin enhances the interaction of EcfP with the RNAP.** Bar graph showing the fold enrichment in co-purification of  $\beta$  and  $\beta'$  subunits of RNAP with sfGFP-EcfP after addition of Polymyxin B. Three biological replicates were performed for this experiment. Error bars indicate SEM and p-values were calculated by Students t-test.

### 3.2.9. $\sigma$ factor phosphorylation occurs in distantly related bacteria

Our bioinformatics results suggest that this type of transcriptional regulation by ECF  $\sigma$  factor phosphorylation is a general mechanism employed by many classes of bacteria, such as  $\gamma$ -,  $\alpha$ - and  $\Delta$ -proteobacteria, Planctomycetia, Acidobacteria, Verrucomicrobiae and several others (Figure 42), which all encode ECF  $\sigma$  factors with an extended region between  $\sigma 2.1$  and  $\sigma 2.2$ , have a degenerate DAED motif replaced by a deviant non-charged motif, and harbor the highly conserved Thr63 that is the site of phosphorylation in EcfP (Figure 34, Figure 36, Figure 37, Figure 42).





\* B. subtilis is used as outlier species to build the phylogenetic tree

**Figure 42. Phylogenetic tree of species encoding EcfP homologs in their genomes.** The phylogenetic tree represents the phylogenetic distance (as calculated by IQ-tree using default parameters over a MSA computed by ClustalO) of the 16S rDNA sequences of representative and reference organisms (as defined by NCBI), containing an ECF  $\sigma$  factor with Ser or Thr in a position equivalent to Thr63 in EcfP of *V. parahaemolyticus*. In most of the cases, there is a perfect correlation between tree architecture and class of the organisms, indicated by the shades of the tree and the accompanying labels. The tree was rooted in the 16S rDNA of *Bacillus subtilis* (used as outlier), since Firmicutes do not contain any ECF sequence with Ser/Thr63. The heatmap on the right shows the frequency of ECF variants with S63, T63, with an extended region between  $\sigma 2.1$  and  $\sigma 2.2$  and their membership to group ECF43. Frequencies identical to 1 (=100%) indicate that all ECFs in this species exhibit the respective feature, while frequencies below 1 indicate that there exist other EcfP homologs in the species, which do not exhibit the given feature.

To test if  $\sigma$  factor phosphorylation is a general mechanism in bacteria, we analyzed for  $\sigma$  factor phosphorylation in the distantly related  $\alpha$ -proteobacterium *Hyphomonas neptunium*. Based on our bioinformatics analysis we identified a putative ECF  $\sigma$  factor (HNE1495) flanked by a putative STK (HNE1496) in *H. neptunium*, which we here refer to as EcfHn and STKHn, respectively. We translationally fused sfGFP to the N-terminus of EcfHn (sfGFP-EcfHn) and expressed it ectopically in the heterologous host *E. coli* in the presence or absence of the predicted kinase STKHn. When analyzed on phostag gels, we observed a clear phosphorylation band of EcfHn in the presence of STKHn, but not in its absence (Figure 43A). Additionally, we performed immunoprecipitation of EcfHn expressed in *E. coli* in the presence and absence of STKHn followed by MS/MS analysis. Importantly, we identified one EcfHn phospho-peptide (Figure 43B) when EcfPHn was expressed in the presence of STKHn, but not in its absence (Figure 43C).



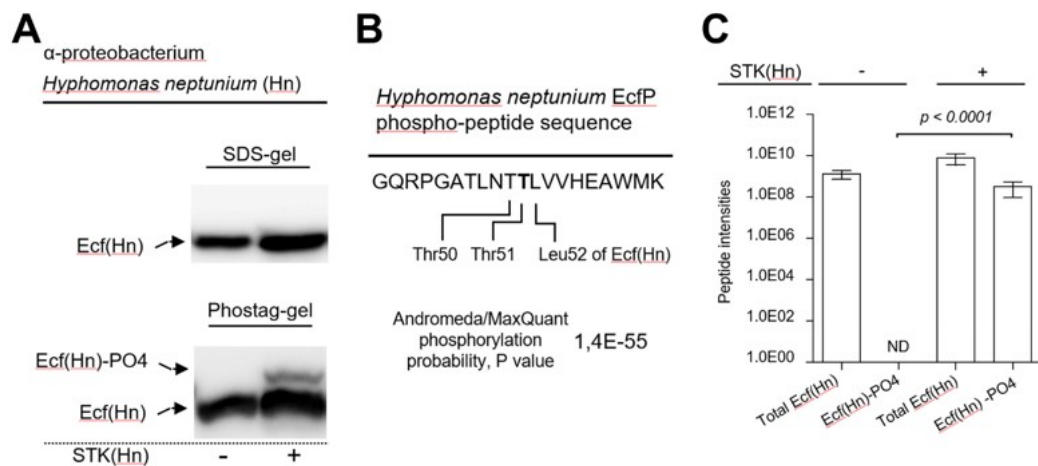


**Figure 43. ECF  $\sigma$  factor phosphorylation in *Hyphomonas neptunium*.** (A) Western-blot using anti-GFP antibodies on *E. coli* cells ectopically expressing the ECF43  $\sigma$  factor EcfHn N-terminally fused to sfGFP (sfGFP-EcfHn) in the presence or absence of ectopic expression of the predicted STK, STKHn. Cells were analyzed on phostag gel to assay for EcfHn phosphorylation. Samples were additionally analyzed on a standard SDS gel acting as a loading control. (B) Sequence of the detected phosphorylated EcfHn peptide with its corresponding phosphorylation probability as calculated by Andromeda embedded in MaxQuant. (C) Upon co-IP-MS experiments using anti-GFP beads of *E. coli* strains expressing sfGFP-EcfHn, label-free quantification was performed. Bar graphs show summed peptide intensities of total sfGFP-EcfHn and phosphorylated EcfHn peptides in the absence (-) or presence (+) of ectopic overexpression of STKHn. "ND": non-detected. Three biological replicates were performed for each experiment. Error bars indicate SEM and p-values were calculated by Student's t-test.

To further identify at which residue EcfHn is phosphorylated, we expanded on our MS/MS analysis of immuno-purified sfGFP-EcfHn. The MS/MS spectrum clearly showed that the detected phosphopeptide was phosphorylated on one specific threonine (Thr) residue – particularly Thr51 of EcfHn (Figure 44). Strikingly, Thr51 of EcfHn corresponds exactly to the highly conserved and phosphorylated residue Thr63 of EcfP from *V. parahaemolyticus* (Figure 36).

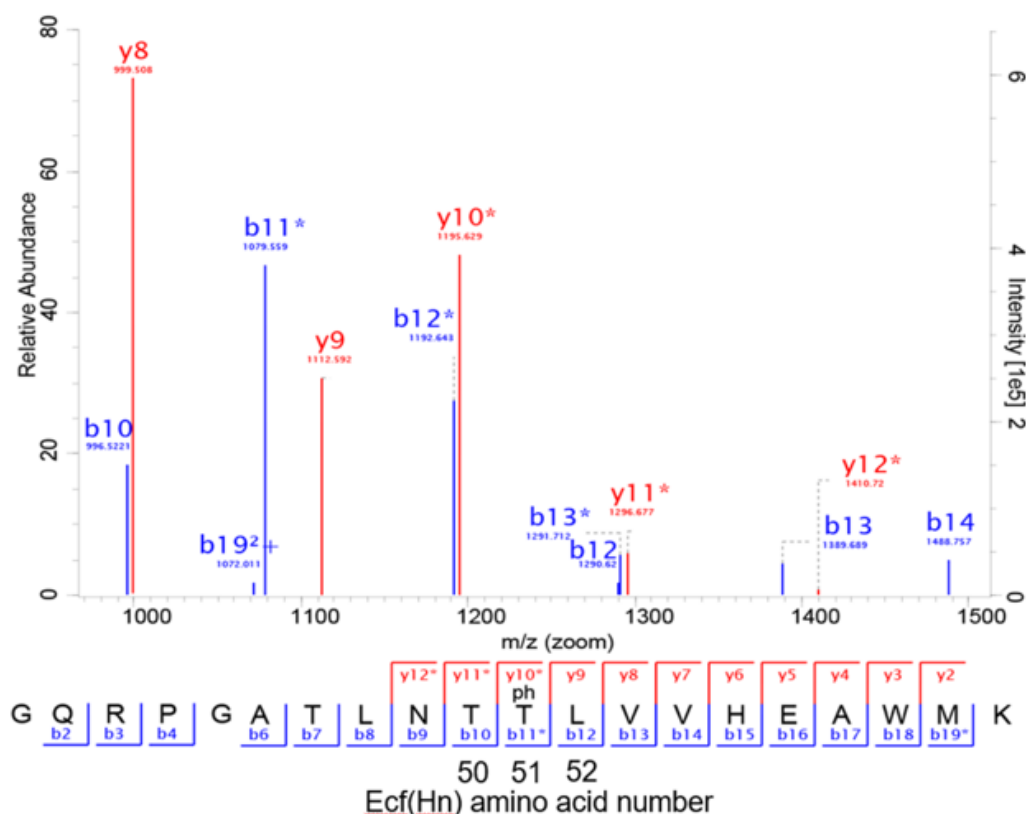


**Figure 44. Identification of the phosphorylated residue in the ECF  $\sigma$  factor of *H. neptunium*.** MS/MS spectrum of the mapped phosphorylation site in the phosphopeptide of ECF  $\sigma$  factor EcfHn. The identified b- and y-fragment ions are shown in blue and red, respectively. Both the b-ion and y-ion series allowed identification of the phosphorylation modification at residue Thr51. A neutral loss of the phosphate (H<sub>3</sub>PO<sub>4</sub>-98Da) ion was detected and the neutral loss peak is marked with an asterisk.

These results show that ECF  $\sigma$  factor phosphorylation by threonine kinases is not restricted to the  $\gamma$ -proteobacterium *V. parahaemolyticus* but also occurs in the distantly related  $\alpha$ -proteobacterium *H. neptunium*. Similar to EcfP from *V. parahaemolyticus*, and almost all other ECFs from group ECF43, EcfHn also carries the deviant region between  $\sigma$ 2.1 and  $\sigma$ 2.2 (Figure 36) that we have identified here, where the usually negatively charged DEAD motif has been replaced with a non-charged motif – NTTL in the case of EcfHn. This NTTL motif includes Thr51 (bold and underlined), which is phosphorylated in the presence of the kinase STKHn. These results further support that  $\sigma$  factor activation by  $\sigma$  phosphorylation is a widespread mechanism across the bacterial kingdom.

### 3.3. Discussion

#### 3.3.1. Overview of ECF $\sigma$ factor phosphorylation regulation transcription

Over the last 25 years, several paradigms in regulation of ECF  $\sigma$  factor activity have been reported, most of which serve to sequester the  $\sigma$  factor in an inactive state when its action is not warranted (Brooks & Buchanan, 2009; M. S. Paget, 2015; Treviño-Quintanilla et al., 2013). The mechanism of  $\sigma$  factor regulation that we report here is fundamentally different from previously characterized mechanisms. Our data indicate that in *V. parahaemolyticus*, regulation of EcfP does not rely on the action of an anti- $\sigma$  factor. Instead, our results indicate that EcfP is intrinsically inactive due the lack of the DAED motif in the  $\sigma$ 2.2 region, which imparts the the negative charges that usually mediate interaction to the RNAP. In fact, the DAED motif of EcfP has been replaced by a deviant non-charged ST**I**A motif including the highly conserved Thr63 residue (bold and underlined) undergoing phosphorylation by PknT. Our results suggest that only upon direct phosphorylation by PknT on Thr63, the negative charge in the STTA motif of  $\sigma$ 2.2 is restored. Phosphorylation results in EcfP activation as it reestablishes EcfP's ability to interact with  $\beta'$  of RNAP in formation of the RNAP holoenzyme, which in turn is directed to EcfP specific promoters (Figure 45).

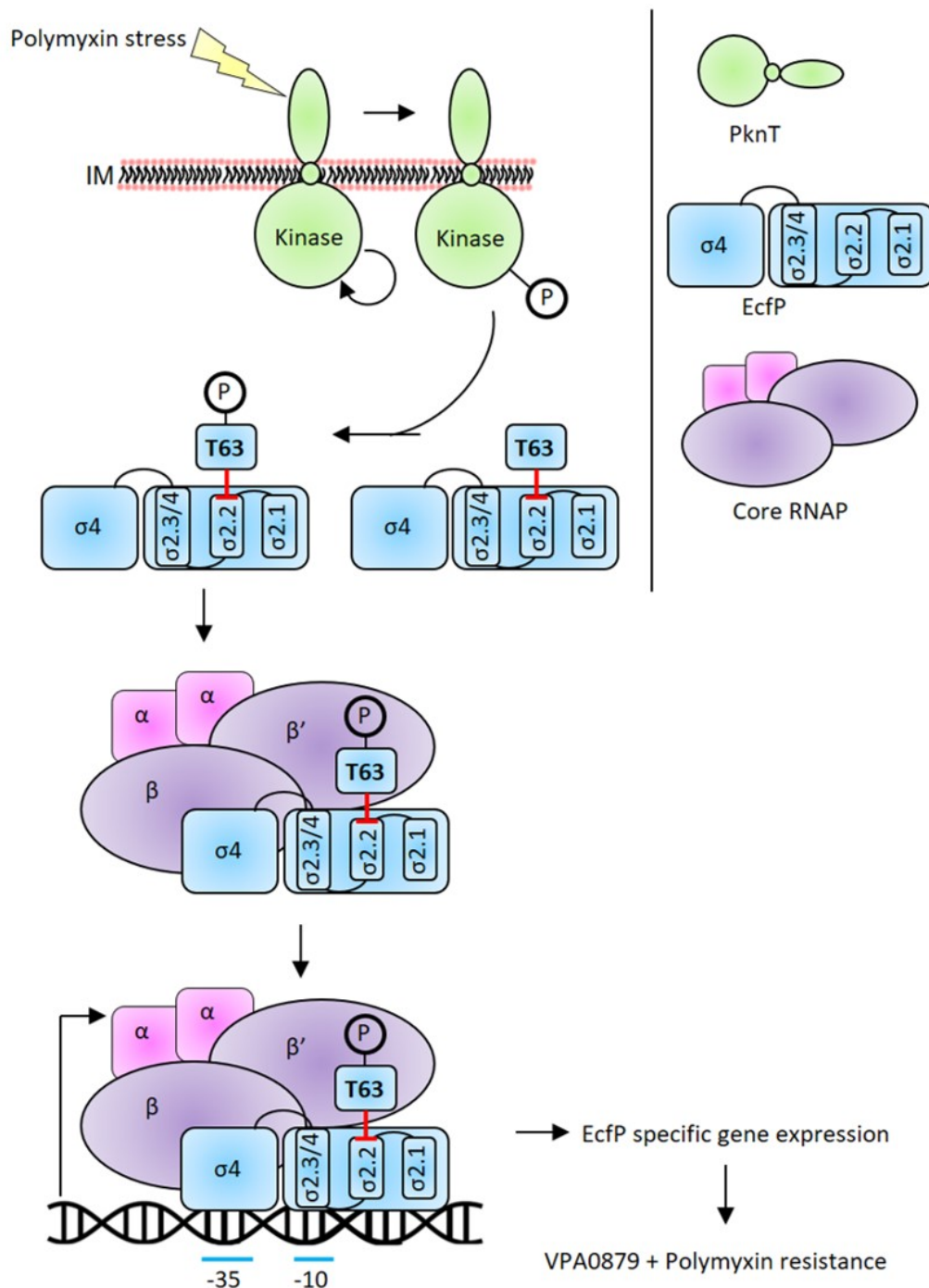


**Figure 45. Transcriptional regulation by  $\sigma$  factor phosphorylation.** Schematic depicting the  $\sigma$  factor phosphorylation signaling cascade that mediates transcriptional regulation. The figure is discussed in detail in the text.

### 3.3.2. Importance of the highly conserved Thr63 residue of EcfP

Our results indicate the nearly invariant nature of the Thr63 residue of EcfP that is being phosphorylated by PknT towards interaction with the RNA polymerase. In fact,

mutation of T63 to alanine (EcfPT63A) did not result in enhanced binding of EcfP with the RNA polymerase. Additionally, studies on the *ecfPT63E* strain, encoding the phosphomimetic variant EcfPT63E only resulted in partial complementation of the polymyxin sensitivity seen in the  $\Delta$ *ecfP* mutant, further highlighting the importance of this residue. While phosphomimetic studies are widely used, it is also possible that these substitutions could result in changes within the structure of the protein, given the differences in the side chain moieties.

The high conservation of this T63 residue among ECF  $\sigma$  factors, with associated STKs (group ECF43) suggests that this mechanism of transcriptional activation by phosphorylation is a widespread mechanism in bacteria. Indeed, we have also shown phosphorylation of an ECF  $\sigma$  factor in the distantly related alpha-proteobacterium, *H. neptunium* at a Thr residue corresponding to that of T63 of EcfP by its cognate STK.

Interestingly, our bioinformatics results also suggest that  $\sigma$  factor phosphorylation might occur in the ECF groups, ECF59 and ECF60. Both groups show microsynteny to STKs and, in the case of ECF59, the negatively charged glutamate of the DAED motif has been substituted for a non-charged Ser residue, suggesting this group could be regulated by Ser phosphorylation at this site. In the case of ECF60, the negative charges of the DAED motif are conserved, but a another negative residue downstream in helix  $\sigma$ 2.2 that performs a similar function as the DAED motif is substituted by a conserved Ser (92%), suggesting that this group could be regulated by Ser phosphorylation on this particular site. Future analyses will be required to test these predictions experimentally.

### **3.3.3. Reception of the external polymyxin stimulus by the PknT/EcfP system**

The results presented here show that the PknT/EcfP system is required for the sensing of polymyxin-induced cell envelope stress and to ensure polymyxin resistance in *V. parahaemolyticus*. This organism responds to polymyxin treatment by elevated kinase activity of PknT, resulting in phosphorylation-activation of EcfP and expression of the EcfP dependent gene *vpa0789*, which is required for polymyxin resistance (Figure 45). While the function of most STKs in bacteria is only beginning to be revealed (Pereira, Goss, & Dworkin, 2011a), our results have now uncovered a specific function for STKs in bacteria, namely the direct regulation of ECF  $\sigma$  factor activity via phosphorylation at a specific Thr residue in response to polymyxin antibiotics.

The mechanism by which polymyxin stress is sensed and how it regulates PknT activity remains to be elucidated. However, PknT does possess a C-terminal domain, which is positioned in the periplasm. It is intriguing to speculate that this domain could exert a regulatory role on PknT kinase activity, either via interactions with other sensory proteins or by direct sensing of polymyxin molecules. Whether resistance to polymyxin antibiotics, as in the case of *V. parahaemolyticus*, is a conserved response in members of ECF43 is unclear. An analysis of the extracytoplasmic domains of the protein kinase associated to members of ECF43 revealed a broad array of sensing modules, indicating either the direct sensing of different ligands or a different sensing mechanism involving a distinct set of intermediate proteins (Figure 34). The closest homologs to PknT appear only in Vibrionales and contain an extracytoplasmic region of ~100 amino acids that does not feature any annotated domain. These proteins could indeed share a similar ligand. Other members of ECF43 instead contain longer extracytoplasmic regions (approx. 400 amino acids) with tetratricopeptide repeats, domains homologous to the S-layer (Pfam: PF00395) or Ser-Thr-rich glycosyl-phosphatidylinositol-anchored membrane protein (Pfam: PF10342).

Even though it is difficult to assign an input cue to ECF  $\sigma$  factors from *in silico* studies, here we show that this signal is likely different for members of ECF43, but could be conserved in members of Vibrionales, suggesting their evolution from an ancient variant and their putative specialization to respond to polymyxin antibiotics. This indicates that similar to two-component systems, the signal transduction mechanism is conserved in PknT/EcfP homologs, while the sensory input and the regulatory outputs are modular – that is, they are dependent on the distinct sensing module fused to the kinase and the genes under control of the  $\sigma$  factor specific promoter, respectively.

### 3.3.4. Genes downregulated by the PknT/EcfP system

Upon comparing the transcriptomes of the  $\Delta ecfP$  and  $\Delta pknT$  mutant strains, one can see that only a fraction of these targets are commonly regulated by both genes. The significantly higher number of downregulated targets in the  $\Delta ecfP$  mutant could reflect that its activity is regulated by proteins other than PknT. However, regulation by other proteins likely does not involve phosphorylation as no phosphorylated EcfP was detected in a strain where *pknT* was deleted. Similarly, the significantly higher number of upregulated targets in the  $\Delta pknT$  mutant suggests that the kinase has targets other than EcfP. This is quite common among STKs, as they are known for their promiscuous nature

and can phosphorylate a wide range of targets resulting in several signaling cascades (Cousin et al., 2013; Dworkin, 2015b; Pereira et al., 2011a).

One of the key targets that the PknT/ EcfP system regulates is *vpa0879*, which encodes for a putative UDP-glucose-4-epimerase. This enzyme is involved in the epimerization of UDP-glucose to UDP-galactose and plays a role in lipopolysaccharide (LPS) synthesis. The LPS layer is composed of three components namely the hydrophobic lipid A, the hydrophilic core polysaccharide chain and the repeating O-antigen oligosaccharide chain that is variable and dependent on the bacterial serotype (Gronow & Brade, 2001). Given that galactose is one of the sugars found in the O-antigen oligosaccharide layer of the LPS in *V. parahaemolyticus* (Hisatsune, Kiuye, & Kondo, 1980), disruption of the enzyme that results in synthesis of UDP-galactose and subsequent incorporation into the LPS could compromise the integrity of this layer.

Our results also suggest that deletion of *vpa0879* results in very high sensitivity to polymyxin B. Polymyxins are a class of antibiotics that are used as a last resort of action against gram-negative infections (Arnold, Forrest, & Messmer, 2007). These antibiotics exert their action through electrostatic interactions between their positively charged side chain and the negatively charged LPS of the bacteria (Domingues et al., 2012; McInerney et al., 2016). Given the possibly compromised integrity in the structure of the LPS upon deletion of *vpa0879*, this could serve to also explain the increased sensitivity to polymyxin B. Our results also indicate that resistance to polymyxins is conferred in *V. parahaemolyticus* through regulation of VPA0879 by the PknT/EcfP system. Further studies are required to characterize if EcfP specifically recognizes the promoter of *vpa0879* and also if the LPS composition of the mutants are compromised, particularly in the O-antigen repeating units compared to wild type.

Besides *vpa0879*, genes involved in the TTSS1 (Type III secretion system 1) of *V. parahaemolyticus* are also among those that are significantly downregulated in both the  $\Delta$ *ecfP* and  $\Delta$ *pknT* mutants. Among the two TTSS found in *V. parahaemolyticus*, TTSS2 was found to be the only contributor to intestinal infection. However, TTSS1 was shown to be essential for infection of a murine model and also in induction of cytotoxicity in several cell lines (Hiyoshi et al., 2010). This indicates an additional role for the PknT/EcfP system in virulence. However, this needs to be tested by further experiments.

### 3.3.5. Genes upregulated by the PknT/EcfP system

Upon looking at the targets that are commonly upregulated in both the  $\Delta ecfP$  and  $\Delta pknT$  mutants, three genes that belong to a putative operon stand out. These include *vpa0807*, *vpa0808* and *vpa0809* which encode for a putative multidrug resistance protein, a putative periplasmic linker protein and a putative AcrB/ AcrD/ AcrF family transporter protein respectively. It appears that these three targets function collectively as a multidrug efflux pump. The function of these multidrug efflux pumps also involves extrusion of small molecules including quorum sensing (QS) signals (Alcalde-Rico, Hernando-Amado, Blanco, & Martínez, 2016; J. Sun, Deng, & Yan, 2014). Interestingly, repression of several virulence determinants in pathogenic bacteria occurs with the help of these signals (Rutherford & Bassler, 2012). We surmise that extrusion of these signals is prevented by repression of the aforementioned operon by the PknT/ EcfP system, reaffirming its role in virulence. In fact, studies on the gram-negative bacterium, *P. aeruginosa* have shown that upon overexpression of multidrug efflux pumps, a significant reduction in the Type III secretion system ensues (Linares et al., 2005). Another instance is the control of high energy consumption by the *Vibrio harveyi* Type III secretion system by repression of it through quorum sensing master regulators such as LuxR, for example (Ruwandeeepika et al., 2015). Further studies are required to validate the combined role of the *vpa0807-09* set of genes and the PknT/ EcfP system in virulence.

### 3.3.6. PknT possesses basal activity in the absence of polymyxin

Additionally, our data show that a small basal fraction of EcfP is phosphorylated in wild type *V. parahaemolyticus* (Figure 17A, orange bars), consistent with the observation that the PknT kinase does have residual activity even in the absence of polymyxin (Figure 31A-B). We speculate that PknT possesses this residual activity, even in the absence of polymyxin, to ensure a continuous basal production of VPA0879 (Figure 26B) in order to ensure *V. parahaemolyticus* is always protected against polymyxin stress to a certain degree. This likely allows cells to survive the initial stress before a response via polymyxin-induced PknT activation and EcfP phosphorylation is elicited.

In summary, the current work has identified a new cellular response and signaling pathway that regulates resistance to polymyxin antibiotics in *V. parahaemolyticus*,



opening up a potential target for novel compounds in order to combat the increasing threat (Srinivas & Rivard, 2017) of multi-resistant organisms. More work will need to be done to investigate the purpose of ECF  $\sigma$  factor regulation via phosphorylation and its potential advantages over the more common regulation via anti- $\sigma$  factors. Nevertheless, phosphorylation can be thought of as a very elegant way by which to regulate the activity of ECF  $\sigma$  factors, in that it is a rapid and easily reversible mechanism. It could also serve as an energy-saving mechanism as regulation by sequestration of ECF  $\sigma$  factors into complexes with anti- $\sigma$  factors requires constant degradation and subsequently, constant regeneration of the latter. Additionally, the often-promiscuous nature of STKs might rapidly lead to activation of a variety of outputs with only one kinase detecting a certain signal.

Collectively, our discoveries reveal how nature has merged two mechanisms for signal transduction – STK signaling and ECF  $\sigma$  factor activity – in order to regulate RNAP holoenzyme formation and transcriptional activation.



**Chapter 4. Regulation of swarming behavior by  
the PknT/EcfP system in *V. parahaemolyticus***



## 4.1. Introduction

### 4.1.1. Swarming motility in bacteria

Bacteria exhibit several kinds of motility such as swimming, gliding, twitching, darting, swarming and sliding (Burchard, 1974; Henrichsen, 1972; Martínez, Torello, & Kolter, 1999; Mattick, 2002; Murray & Kazmierczak, 2008; Spormann, 1999; Youderian, 2004). This chapter will focus on dissecting the details specific for swarming behavior. Swarming was identified as early as 1885 in *Proteus* species as a distinct type of surface translocation, characterized by elongated cells (Vogel, 1885). In this organism, vegetatively growing cells differentiate into the morphologically distinct swarmer population upon encountering solid surfaces (Smith, 1972). This process can in turn be classified into three different stages, namely the differentiation process itself, migration of the cells in the form of rafts and reversion of swarmer cells into vegetative cells (Copeland & Weibel, 2009; Morrison & Scott, 1966). As a result of the three different stages, the swarmer cells of *P. mirabilis* exhibit a classic “bulls-eye” pattern wherein distinct consolidation zones are evident (C. Allison & Hughes, 1991). Currently, there are several well-characterized examples of swarming behavior among *Bacillus*, *Vibrio*, *Clostridium* and *Pseudomonas* species, to name a few (Déziel, Comeau, & Villemur, 2001; Hernández & Rodríguez, 1993; Kohler, Curty, Barja, Van Delden, & Pechere, 2000; Ulitzur, 1974).

### 4.1.2. Characteristics of swarming behavior

Swarmer cells have distinct advantages over other populations of cells. For instance, they are significantly more resistant to antibiotics that interfere with cell envelope synthesis, protein translation and DNA replication, as shown by the cells of *Salmonella enterica* (W. Kim, Killam, Sood, & Surette, 2003). Among other reasons, high cell densities and circulation within the swarm colony have been proposed as likely reasons for the resistance of these cells to antibiotics (Butler, Wang, & Harshey, 2010). A striking feature of swimmers in *P. mirabilis* is the marked elongation of cells that occurs in the form of multinucleate filaments (Robert Belas, Schneider, & Melch, 1998; Hernandez, Ramisse, & Cavallo, 1999). Swarmer cells also possess numerous flagella throughout the length of the cell (M. Sharma & Anand, 2002). This is once again evident in *P. mirabilis*, wherein flagellar densities were found to be the highest in swarmer cells, followed by the cells within the consolidated population and eventually, vegetative cells

(Tuson, Copeland, Carey, Sacotte, & Weibel, 2013). Additionally, in *P. mirabilis*, only one kind of flagellum is produced for both swimming and swarming motilities. (R. Belas, Erskine, & Flaherty, 1991). This type of single flagellar system can also be observed in the case of the gram-negative enteric bacterium, *Serratia marcescens* (Alberti & Harshey, 1990). However in certain other bacteria such as *Vibrio parahaemolyticus*, two distinct flagellar systems can be found (Sar et al., 1990).

### 4.1.3. Factors that regulate swarming behavior

Swarming is not a behavioral response to starvation but rather a response to different environmental cues. A primary requirement for this motility is surface contact or the presence of a viscous environment (Belas et al., 1991). Yet another important factor that can regulate swarming is the composition of the medium (JONES & PARK, 1967; Julkowska, Obuchowski, Holland, & Séror, 2005). For instance, certain species of bacteria like *Proteus* and *Vibrio* are able to swarm in media containing high agar concentrations (Little, Austerman, Zheng, & Gibbs, 2018; Partridge & Harshey, 2013). This adaptation suggests the importance of both water content and surface tension of the medium, which in turn likely depends on the secretion of various extracellular substances that helps promote motility on these surfaces (Kearns, 2011; Srinivasan, Kaplan, & Mahadevan, 2019; A. Yang, Tang, Si, & Tang, 2017). This is exemplified by the role the O-antigen of the lipopolysaccharide (LPS) plays in improving the wettability of the surface and thereby, facilitating swarming behavior in *S. enterica* (Toguchi, Siano, Burkart, & Harshey, 2000). Other factors including chemotaxis and quorum sensing have also been found to influence swarming behavior (Clive Allison, Lai, Gygi, & Hughes, 1993; Burkart, Toguchi, & Harshey, 1998; Eberl, Christlansen, Molin, & Givskov, 1996; Harshey & Matsuyama, 1994; Tremblay, Richardson, Lépine, & Déziel, 2007).

### 4.1.4. Swarming in *V. parahaemolyticus*

Upon encountering solid surfaces, *V. parahaemolyticus* differentiates into swarmer cells (Ulitzur, 1974). This population represents a unique cell type that can also enable the bacteria to move through highly viscous environments (L McCarter, 1999). The swarmer cells are highly elongated and multinucleoid in nature (Jaques & McCarter, 2006; Kearns & Losick, 2003). In addition, these cells also possess numerous peritrichous lateral flagella (Patrick & Kearns, 2012; Turner, Zhang, Darnton, & Berg, 2010). This will be discussed at some length in the upcoming section.

#### 4.1.4.1. Dual flagellar systems of *V. parahaemolyticus*

Initial studies on swarming behavior resulted in the identification of two distinct flagella in the organism (Figure 46). These were the monotrichous polar M flagellum and the peritrichous L (lateral) flagella (Shinoda & Okamoto, 1977). The L flagella were an exclusive adaptation to growth upon solid medium and henceforth, were directly related to swarming behavior. The M flagellum, on the other hand was associated with swimmer cells (Shinoda & Okamoto, 1977). Luciferase assays showed stimulation of the *laf* genes when the viscosity of the medium and the wettability of the agar were increased. Increase in light intensity was found to correlate with a corresponding increase in the number of lateral flagella (R. Belas, Simon, & Silverman, 1986).

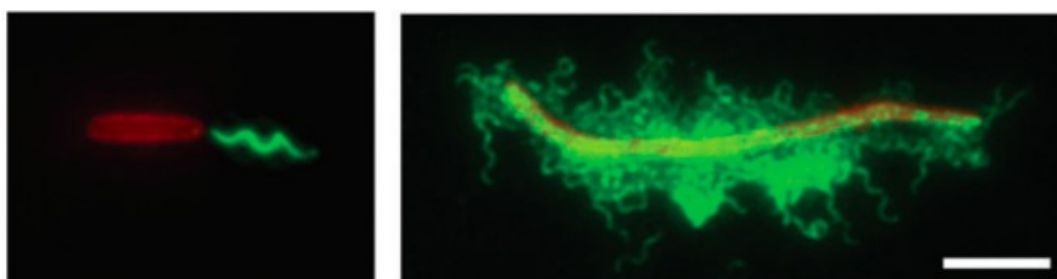


**Figure 46. Swimmer and swarmer cells of *V. parahaemolyticus*.** Immunofluorescence microscopy helps shed light on the two distinct types of cells in *V. parahaemolyticus*. In free-living conditions (in liquid), the bacteria exist as short swimmer cells (left panel) that are characterized by the presence of a single polar flagellum (colored green). Upon encountering highly viscous environments or a solid surface, swimmer cells differentiate into elongated swarmer cells (right panel) that are characterized by the presence of numerous peritrichous lateral flagella (colored green). Adapted from (Gode-Potratz & McCarter, 2011).

The two flagellar structures have distinct features. The polar flagellum consists of a sheath, which is essentially an extension of the outer membrane of the cell and is constitutively expressed (Y. K. Kim & McCarter, 2000). Attachment to solid surfaces or the presence of viscous environments results in induction of the lateral flagella (Merino, Shaw, & Tomás, 2006; Stewart & McCarter, 2003). The energy of the flagellar motor is also different, in that the polar flagellum is driven by sodium motive force just as in the case of *V. alginolyticus* (Kojima, Yamamoto, Kawagishi, & Homma, 1999), whereas the lateral flagella was driven by proton motive force, similar to *E. coli* and *B subtilis* (Manson, Tedesco, Berg, Harold, & Van der Drift, 1977). Increase in viscosity of the medium results in significant reduction in the speed of the polar flagellum (Atsumi, McCarter, & Imae, 1992). Furthermore, the unsheathed lateral flagella are much more sensitive to mechanical stresses (Zhu, Kojima, & Homma, 2013).

The two flagellar systems are encoded by distinct sets of genes (Y. K. Kim & McCarter, 2004). In the case of the polar flagellin, there was some structural similarity, especially at the N and C termini, to lateral flagellin (L. L. McCarter, 1995). The former was characterized by the presence of hydrophobic heptad repeats that, in turn have a significant role in polymerization (L. L. McCarter, 1995). The genes encoding the polar flagellin were found to be organized in two loci: *flaBAGH* and *flaEFCD* (L. McCarter, 1999). Identification of the *laf* set of genes encoding the lateral flagella revealed that expression of the essential gene, *lafA* was dependent on the *lafLSTUV* set of genes in a  $\sigma^{28}$ -dependent manner (Merino et al., 2006). Mutations in all the above candidates resulted in significant reduction in swarming (L. L. McCarter & Wright, 1993). Further dissection of the *laf* genes led to the identification of two distinct regulators, one dependent on  $\sigma^{54}$  (*lafK*) and the other on  $\sigma^{28}$  that were responsible for the control of early and late flagellar genes, respectively (Stewart & McCarter, 2003).

#### **4.1.4.2. Regulation of swarming behavior of *V. parahaemolyticus***

There are many different ways through which swarming is regulated in *V. parahaemolyticus*. For instance, the hydrophilic polysaccharide ficoll induces expression of the lateral flagella, thereby suggesting that cells are able to sense microviscosity within the medium (Kühn, Schmidt, Eckhardt, & Thormann, 2017). The polar flagellum of the bacteria has been shown to act as a sensor, in that it induces expression of the lateral flagella through negative regulation (Stewart & McCarter, 2003). This can be seen through mutations of the gene, *flaC* which results in a wobbly appearance and poor swimming motility but is able to stimulate production of lateral flagella in liquid medium (Linda McCarter, Hilmen, & Silverman, 1988). Mutations in *flaC* were found to induce expression of the *laf* genes in a medium-specific manner, in that expression was found to occur only when the bacteria were grown on marine broth but not in Heart Infusion (HI) broth. Upon comparing the composition of the two media, the biggest difference was the availability of iron in the latter (Drake, Depaola, & Jaykus, 2007; L. McCarter & Silverman, 1989). Consequently, addition of iron chelators to the HI broth stimulated synthesis of lateral flagella. Transcription of the essential gene, *lafA* was found to be dependent on both interference of the polar flagellum and conditions of iron limitation (L. McCarter & Silverman, 1989). When grown on normal agar plates, *V. parahaemolyticus* has an appearance that is characteristic of iron starvation, in that several outer membrane proteins that show similarity to iron uptake proteins were synthesized (Jaques



& McCarter, 2006). This whole phenomenon essentially resembles an iron stress response as seen in other bacterial species (L. McCarter & Silverman, 1990).

Other factors such as the master regulator, OpaR that controls duality between the opaque and translucent colony morphologies and also the *scr* operon of genes that affects quorum sensing have been shown to significantly influence swarming behavior in *V. parahaemolyticus* (Boles & McCarter, 2002; Gode-Potratz & McCarter, 2011; Jaques & McCarter, 2006; Trimble & McCarter, 2011).

Given that swarming behavior in bacteria has also been implicated in virulence and pathogenicity (Clive Allison, Emody, Coleman, & Hughes, 1994; Clive Allison et al., 1993; Ottemann & Miller, 1997; Overhage, Bains, Brazas, & Hancock, 2008; Rather, 2005; Senesi et al., 2002), it is extremely appealing to characterize the molecular targets that might affect this behavior in the pathogen, *V. parahaemolyticus*. Additionally, since STKs have multifaceted signaling roles that in turn affect several important physiological functions, one of the main focuses of this thesis was to address if they were also involved in regulation of the highly coordinated swarming motility in *V. parahaemolyticus*.

### 4.2. Results

Swarming in bacteria is a highly organized process of differentiation that initiates upon surface contact or the presence of viscous environments (C. Allison & Hughes, 1991; Copeland & Weibel, 2009). In *V. parahaemolyticus*, the process is characterized by significant elongation of the cell and the presence of numerous peritrichous lateral flagella. Swarming behavior of *V. parahaemolyticus* in the laboratory is facilitated by spotting cells upon a specialized medium (Heart Infusion agar) containing salt (calcium chloride) and an iron chelator (2, 2'-dipyridyl) (Gode-Potratz, Chodur, & McCarter, 2010). A typical swarm colony of *V. parahaemolyticus* is depicted in Figure 47. It comprises of three distinct layers, namely the center, middle and periphery (Freitas et al, in preparation). As one can see from the figure, the three layers are morphologically different. The cells in the center layer are the smallest and resemble those found in free-living liquid media and those at the periphery are the most representative of the swarmer population, comprising of highly elongated cells that exhibit close cell-cell contact.

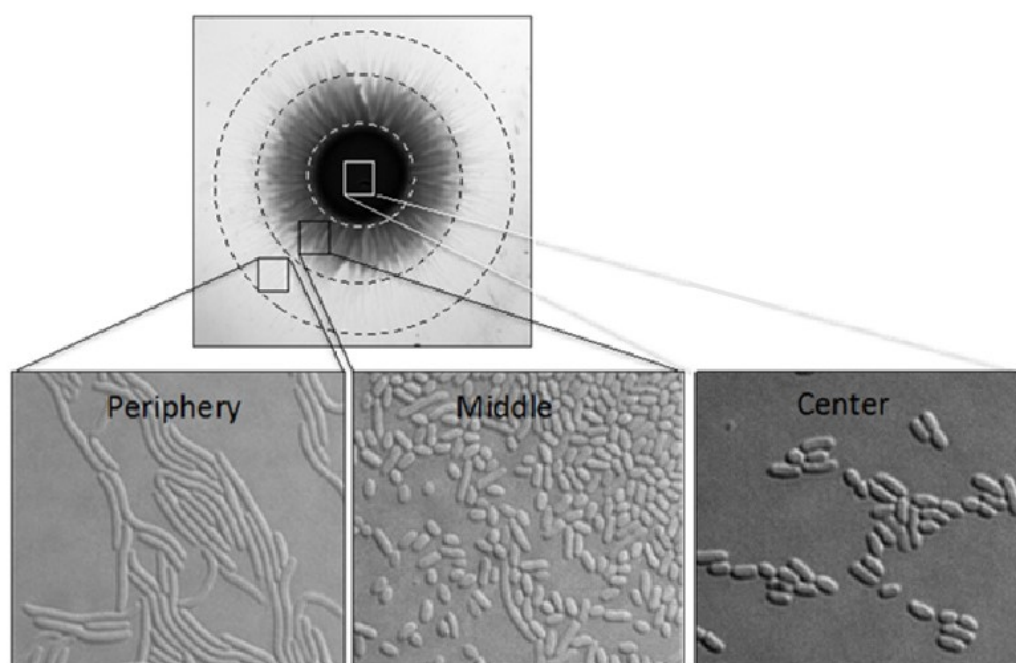


**Figure 47. Distinct layers within the swarm colony of *V. parahaemolyticus*.** Three distinct layers can be found in a typical swarm colony of *V. parahaemolyticus*. The cells in the innermost layer, namely the center are made up of very short cells, whereas those in the periphery consist of extremely elongated cells that are the most characteristic swimmers. For proteomics, cells from the periphery were chosen. Images were kindly provided by Stephan Wimmi and Dr. Samada Muraleedharan.

### 4.2.1. PknT is important for swarming behavior

Given the wide range of physiological processes that Serine/Threonine kinases (STKs) control, we wanted to assess whether the STK in *V. parahaemolyticus*, PknT played a role in regulation of swarming behavior. In order to do so, we created a deletion mutant ( $\Delta pknT$ ) and performed several phenotypic tests. The growth profile, swimming and biofilm formation abilities of the mutant were unaffected when compared to wild type (Figure 48).

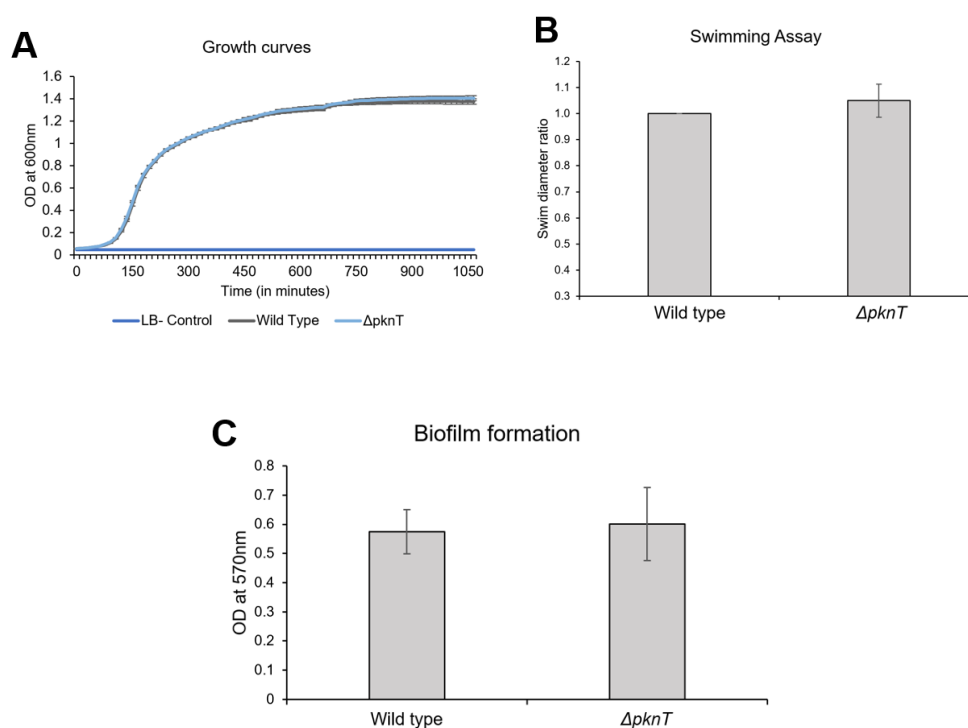


**Figure 48. Phenotypic characterization of PknT.** Deletion of the Serine/Threonine kinase, *pknT* had no effect on the growth profile, swimming or biofilm forming abilities of *V. parahaemolyticus*, when compared to wild type.

However, we found a significant defect in swarming (an approximately 50% reduction in the size of the swarm colony) in the  $\Delta pknT$  mutant strain compared to wild type (Figure 49). In order to rule out the possibility of this phenotype occurring due to polar effects of genes within the operon that *pknT* belongs to, we aimed to complement the aforementioned swarming defect. This was achieved by inserting the *pknT* gene – alongside its native promoter – elsewhere within the genome of *V. parahaemolyticus* (the intergenic regions used here were carefully chosen so as to not disrupt the function of any other essential genes). The resulting strain was able to successfully complement the swarming defect, thus showing that the swarming defect of the  $\Delta pknT$  mutant strain is truly due to the absence of PknT (Figure 49).

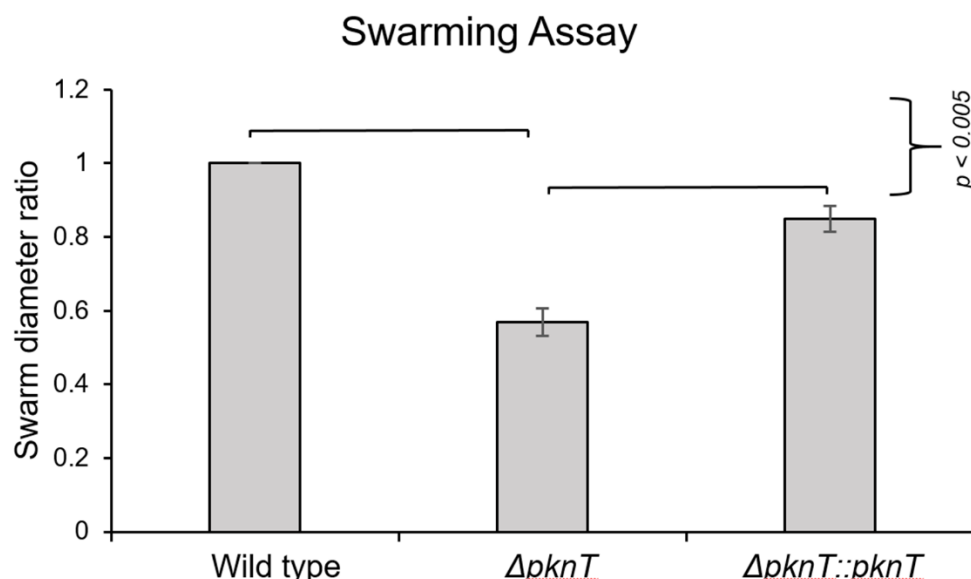


**Figure 49. PknT is required for swarming behavior.** Deletion of *pknT* resulted in a severe (almost 50%) defect in the diameter of the swarm colony, when compared to wild type.

In order to observe if there were significant morphological differences in the swarm colony, stereo microscopy images of the  $\Delta pknT$  and wild type strains were compared (Figure 50). Strikingly, the peripheral area of the swarm colony was significantly smaller in the mutant when compared to wild type. Additionally, the flares that characterize the periphery in the swimmers of the  $\Delta pknT$  mutant strain were also considerably smaller and markedly different in their appearance than those found in the wild type strain.

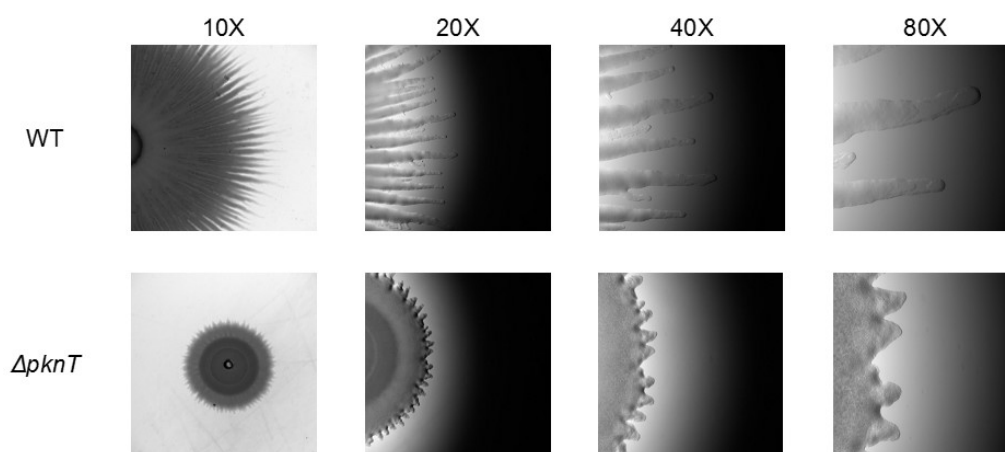


**Figure 50. The swarm colony of  $\Delta pknT$  appears to be morphologically different than wild type.** Stereo microscopy images of  $\Delta pknT$  and wild type strains indicate a significantly different appearance in the flares in the periphery of the swarm colony.

### 4.2.2. VP0054, VP0056 and EcfP also regulate swarming behavior

As seen in Chapter 3, *pknT* exists in an operon with the ECF  $\sigma$  factor encoding gene, *ecfP* and two other genes of unknown function, namely *vp0054* and *vp0056* (Figure 15). Deletion mutants of these genes were generated and their swarming abilities were evaluated and compared to wild type. The results are summarized in Figure 51. Strikingly, deletion of the ECF  $\sigma$  factor encoding gene, *ecfP* resulted in a significant swarming defect and the degree of this defect was similar to that observed for the  $\Delta pknT$  mutant strain. On the contrary, deletion of both *vp0054* and *vp0056* resulted in significantly higher swarming than wild type. These results suggest that PknT and EcfP act as positive regulators of swarming, whereas VP0054 and VP0056 act as negative regulators.

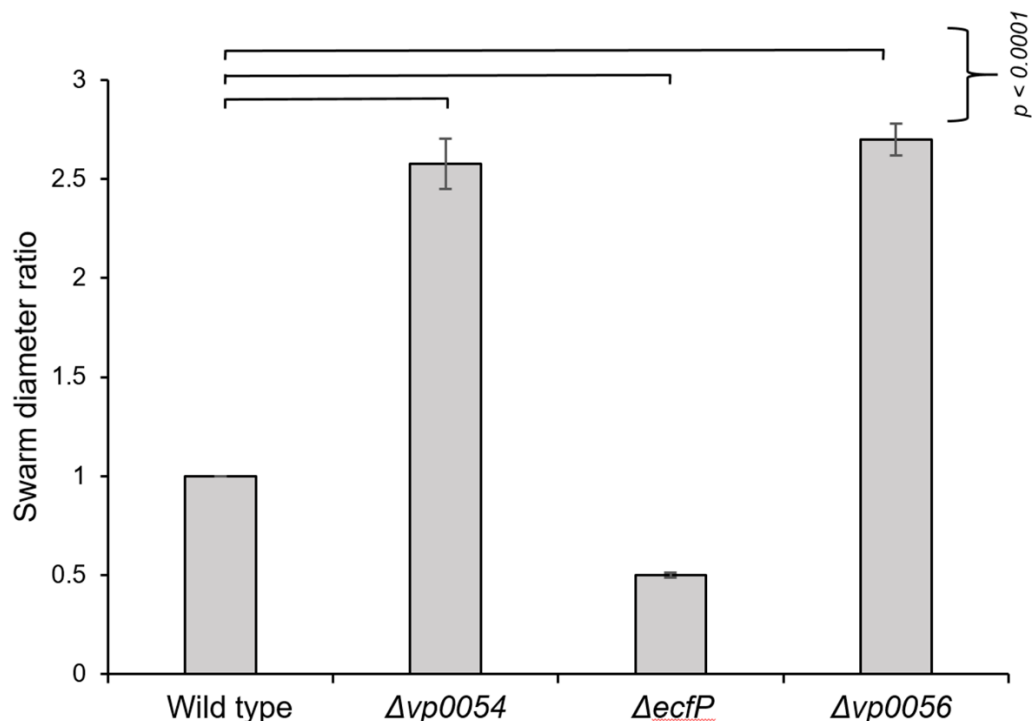


**Figure 51. Swarming phenotypes of  $\Delta vp0054$ ,  $\Delta ecfP$  and  $\Delta vp0056$  mutant strains.** Swarming assays were performed on the deletion mutants of the genes present in the same operon as that of *pknT*.  $\Delta vp0054$  and  $\Delta vp0056$  mutants swarmed significantly more than wild type, whereas  $\Delta ecfP$  showed a significant swarming defect.

Just as in the case of the  $\Delta pknT$  strain, we looked at the morphologies of the swarm colonies of  $\Delta vp0054$ ,  $\Delta ecfP$  and  $\Delta vp0056$  mutant strains through stereo microscopy (Figure 52). However, despite the clear differences in swarming ability compared to wild type, unlike the case of the  $\Delta pknT$  strain, no significant differences in

## Results – Part II

the appearance of the swarm colony periphery were found for the above mentioned mutants when compared to wild type.

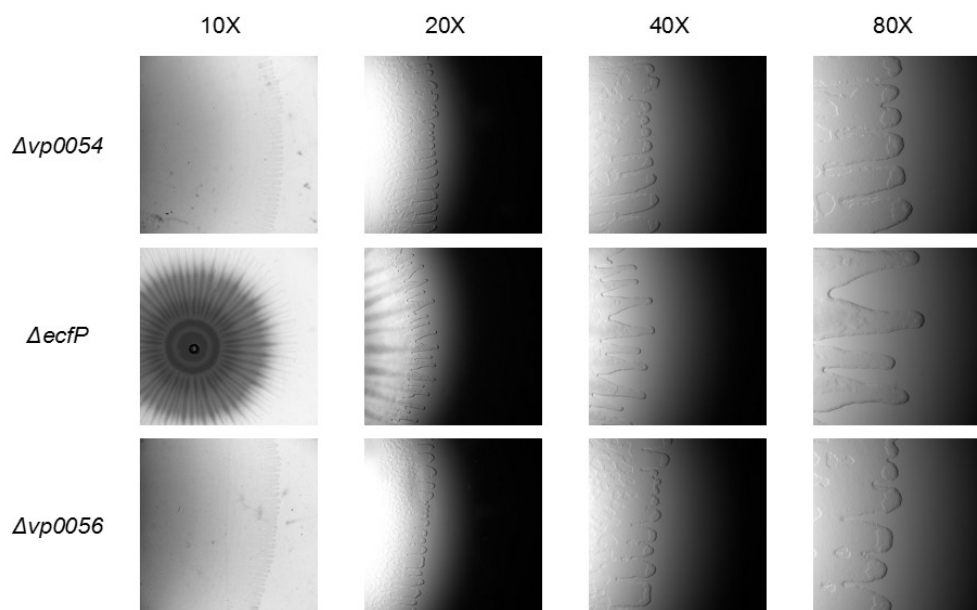


**Figure 52. Colony morphologies of  $\Delta vp0054$ ,  $\Delta ecfP$  and  $\Delta vp0056$  mutants.** Stereo microscopy images of  $\Delta vp0054$ ,  $\Delta ecfP$  and  $\Delta vp0056$  mutants showed no significant differences in the appearance of the swarm flares in the peripheral area of the colony.

To further establish the importance of the genes within the operon, combinatorial deletions were made followed by examination of their swarm diameters. Interestingly, a strain that was deleted for both *ecfP* and *pknT* showed the same swarm defect as the individual  $\Delta pknT$  or  $\Delta ecfP$  mutant strains, indicating that the effect of these two genes on swarming is not cumulative and that they possibly exert their effect by functioning in the same pathway (Figure 53). Furthermore, a strain that was deleted for both *vp0054* and *pknT* showed a significant defect in swarming compared to wild type, as did deletion of all the genes within the operon ( $\Delta vp0054\Delta ecfP\Delta vp0056\Delta pknT$ ) (Figure 53). This indicates that the effect of *pknT* and possibly, *ecfP* is dominant and masks the effect of the other two genes (*vp0054* and *vp0056*) within the operon. Altogether, these results suggest that PknT and EcfP regulate swarming behavior in *V. parahaemolyticus* by functioning in the same signaling pathway.

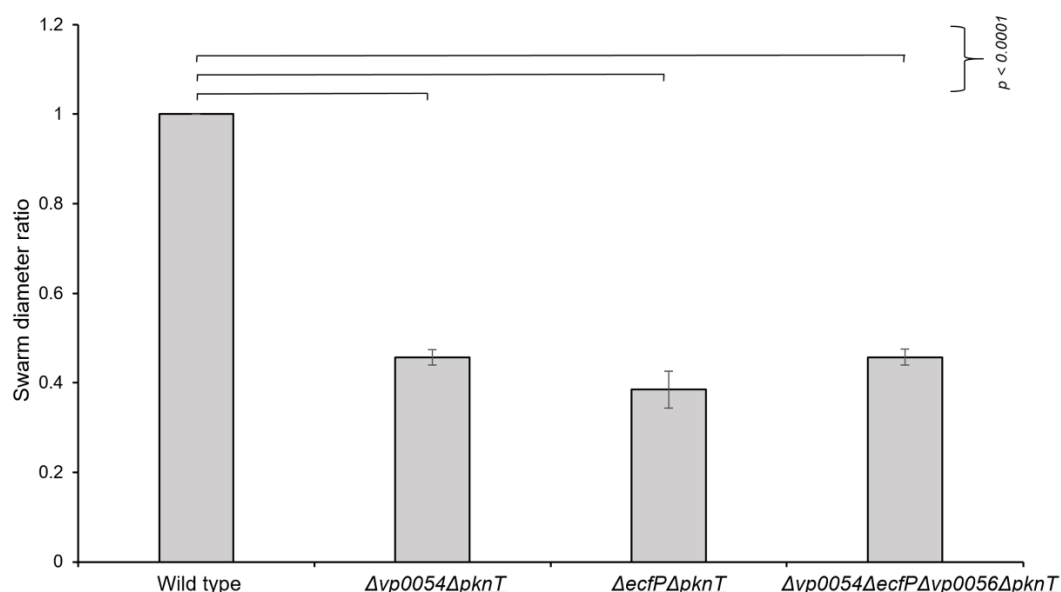


**Figure 53. Swarming behavior of combinatorial deletions of genes within the operon.** A  $\Delta vp0054\Delta pknT$  double deletion mutant showed a significant swarming defect. Deletion of both *ecfP* and *pknT* gave rise to the same swarming defect as the individual deletions. Deletion of the entire operon ( $\Delta vp0054\Delta ecfP\Delta vp0056\Delta pknT$ ) also gave rise to a similar swarming defect as above. These results indicate that the effect of *ecfP* and *pknT* on swarming behavior is not cumulative.

#### 4.2.3. The catalytic activity of PknT and the conserved Thr63 residue of EcfP are indispensable for swarming behavior

Previous results, as discussed in Chapter 3, showed strong evidence that EcfP is phosphorylated by PknT at the highly conserved threonine residue (Thr63) (Figure 17, Figure 20). We hypothesized that phosphorylation could be the means through which the PknT/EcfP system regulates swarming behavior in *V. parahaemolyticus*. Therefore, we substituted the native locus of *ecfP* with *ecfPT63A*, which encodes the phosphoablative EcfPT63A variant. Additionally, since the conserved catalytic aspartate residue of PknT was found to be required for the phosphorylation of EcfP (Figure 31A-B), we substituted the native locus of *pknT* with *pknTD202A*, encoding the catalytically inactive PknTD202A variant. Upon performing swarming motility assay, we observed a strikingly significant defect in swarm diameter for the both the *ecfPT63A* and *pknTD202A* strains, when compared to wild type (Figure 54).

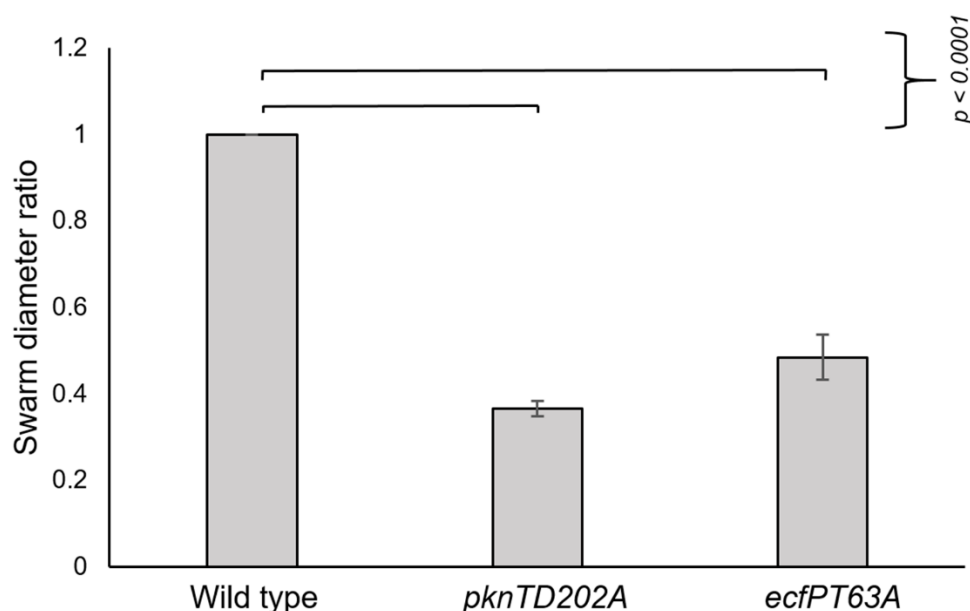


**Figure 54. Swarming behavior of the catalytically inactive *pknTD202A* and the phosphoablative *ecfPT63A* mutants.** Introduction of the D202A mutation in the native locus of *pknT* resulting in the *pknTD202A* strain, encoding the PknTD202A variant resulted in a significant swarming defect when compared to wild type. A significant swarming defect was also seen in the case of the *ecfPT63A* strain, which encodes for the phosphoablative EcfPT63A variant.

Furthermore, upon examining the morphologies of the swarm colonies of the *ecfPT63A* and *pknTD202A* mutant strains, one thing that immediately stands out is the fact that both the peripheral region of the *ecfPT63A* and *pknTD202A* strains and the characteristic swarm flares associated with that region resemble those found in the  $\Delta ecfP$  and  $\Delta pknT$  strains, respectively (Figure 55). Altogether, these results indicate that PknT-mediated phosphorylation of EcfP at the highly conserved threonine residue (Thr63) is important for regulation of swarming behavior in *V. parahaemolyticus*.

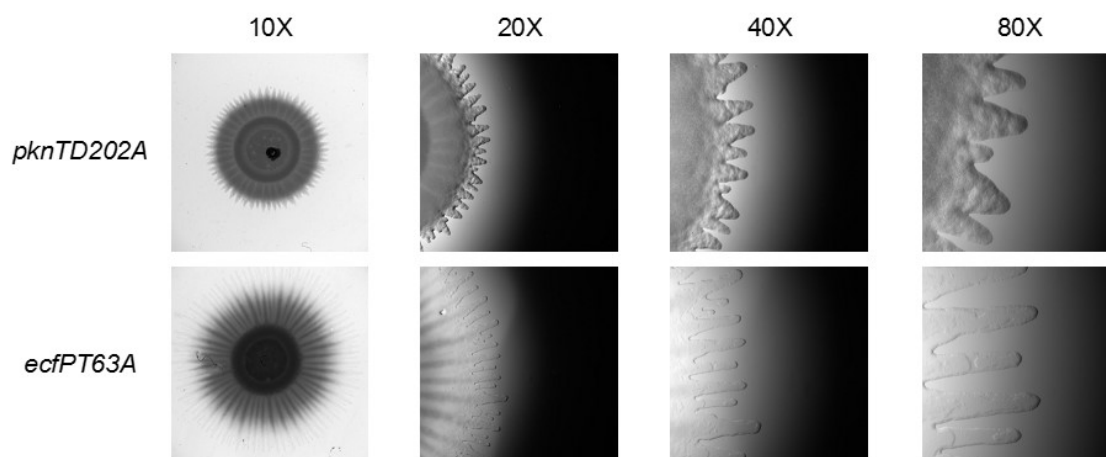


**Figure 55. Morphological differences in the swarm colonies of the *pknTD202A* and *ecfPT63A* mutants.** Stereo microscopy images of the *pknTD202A* mutant, encoding the PknTD202A variant showed similarity with the  $\Delta pknT$  strain, with respect to the appearance of



flares in the periphery of the swarm colony. Similarities were also found between the *ecfPT63A* strain, encoding the EcfPT63A variant and the  $\Delta$ *ecfP* mutant strain, in terms of morphological appearance.

#### 4.2.4. Swarming-specific proteins that are regulated by PknT

To better understand the cellular output of PknT, we performed global LC-MS proteomics experiments on quadruplicate samples of the  $\Delta$ *pknT* swarmer cells in comparison to those of wild type. For this experiment, the cells were obtained from the periphery of the colony as these were the most representative of the swarm population (Figure 47). The results of these proteomics experiments are depicted in Figure 56, in the form of volcano plots that show fold-changes (mutant with respect to wild type) for the individual targets with respect to the corresponding statistical significance values (p-value).

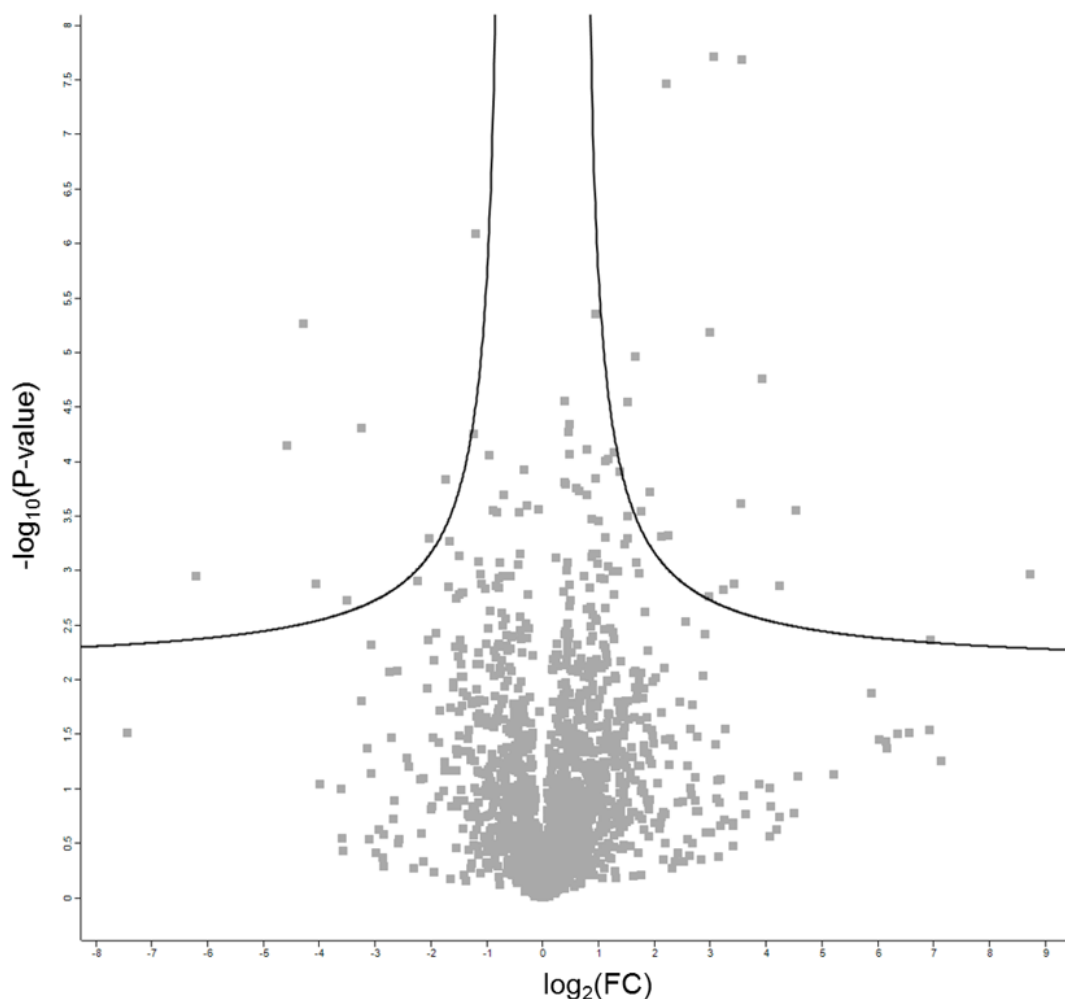


**Figure 56. Global LC-MS proteomics on  $\Delta pknT$  mutant compared to wild type.** Volcano plots of the targets obtained from global LC-MS proteomics analyses on the swarmer cells (cells in the periphery of the swarm colony) of  $\Delta pknT$  mutant strain, when compared to wild type. While the X-axis represents fold change (mutant/ wild type) of the individual hits, the Y-axis represents the statistical significance of the corresponding targets. The two curves (black) depict the set threshold (dictated by these parameters: FDR=0.01,  $S_0=0.2$ ). All the points (filled grey squares) to the left of the leftmost curve indicate significantly downregulated targets, whereas those to the right of the rightmost curve indicate significantly upregulated hits.

The two curved lines in Figure 56 indicate the threshold ( $S_0$  of 0.1 and a False Discovery Rate (FDR) of 0.01) that was used to delineate significant hits. The points found to the left of the leftmost curve represent significantly downregulated targets and those that were found to the right of the rightmost curve were found to be significantly upregulated. A zoomed-in view of the significantly regulated targets is shown in Figure 57.

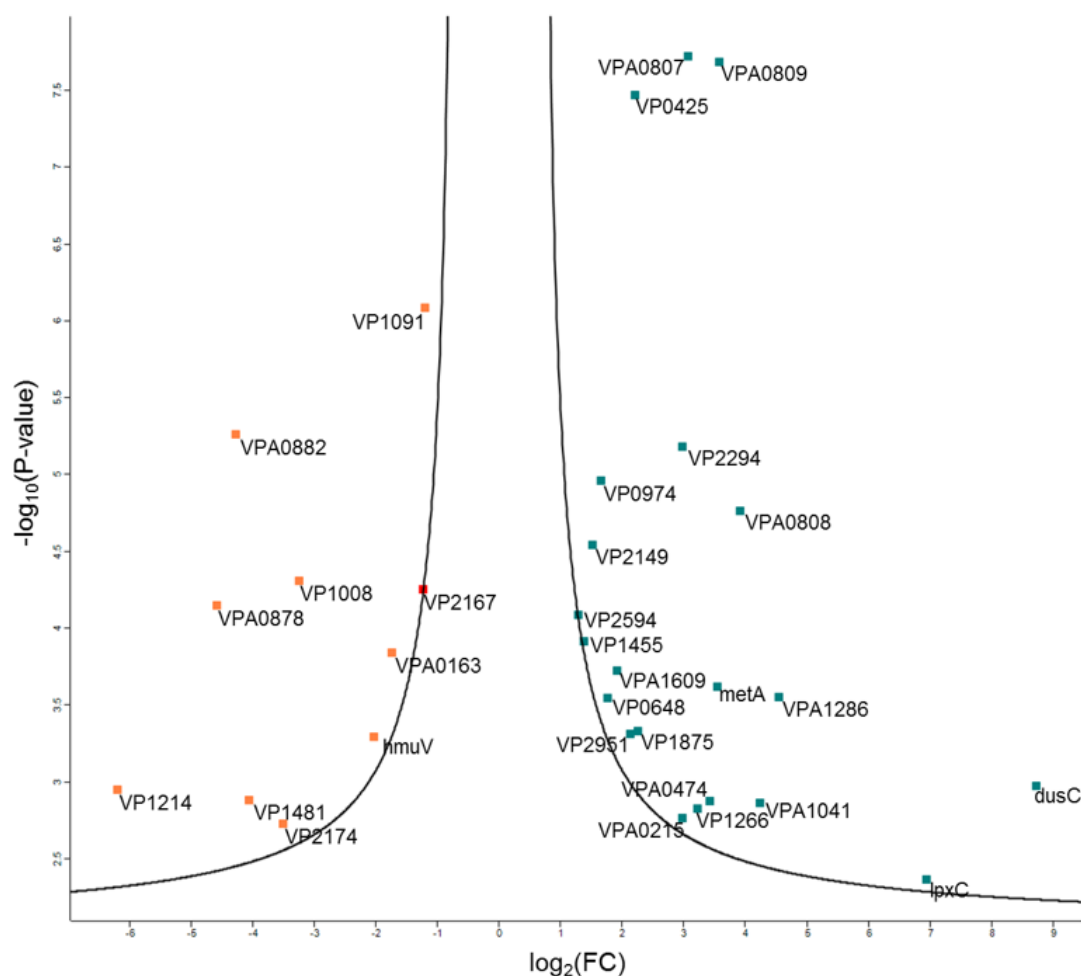


**Figure 57. An overview of the targets that are significantly regulated by PknT swarmers.** This figure represents a Volcano plot, showing a zoomed-in view of the targets on either side of the black curves from Figure 56. While the X-axis represents fold change (mutant/ wild type) of the individual hits, the Y-axis represents the statistical significance of the corresponding targets. Blue colored squares represent significantly upregulated targets, whereas orange

colored squares show significantly downregulated hits. The data labels for each point represents the gene names encoding the corresponding proteins.

In order to assess the nature of the targets that were significantly regulated in the *ΔpknT* swarmer cells with respect to wild type, we decided to group them according to their gene ontology (GO) functions. In the event where a GO function could not be obtained, the target under question was categorized as an uncharacterized protein. The results for this GO analysis of the significant targets regulated by PknT swarmers is depicted as a pie chart (Figure 58). Among the significantly regulated targets, transporters seem to constitute the largest fraction (23%), followed by proteins involved in the genetic machinery (19%). Most of the transporters that are regulated by PknT appear to be part of the outer membrane.

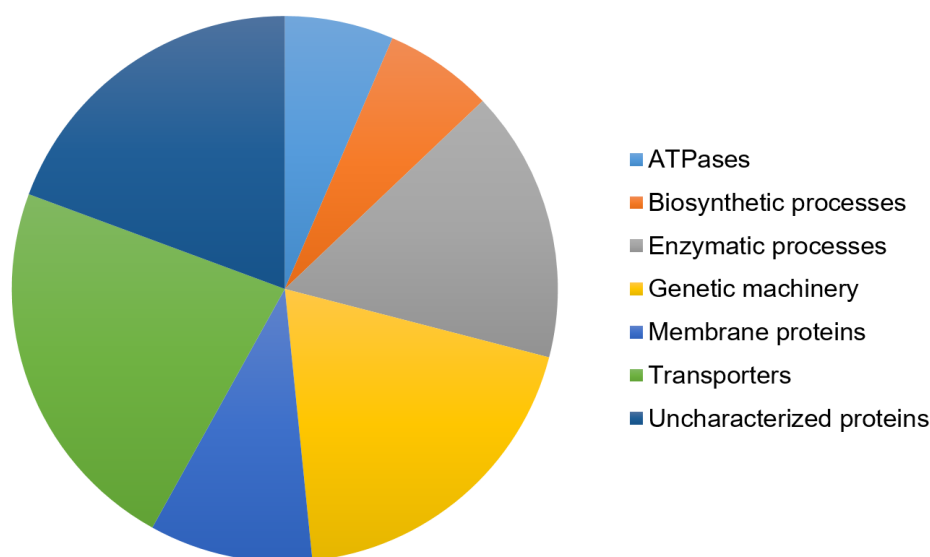
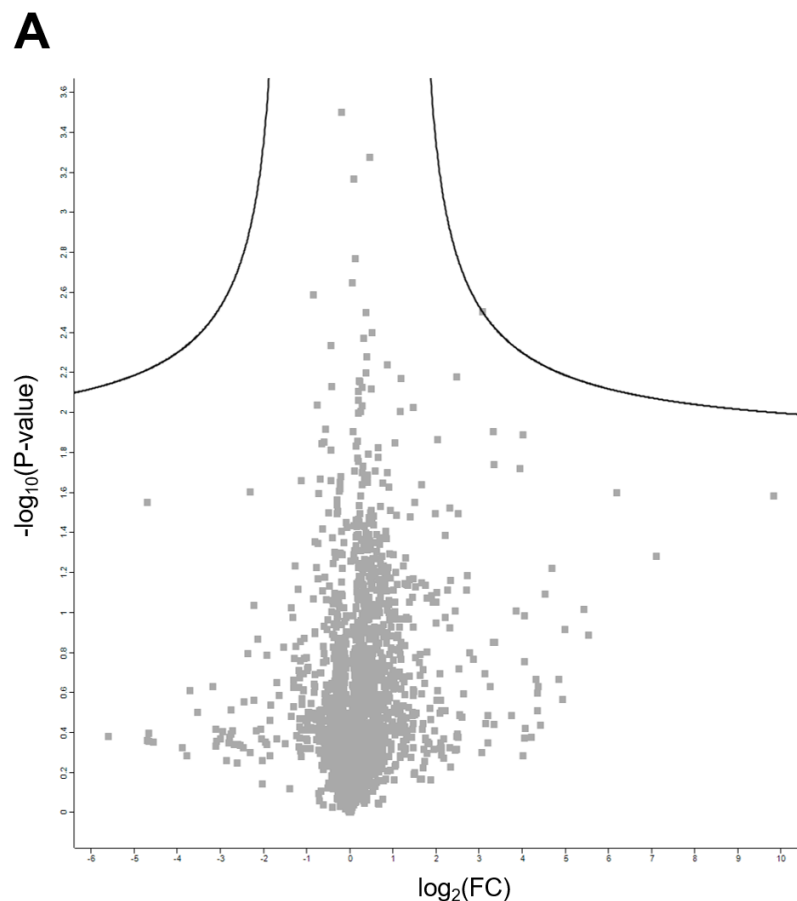


**Figure 58. Functional groups of the proteins significantly regulated by PknT swarmers.** The significantly regulated targets of PknT swarmers, when compared to wild type obtained by global LC-MS proteomics studies (Figures 53, 54) were categorized into different functional groups based on the gene ontologies of the targets.

Interestingly, despite the commonality among majority of the functional categories, some of them appear to be exclusive. For instance, while ATPases feature exclusively among the significantly downregulated targets, proteins involved in biosynthetic processes appear only among the significantly upregulated hits. A complete list of all the significantly regulated targets can be found in Table 18 and Table 19.

### 4.2.5. Swarming-specific proteins that are regulated by VP0054, EcfP and VP0056

In order to obtain a better understanding of how proteins encoded by the other genes within the same operon as that of *pknT* (Figure 15) regulate swarming behavior, we performed global LC-MS proteomics experiments on the respective deletion mutants. These experiments were done on (triplicate) samples collected from the periphery of swarmer cells from wild type,  $\Delta vp0054$ ,  $\Delta ecfP$  and  $\Delta vp0056$  mutants. The results for these experiments are shown in the form of volcano plots in Figure 59. Unfortunately, none of the targets matched the set threshold ( $S_0$  of 0.1 and a False Discovery Rate (FDR) of 0.01), in that no hits were found beyond the two curved lines, as in the case of the  $\Delta pknT$  swarmer. However, even though we were unable to extract significant hits out of these experiments, we were able to find some similarities in the pattern of regulation among the  $\Delta ecfP$  and  $\Delta pknT$  mutants. This is once again suggestive of their role in regulation of swarming behavior by acting in the same signaling pathway. Some of these targets are discussed at some length in the upcoming “Discussion” section (Section 4.3).



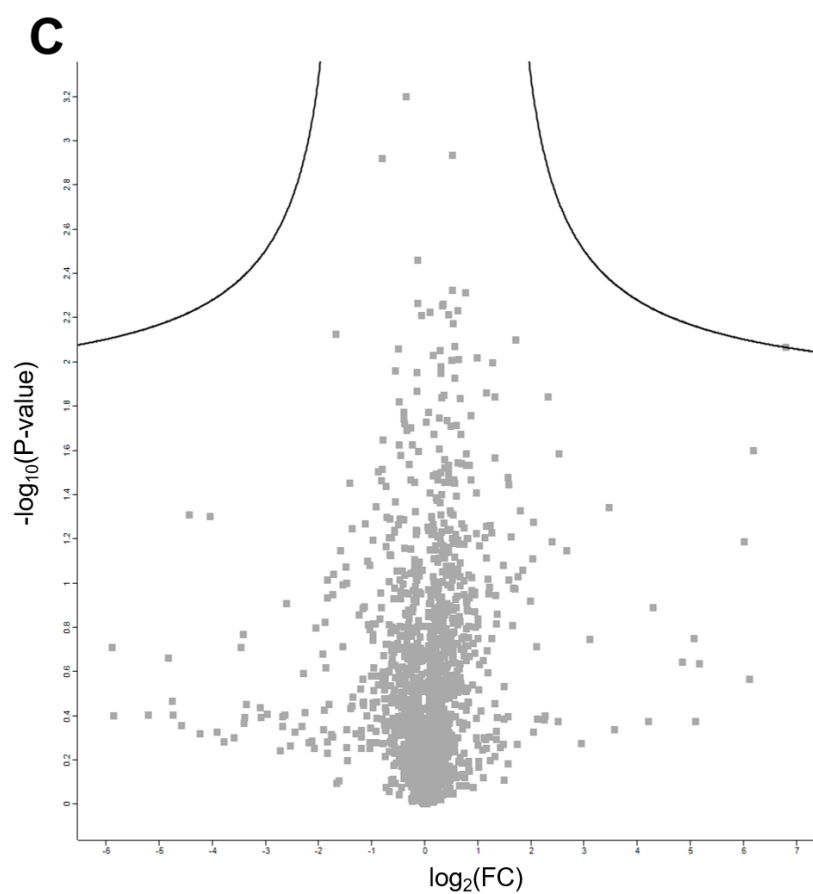
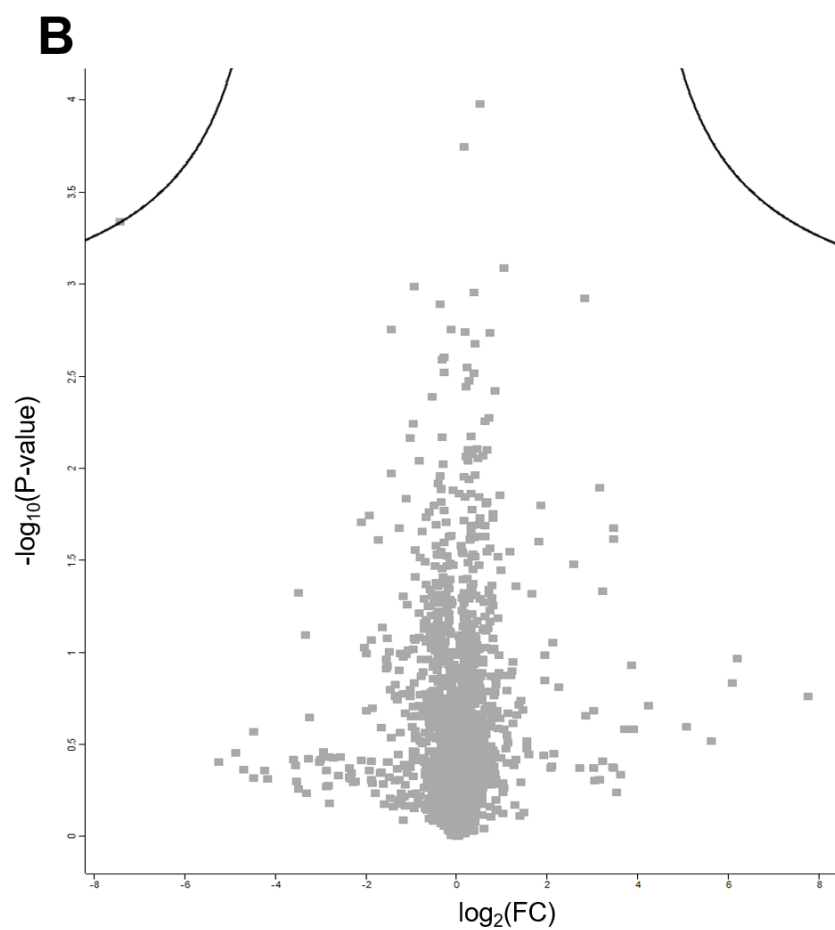


**Figure 59. Global LC-MS proteomics studies on  $\Delta vp0054$ ,  $\Delta ecfP$  and  $\Delta vp0056$  mutant strains compared to wild type.** Global LC-MS proteomics studies were performed on the swarmer cells of the deletion mutants of the three other genes in the same operon as that of *pknT*. This was compared with wild type to look for significantly regulated targets and volcano plots were generated. While the X-axis represents fold change (mutant/ wild type) of the individual hits, the Y-axis represents the statistical significance of the corresponding targets. None of the obtained hits passed the threshold set by the two black curves (dictated by these parameters: FDR=0.01,  $S_0=0.2$ ). Therefore, no significant targets were obtained for (A)  $\Delta vp0054$  swarmers, (B)  $\Delta ecfP$  swarmers and (C)  $\Delta vp0056$  swarmers.

Altogether, our findings indicate that both PknT and EcfP regulate swarming behavior. Furthermore, our results also suggest that they act in the same signaling pathway, possibly via a phosphorylation-driven mechanism. Further exploration of the proteomics targets and subsequent experiments are required to better understand the exact role of phosphorylation and the specific downstream targets in this regulation of swarming behavior in *V. parahaemolyticus*.

### 4.3. Discussion

Our findings reveal a novel and combined role for both STKs and ECF  $\sigma$  factors in bacteria, namely regulation of swarming behavior. Swarming is a highly coordinated behavior that bacteria adopt upon encountering solid surfaces or highly viscous environments. Our results indicate that the PknT/EcfP system induces swarming in *V. parahaemolyticus*. This regulation appears to be dependent on phosphorylation of EcfP by PknT. Interestingly, our findings also indicate that the proteins encoded by the other two genes within the operon, namely VP0054 and VP0056 repress swarming behavior. Furthermore, among the targets regulated by PknT, transport proteins seem to play a key role in regulation of swarming. Altogether, we are able to show the importance of the PknT/EcfP system, alongside the proteins encoded by the other two genes within the same operon in regulation of swarming behavior in *V. parahaemolyticus*.

Given the similarity in swarming defect and morphological appearances of the swarm colonies in the  $\Delta pknT$  and *pknTD202A* (which encodes the catalytically inactive PknTD202A variant) strains, it is likely that the catalytic activity of the kinase is important for its regulatory role on swarming. Furthermore, the significant defect in swarming in the *ecfPT63A* strain (encoding the phosphoablative EcfPT63A variant), when compared to wild type supports the idea of swarming being regulated by the PknT/EcfP system via a phosphorylation-driven mechanism. Interestingly, differences were found in the colony morphology of the periphery of the swarm colony only in the  $\Delta pknT$  mutant strain when compared to wild type (Figure 50). The morphology of the  $\Delta ecfP$  mutant strain, on the other hand, was similar to that of wild type (Figure 52). This suggests that despite the possibility of the kinase and the ECF  $\sigma$  factor functioning within the same signaling pathway, PknT might have additional targets that might help regulate swarming behavior in *V. parahaemolyticus*.

Since ECF  $\sigma$  factors usually respond to external stresses by turning on appropriate response pathways, we surmise that in the case of swarming, they likely play a role in sensing stresses such as iron and excess salt, which in turn affect swarming behaviour. A salient reason for this speculation is that the HI medium in the laboratory that is used to study swarming motility is supplemented with both salt (calcium chloride) and an iron chelator (2,2'-dipyridyl).

## Discussion – Part II

---

Sensing of these external stresses could occur either through the periplasmic domain of PknT or through the large extracytoplasmic domains of VP0054 and VP0056. The latter is a particularly appealing theory as both VP0054 and VP0056 also play a role in regulation of swarming behavior. However, considering that these two proteins act as repressors of swarming behavior, one can speculate that upon sensing external stresses, conformational changes could ensue, thereby inactivating these two proteins and this signal could then be transmitted to the PknT/EcfP system.

There have been several studies in the past that have implicated STKs in bacterial motility. For instance, the *Mycoplasma pneumonia* kinase PrkC was found to influence gliding motility by working in opposition to its cognate phosphatase, PrpC (Page & Krause, 2013). Yet another example is the kinase, SpkA of the *Synechocystis* sp. of cyanobacteria. This Hanks-type kinase was found to regulate cellular motility, primarily via phosphorylation of certain membrane proteins (Kamei, Yuasa, Orikawa, Xiao Xing Geng, & Ikeuchi, 2001). Despite these examples, our findings implicate STKs for the first time in the regulation of the specialized swarming motility in bacteria.

Upon inspecting the functional categories of proteins that are significantly regulated by PknT, we found that ATPases appear to be exclusively downregulated in the  $\Delta pknT$  swimmers when compared to wild type. One of the reasons for this downregulation in ATPases could simply be the deletion of one of the four STKs in *V. parahaemolyticus* and subsequent reduction of the ATP-binding/ hydrolysis load.

Interestingly, the connection between ATPases and regulation of swarming behavior has been well established in several previous studies. For instance, in *P. mirabilis*, a mutant that had lost a P-type ATPase was found to be defective in swarming behavior, in that there was a considerable reduction in both velocity and initiation of swarming (Lai, Gygi, Fraser, & Hughes, 1998). Interestingly, studies on the global gene expression profile of the bacterium, *Bacillus cereus* revealed a significant enhancement in the levels of proteins encoding distinct ATPase subunits among the swimmer cells when compared to non-swimmers (Salveti, Faegri, Ghelardi, Kolstø, & Senesi, 2011). These examples could provide certain gateways into explaining the markedly downregulated levels of ATPases in a mutant strain that exhibits a significant swarming defect ( $\Delta pknT$ ) when compared to wild type.

A notable target from the global LC-MS proteomics experiments on  $\Delta pknT$  swimmers was the putative heme transport protein, VPA0882, which was found to be



significantly downregulated. In addition to direct capture from host cells, most pathogenic bacteria also take up iron through heme (either free heme or through proteins containing heme). While iron limitation has been shown to induce swarming behavior (L. McCarter & Silverman, 1989), it has also been proposed that uptake of sufficient iron is essential for the initial induction of swarming behavior and this uptake mechanism can be overridden when enough iron is supplied to the cells (Burbank, Mohammadi, & Roper, 2015). With this in mind, we hypothesize that in the case of *V. parahaemolyticus*, PknT plays a role in sensing iron in the environment and its subsequent uptake, possibly through VPA0882.

Among the proteins that were significantly upregulated in  $\Delta pknT$  swimmers when compared to wild type were those involved in biosynthetic processes. One of the proteins found in this category, namely VP0465 was found to have a putative function in lipid A biosynthesis. Given the role that LPS plays in promoting the wettability of the agar surface (Chen, Turner, & Berg, 2007; Copeland & Weibel, 2009), we hypothesize that PknT regulates the synthesis of lipid A, thereby playing a significant role in assembly of the core LPS structure. Interestingly, a *S. typhimurium* mutant that was defective in LPS biosynthesis resulted in premature onset of swarming as a result of increased production of the extracellular matrix (Toguchi et al., 2000).

One of the proteins that was significantly upregulated in  $\Delta pknT$  swimmers was VP1751 which was predicted to have a role in the biosynthesis of L-methionine. Interestingly, methionine has been shown to promote swarming behavior but in a concentration dependent manner (Bamidele & Babatunde, 2015). We surmise that methionine imbalance could be one of the factors that might result in the observed defect in swarming behavior in the  $\Delta pknT$  mutant strain.

Three proteins, namely VPA0807, VPA0808 and VPA0809 which altogether appear to encode a multidrug efflux pump were also found to be significantly upregulated in  $\Delta pknT$  swimmers, when compared to wild type (individual putative functions of these three proteins are mentioned in the "Discussion" section of Chapter 3). Despite the lack of significant hits, the three aforementioned proteins were also found to be upregulated to some degree in the  $\Delta ecfP$  swimmers when compared to wild type. As mentioned previously, these multidrug efflux pumps are also involved in the extrusion of certain molecules such as quorum signals (Alcalde-Rico et al., 2016; J. Sun et al., 2014). Given the importance of these quorum signals in swarming behavior (Trimble & McCarter, 2011), we hypothesize that the PknT/EcfP-mediated control of the *vpa0807-09* operon

## Discussion – Part II

---

of genes constitutes a previously uncharacterized player for quorum sensing and in turn, swarming behavior in *V. parahaemolyticus*.

Swarming behavior in *V. parahaemolyticus* has been shown to be regulated by quorum sensing through the *scr* operon of genes that requires the presence of an S signal (Trimble & McCarter, 2011). However, since none of these candidates were identified in the proteomics analyses on the swarmer cells of  $\Delta pknT$  when compared to wild type, we believe that PknT exerts its influence on swarming through a different mechanism that does not involve the aforementioned operon of genes. Furthermore, the global transcriptional regulator, OpaR, which governs the switch between opaque (OP) and translucent (TR) colony morphologies was also not identified to be one of the targets regulated by PknT swarmer cells. This further indicates that swarming behavior in *V. parahaemolyticus* is induced by PknT through a distinct mechanism that does not involve OpaR. Collectively, the aforementioned findings indicate that the regulatory role of PknT on swarming behavior of *V. parahaemolyticus* involves an entirely novel mechanism (possibly, through the *vpa0807-09* operon).

Altogether, our results suggest that phosphorylation of the ECF  $\sigma$  factor, EcfP by the kinase, PknT plays a role in regulation of swarming behavior in *V. parahaemolyticus*. This in turn appears to be dependent on the regulatory role of the kinase on a multitude of protein families, as indicated by our proteomics analyses. These protein families include ATPases, proteins involved in biosynthetic processes and heme transport proteins.

## **Chapter 5: Conclusions and future prospects**



One of the main outcomes of this thesis work sheds light on an entirely novel mechanism of regulation of ECF  $\sigma$  factors. Our findings show that in the marine pathogenic bacterium *V. parahaemolyticus*, the  $\sigma$  factor EcfP exists in a phosphorylated state. This is the first time that ECF  $\sigma$  factors have been shown to be phosphorylated in any bacterial species. Given the weight of this finding, upon investigation of the genetic neighborhood, we found that the gene encoding EcfP was cotranscribed with a gene that encodes for an STK, namely PknT. In fact, we were able to show that PknT is a genuine threonine kinase that was responsible for phosphorylation of EcfP. This phosphorylation was found to occur on a specific threonine residue (Thr63) on EcfP.

Additionally, the PknT/EcfP system was found to be essential for conferring polymyxin resistance in a phosphorylation-driven manner. In other words, the catalytically important aspartate residue of PknT (D202) and the phosphorylatable residue of EcfP (T63) were both found to be important for polymyxin resistance. Upon assessing the cellular output of the PknT/EcfP system through transcriptomics and proteomics analyses, we found that both proteins were responsible for the regulation of a putative UDP-glucose-4-epimerase, namely VPA0879 of unknown function. Interestingly, VPA0879 was found to be an essential polymyxin determinant, in that deletion of the gene encoding the protein resulted in severe polymyxin sensitivity. Our findings also indicate that regulation of VPA0879 was dependent on phosphorylation of EcfP, in that the peptides corresponding to VPA0879 were not detected through global LC-MS proteomics analyses, when the Thr63 residue of EcfP was replaced by alanine (T63A).

Furthermore, phosphorylation of EcfP was found to promote its interaction with the  $\beta/\beta'$  subunits of the RNA polymerase. Our results also indicate that the PknT/EcfP system is induced by polymyxin stress. The level of phosphorylated EcfP was significantly enhanced after the addition of polymyxin B. More strikingly, polymyxin treatment also resulted in a marked enrichment in the amount of  $\beta/\beta'$  subunits of the RNA polymerase that were co-immunoprecipitated with EcfP.

Moreover, through bioinformatics analyses, we found several instances of ECF  $\sigma$  factors that were found in association with STKs across the bacterial kingdom. Most of these proteins were found to belong to the ECF43 group. Our analyses also showed that among these  $\sigma$  factors, the invariant DAED motif that facilitates interaction with the RNA

## Conclusions and future prospects

---

polymerase was replaced by a stretch of uncharged amino acids. This can be seen in the case of EcfP, where the aforementioned motif is replaced by ST**I**A, comprising of the conserved Thr63 residue that is phosphorylated (bold and underlined). We propose that phosphorylation of Thr63 restores the negative charge (as in the case of the DAED motif) within EcfP, which then enables interaction with the positively charged helices of the RNA polymerase.

In line with our bioinformatics results, we also show that ECF sigma factor phosphorylation occurs in the distant bacterium, *Hyphomonas neptunium*. Collectively, our findings indicate that phosphorylation of ECF  $\sigma$  factors and eventual transcriptional regulation is a widespread mechanism in bacteria. Given the wide range of physiological processes that are affected by STKs and the abundance of ECF  $\sigma$  factors within the realm of signal transduction, the convergence of these two mechanisms is very appealing.

One of the key areas that warrants further research is the means through which polymyxin is sensed by the cells. The closest homologs of PknT appear to be proteins that are exclusive to Vibrionales and examination of conserved residues within these proteins could prove beneficial in mapping potential ligand binding sites. In the event wherein the kinase does not directly participate in sensing polymyxins, examination of the targets regulated by the PknT/EcfP system to assess levels of proteins within the outer membrane could help understand how the signal is transmitted to PknT and eventually to EcfP.

An interesting area of future research would be investigation of the promoter region of *vpa0879* to look for conserved -10 and -35 regions and eventually, assess for direct binding of EcfP through gel-shift assays. This aforementioned experiment could be modified to include the phosphoablative variant of EcfP (EcfPT63A), in order to provide direct evidence for the role of phosphorylation in promoter binding. Given that *vpa0879* encodes for a putative UDP-glucose-4-epimerase, metabolomics studies could help shed light on the levels of key metabolites that in turn aid in the assembly of the LPS layer. Furthermore, inspection of the LPS composition of  $\Delta$ *ecfP*,  $\Delta$ *pknT* and  $\Delta$ *vpa0879* mutants in comparison to wild type would also be beneficial in understanding the increased sensitivity to polymyxin antibiotics.

The transcriptomics results show that almost the entirety of the genes involved in Type III secretion system 1 (TTSS1) in *V. parahaemolyticus* were significantly

downregulated in both the  $\Delta ecfP$  and  $\Delta pknT$  mutants when compared to wild type. Future work on infection of the  $\Delta pknT$ ,  $\Delta ecfP$  and consequently,  $\Delta vpa0879$  mutants on infection of mammalian cells in the laboratory would definitely shed more insights on the biological importance of the system.

Yet another interesting area of research is the investigation on how the PknT/EcfP system itself could be regulated at the molecular level. Phosphorylation is a readily reversible process that requires the presence of specific protein phosphatases. Examination of the proteomics and transcriptomics profile of the PknT/EcfP system to identify these phosphatases and their eventual characterization remains one of the key aims of future research.

In addition to the above findings, the current work also provides evidence of a role for the PknT/EcfP system in regulation of swarming behavior in *V. parahaemolyticus*. Interestingly, while PknT and EcfP appear to be responsible for induction of swarming, the proteins encoded by the other two genes with the same operon (VP0054 and VP0056) appear to repress swarming behavior. Furthermore, our findings also indicate that the PknT/EcfP system function in a phosphorylation-based mechanism to regulate swarming motility. In other words, the catalytically significant aspartate residue of PknT (D202) and the phosphorylatable residue of EcfP (T63) were both found to be important for proper swarming behavior. Through global LC-MS proteomics analyses, we were able to discern several key categories of proteins that were regulated by PknT swimmers including transporters, proteins involved in biosynthetic functions and enzymatic processes.

Several key questions remain to be addressed with respect to these findings. In line with previous research done on swarming behavior in *V. parahaemolyticus* (Gode-Potratz et al., 2010; L. McCarter & Silverman, 1989) and the identification of the heme transport protein, VPA0882 in the current study as a key target of PknT, we hypothesized that EcfP could be involved in sensing iron. Further experiments are required to directly testing if an iron-containing salt could possibly turn on the PknT/EcfP system and if so, discerning the exact concentration at which this occurs. Additionally, examination of the levels of phosphorylated EcfP after addition of the appropriate concentration of iron could help discern whether iron stress stimulates phosphorylation of EcfP (as observed in the case of polymyxins – Chapter 3) and thereby, regulates swarming behavior in *V. parahaemolyticus*.

## Conclusions and future prospects

---

In order to obtain proof that EcfP directly regulates VPA0882 levels, one can inspect the promoter region of *vpa0882* to look for conserved -10 and -35 regions. These findings can in turn be used to evaluate direct binding of EcfP through gel-shift assays and thereby, transcriptional regulation. Further, the aforementioned experimental setup could be modified to include the phosphoablative variant of EcfP, in order to provide direct evidence for the role of phosphorylation in promoter binding and subsequently, transcriptional regulation.

Altogether, we have identified a novel and widespread mechanism of transcriptional regulation by  $\sigma$  factor phosphorylation in bacteria. In addition, our findings also indicate that this new mechanism of  $\sigma$  factor phosphorylation helps regulate polymyxin resistance and swarming behavior in *Vibrio parahaemolyticus*.



## **Chapter 6: Materials and Methods**



## 6.1. Chemicals, equipments and software

The reagents, kits, equipments and software used for the entirety of this thesis can be found in Table 1, Table 2, Table 3 and Table 4 respectively. The corresponding manufacturer information and identifier number are also recorded. In cases of microorganisms that belong to biosafety level 2, all necessary experiments, microbiological and molecular biological, were performed as per the guidelines set in place for the respective level.

**Table 1. List of reagents**

Reagents	Supplier	Identifier
<b>Genetic reagents</b>		
Restriction enzymes	New England Biolabs (NEB) (Frankfurt a.M.)	
2-Log DNA Ladder (0.1-10.0KB)	New England Biolabs (NEB) (Frankfurt a.M.)	NEB Cat#: N3200S
Color Pre-stained Protein Standard Broad Range (11-245 KDA)	New England Biolabs (NEB) (Frankfurt a.M.)	NEB Cat#: P7712S
T4 Ligase	New England Biolabs (NEB) (Frankfurt a.M.)	NEB Cat#: M0202L
10X Buffer for T4 DNA Ligase with 10mM ATP	New England Biolabs (NEB) (Frankfurt a.M.)	NEB Cat#: B0202S
Q5 Hot Start High Fidelity DNA Polymerase	New England Biolabs (NEB) (Frankfurt a.M.)	NEB Cat#: M0493S
Q5 High GC Enhancer	New England Biolabs (NEB) (Frankfurt a.M.)	NEB Cat#: B9028A
Q5 Reaction buffer	New England Biolabs (NEB) (Frankfurt a.M.)	NEB Cat#: B9027S
Desoxyribonucleotide (dNTP) Solution Mix	New England Biolabs (NEB) (Frankfurt a.M.)	NEB Cat#: N04475
Alkaline Phosphatase Calf Intestinal (CIP)	New England Biolabs (NEB) (Frankfurt a.M.)	NEB Cat#: M0290L
<b>Antibodies</b>		

## Materials and Methods

Living Colors A.v.	Clontech Laboratories, Inc.	Cat#: 632381
Monoclonal Antibody (JL-8)	(USA)	
Sheep anti-mouse $\alpha$ -GFP	GE, Amersham (UK)	Nr.: NXA931-1ML
<b>Chemical compounds/ drugs</b>		
Antibiotics: Chloramphenicol; Ampicillin sodium salt; Streptomycin sulfate; kanamycin sulfate	Carl Roth GmbH + Co KG (Karlsruhe)	Art.-Nr.: 3886.3; k029.3; 0236.2
Isopropyl $\beta$ -D-1 thiogalactopyranoside (IPTG)	Peqlab (Erlangen)	Nr.: 35-2030
Difco Agar, Granulated	Beckton Dickinson GmbH (Heidelberg)	Ref#: 214510
LB-Medium (Luria/Miller)	Carl Roth GmbH + Co KG (Karlsruhe)	Art.-Nr.: X968,3
L(+)-Arabinose	Carl Roth GmbH + Co KG (Karlsruhe)	Art.-Nr.: 5118.3
peqGOLD Universal Agarose	Peqlab (Erlangen)	Nr.: 35-1020
Agarose NEEP Ultra-Quality	Carl Roth GmbH + Co KG (Karlsruhe)	Art.-Nr.: 2267.3
D(+) Saccharose	Carl Roth GmbH + Co KG (Karlsruhe)	Art.-Nr.: 4621.1
Instant Blue	Expediton (United Kingdom)	Nr.: ISB1L
Gel loading dye purple 6X	New England Biolabs (NEB) (Frankfurt a.M.)	#B7025S
5-Bromo-4-Chloro-3-Indolyl- $\beta$ -D-Galactopyranoside (X- Gal)	Carl Roth GmbH + Co KG (Karlsruhe)	Art.-Nr.: 2315.4
Ethidium bromide	Carl Roth GmbH + Co KG (Karlsruhe)	Nr.: 1239-45-8
Red-gal	Sigma-Aldrich (Steinheim)	Nr.:1364C-A103X
X-Phos	Carl Roth GmbH + Co KG (Karlsruhe)	Nr.: A155.3
GFP bead slurry	Chromotek (USA)	Nr.: GTA-20
cOmplete, EDTA free protease inhibitor cocktail tablets	Roche diagnostics (Mannheim)	Nr.: 11873580001

Difco HI agar	Beckton Dickinson GmbH (Heidelberg)	Ref#: 244400
Crystal Violet	Carl Roth GmbH + Co KG (Karlsruhe)	Nr.: 548-62-9
2,2'-bipyridyl	Sigma-Aldrich (Steinheim)	Lot#: STBD3612V
Super-Sep phos-tag precast gel	Fujifilm WAKO (USA)	Nr.: 195-17991
<b>Materials</b>		
96-well plates	Greiner Bio-One GmbH (Frickenhausen)	
Petri dish (round) 92x16mm	Sarstedt AG (Nümbrecht)	Cat#: 82.1472.001
Petri dish (round) 150x20mm	Sarstedt AG (Nümbrecht)	Cat#: 82.1184.500
Microspin C18 columns	The Nest Group Inc. (USA)	Cat#: NC9270379
Petri dish (square) 100x100x20mm	Sarstedt AG (Nümbrecht)	Cat#: 82.9923.422

**Table 2. List of commercial kits and assays**

Name	Manufacturer	Identifier
NucleoSpin Gel and PCR Clean-up kit	Macherey-Nagel (Düren)	Ref.: 740609.250
NucleoSpin Plasmid Kit	Macherey-Nagel (Düren)	Ref.: 740588.250
Bacterial Two Hybrid Kit	Euromedex (Sooudelweyersheim, France)	Cat#: EUK001

**Table 3. List of software and online resources**

Name	Source/Reference	Additional information
SeqBuilder v12.3.1	DNASTAR Software for Life Scientists (Madison, WI)	
SeqMan Pro v12.3.1	DNASTAR Software for Life Scientists (Madison, WI)	
ImageJ-Fiji	(Schindelin et al., 2012)	<a href="http://rsbweb.nih.gov/ij">http://rsbweb.nih.gov/ij</a>
GraphPad Prism version 6.07	GraphPad Software (La Jolla CA)	<a href="https://www.graphpad.com/">https://www.graphpad.com/</a>

## Materials and Methods

NIS-Elements	NIS-Elements	Software	AR
Software	AR	5.02.00 (Nikon)	
4.60.00 (Nikon)			
Oligo	Calc:	(Kibbe, 2007)	<a href="http://biotools.nubic.northwestern.edu/Oligo%20Calc.html">http://biotools.nubic.northwestern.edu/Oligo° Calc.html</a>
Oligonucleotide Properties Calculator			
MaxQuant	v	(Cox & Mann, 2008)	
1.5.3.17			
Perseus		(Tyanova et al., 2016)	
Computational platform			
Scaffold v4.8.9		Proteome Software (Oregon, USA)	<a href="http://www.proteomesoftware.com/products/scaffold/">http://www.proteomesoftware.com/products/scaffold/</a>
Bowtie 2		(Langmead & Salzberg, 2012)	
SAMTool		(H. Li et al., 2009)	
BEDtools		(Quinlan & Hall, 2010)	
HMMER suite		(Finn, Clements, & Eddy, 2011)	
Clustal Omega		(Sievers & Higgins, 2014)	
v1.2.3			
NCBI (February 2019)		National Library of Medicine (USA)	<a href="https://www.ncbi.nlm.nih.gov/">https://www.ncbi.nlm.nih.gov/</a>
iTASSER		(Jianyi Yang et al., 2014)	<a href="https://zhanglab.ccmb.med.umich.edu/I-TASSER/">https://zhanglab.ccmb.med.umich.edu/I-TASSER/</a>
Chimera		(Pettersen et al., 2004)	<a href="http://www.rbvi.ucsf.edu/chimera/">http://www.rbvi.ucsf.edu/chimera/</a>

#### Table 4. List of essential equipments

Application	Device	Manufacturer
Electroporation	MicroPulser electroporator	Bio-rad (München)
PCR	Mastercycler nexus PCR System	Eppendorf (Hamburg)
Centrifugation	Centrifuge 5424 and 5424R.	Eppendorf (Hamburg)
	Multifuge 1 S-R, Fresco 17,	Heraeus/Thermo
	Multifuge X1R, Sorvall RC 6+	Scientific (Dreieich)
	Avanti JXN-26	Beckman Coulter (Krefeld)

Thermomixing	Thermomixer compact	Eppendorf (Hamburg)
DNA illumination and documentation	E-BOX VX2 imaging system	PeqLab (Eberhardzell)
DNA illumination	UVT_20 LE	Herolab (Wiesloch)
Protein electrophoresis	Mini-PROTEAN 3 cell	Bio-rad (München)
Western blotting	Transfer system from PeqLab	PeqLab (Eberhardzell)
Chemical-luminescence detection	Luminescent image analyzer LAS-4000	Fujifilm (Düsseldorf)
Stereo microscopy	Nikon H600L	Nikon (Düsseldorf)
Speed vacuum concentrator	Sovant SPD131DDA	Thermo Scientific (Dreieich)
Mass spectrometry	Q Exactive Plus Hybrid Quadrupole-Orbitrap Mass Spectrometer	Thermo Scientific (Dreieich)
Plate reader for absorbance measurements	Infinite M200 Pro	Tecan (Crailsheim)
Nanodrop for concentrations and purity of DNA/ RNA	ND-1000 Spectrophotometer	PeqLab (Eberhardzell)
Ultrasonicator	Sonopuls mini20	Bandelin (Berlin)
	UP200st Ultrasonic Processor	Hielscher (Teltow)

## 6.2. Media, buffers and solutions

The compositions of all the media, buffers and miscellaneous solutions that were used for experiments throughout the course of this thesis can be found in Table 5.

**Table 5. List of media, buffer and solutions**

Media/ Buffer	Composition
Luria Bertani (LB)	1% (w/v) tryptone; 0.5% (w/v) yeast extract; 1% (w/v) NaCl
Phosphate buffered saline (PBS)	For 10x solution: 25.6 g Na <sub>2</sub> HPO <sub>4</sub> ·7H <sub>2</sub> O

## Materials and Methods

HNN lysis buffer	80 g NaCl 2 g KCl 2 g KH <sub>2</sub> PO <sub>4</sub> Bring to 1 liter with H <sub>2</sub> O. Autoclave for 40 minutes at 121°C. 50 mM HEPES pH 7.5, 150 mM NaCl and 5 mM EDTA
TAE Buffer	For 50X solution: 50mM EDTA, 2M Tris base, 1M acetic acid, adjust pH to 8.7
Milk solution for Western Blot	For 1L: 50g dry non-fat milk powder, 100ml 10X PBS, 1ml Tween-20 and appropriate volume of distilled water
Cathode buffer	25mM Tris base; 40mM glycine; 10% methanol, adjust pH to 9.4 (For phostag gels, 10mM EDTA was added)
Anode buffer I	25mM Tris base; 10% methanol, adjust pH to 10.4
Anode buffer II	0.3M Tris base; 10% methanol, adjust pH of 10.4
Luria-Bertani (LB)	1% (w/v) tryptone; 0.5% (w/v) yeast extract; 1% (w/v) NaCl
Difco Heart Infusion (HI) agar	For 1L: 10g Beef Heart (Infusion from 500g); 10g Tryptone; 5g sodium chloride; 15g agar
SDS PAGE Resolving gel buffer	1.5M Tris-HCl pH 8.8; 0.4% (w/v) SDS
SDS PAGE Stackinng gel buffer	1.5M Tris-HCl pH 6.8; 0.4% (w/v) SDS
2X SDS sample buffer	125mM Tris pH 6.8; 20% (w/v) glycerol; 4% (w/v) SDS; 0.02% bromophenol blue; 10% BME

### 6.3. Microbiological methods

#### 6.3.1. Bacterial growth conditions

If not otherwise stated, *V. parahaemolyticus* and *E. coli* were grown in LB medium (Carl-Roth) or on LB agar (Beckton, Dickinson and Company) plates at 37 °C, containing antibiotics in the following concentrations: streptomycin 200 µg/ml; kanamycin 50 µg/ml; ampicillin 100 µg/ml; chloramphenicol 20 µg/ml for *E. coli* and 5 µg/ml for *V. parahaemolyticus*. Polymyxins (B and E) were added in the concentrations indicated in the figures and figure legends. When needed, L-arabinose (Carl-Roth) and IPTG (Carl-



Roth) were added to final concentrations of 0.2% w/v and 500  $\mu$ M (if not otherwise specified), respectively.

### 6.3.2. Bacterial strains

Deletion of genes in *V. parahaemolyticus* was performed through the principle of homologous recombination. *E. coli* strain DH5 $\alpha$ pir was used for standard cloning and *E. coli* strain SM10 $\lambda$ pir was for conjugative transfer of pDM4 derivatives from *E. coli* to *V. parahaemolyticus*. The procedure is described as follows.

Both the donor *E. coli* strain (SM10 $\lambda$ pir) harboring the corresponding plasmid (pDM4 derivative) and the recipient *V. parahaemolyticus* strain were grown in LB until the cultures reach an OD<sub>600</sub> of approximately 0.5. 1 ml of each of these cultures was then harvested and the obtained pellet was resuspended in 100  $\mu$ l of LB. 40  $\mu$ l of each of these suspensions was then mixed together in a separate tube. From this, triplicates of 20  $\mu$ l of the mixture were spotted on LB-agar plates and incubated at 37 °C. The grown spots were then scraped off and resuspended in 1ml of LB medium. Dilution series of the aforementioned suspension were plated on LB+Amp+Cm plates and incubated at 37 °C. Single colonies that were obtained from these dilution series were then restreaked onto fresh LB+Amp+Cm plates and once again incubated at 37 °C. The colonies thus obtained were the single crossovers and if the next step is not carried out immediately after, the single crossovers obtained can be suspended in glycerol and stored at -80 °C for storage.

The single crossovers obtained above were grown in LB broth containing Cm with shaking at 37 °C for at least 5-6 hours. From this grown culture, 50  $\mu$ l was taken out and mixed with a solution containing 2 ml of LB broth and 1 ml of 33% sucrose solution. This mixture was grown with shaking at 37 °C for around 20-24 hours. Dilution series of this grown culture were then plated on to LB agar plates containing 33% sucrose and incubated overnight at 30 °C. The colonies thus obtained were streaked on to both LB+Amp+Cm plates and LB+Amp plates. Those that were found to be sensitive to Cm were further tested by colony PCR to assess for the corresponding deletion. If positive results were obtained through agarose gel electrophoresis, the respective patches were further restreaked onto LB+Amp plates and incubated at 37 °C to obtain single colonies. These single colonies were once again tested with colony PCR to assess for deletion of the gene. The PCRs were performed alongside genomic DNA of *V. parahaemolyticus* to assess for the size shift in the DNA band, indicative of the deletion.

## Materials and Methods

The aforementioned procedure of conjugative transfer/ homologous recombination was also carried out to obtain insertions within the genome of *V. parahaemolyticus*. Colony PCR of the positive patches and colonies at the end of the double crossover step were performed alongside genomic DNA to assess for an increase in the desired DNA band, indicative of an insertion within the genome.

*E. coli* strain MG1655 was used for Phos-tag and Co-IP/MS experiments. The wild-type strain of *V. parahaemolyticus* used was the clinical isolate 2210633 and all mutants are derivatives of this strain. All strains used are listed in Table 6.

**Table 6. List of strains**

Strains	Description/genotype	References
<i>Vibrio parahaemolyticus</i> RIMD2210633	Clinical isolate, wild-type	(Makino et al., 2003)
SI1	$\Delta vp0057 (\Delta pknT)$	This work
SI6	$\Delta vp0054$	This work
SI7	$\Delta vp0055 (\Delta ecfP)$	This work
SI8	$\Delta vp0056$	This work
SI14	$\Delta vp0054 \Delta vp0057$	This work
SI15	$\Delta vp0054 \Delta vp0055 \Delta vp0056 \Delta vp0057$	This work
SI16	$\Delta vp0057 \Omega vp0057$	
SI17	$vp0057D202A$	This work
SI51	$\Delta vp0054 \Delta vp0055$	This work
SI52	$\Delta vp0056 \Delta vp0057$	This work
SI53	$\Delta vp0054 \Delta vp0056$	This work
SI62	$vp0055T63A$	This work
SI70	$\Delta vpa0879$	This work
SI95	$vp0055T63E$	This work
<i>Escherichia coli</i> DH5 $\alpha$ pir	sup E44, $\Delta lacU169 (\Phi lacZ \Delta M15)$ , recA1, endA1, hsdR17, thi-1, gyrA96, relA1, $\lambda$ pir	
<i>Escherichia coli</i> SM10 $\lambda$ pir	KmR, thi-1, thr, leu, tonA, lacY, supE, recA::RP4-2-Tc::Mu, $\lambda$ pir	
<i>Escherichia coli</i> BTH101	F-, cya-99, araD139, galE15, galK16, rpsL1 (StrR), hsdR2, mcrA1, mcrB1, relA1	(G Karimova, Pidoux,

<i>Escherichia coli</i> MG1655	F- $\lambda$ - ilvG- rfb-50 rph-1	Ullmann, & Ladant, 1998)
-----------------------------------	-----------------------------------	-----------------------------

### 6.3.3. Swimming assays

A single *V. parahaemolyticus* bacterial colony from a plate was inoculated into 5 ml of LB medium and grown until the cells reach stationary phase ( $OD_{600} \geq 3.0$ ). This was followed by immersing a sterile toothpick into the culture and pricking it onto the surface of LB plates containing 0.3% agar (swimming medium). The plates were then incubated at 30 °C for at least 10 hours. Subsequently, the diameter of the swimming colony was measured and eventually plotted in the form of bar graphs. Calculations were made with respect to the wild type strain.

### 6.3.4. Growth curves

A single *V. parahaemolyticus* bacterial colony from a plate was inoculated into 5 ml of LB medium and grown until the cells reach stationary phase ( $OD_{600} \geq 3.0$ ). From this culture, 10  $\mu$ l was taken and resuspended into 1 ml of LB medium. After proper mixing, 1  $\mu$ l of the cells were inoculated into 200  $\mu$ l of LB medium in microtiter plates. At least 3-4 replicates were performed for each strain that was used. The microtiter plates were incubated at 37 °C (with shaking) in a TECAN Microplate Reader (Infinite 200 PRO). Absorbance ( $OD_{600}$ ) values were recorded every 15 minutes for 18 hours and subsequently, the average values of the replicates was plotted against time.

### 6.3.5. Swarming assays

A single *V. parahaemolyticus* bacterial colony from a plate was inoculated into 5 ml of LB medium and grown until the cells reach an  $OD_{600}$  of approximately 1.0. This was followed by spotting 1  $\mu$ l of the culture onto a plate containing HI agar supplemented with 4M calcium chloride and 50mM 2, 2' dipyridyl. The plate was incubated at 24 °C for 17 hours to allow swarming motility to take place. The diameter of the swarm colony was calculated the next day and plotted in the form of a bar graph. All calculations were done with respect to wild type.

### 6.3.6. Submerged biofilm formation assay

*V. parahaemolyticus* cells were grown on agar plates and from this, a single colony was inoculated into 5 ml of HI medium (containing 2% sodium chloride) and incubated overnight at 37 °C with shaking. From this overnight culture, dilution series were prepared in a solution containing HI medium (with 2% sodium chloride) in a microtiter plate (total volume of 200 µl). This plate was then incubated at 30 °C for 16 hours to enable formation of pellicles. After this incubation period, the pellicles (formed on the surface) were removed using a sterile Q-tip. The remaining liquid was then removed using a multichannel pipette. This was followed by the addition of 225 µl of 0.1% Crystal Violet dye into the wells and incubation at room temperature for 15 minutes. The dye solution was subsequently drained and the wells were washed three times with distilled water. Finally, 300 µl of DMSO was added to the wells and the absorbance values were measured at 570 nm and plotted in the form of bar graphs.

### 6.3.7. Bacterial two hybrid assays

In order to detect protein-protein interactions by reconstituting certain proteins in *E. coli*, the bacterial two hybrid (BACTH) assay was employed (G Karimova et al., 1998). The assay makes use of the T18 and T25 domains of the adenylate cyclase within the organism, *Bordetella pertussis*. In order to carry out the experiment, plasmids that encode either the T18 domain (pUT18 or pUT18C) or the T25 domain (pKNT25 or pKT25) were purified and the corresponding genes whose products are to be tested for interaction were fused to the aforementioned plasmids. The plasmids in the study were all provided by the manufacturer (Euromedex, Soouddelweyheim, France).

After designing the appropriate constructs, two plasmids (one encoding for the T18 and the other encoding for the T25 domain), carrying either N-terminal or C-terminal fusions of the gene of interest were co-transformed into the *E. coli* strain, BTH101. The reason for using this particular strain of *E. coli* is that it lacks the *cyaA* gene which in turn encodes for the catalytic domain of adenylate cyclase. Therefore, on its own this strain is unable to produce the messenger molecule, cyclic adenosine monophosphate (cAMP). Interaction between the genes used in the aforementioned co-transformation experiment in turn results in bringing the T18 and the T25 domains closer to each other and subsequently, reconstitution of the catalytic domain of the adenylate cyclase enzyme. As a result of this, the strain is able to produce cAMP which is then able to activate transcription of the *lac* operon and subsequently, expression of  $\beta$ -galactosidase

( $\beta$ -gal). This can be visualized by employing the indicator, X-gal which is in turn cleaved by the  $\beta$ -gal enzyme and resulting in the formation of blue colonies.

The experimental workflow of a typical BACTH assay in the laboratory is described as follows. 20-25 ng of the purified plasmid DNA (from both T18 and T25) were used for transformation into BTH101. The transformed cells were in turn plated onto LB agar plates with the following antibiotics: 100  $\mu$ g/ml of ampicillin, 50  $\mu$ g/ml of kanamycin. In order to permit blue-white screening, the plates were also supplemented with 500  $\mu$ M of IPTG and 80  $\mu$ g/ml of X-gal. The plates were then incubated at 30 °C for a period not lasting longer than 2 days. From each of these plates, three colonies (standing for three replicates) were selected and resuspended into 1 ml of LB medium containing the aforementioned antibiotics. The Eppendorf tubes were then shaken at 30 °C for at least 2 hours. They were then spotted onto LB-agar plates containing the aforementioned antibiotics and indicators and incubated at 30 °C for a maximum period of 2 days. Pictures were taken of the above plates at regular intervals. In all cases, co-transformation of pUT18C-zip and pKNT25-zip (Euromedex, Soouddelweyrsheim, France) into BTH101 was carried out and this served as the positive control. On the other hand, transformations were also done with empty vectors which in turn served as negative controls.

### 6.3.8. Stressor sensitivity assay

The effect of the following stressors was tested on *V. parahaemolyticus* wild type and mutant strains: Streptomycin (Carl-Roth) was used to test if deletion of either the kinase or the sigma factor had any effect on protein synthesis. In order to gauge the effects of the above deletions to changes in the cell membrane, several compounds were tested: salt (specifically, sodium chloride) (Carl-Roth), detergent (sodium dodecyl sulphate (SDS) (Carl-Roth) – both of which have denaturing properties on the outer membrane, heat which affects permeability of the cell and benzopenicillin (or Penicillin G) (Sigma-Aldrich), a beta-lactam antibiotic which has been shown to disrupt the peptidoglycan cross-links within the cell envelope. Finally, polymyxins (Polymyxin B and E) (EMD Millipore Corporation) were used to test the effect of the genes on lipopolysaccharides (LPS) and the cell envelope.

The appropriate stressor concentration was mixed with 50 ml of LB-agar. Serial dilutions of stationary phase-grown cells were then spotted onto the LB-agar plates and incubated at 37 °C overnight. In order to measure colony forming units (CFU's), cells

## Materials and Methods

---

from each dilution series were spread on LB-agar plates with the indicated concentration of stressor compound. They were then incubated at 37 °C overnight and the number of colonies were enumerated by hand and the CFU per mL was calculated. For each experiment, a minimum of three biological replicates were performed.

### 6.3.9. Membrane orientation assay

To assess membrane topology of the kinase PknT, the plasmids pSI049 and pSI076 were transformed into *E. coli* DH5 $\alpha$ pir and the resulting colonies were streaked on LB-agar containing two indicators, 80  $\mu$ g/ml of 5-bromo-4-chloro-3-indolyl phosphate disodium salt (X-Phos) (Sigma-Aldrich) and 100  $\mu$ g/ml of 6-chloro-3-indolyl-D-galactoside (Red-Gal) (Sigma-Aldrich), in addition to 1mM of the inducer, IPTG dissolved in 50 mM of phosphate buffer (pH 7.0) and the appropriate antibiotic. The plates were then incubated overnight at 37 °C and the coloration of the bacterial colonies was assessed the following day. A red color is indicative of high  $\beta$ -galactosidase activity indicating a cytosolic localization of the PknT site at which PhoA/LacZ $\alpha$  is translationally fused to. A blue coloration indicates a high alkaline phosphatase activity indicating a periplasmic localization of the PhoA/LacZ $\alpha$  fusion site of PknT.

## 6.4. Molecular cloning

### 6.4.1. Isolation of genomic DNA from *V. parahaemolyticus*

The corresponding *V. parahaemolyticus* strain was streaked out on LB-agar plates containing the respective antibiotic and incubated overnight at 37 °C. The following day, a small portion of the grown cells was resuspended in distilled water and boiled for 10 minutes in a Thermomixer (Eppendorf Thermomixer C). This was followed by centrifugation of the samples at 10,000 rpm for 10 minutes. The resulting supernatant (the genomic DNA) was then transferred to a fresh Eppendorf tube for further use.

### 6.4.2. Isolation of plasmid DNA from *E. coli*

*E. coli* strains containing the corresponding plasmid(s) were grown in 5 ml of LB (with the relevant antibiotic) at 37 °C with shaking until the cells reach stationary phase (OD<sub>600</sub>  $\geq$  3.0). Plasmid DNA was obtained from these cells by following the NucleoSpin Plasmid kit (Macherey-Nagel). The concentration of the obtained plasmid DNA was then measured using a Nanodrop spectrophotometer.

### 6.4.3. Polymerase chain reaction (PCR)

Amplification of corresponding DNA fragments were carried out either with the Q5 Hot Start High Fidelity DNA Polymerase or Phusion High-Fidelity DNA Polymerase. The total reaction volume used for the PCR was 50  $\mu$ l. However, in case of colony PCR, the total reaction volume used was 20  $\mu$ l. The composition of the PCR mixtures for Q5 Hot Start Polymerase and Phusion Polymerase are shown in Table 7 and Table 8 respectively. The conditions that were used for PCR largely depend on the size of the product that is desired.

**Table 7. Components of the Q5 PCR reaction mix**

Reagents	Volumes ( $\mu$ l)
10mM dNTPs	1
5X Q5 reaction buffer	10
5X Q5 High GC enhancer	10
0.5 $\mu$ M forward primer	2
0.5 $\mu$ M reverse primer	2
Polymerase	0.5
Template DNA	1
Nuclease-free water	Up to 50 $\mu$ l

**Table 8. Components of the Phusion PCR reaction mix**

Reagents	Volumes ( $\mu$ l)
10mM dNTPs	1
10X Buffer	5
0.5 $\mu$ M forward primer	2
0.5 $\mu$ M reverse primer	2
Polymerase	1
Template DNA	1
Nuclease-free water	Up to 50 $\mu$ l

### 6.4.4. Separation and detection of DNA using agarose gel electrophoresis

Separation of DNA was facilitated by agarose gel electrophoresis by employing 1% agarose gels. The agarose gels were made by mixing the corresponding amount of agarose in 0.5X TAE buffer and 0.01% of ethidium bromide. The DNA samples were in turn suspended in 6X Gel loading dye purple (New England Biolabs). A 2-log DNA ladder (New England Biolabs) was used as the marker to help assess the size of the DNA fragment. The gels were in turn visualized with the help of the E-BOX VX2 imaging system (PeqLab). If needed, specific DNA fragments were excised for further use.

### 6.4.5. Site-directed mutagenesis

The rolling-circle method of DNA amplification was employed to facilitate site-directed mutagenesis (Lizardi et al., 1998). The appropriate plasmid DNA was amplified using Q5 Hot Start High Fidelity DNA Polymerase with the corresponding primers. The PCR product was then immediately purified with the NucleoSpin Gel and PCR Clean-up kit (Macherey-Nagel). This was followed by digestion of the purified product with DpnI and subsequent clean-up with the above mentioned kit. The digested DNA was then transformed into *E. coli* and the resulting colonies were sent for sequencing to confirm the introduction of the respective point mutations into the plasmid DNA.

### 6.4.6. Restriction digestion of DNA

Digestion of DNA was carried out using restriction endonucleases and the corresponding buffers that the enzymes are compatible with (NEB Germany; Fermentas, Canada). 1 µg of DNA (both insert and vector) was incubated with the appropriate restriction enzymes and buffers for at least 1.5 hours at 37 °C. This was followed by the addition of 1 µl of calf intestine alkaline phosphatase (CIP) to the vector to prevent self-ligation. The resulting digested product was then separated through agarose gel electrophoresis. The desired band was then excised and eluted using the NucleoSpin Gel and PCR Clean-up kit (Macherey-Nagel).

### 6.4.7. Ligation of DNA

Ligation of DNA was carried out using the T4 DNA ligase and the appropriate buffer (New England BioLabs). The reaction was carried out as follows. A 1:5 ratio of the digested vector:insert DNA was mixed in an Eppendorf tube. To this mix, 1 µl of T4 DNA



ligase and the corresponding volume of 10X ligase buffer was added and the total volume was made up with water to 20  $\mu$ l. The ligation reaction was allowed to carry out at room temperature for a minimum period of 1 hour. This was followed by transformation of the ligation reaction mixtures into corresponding *E. coli* strains.

### 6.4.8. Preparation of chemically competent *E. coli* cells

A single *E. coli* bacterial colony from a plate was inoculated into 5 ml of LB medium with the corresponding antibiotic and grown at 37 °C with shaking until the cells reach an OD<sub>600</sub> of 0.7-1.0. From this culture, subsequent inoculation was done into a larger volume of LB such that the initial OD<sub>600</sub> of the cells was approximately 0.05. The culture was grown at 37 °C with shaking until the cells reach an OD<sub>600</sub> of 0.5-0.7. This was followed by centrifugation of the samples at 4700 rpm for 10 minutes at 4 °C. The resulting pellet was then washed twice with 50mM ice-cold calcium chloride. The pellet obtained after the second wash was in turn resuspended in a solution of 50 mM (ice-cold) calcium chloride and 1/10<sup>th</sup> volume of glycerol. After resuspension, aliquots of approximately 50 $\mu$ l were snap-chilled in liquid nitrogen and subsequently stored at -80 °C.

### 6.4.9. Transformation of chemically competent *E. coli* cells

50  $\mu$ l of the (above-obtained) chemically competent *E. coli* cells was added to 50-100 ng of the corresponding plasmid. The resulting mixture was gently mixed and placed on ice for approximately 30 minutes. This was followed by subjecting the cells to heat-shock in order to facilitate plasmid uptake by incubating them in a water bath set to 42 °C for 1 minute. Subsequently, the cells were immediately transferred back to ice and resuspended in 500  $\mu$ l of LB medium. The cells were then shaken for 45 minutes at 37 °C followed by centrifugation. After decanting a substantial amount of the supernatant, approximately 50-100  $\mu$ l of the cells was plated onto LB-agar plates containing the relevant antibiotic.

### 6.4.10. Preparation of electro-competent *Vibrio parahaemolyticus* cells

A single *V. parahaemolyticus* bacterial colony from a plate was inoculated into 200 ml of LB medium and grown at 37 °C with shaking until the cells reach an OD<sub>600</sub> of 1.0. This was followed by centrifugation of the samples at 4700 rpm for 10 minutes at 4 °C. The resulting pellet was then washed twice with 273 mM ice-cold sucrose solution (that is in turn buffered with KOH to a pH of 7.2-7.4). The pellet obtained after the second wash was in turn resuspended in a solution of 273 mM (ice-cold) sucrose solution and 1/10<sup>th</sup> volume of glycerol. After resuspension, aliquots of approximately 100µl were snap-chilled in liquid nitrogen and subsequently stored at -80 °C.

### 6.4.11. Transformation of electro-competent *V. parahaemolyticus* cells

100 µl of the (aforementioned) electro-competent *V. parahaemolyticus* cells was added to 100-1000 ng of the corresponding plasmid. The resulting mixture was gently mixed and placed on ice for approximately 1 hour. This mixture was transferred into a pre-chilled electroporation cuvette. Immediately, electroporation was carried out using a MicroPulser electroporator (Bio-Rad) at the following conditions: voltage 2200, µF 25 and 200 Ω. Subsequently, the cells were immediately transferred back to ice and resuspended in 1 ml of LB medium. The cells were then transferred back into a 1.5 ml Eppendorf tube and shaken for at least 2 hours at 37 °C, followed by centrifugation. After decanting a substantial amount of the supernatant, approximately 50-100 µl of the cells was plated onto LB-agar plates containing the relevant antibiotic.

### 6.4.12. Plasmids

A comprehensive list of all plasmids used in this work is provided in Table 9. This section also details the construction of each of the plasmids mentioned in the table.

**Table 9. List of plasmids**

Plasmids	Description/genotype	References
pDM4	Suicide vector for gene deletions and insertions	(Donnenberg & Kaper, 1991)

pBAD33	Pbad	(Guzman, Belin, Carson, & Beckwith, 1995)
pKTOP	phoA-lacZ $\alpha$	(Gouzel Karimova, Robichon, & Ladant, 2009)
pKNT25	Plac::T25	(G Karimova et al., 1998)
pUT18	Plac::T18	(G Karimova et al., 1998)
pKT25	Plac::T25	(G Karimova et al., 1998)
pUT18C	Plac::T18	(G Karimova et al., 1998)
pJH036	Pbad::sfGFP	This work
pSI001	Plasmid for the deletion of <i>vp0057</i>	This work
pSI008	Plasmid for the deletion of <i>vp0054</i> , <i>vp0055</i> , <i>vp0056</i> and <i>vp0057</i>	This work
pSI010	Pbad::sfGFP- <i>vp0055</i>	This work
pSI016	Plac:: <i>vp0055</i> -t25	This work
pSI017	Plac:: <i>vp0055</i> -t18	This work
pSI018	Plac::t25- <i>vp0055</i>	This work
pSI019	Plac::t18- <i>vp0055</i>	This work
pSI024	Plac:: <i>vp0057</i> -t25	This work
pSI025	Plac:: <i>vp0057</i> -t18	This work
pSI026	Plac::t25- <i>vp0057</i>	This work
pSI027	Plac::t18- <i>vp0057</i>	This work
pSI046	Plasmid for the deletion of <i>vp0054</i>	This work
pSI047	Plasmid for the deletion of <i>vp0055</i>	This work
pSI048	Plasmid for the deletion of <i>vp0056</i>	This work
pSI049	Plac:: <i>vp0057</i> -PhoA-LacZ $\alpha$	This work
pSI050	Plasmid for the insertion of <i>vp0057</i> in between intergenic regions <i>vp2408</i> and <i>vp2409</i> cloned into PDM4	This work
pSI051	Plasmid for replacing the native <i>vp0057</i> locus with <i>vp0057D202A</i>	This work
pSI068	Plac::t18- <i>vp0057D202A</i>	This work
pSI076	Plac::PhoA-LacZ $\alpha$ - <i>vp0057</i>	This work
pSI077	Plasmid for the deletion of <i>vpa0879</i>	This work
pSI080	Plac::t25- <i>vp0055T63A</i>	This work

## Materials and Methods

pSI084	Plasmid for insertion of <i>vp0055T63A</i> on the chromosome replacing the native <i>vp0055</i> locus	This work
pSI109	Plac:: <i>vp0057</i>	This work
pSI120	Plasmid for the deletion of the genes <i>vp0054</i> and <i>vp0055</i>	This work
pSI121	Plasmid for the deletion of the genes <i>vp0056</i> and <i>vp0057</i>	This work
pSRKKm	pBBR1MCS-2-derived broad-host-range expression vector containing lac promoter and lacIq, lacZ $\alpha$ , and Kmr	(Khan, Gaines, Roop, & Farrand, 2008)
pSI127	PBAD::sfGFP- <i>vp0055</i> T63E	This work
pSI128	Pbad::sfGFP- <i>vp0055T63A</i>	This work
pSI130	Plasmid for insertion of <i>vp0055T63E</i> on the chromosome replacing the native <i>vp0055</i> locus	This work
pSI132	Pbad::sfGFP- <i>hne1495</i>	This work
pSI135	Plac:: <i>hne1496</i>	This work

### 6.4.12.1. Construction of plasmids

#### Plasmid pSI001

The upstream and downstream flanking regions of the gene *vp0057* were amplified from *V. parahaemolyticus* using the primers *vp0057-del-a/vp0057-del-b* and *vp0057-del-c/vp0057-del-d* respectively. The resulting fragments were then fused together in a third PCR reaction by using primers *vp0057-del-a/vp0057-del-d*. This DNA fragment was then digested with XbaI and then inserted into the corresponding site of pDM4, resulting in the plasmid pSI001.

#### Plasmid pSI008

The upstream region of the gene *vp0057* and the downstream region of the gene *vp0054* were amplified from *V. parahaemolyticus* using the primers *VP0057Operon-del-a/VP0057Operon-del-b* and *VP0057Operon-del-c/VP0057Operon-del-d* respectively. The resulting fragments were then fused together in a third PCR reaction by using primers *VP0057Operon-del-a/VP0057Operon-del-d*. This DNA fragment was then

digested with the enzymes, XbaI and SphI and then inserted into the corresponding site of pDM4, resulting in the plasmid pSI008.

### **Plasmid pSI046**

The upstream and downstream flanking regions of the gene *vp0054* were amplified from *V. parahaemolyticus* using the primers VP0054-del-a/VP0054-del-b and VP0054-del-c/VP0054-del-d respectively. The resulting fragments were then fused together in a third PCR reaction by using primers VP0054-del-a/VP0054-del-d. This DNA fragment was then digested with the enzymes, XbaI and SphI and then inserted into the corresponding site of pDM4, resulting in the plasmid pSI046.

### **Plasmid pSI047**

The upstream and downstream flanking regions of the gene *vp0055* were amplified from *V. parahaemolyticus* using the primers VP0055-del-a/VP0055-del-b and VP0055-del-c/VP0055-del-d respectively. The resulting fragments were then fused together in a third PCR reaction by using primers VP0055-del-a/VP0055-del-d. This DNA fragment was then digested with the enzymes, XbaI and SphI and then inserted into the corresponding site of pDM4, resulting in the plasmid pSI047.

### **Plasmid pSI048**

The upstream and downstream flanking regions of the gene *vp0056* were amplified from *V. parahaemolyticus* using the primers VP0056-del-a/VP0056-del-b and VP0056-del-c/VP0056-del-d respectively. The resulting fragments were then fused together in a third PCR reaction by using primers VP0056-del-a/VP0056-del-d. This DNA fragment was then digested with the enzymes, XbaI and SacI and then inserted into the corresponding site of pDM4, resulting in the plasmid pSI048.

### **Plasmid pSI077**

The upstream and downstream flanking regions of the gene *vpa0879* were amplified from *V. parahaemolyticus* using the primers vpa0879-del-a/vpa0879-del-b and vpa0879-del-b/vpa0879-del-d respectively. The resulting fragments were then fused together in a third PCR reaction by using primers vpa0879-del-a/vpa0879-del-d. This DNA fragment was then digested with the enzymes, SalI and SacI and then inserted into the corresponding site of pDM4, resulting in the plasmid pSI077.

## Materials and Methods

---

### Plasmid pSI120

The upstream flanking region of the gene *vp0055* and the downstream flanking region of the gene, *vp0054* were amplified from *V. parahaemolyticus* using the primers VP0055-del-a/delvp0054delvp0055-b and VP0054-del-c/VP0054-del-d respectively. The resulting fragments were then fused together in a third PCR reaction by using primers VP0055-del-a/VP0054-del-d. This DNA fragment was then digested with the enzymes, XbaI and SphI and then inserted into the corresponding site of pDM4, resulting in the plasmid pSI088.

### Plasmid pSI121

The upstream flanking region of the gene *vp0057* and the downstream flanking region of the gene *vp0056* were amplified from *V. parahaemolyticus* using the primers vp0057-del-a/delvp0056delvp0057 b and VP0056-del-c/VP0056-del-d respectively. The resulting fragments were then fused together in a third PCR reaction by using primers vp0057-del-a/VP0056-del-d. This DNA fragment was then digested with the enzymes, XbaI and SacI and then inserted into the corresponding site of pDM4, resulting in the plasmid pSI089.

### Plasmids pSI016 and pSI017

The gene *vp0055* was amplified from *V. parahaemolyticus* using primers vp0055 pKNT25 cw/vp0055 pKNT25 ccw and the DNA fragment produced from the PCR was digested with the enzymes, XbaI and KpnI and inserted into the corresponding sites of the plasmids, pKNT25 and pUT18, resulting in the plasmids pSI017 and pSI018 respectively.

### Plasmids pSI018 and pSI019

The gene *vp0055* was amplified from *V. parahaemolyticus* using primers vp0055 pKT25 cw/vp0055 pKT25 ccw and the DNA fragment produced from the PCR was digested with the enzymes, XbaI and KpnI and inserted into the corresponding sites of the plasmids, pKT25 and pUT18C, resulting in the plasmids pSI019 and pSI020 respectively.

### Plasmids pSI024 and pSI025

The gene *vp0057* was amplified from *V. parahaemolyticus* using primers vp0057 full pKNT25 cw/vp0057 full pKNT25 ccw and the DNA fragment produced from the PCR was digested with the enzymes, XbaI and KpnI and inserted into the corresponding sites of the plasmids, pKNT25 and pUT18, resulting in the plasmids pSI025 and pSI026 respectively.

### Plasmids pSI026 and pSI027

The gene *vp0057* was amplified from *V. parahaemolyticus* using primers *vp0057* full pKT25 cw/*vp0057* full pKT25 ccw and the DNA fragment produced from the PCR was digested with the enzymes, XbaI and KpnI and inserted into the corresponding sites of the plasmids, pKT25 and pUT18C, resulting in the plasmids pSI027 and pSI028 respectively.

### Plasmid pSI068

Generation of pSI068 for bacterial two hybrid screen was achieved by rolling circle PCR using pSI028 as a template with primers VP0057-D202A B Primer/VP0057-D202A C Primer.

### Plasmid pSI080

Two PCRs were performed on the gene *vp0055* of *V. parahaemolyticus* with primers *vp0055* pKT25 cw/55 T63A CCW and 55 T63A CW/*vp0055* pKT25 ccw, respectively. The resulting fragments were then fused together in a third PCR using the primers *vp0055* pKT25 cw/*vp0055* pKT25 ccw. This third DNA fragment was then digested with the enzymes, XbaI and KpnI and fused into the corresponding site of pKT25, resulting in the plasmid pSI080.

### Plasmid pSI130

Two PCRs were performed on the gene *vp0055* of *V. parahaemolyticus* with primers *vp0055* pKT25 cw/VP0055 T63E CCW and VP0055 T63E CW/*vp0055* pKT25 ccw, respectively. The resulting fragments were then fused together in a third PCR using the primers *vp0055* pKT25 cw/*vp0055* pKT25 ccw. This third DNA fragment was then digested with the enzymes, XbaI and KpnI and fused into the corresponding site of pKT25, resulting in the plasmid pSI130.

### Plasmid pSI050

Plasmid pSI050 was created to facilitate chromosomal insertion of the gene *vp0057* in a different part of the genome of *V. parahaemolyticus*. The region between genes *vp2408* and *vp2409* was chosen for insertion. Three separate PCR reactions were carried out. The gene *vp2408* and a part of the flanking region between *vp2408* and *vp2409* were amplified from *V. parahaemolyticus* using primers 57ChrIns-A/57ChrIns-B. The gene *vp0057* alongside its native promoter was amplified using primers 57ChrIns-C/57ChrIns-D. Finally, the gene *vp2409*, alongside a part of the flanking region between *vp2408* and

## Materials and Methods

---

*vp2409* was amplified using primers 57Chrlns-E/57Chrlns-F. The products of the three PCR reactions were fused together with primers 57Chrlns-A/57Chrlns-F and the resulting DNA was restricted with XbaI and SacI and fused into the corresponding site of pDM4, resulting in the plasmid pSI050.

### Plasmid pSI051

In order to obtain plasmid pSI051, three separate PCR reactions were carried out. The upstream and downstream regions of the gene *vp0057* of *V. parahaemolyticus* were amplified using primers *vp0057-del-a*/VP0057 Point Mutant Del B and VP0057 Point Mutant Del D/*vp0057-del-d*. *vp0057D202A*, encoding the catalytically inactive VP0057D202A variant was amplified using the plasmid pSI068 as a template with primers VP0057 Point Mutant Del C/VP0057 Point Mutant Del E. These fragments of these three PCRs were fused together with the primers *vp0057-del-a*/*vp0057-del-d* and the resulting DNA was then restricted with XbaI and fused into the corresponding site of pDM4, resulting in the plasmid pSI051.

### Plasmid pSI084

In order to obtain plasmid pSI084, three separate PCR reactions were carried out. The upstream and downstream regions of the gene *vp0055* of *V. parahaemolyticus* were amplified using primers VP0055-del-a/55 Pmu Ins B and VP0055-del-c/VP0055-del-d. *vp0055T63A*, encoding for the phosphoablative VP0055T63A variant was amplified using the plasmid pSI080 as a template with primers 55 Pmu Ins C/55 Pmu Ins D. These fragments of these three PCRs were fused together with the primers VP0055-del-a/VP0055-del-d and the resulting DNA was then restricted with the enzymes, XbaI and SphI and fused into the corresponding site of pDM4, resulting in the plasmid pSI084.

### Plasmid pSI130

In order to obtain plasmid pSI139, three separate PCR reactions were carried out. The upstream and downstream regions of the gene *vp0055* of *V. parahaemolyticus* were amplified using primers VP0055-del-a/55 Pmu Ins B and VP0055-del-c/VP0055-del-d. *vp0055T63E*, encoding for the phosphomimetic VP0055T63E variant was amplified using the plasmid pSI127 as a template with primers 55 Pmu Ins C/55 Pmu Ins D. These fragments of these three PCRs were fused together with the primers VP0055-del-a/VP0055-del-d and the resulting DNA was then restricted with the enzymes, XbaI and SphI and fused into the corresponding site of pDM4, resulting in the plasmid pSI139.



### Plasmid pSI010

The gene *vp0055* was amplified from *V. parahaemolyticus* using primers VP0055 SFGFP CW/VP0055 SFGFP CCW and the DNA fragment obtained was restricted with the enzymes, XbaI and SphI and fused into the corresponding site of the plasmid pJH036, resulting in the plasmid pSI011.

### Plasmid pSI049

The gene *vp0057* was amplified from *V. parahaemolyticus* using primers VP0057-pkTOP CW/VP0057-pkTOP CCW and the DNA fragment obtained was restricted with the enzymes, XbaI and KpnI and fused into the corresponding site of the plasmid, pkTOP resulting in the plasmid pSI049.

### Plasmid pSI076

The plasmid pkTOP was used as a template to amplify the *phoA* and *lacZα* encoding regions using the primers PhoA-LacZa-A Primer/PhoA-LacZa-B Primer. The gene *vp0057* was amplified using the primers VP0057 Full C Primer/VP0057 Full D Primer. The above two DNA fragments were fused together and restricted with the enzymes, XbaI and HindIII and inserted into the corresponding site of pKNT25 resulting in the plasmid pSI076.

### Plasmid pSI109

The gene *vp0057* was amplified from *V. parahaemolyticus* using primers VP0057 Srkkan cw/ VP0057 Srkkan ccw and the DNA fragment obtained was restricted with the enzymes, NdeI and SacI and fused into the corresponding site of the plasmid, pSRKKm resulting in the plasmid pSI115.

### Plasmid pSI128

*vp0055T63A*, encoding for the VP0055T63A variant was obtained by a PCR reaction with the primers VP0055 SFGFP CW/VP0055 SFGFP CCW and the plasmid, pSI080 as a template. The resulting DNA fragment was restricted with the enzymes, XbaI and SphI and fused into the corresponding site of the plasmid pJH036, resulting in the plasmid pSI142.

### Plasmid pSI132

A DNA sequence, codon-optimized for *E. coli*, including the ORF (hne1495) encoding the ECF-σ factor HNE1495 of *H. neptunium* ATCC 15444 was obtained from

## Materials and Methods

ThermoFisher Scientific. The DNA sequence was designed to include the restriction sites XbaI and SphI at the 5' and 3' ends, respectively, for direct insertion into the vector pJH036 (kindly provided by Jan Heering), resulting in plasmid pSI143. Particularly, we ordered the Strings™ DNA Fragments (ThermoFisher Scientific) and used the built-in codon optimization tool (ThermoFisher Scientific) using their *E. coli* codon usage table and avoiding the restriction sites XbaI and SphI.

### Plasmid pSI135

A DNA sequence, codon-optimized for *E. coli*, including the ORF (hne14956) encoding the predicted STK HNE1496 of *H. neptunium* ATCC 15444 was obtained from ThermoFisher Scientific. The DNA sequence was designed to include the restriction sites NdeI and SacI at the 5' and 3' ends, respectively, for direct insertion into the vector pSRKKm, resulting in plasmid pSI146. Particularly, we ordered the Strings™ DNA Fragments (ThermoFisher Scientific) and used the built-in codon optimization tool (ThermoFisher Scientific) using their *E. coli* codon usage table and avoiding the restriction sites NdeI and SacI.

### 6.4.13. Primers

A comprehensive list of all primers used for molecular cloning in the current work is provided in Table 10.

**Table 10. List of primers**

Primer name	Sequence
vp0057-del-a	ccccctctagaaattccatggtttcgaccactg
vp0057-del-b	acgtgtatacatctgttttaagccagtgccgtatatcttattgtttacg
vp0057-del-c	ggcttaaaacaagatgtatacacgt
vp0057-del-d	ccccctctagaacgaatctttggtgatggtgaatc
vp0055 pKNT25 cw	ccccctctagaatggcaacgacttcagccctaa
vp0055 pKNT25 ccw	cccccggtacccgtgCGTgtgccattcttgattg
vp0055 pKT25 cw	ccccctctagagatggcaacgacttcagcccta
vp0055 pKT25 ccw	cccccggtaccttatgCGTgtgccattcttgattg
vp0057 full pKNT25 cw	ccccctctagaatgcagttaggctccagcgaa
vp0057 full pKNT25 ccw	cccccggtacccgttggttggtgctgtccttagac

vp0057 full pKT25 cw	ccccctctagagatgcagttaggctccagcg
vp0057 full pKT25 cw	cccccggtaccttattggttggtgctgccttag
VP0054-del-a	ccccctctagaacaatgacgaaccgaaagcc
VP0054-del-b	aaataacattatgtattttaagtgggatttatgcgtgtgccattcttg
VP0054-del-c	ccacttaaaatacataatgttattt
VP0054-del-d	cccccgcatgccactgtacagatcaatcggagct
VP0055-del-a	ccccctctagaagacccgattcaccatcaccaa
VP0055-del-b	aatccacagtttcttggtcatgatggtataacctcctcgctcact
VP0055-del-c	atcatgaccaagaaactgtggatt
VP0055-del-d	cccccgcatgccacttcatacgctacgcgat
VP0056-del-a	ccccctctagaattgctcgattcaacctgacgc
VP0056-del-b	ggctgaagtcggtgccatggcttgtttaagccttatgggtgg
VP0056-del-c	ccatggcaacgacttcagcc
VP0056-del-d	cccccgagctctgcttcacctcaattaacgacg
VP0057-D202A B Primer	ttcaggcttgagagcggcgtgtaac
VP0057-D202A C Primer	gttacacgccgctctcaagcctgaa
VP0057-pkTOP CW	ccccctctagagggtgcagttaggctccagcgaa
VP0057-pkTOP CCW	cccccggtacccggtggttggtgctgccttagac
PhoA-LacZa-A Primer	ccccctctagagcccggacaccagaaatgcc
PhoA-LacZa-B Primer	gcgccattcgccattcaggct
VP0057 Full C Primer	gtgcagttaggctccagcgaaagcctgaatggcgaatggcgc
VP0057 Full D Primer	cccccaagctttattggttggtgctgccttag
VP0055 SFGFP CW	ccccctctagagtcaggggcccatctgcaacgacttcagccctaacc
VP0055 SFGFP CCW	cccccgcatgcttatgcgtgtgccattcttgattg
VP0057Operon-del- a	cccccgcatgcatgggtgcgtttgccagcgtc

## Materials and Methods

VP0057 Operon-del-b	aaataacattatgtattttaagtgccacagtcgctgatatcttattgttt
VP0057 Operon-del-c	ccacttaaaatacataatgttattt
VP0057 Operon-del-d	ccccctctagacctccaatgctttgtttacgtt
VP0057 Point Mutant Del B	tttcgctggagcctaactgcacagtcgctgatatcttattgttttac
VP0057 Point Mutant Del C	gtgcagttaggctccagcgaaa
VP0057 Point Mutant Del D	tctaaggacagcaccaaccaataaggcttaaaacaagatgtatacacgt
VP0057 Point Mutant Del E	ttattggttggtgctgtccttaga
vpa0879-del-a	cccccgctcgacaactatggcgtatggcaaggg
vpa0879-del-b	tttgttattattgtgtaagtaaaaattatcaatccttctgacgcgaat
vpa0879-del-c	tttacttaacacaataataacaaa
vpa0879-del-d	cccccgagctctttcgtggaacaagttcatgcc
delvp0054delvp0055b	aaataacattatgtattttaagtgggatggttatacctcctcgctca
delvp0056delvp0057b	ggctgaagtcgttgccatggctgttttaagccagtcgctgat
55 T63A CW	agcaccgcccgcattgattcatg
55 T63A CCW	catgaatcaatgcggcgggtgctgttgacgctgtctgccaatc
55 Pmu Ins B	ttagggctgaagtcgttgccatggttatacctcctcgctcact
55 Pmu Ins C	atggcaacgacttcagccctaa
55 Pmu Ins D	aatccacagtttcttggtcatgatttatgcgtgtgccattcttgattg
sfGFP-1-cw	cccccaggcctaaggagtggtgaaatgagcaaaggagaagaactttcac
sfGFP-1-ccw	ccccctctagattttagagctcatccatgccatg
VP0057 Srkkan cw	ccccccataggtgcagttaggctccagcgaa
VP0057 Srkkan ccw	cccccgagctcttattggttggtgctgtcctta
57ChrIns-A	ccccctctagatgttgatcagagcttgattgaac
57ChrIns-B	actctataacaataagtgcattgttccgctgctatggcgagagt
57ChrIns-C	aatcatgcacttattgttatagagt
57ChrIns-D	ttattggttggtgctgtccttag
57ChrIns-E	ctaaggacagcaccaaccaataagtgtcttttcattgaatatttact
57ChrIns-F	cccccgagctcagccttctgctcatcgcttgc

VP0055 T63E CW	agcaccgaggcattgattcatg
VP0055 T63E CCW	catgaatcaatgcctcggtgctgttgacgctgtctgccaataacc

## 6.5. Biochemical methods

### 6.5.1. Separation and detection of proteins by SDS PAGE

SDS-PAGE (SDS-Polyacrylamide gel electrophoresis) was used for separation of proteins (Laemmli, 1970). *V. parahaemolyticus* samples were grown until they reach an OD<sub>600</sub> of approximately 0.4. The cells were then harvested and resuspended in 2X Laemmli buffer (Composition in Table 5). The obtained suspension was then boiled for approximately 10 minutes and loaded on to an SDS gel comprised of the desired percentage of stacking gel and resolving gel. As a reference, the typical compositions of a 5% stacking gel and an 11% resolving gel are shown in Table 11. A standard protein ladder was used for comparison (Color Prestained Protein Standard Broad Range, NewEngland BioLabs). Separation through electrophoresis was carried out between 150 and 160V in SDS running buffer (TGS buffer, Bio-Rad) with the help of a Bio-Rad MiniPROTEAN 3 Cell or MiniPROTEAN TetraCell. The gels were subsequently stained with Instant Blue™ (Expedeon, UK) for a minimum period of 10 minutes. A list of all buffers used and their respective compositions can be found in Table 5.

**Table 11. List of SDS PAGE gels**

Reagents	11% Resolving gel (10mL)	5% Stacking gel (5mL)
Resolving gel buffer	3.8mL	-
Stacking gel buffer	-	2.8mL
30% Acrylamide	2.5mL	1.25mL
ddH <sub>2</sub> O	3.7mL	825μL
TEMED	80μL	50μL
10% APS	6μL	3.75μL

### 6.5.2. Immunoblot analysis

In order to detect proteins of interest, immunoblot analysis was undertaken. The first step here was separation of proteins with SDS PAGE, as described earlier. This was followed by transfer onto a PVDF membrane using the semi-dry transfer procedure. For each gel, six pieces of Whatman paper and one PVDF membrane (that were all cut

## Materials and Methods

---

corresponding to the gel size) were used. The PVDF membrane was soaked in 100% methanol for approximately 15 minutes and rinsed in distilled water for at least a couple of minutes. The PeqLab semi-dry system was used for the transfer procedure. From the bottom (anode) plate to the top (cathode) plate, the components are described as follows.

Immediately following the base plate were 2 pieces of Whatman paper soaked in Anode buffer I followed by a single piece of Whatman paper soaked in Anode buffer II. This was followed by the PVDF membrane (pre-soaked in methanol and rinsed), the SDS gel and eventually, 3 pieces of Whatman paper soaked in cathode buffer before placing the top (cathode) plate and connecting the entire setup to the power supply (50 mA for around 1.5 hours). The composition of the buffers are provided in Table 5.

After the transfer procedure is completed, the setup was carefully dismantled and the membrane was taken out and transferred in milk solution (composition provided in Table 5). Blocking of the membrane was carried out at room temperature with shaking for a minimum period of 1 hour. Immediately after this, the membrane was transferred into the same milk solution as above containing the corresponding primary antibody (1:4000 v/v ratio of antibody to milk solution). This was incubated overnight with shaking at 4 °C. The following day, the membrane was washed three times with the aforementioned milk solution and eventually transferred to the same solution consisting of the corresponding secondary antibody (1:5000 v/v ratio of antibody to milk solution). This was incubated at room temperature with shaking for at least one hour. This was followed by washing the membrane with 1X PBS at least three times. After the final wash, excess liquid was gently drained off the membrane and it was transferred on to a clean plate. Approximately, 2 ml of horse radish peroxidase (Luminata™ Forte Western HRP Substrate, Millipore) was added to the membrane and it was incubated at room temperature for at least a couple of minutes. This was followed by development of the blot using the luminescent image analyzer LAS-4000 (Fujifilm, Düsseldorf).

### **6.5.3. Immunoprecipitation and co-immunoprecipitation assays followed by LC-MS analysis**

#### **6.5.3.1. *Vibrio parahaemolyticus***

In the case of overexpression of just the sigma factor in the absence of the kinase, two plasmids - one containing sfGFP fused to the N-terminal of EcfK (pSI010) and the

other being just the empty pSRKKm vector – were introduced into *V. parahaemolyticus* cells. Overexpression of both the kinase and the ECF sigma factor was achieved by introducing two plasmids – pSI010 and the other containing PnkT fused into the vector pSRKKm (pSI109) – into *V. parahaemolyticus* cells.

A minimum of three biological replicates were performed for each experiment. A single bacterial colony was inoculated into 20 ml LB medium, with the appropriate antibiotics and approximately 30 minutes later, the inducers, namely IPTG (for pSRKKm and pSI115) and L-arabinose (for pSI011) were added. Upon reaching an OD<sub>600</sub> of approximately 1.0, the cultures were diluted into 250 ml of LB already containing the antibiotics and inducers to an initial OD<sub>600</sub> of 0.05. The cultures were grown until they reach an OD of roughly 0.39-0.41. They were then harvested and the pellet was resuspended in 10 ml of lysis buffer (50 mM HEPES, 150 mM NaCl and 5 mM EDTA) pre-mixed with protease inhibitors (cComplete EDTA free, Sigma-Aldrich). NP-40 (Sigma-Aldrich) was added to a final concentration of 0.5%. This was followed by ultrasonication to break open the cells (Amplitude 100%, three 20s pulses) after which the samples were incubated at 4 °C on an overhead rotator to ensure uniform mixing. Immediately after this, another step of ultrasonication (same conditions) was performed, followed by centrifugation for 10 minutes. The supernatant was then mixed with 20 µl of anti-GFP bead slurry (Chromotek) and incubated for an hour with rotation at 4 °C.

The beads were then washed four times with 700 µl of 100 mM ammoniumbicarbonate (Sigma-Aldrich). For elution, an on-bead digestion was performed by adding 200 µl trypsin-containing elution buffer 1 (1.0 M urea, 100 mM ammoniumbicarbonate, 1 µg trypsin (Promega)) to each sample. After 30 min shaking incubation (1400 rpm) at 30 °C, the supernatant containing digested proteins was collected. Beads were then washed twice with 80 µL of elution buffer 2 (1.0 M urea, 100 mM ammoniumbicarbonate, 5 mM Tris(2-carboxyethyl)phosphine (TCEP)) (Thermo Scientific) and the supernatant was added to the first elution fraction. Digestion was allowed to proceed overnight at 30°C.

Following digestion, the peptides were incubated with 10 mM iodoacetamide (IAA, Sigma-Aldrich) for 30 min at 25°C in the dark. The peptides were acidified with 1% trifluoroacetic acid (TFA, Thermo Scientific) and desalted using solid-phase extraction (SPE) on C18-Microspin columns (Harvard Apparatus). SPE columns were prepared by adding acetonitrile (ACN), followed by column equilibration with 0.1% TFA. Peptides were loaded on equilibrated Microspin columns and washed twice with 5% ACN/0.1%

## Materials and Methods

---

TFA. After peptide elution using 50% ACN/0.1% TFA, peptides were dried in a rotating concentrator (Thermo Scientific), reconstituted in 0.1% TFA, sonicated (Vial-Tweeter Sonotrode, Hielscher Ultrasonics) and subjected to liquid chromatography-mass spectrometry (LC-MS) analysis.

LC-MS analysis of the peptide samples was carried out on a Q-Exactive Plus instrument connected to an Ultimate 3000 RSLC nano and a nanospray flex ion source (Thermo Scientific). Peptide separation was performed on a reverse phase HPLC column (75  $\mu$ m x 42 cm) packed in-house with C18 resin (2.4  $\mu$ m). The peptides were loaded onto a PepMap 100 precolumn (Thermo Scientific) and then eluted by a linear ACN gradient from 2-35% solvent B over 60 minutes (solvent A: 0.15% formic acid; solvent B: 99.85% ACN in 0.15% formic acid). The following parameters were used for testing: a flow rate of 300 nl/min, spray voltage of 2.5 kV and heated capillary temperature of 300 °C. The peptides were analyzed in positive ion mode. Survey full-scan MS spectra ( $m/z$  = 375-1500) were acquired in the Orbitrap with a resolution of 70,000 full width at half maximum at a theoretical  $m/z$  200 after accumulation of a maximum of  $3 \times 10^6$  ions in the Orbitrap. Based on the survey scan, up to 10 most intense ions were subject to fragmentation using high collision dissociation (HCD) at 27% normalized collision energy. Fragmented spectra were acquired at a resolution of 17,500. The ion accumulation time was set to 50 ms for both MS survey and MS/MS scans. To increase the efficiency of MS/MS attempts, the charged state screening modus was enabled to exclude unassigned and singly charged ions. The dynamic exclusion duration was set to 30 sec.

Label-free quantification (LFQ) of the samples was performed using MaxQuant (Version 1.5.3.17) (Cox & Mann, 2008). For Andromeda database searches implemented in the MaxQuant environment, the protein databases for *V. parahemolyticus* were downloaded from Uniprot. The search criteria were set as follows: full tryptic specificity was required (cleavage after lysine or arginine residues); two missed cleavages were allowed; carbamidomethylation (C) was set as fixed modification; oxidation (M) and phosphorylation (ST) as variable modifications. MaxQuant was operated in default settings with the “Match-between-run” options. Peptide phosphorylation probability was carried out using MaxQuant.



### 6.5.3.2. *Escherichia coli*

The desired plasmid(s), as mentioned above in the case of *Vibrio parahaemolyticus*, were introduced into *E. coli* MG1655 cells. Again, a minimum of three biological replicates were performed for each experiment. The cultures were induced and harvested as in the case of the *V. parahaemolyticus* samples. The obtained pellet was then washed with 50ml of 1X PBS followed by centrifugation under similar conditions. The pellets were then snap-chilled in liquid nitrogen before freezing them at -80 °C overnight.

The following day, the frozen pellets were resuspended in 25ml of lysis buffer (Refer to the *V. parahaemolyticus* section for the composition). This was followed by cell disruption through French press - three rounds per sample. 10ml of the lysate was transferred to a fresh tube and treated with the following detergents: 0.1% SDS and 0.5% NP-40. The samples were then incubated at 4 °C on an overhead rotator to ensure uniform mixing. Upon centrifugation of these samples for 10 minutes (4000 rpm), the supernatant was mixed with 20 µl of anti-GFP bead slurry (Chromotek) and incubated for an hour with rotation at 4 °C. The beads were then washed four times with 700 µl of 100 mM ammonium bicarbonate. At this point, if Western blotting is to be performed to assess for protein levels, the beads were resuspended into 100 µl of 4X SDS solubilization buffer (Laemmli Buffer) and boiled at 95 °C for 10 minutes. The samples were then loaded onto an 8% SDS gel and Western blotting was carried out with an antibody against the  $\beta'$  subunit of the RNAP of *E. coli*. If the samples were to be analyzed by mass spectrometry, then after the four washes with 100mM ammonium bicarbonate, they were treated the same way as in the case of *V. parahaemolyticus*.

### 6.5.4. Co-immunoprecipitation upon Polymyxin treatment

A minimum of three biological replicates were performed for each experiment. A single *V. parahaemolyticus* colony was inoculated into 20 ml LB medium, with the appropriate antibiotics and approximately 30 minutes later, the inducers, namely IPTG (for pSRKKm and pSI109) and L-arabinose (for pSI010) were added. Upon reaching an OD<sub>600</sub> of approximately 1.0, the cultures were diluted into 500ml of LB already containing the antibiotics and inducers to an initial OD<sub>600</sub> of 0.05. Upon reaching exponential phase (OD<sub>600</sub> 0.39-0.41), the cultures were divided into two flasks of 250 ml each. To the “experimental” flask, polymyxin B was added to a final concentration of 5 µg/ml (Stock

concentration: 50 mg/ml). To the “control” flask, no polymyxin B was added. The cultures were then incubated at 37 °C under standard laboratory shaking conditions for five minutes. Subsequently, the samples were harvested and prepared for co-immunoprecipitation with anti-GFP beads as described in the previous section (Section 6.5.3).

### 6.5.5. Detection of phosphorylation by Phostag gels

In the case of overexpression of just the sigma factor in the absence of the kinase, two plasmids - one containing sfGFP fused to the N-terminal of EcfK (pSI010) and the other being just the empty pSRKKm vector – were introduced into *V. parahaemolyticus* or *E.coli* MG1655 cells. Overexpression of both the kinase and the ECF sigma factor was achieved by introducing two plasmids – pSI010 and the other containing PnkT fused into the vector, pSRKKm (pSI109) –into *V. parahaemolyticus* or *E.coli* MG1655 cells.

A minimum of three biological replicates were performed for each experiment. A single bacterial colony was inoculated into 5 ml LB medium, with the appropriate antibiotics and approximately 30 minutes later, the inducers, namely IPTG (for pSRKKm and pSI115) and L-arabinose (for pSI011) were added. Upon reaching an OD<sub>600</sub> of approximately 1.0, the cultures were diluted into 10 ml of LB already containing the antibiotics and inducers to an initial OD<sub>600</sub> of 0.05. The cultures were grown until they reach an OD<sub>600</sub> of roughly 0.39-0.41. The samples were subject to TCA/acetone precipitation and the obtained pellet was resuspended in the desired amount of lysis buffer (containing 50 mM HEPES and 150 mM NaCl) and normalized to the same OD<sub>600</sub>. The samples were then loaded on a SuperSep™ Phostag™ (Fujifilm Wako Pure Chemical Corporation). Subsequently the gel was washed a minimum of three times in transfer buffer (without EDTA) followed by an additional washing step in the same transfer buffer (with EDTA). Western blotting was carried out using a semi-dry transfer procedure and the samples were probed with an antibody against GFP (primary antibody, Living Colors® A.v. Monoclonal Antibody (JL-8), used 1:4000) and anti-mouse HRP conjugated as the subsequent secondary antibody (secondary antibody, Amersham ECL Mouse IgG, HRP-linked whole Ab (from sheep), used 1:5000).

#### 6.5.5.1. Detection of phosphorylation by Phostag gels upon polymyxin treatment

A minimum of three biological replicates were performed for each experiment. A single *V. parahaemolyticus* colony was inoculated into 5 ml LB medium, with the appropriate antibiotics and approximately 30 minutes later, the inducers, namely IPTG (for pSRKKm and pSI115) and L-arabinose (for pSI011) were added. Upon reaching an OD of approximately 1.0, the cultures were diluted into 20 ml of LB already containing the antibiotics and inducers to an initial OD of 0.05. The cultures were grown until they reach an OD of roughly 0.39-0.41 and then divided into two flasks of 10 ml each: the “experimental” flasks containing a final concentration of 5 µg/ml of polymyxin B and the “control” flask containing none. The flasks were then shaken under standard laboratory conditions for five minutes. They were then harvested and treated as described in the above section before being loaded on a phostag gel.

### **6.6. Label-free quantification of total cell lysates using LC-MS-based proteomics**

Overnight cultures of *V. parahaemolyticus* were sub-cultured to an initial OD<sub>600</sub> of approximately 0.05 in 20 ml of LB and were grown until they reach an OD<sub>600</sub> of 0.39-0.41. These cultures were then centrifuged for 10 minutes at 4700 rpm, 4 °C. Upon discarding the supernatant, the pellets were washed with 1ml of distilled water and the solution was transferred to a 2 ml Eppendorf tube which was then centrifuged on a bench table-top centrifuge for 2 minutes at 6000 rpm, 4 °C. At this step, the pellets can be frozen at -80 °C or can be lysed immediately.

The pellets were lysed with 400 µl of 1 % sodium laureth sulphate (SLS) (prepared from a 2 % stock solution by dissolving the desired volume in ammonium bicarbonate). After proper resuspension, the solution was boiled at 90 °C for 5 minutes. This was followed by ultrasonication of the samples for a pulse of 20 seconds (Amplitude 100%) and yet another boiling step at 90 °C for 15 minutes. In order to estimate the concentration of protein obtained, the Bicinchoninic acid (BCA) assay was performed using the Thermo Scientific Pierce BCA Protein Assay Kit. After this step, 10 µl of 0.2 M tris (2-carboxyethyl)phosphine (TCEP) (Thermo Scientific) was added to the samples, followed by incubation at 90 °C for 15 minutes. This was followed by the addition of 10 µl of 0.4 M iodoacetamide and incubation in the dark at 25 °C for at least 30 minutes.

For the next step, namely tryptic digestion, only 50 µg of the total protein concentration (calculated above through the BCA assay) was used. 1µg of trypsin

## Materials and Methods

---

(Promega) was added to all the samples and digestion was carried out in 100 µl of 0.5 % SLS. The mixture was vortexed thoroughly and the reaction was allowed to proceed at 30 °C overnight.

The following day, the samples were spun down and trifluoroacetic acid (TFA) was added to a final concentration of 1.5 %. The pH of the samples was checked using pH indicator strips (LLG Labware) and it was ensured that the value was not higher than 2. After letting the samples rest for 10 minutes at room temperature, they were centrifuged at 21,130 g and 4 °C till complete clearing of the supernatant from detergent occurs (precipitation). The supernatant was transferred to a new tube and used for C18 extraction through the procedure described in section 6.5.3.1. Upon elution, the peptides were concentrated under vacuum to dryness and dissolved in 100 µl of 0.1% TFA, followed by 20 seconds of ultrasonication (Hielscher Ultrasonics) and shaking at 1400 rpm at 25 °C for 5 minutes. The samples were then transferred into Liquid Chromatography (LC) vials; upon ensuring the removal of air bubbles, they were either handed in for loading into the mass spectrometry directly or were frozen at -20 °C.

The LC-MS analysis of total cell lysates was carried out as described in Section 6.5.3.1 with modifications on gradient length and label-free quantification strategy. The procedure has been described previously in more detail in (Yuan, Jin, Glatter, & Sourjik, 2017).

The Perseus tool (Tyanova et al., 2016) was employed to analyze the data obtained through LC-MS global proteomics. The reference *V. parahaemolyticus* proteome was chosen and the replicates were grouped together to analyze variance. Furthermore, in order to generate volcano plots, the P-values were calculated using a standard Student's T-test and fold changes were generated upon comparison of the peptide levels of different strains with respect to those of wild type.

### 6.6.1. Proteomics upon polymyxin treatment

Overnight cultures (5 ml) of *V. parahaemolyticus* were sub-cultured to an initial OD<sub>600</sub> of approximately 0.05 in 40 ml of LB and were grown until they reach an OD<sub>600</sub> of approximately 0.39-0.41. The cultures were then divided into two flasks of 20 ml each: to the “experimental” flask, polymyxin B was added to a final concentration of 10 µg/ ml, whereas nothing was added to the other “control” flask. The two were then shaken under

standard laboratory conditions for five minutes. This was proceeded by harvesting and subsequent sample treatment as described in the above section (Section 6.6).

### **6.7. RNA sequencing/ Transcriptomics**

#### **6.7.1. Isolation of total RNA**

Twenty ml of exponentially grown cultures were centrifuged for 10 minutes at 16,000 g, 4 °C and the pellet was resuspended in 1 ml of Trizol (Sigma-Aldrich) and incubated at 65 °C for 10 minutes. This was followed by the addition of 200 µl of chloroform and gentle mixing by pipetting up and down. The samples were then incubated at room temperature for 5 minutes while being shaken vigorously, followed by centrifugation for 15 minutes at 16,000 g, 4 °C. The aqueous layer from this step is then transferred into a fresh 1.5 ml Eppendorf tube. 500 µl of isopropanol was added to the same and the solution was mixed by inverting the tube gently. This was followed by incubation of the samples for 1 hour at -20 °C and centrifugation for 30 minutes at 16,000 g, 4 °C. The RNA pellet was washed with 1 ml of 70 % ethanol and spun for 5 minutes at 16,000 g, 4 °C. The supernatant was decanted and the samples were spun again for 30 seconds at 16,000 g, 4 °C followed by gentle removal of any residual ethanol with a pipette. The samples were air-dried under a clean fume hood if necessary, in order for the remainder of ethanol to evaporate. The RNA pellet was finally resuspended in 50 µl of RNase-free water (Carl-Roth).

This was followed by DNase treatment, whereby 2 µl of DNase I (Ambion by Life Technologies) with the desired amount of buffer was added and the samples were incubated for at least 1 hour at 37 °C. Upon completion of the reaction, 150 µl of RNase-free water and 200 µl of acidic phenol:chloroform (5:1) mixture were added, followed by vigorous vortexing. The samples were then spun for 5-10 minutes at 16,000 g, 4 °C and the upper phase was transferred to a fresh tube. 20 µl of 3M sodium acetate (NaOAc, Carl-Roth) and 500 µl of (cold) 100 % ethanol were added to the tubes and the samples were kept overnight at -80 °C. The following day, upon centrifugation of the samples for 10 minutes at 16,000 g, 4 °C, the supernatant was poured out. 1 ml of 70 % ethanol was added to the tubes followed by gentle resuspension and centrifugation for 5 minutes at 16,000 g, 4 °C. After discarding the supernatant (with multiple centrifugation steps, if necessary), the RNA pellet was resuspended in 40 µl of RNase-free water.

## Materials and Methods

---

At this step, the concentration/ purity of the samples was measured by a Nanodrop machine and by running them on an agarose gel through electrophoresis. The RNA samples were stored at -20 °C (in aliquots if desired). 15 µl of the total RNA (concentration: 200 ng/µl) was sent to the Max Planck Genome Center in Cologne, Germany for transcriptomics analyses. De novo sequencing was done on the samples facilitated by the Illumina HiSeq3000 sequencer.

### 6.7.2. Data analysis

The obtained reads were mapped individually on to *V. parahaemolyticus* chromosomes I and II (Ref-Seq NC\_004603.1 and NC\_004605.1) using Bowtie 2 (Langmead & Salzberg, 2012). The reference genome and annotation were provided by RefSeq (Pruitt, Tatusova, & Maglott, 2007). The output BAM files were sorted using SAMTool (H. Li et al., 2009). The genome coverage and conversion to BED files were done using BEDtools (Quinlan & Hall, 2010). The differential gene expression analyses were performed based on the calculated Reads Per Kilobase Million (RPKM) normalization (Mortazavi, Williams, McCue, Schaeffer, & Wold, 2008). Fold-change (with respect to wild type) was calculated to identify significant up- and down regulated genes. To improve the accuracy of the fold-change data, a pseudo-count was used before normalization. The p-values were calculated using an unpaired hypothesis test with a false discovery rate (FDR) (Storey, 2002). All differential gene expression analyses were done using MATLAB (Mathworks).

## 6.8. Stereo microscopy

In order to visualize morphologies of the swarm colonies of the different mutants and also wild type, stereo microscopy images were taken. In order to do this, the plate containing the swarm colony was directly placed underneath the microscope (Nikon H600L) and images were analyzed and captured using the NIS Elements AR (v 5.02.00) tool. The magnification of the lens used is indicated in the respective pictures. Further, the time of exposure was adjusted according to the user's choice and ease of comparison.

## 6.9. Bioinformatic analysis

### 6.9.1. Identification of targets for analysis

To identify proteins similar to EcfP with a STK encoded in the vicinity of their coding sequence, we built Hidden Markov models (HMMs; HMMER suite (Finn et al., 2011)) from the multiple sequence alignment (Clustal Omega 1.2.3 (Sievers & Higgins, 2014)) of the ECFs and STKs extracted from a PSI-BLAST search (Altschul, Gertz, Agarwala, Schäffer, & Yu, 2009) (E-value < 10) of EcfP and PknT. We used these HMMs to look for homologs of EcfP and PknT in the annotated genomes in NCBI (version from February 2017). We then filtered for pairs of ECF-STK whose coding sequences were separated by less than 5000bp. The 224 unique matches where several ECFs or several STKs are found in the same neighborhood were discarded, since the interaction pair was not clear. We also discarded 12 variants where the ECF and the kinase coding sequences were fused. The search yielded 1617 pairs with a combined amino acid sequence identity <98%, that is, these pairs of STK and ECF share less than 98% sequence identity when concatenated. From those, 14 putative STKs were found to not match the PFAM model for proteins kinases (PFAM: PF00069) and were discarded. We eventually ended with 1,603 pairs of ECF-STK.

### 6.9.2. Generation of the phylogenetic tree

We aligned the resulting ECFs with Clustal Omega 1.2.3 (Sievers & Higgins, 2014). A maximum likelihood phylogenetic tree was built from the manually curated alignment using IQ-Tree with automatic model selection and default parameters (Nguyen, Schmidt, Von Haeseler, & Minh, 2015). We included as outliers of this phylogenetic tree SigM from *Bacillus subtilis*, RpoE and Fecl from *Escherichia coli*, Ecf41 from *Rhodobacter sphaeroides* and SigE from *Mycobacterium tuberculosis*. The latter is regulated through the phosphorylation of its anti- $\sigma$ -factor, RseA, which is then cleaved by the protease ClpC1P2 (Barik, Sureka, Mukherjee, Basu, & Kundu, 2010). All the remaining outliers are not regulated by STKs. The resulting phylogenetic tree was visualized in iTOL (Letunic & Bork, 2016). The domain architecture of STKs was computed using PFAM database.

### 6.9.3. Analysis of the phylogenetic tree

For the assignment of extracted ECFs to ECF groups, HMMs from the available ECF classifications (Xiaolu Huang, Pinto, Fritz, & Mascher, 2015; Jogler et al., 2012;

Staroń et al., 2009) were used to score every extracted ECF against every ECF group. Proteins were assigned to the group for which the bit score was higher.

The presence or absence of an extended region between helices  $\sigma 2.1$  and  $\sigma 2.2$  was assessed from the alignment of the extracted ECFs, including outliers. We considered that a protein has an extended region when the length between  $\sigma 2.1$  and  $\sigma 2.2$  helices is larger than three times the standard deviation of the length in the outliers, that is, 11-12 amino acids.

### 6.9.4. Homology structural modeling

In order to find regions of importance within EcfP, homology structural modeling was carried out. This was done using iTASSER (Jianyi Yang et al., 2014) with the available sequence of the ECF  $\sigma$  factor, SigH from *M. tuberculosis* (PDB: 5ZX2 (L. Li et al., 2019)). The structural alignment with EcfP was done using Chimera (Pettersen et al., 2004) using the default parameters. Only the  $\sigma 2$  portion was aligned.

### 6.9.5. Identification of domains of kinases similar to PknT

We used HMMs from Pfam to identify cognate STKs that were similar to that associated with EcfP (that is, PknT). The HMMER search tool (Finn et al., 2011) was used to find homologous domains. For the above search, default parameters within the tool were used and no strict parameters for threshold were employed so as to not lose any valuable information with respect to sequence homology.

### 6.9.6. Frequency of essential regions of EcfP within other species

In order to obtain the frequency of S63, T63 and the extended region within EcfP among other species of the bacterial kingdom, a phylogenetic tree was generated using sequences of 16S DNA within NCBI (February 2017 version). A comprehensive list of these species and the corresponding identifiers can be found in Table 20. For our analyses, only representatives of the native organisms were used. Entries that had more than 1200 base pairs or any other sequencing artefacts were removed from the analysis for generation of the tree.



## **Chapter 7: Supplementary Materials**



**Table 12. Genes significantly downregulated in both  $\Delta ecfP$  and  $\Delta pknT$  mutants when compared to wild type.** This table gives a list of all genes that were commonly downregulated in both  $\Delta ecfP$  and  $\Delta pknT$  mutants by a minimum of 4 fold when compared to wild type. The targets were obtained through transcriptomics analyses. p-values were determined by Students t-test.

Gene	Annotation	Fold down-regulated in $\Delta ecfP/WT$	Fold down-regulated in $\Delta pknT/WT$	p-value $\Delta ecfP$	p-value $\Delta pknT$
<i>vp1680</i>	hypothetical protein	11.825	4.142	6.80E-33	8.00E-22
<i>vpa0874</i>	hypothetical protein	5.558	5.709	1.80E-12	6.70E-39
<i>vpa0875</i>	carboxylase	32.607	26.182	4.50E-31	5.20E-52
<i>vpa0876</i>	hypothetical protein	12.734	10.225	7.90E-16	5.60E-19
<i>vpa0877</i>	LamB/YcsF family protein	7.545	6.058	2.90E-09	2.20E-09
<i>vpa0878</i>	hypothetical protein	14.006	11.246	6.00E-17	4.90E-21
<i>vpa0879</i>	UDP-glucose-4-epimerase	185.010	92.817	4.50E-61	7.10E-141
<i>vpa0882</i>	heme transport protein HutA	49.700	39.900	1.00E-81	5.40E-75

**Table 13. Genes significantly upregulated in both  $\Delta ecfP$  and  $\Delta pknT$  mutants when compared to wild type.** This table gives a list of all genes that were commonly upregulated in both  $\Delta ecfP$  and  $\Delta pknT$  mutants by a minimum of 4 fold when compared to wild type. The targets were obtained through transcriptomics analyses. p-values were determined by Students t-test.

Gene	Annotation	Fold up-regulated in $\Delta ecfP/WT$	Fold up-regulated in $\Delta pknT/WT$	p-value $\Delta ecfP$	p-value $\Delta pknT$
<i>vp0018</i>	16 kDa heat shock protein A	6.869	4.820	8.80E-26	1.00E-19
<i>vp1264</i>	hypothetical protein	6.812	12.109	9.60E-30	1.10E-54
<i>vp2034</i>	hypothetical protein	6.261	8.637	8.80E-26	1.70E-40
<i>vp2035</i>	hypothetical protein	6.614	9.524	3.30E-29	1.00E-46
<i>vp2036</i>	DNA polymerase III alpha chain	5.086	7.403	7.80E-23	4.70E-39

## Supplementary Materials

<i>vpa0776</i>	mazG-like protein	12.656	9.331	2.10E-27	1.00E-37
<i>vpa0777</i>	hypothetical protein	8.854	5.061	1.20E-22	7.00E-26
<i>vpa0807</i>	multidrug resistance protein	15.660	13.293	2.40E-36	3.70E-62
<i>vpa0808</i>	periplasmic linker protein	15.360	10.167	6.10E-36	4.10E-55
<i>vpa0809</i>	AcrB/AcrD/AcrF family transporter	12.366	10.465	0.00E+00	0.00E+00

**Table 14. List of genes that were significantly downregulated in the  $\Delta ecfP$  mutant when compared to wild type.** This table gives a list of all genes that were significantly downregulated in the  $\Delta ecfP$  mutant by a minimum of 4 fold when compared to wild type. The targets were obtained through transcriptomics analyses. p-values were determined by Students t-test.

Gene	Annotation	Fold down-regulated in $\Delta ecfP/WT$	p-value
<i>vpa0879</i>	UDP-glucose 4-epimerase	185.010	4.45E-61
<i>vpa0882</i>	heme transport protein HutA	49.749	1.07E-38
<i>vpa0875</i>	putative carboxylase	32.607	4.52E-31
<i>vpa0450</i>	hypothetical protein	17.613	4.94E-30
<i>vpa0451</i>	hypothetical protein	16.639	7.69E-22
<i>vpa0878</i>	hypothetical protein	14.006	5.98E-17
<i>vpa0876</i>	conserved hypothetical protein	12.734	7.69E-16
<i>vp1687</i>	putative type III chaperone	12.177	1.11E-28
<i>vp1680</i>	hypothetical protein	11.825	6.78E-33
<i>vp1686</i>	hypothetical protein	10.792	9.34E-33
<i>vp1657</i>	putative translocator protein PopB	10.703	9.58E-34
<i>vp1682</i>	hypothetical protein	10.420	8.05E-25
<i>vp1683</i>	hypothetical protein	9.820	8.39E-28
<i>vp1692</i>	putative type III export protein	9.170	8.39E-28
<i>vp1656</i>	putative translocator protein PopD	9.059	2.00E-30
<i>vp1664</i>	putative type III secretion protein	8.765	1.18E-23
<i>vp1690</i>	putative type III secretion lipoprotein	8.690	3.53E-26

<i>vp1693</i>	putative type III secretion protein	8.668	9.10E-27
<i>vp1691</i>	type III export protein	8.373	7.53E-24
<i>vp1694</i>	type III export protein YscF	8.331	2.45E-25
<i>vp1658</i>	low calcium response locus protein H	8.166	3.53E-26
<i>vp1688</i>	putative type III secretion protein	8.110	3.89E-24
<i>vp1659</i>	hypothetical protein	8.033	5.95E-27
<i>vp1689</i>	putative type III secretion protein	8.013	2.39E-24
<i>vp1663</i>	putative YscY	7.924	1.33E-21
<i>vp1667</i>	putative outer membrane protein PopN	7.900	6.44E-25
<i>vp1665</i>	putative type III secretion protein	7.602	3.38E-22
<i>vpa0877</i>	putative lactam utilization protein	7.545	2.91E-09
<i>vp1662</i>	low calcium response protein	7.493	1.00E-24
<i>vp1660</i>	putative regulator in type III secretion	7.207	2.35E-19
<i>vp1668</i>	ATP synthase in type III secretion system	7.174	1.26E-23
<i>vp1695</i>	putative type III export protein PscD	7.147	3.80E-24
<i>vp1661</i>	putative LcrR	7.070	1.18E-17
<i>vp1698</i>	hypothetical protein	7.053	9.57E-25
<i>vp1697</i>	putative type III export apparatus protein NosA	6.940	2.76E-22
<i>vp1696</i>	putative type III secretion protein YscC	6.849	4.22E-24
<i>vp1666</i>	hypothetical protein in type III secretion	6.768	1.87E-19
<i>vp1672</i>	translocation protein in type III secretion	6.344	5.41E-19
<i>vp1701</i>	putative exoenzyme S synthesis protein C precursor	6.223	1.14E-14
<i>vp1673</i>	translocation protein in type III secretion	6.164	1.62E-15
<i>vp1670</i>	putative translocation protein in type III secretion	5.776	3.76E-19

## Supplementary Materials

<i>vp1671</i>	putative translocation protein in type III secretion	5.747	3.94E-19
<i>vp1702</i>	hypothetical protein	5.637	4.73E-15
<i>vpa0874</i>	hypothetical protein	5.558	1.76E-12
<i>vp1669</i>	putative type III secretion protein YscO	5.367	1.50E-14
<i>vp1684</i>	hypothetical protein	5.177	5.99E-15
<i>vp1674</i>	translocation protein in type III secretion	4.975	1.57E-14
<i>vp1685</i>	hypothetical protein	4.926	6.02E-12

**Table 15. List of genes that were significantly upregulated in the  $\Delta$ ecfP mutant when compared to wild type.** This table gives a list of all genes that were significantly upregulated in the  $\Delta$ ecfP mutant by a minimum of 4 fold when compared to wild type. The targets were obtained through transcriptomics analyses. p-values were determined by Students t-test.

Gene	Annotation	Fold up-regulated in $\Delta$ ecfP/WT	p-value
<i>vpa0807</i>	putative multidrug resistance protein	15.660	2.45E-36
<i>vpa0808</i>	putative periplasmic linker protein	15.360	6.09E-36
<i>vpa0776</i>	mazG-related protein	12.656	2.08E-27
<i>vpa0809</i>	transporter, AcrB/D/F family	12.366	NA
<i>vpa0777</i>	hypothetical protein	8.854	1.23E-22
<i>vpa0598</i>	hypothetical protein	8.703	1.21E-02
<i>vpa0778</i>	putative Mg transporter MgtE	7.276	9.59E-16
<i>vp0018</i>	16 kDa heat shock protein A	6.869	8.76E-26
<i>vp1264</i>	hypothetical protein	6.812	9.61E-30
<i>vp2035</i>	hypothetical protein	6.614	3.26E-29
<i>vp2034</i>	hypothetical protein	6.261	8.76E-26
<i>vp0061</i>	putative multidrug transmembrane resistance signal peptide protein	5.435	2.66E-17
<i>vp2036</i>	putative DNA polymerase III alpha chain	5.086	7.76E-23
<i>vpa0526</i>	putative OmpU	4.989	7.93E-11
<i>vp2754</i>	hypothetical protein	4.733	2.29E-14
<i>vp0060</i>	putative multidrug transmembrane resistance signal peptide protein	4.445	2.06E-13
<i>vpa0775</i>	hypothetical protein	4.385	3.04E-07

<i>vp1334</i>	hypothetical protein	4.361	3.94E-02
<i>vpa1644</i>	maltose-inducible porin	4.041	1.79E-11
<i>vp2755</i>	hypothetical protein	4.038	1.53E-13

**Table 16. List of genes that were significantly downregulated in the  $\Delta pknT$  mutant when compared to wild type.** This table gives a list of all genes that were significantly downregulated in the  $\Delta pknT$  mutant by a minimum of 4 fold when compared to wild type. The targets were obtained through transcriptomics analyses. p-values were determined by Students t-test.

Gene	Annotation	Fold down-regulated in $\Delta pknT/WT$	p-value
<i>vpa0879</i>	UDP-glucose 4-epimerase	92.817	7.11E-141
<i>vpa0882</i>	heme transport protein HutA	39.946	5.42E-75
<i>vpa0875</i>	putative carboxylase	26.182	5.20E-52
<i>vpa0946</i>	conserved hypothetical protein	12.614	3.27E-12
<i>vpa0945</i>	conserved hypothetical protein	11.641	9.20E-09
<i>vpa0878</i>	hypothetical protein	11.246	4.89E-21
<i>vpa0947</i>	transcriptional regulator, ArsR family	10.268	1.03E-07
<i>vpa0876</i>	conserved hypothetical protein	10.225	5.56E-19
<i>vpa0642</i>	putative glutathione S-transferase	7.857	3.22E-10
<i>vpa0218</i>	hypothetical protein	7.645	5.39E-60
<i>tRNA-Pro-3</i>	tRNA-Pro	7.232	1.78E-05
<i>vpa0217</i>	conserved hypothetical protein	6.847	3.72E-54
<i>vpa0811</i>	PTS system, fructose-specific IIBC component	6.581	1.96E-46
<i>vpa0877</i>	putative lactam utilization protein	6.058	2.17E-09
<i>vpa0812</i>	1-phosphofructokinase	5.879	1.61E-33
<i>vpa0874</i>	hypothetical protein	5.709	6.65E-39
<i>vpa0860</i>	long-chain fatty acid transport protein	5.384	2.98E-23
<i>vpa1250</i>	3,4-dihydroxy-2-butanone 4-phosphate synthase	5.252	2.16E-42
<i>vp0081</i>	putative hyperosmotically inducible periplasmic protein	5.147	4.58E-03
<i>vpa0859</i>	putative lipase	5.106	2.20E-31

## Supplementary Materials

<i>vpa0813</i>	PTS system, fructose-specific IIA/FPR component	4.899	4.17E-27
<i>tRNA-Ser-6</i>	tRNA-Ser	4.772	6.12E-03
<i>tRNA-Gly-12</i>	tRNA-Gly	4.745	1.34E-13
<i>vp1680</i>	hypothetical protein	4.142	8.00E-22
<i>vpa1709</i>	hypothetical protein	4.073	6.77E-05
<i>vp0782</i>	flagellar L-ring protein precursor FlgH	4.070	1.10E-21

**Table 17. List of genes that were significantly upregulated in the  $\Delta pknT$  mutant when compared to wild type.** This table gives a list of all genes that were significantly upregulated in the  $\Delta pknT$  mutant by a minimum of 4 fold when compared to wild type. The targets were obtained through transcriptomics analyses. p-values were determined by Students t-test.

Gene	Annotation	Fold up-regulated in $\Delta pknT/WT$	p-value
<i>vp2015</i>	putative cytochrome c	63.084	1.15E-88
<i>vp2016</i>	hypothetical protein	42.476	6.21E-86
<i>vpa1407</i>	hypothetical protein	34.122	7.66E-50
<i>vp1164</i>	hypothetical protein	26.709	1.22E-67
<i>vpa1406</i>	putative exopolysaccharide biosynthesis protein	25.888	2.91E-59
<i>vpa1494</i>	hypothetical protein	24.739	9.23E-68
<i>vpa1403</i>	putative capsular polysaccharide biosynthesis glycosyltransferase	22.371	2.91E-59
<i>vpa1529</i>	hypothetical protein	20.713	9.28E-63
<i>vpa1404</i>	hypothetical protein	20.295	5.51E-55
<i>vp0294</i>	hypothetical protein	19.543	1.62E-28
<i>vpa1528</i>	hypothetical protein	18.399	3.41E-51
<i>vpa1495</i>	ABC transporter, ATP-binding protein	18.290	2.45E-65
<i>vpa1408</i>	putative lipopolysaccharide biosynthesis protein	17.154	3.51E-46
<i>vp0292</i>	sulfate adenylyl transferase, subunit 2	15.608	8.89E-54
<i>vpa1405</i>	putative polysaccharide export-related protein	15.089	3.22E-36
<i>vpa1660</i>	putative transport protein	13.785	1.37E-45
<i>vp0293</i>	sulfate adenylyl transferase, subunit 1	13.758	1.21E-50



<i>vpa0807</i>	putative multidrug resistance protein	13.293	3.73E-62
<i>vpa1658</i>	hypothetical protein	13.285	1.96E-51
<i>vpa0428</i>	conserved hypothetical protein	12.663	2.85E-59
<i>vpa1659</i>	hypothetical protein	12.644	2.98E-50
<i>vpa0424</i>	TonB system transport protein ExbD1	12.323	4.11E-56
<i>vpa0422</i>	putative hemin ABC transporter, permease protein	12.221	1.01E-58
<i>vp1264</i>	hypothetical protein	12.109	1.13E-54
<i>vpa0427</i>	coproporphyrinogen oxidase homolog PhuW	11.957	3.27E-58
<i>vp0497</i>	formate acetyl transferase-related protein	11.743	9.55E-52
<i>vpa0423</i>	hemin ABC transporter, periplasmic hemin-binding protein HutB	11.665	1.43E-57
<i>vpa0425</i>	ExbB-like protein	11.337	5.29E-55
<i>vpa1661</i>	putative AcsD	11.054	3.50E-43
<i>vpa0809</i>	Transporter, AcrB/D/F family	10.465	0.00E+00
<i>vpa0808</i>	putative periplasmic linker protein	10.167	4.13E-55
<i>vp2873</i>	fumarate hydratase, class II	9.871	3.47E-45
<i>vpa1411</i>	putative glycosyltransferase	9.855	4.71E-29
<i>vpa1409</i>	hypothetical protein	9.849	3.93E-35
<i>vpa1410</i>	hypothetical protein	9.821	6.07E-32
<i>vpa0421</i>	hemin ABC transporter, ATP-binding protein HutD	9.740	5.12E-52
<i>vp2035</i>	hypothetical protein	9.524	1.00E-46
<i>vpa0776</i>	mazG-related protein	9.331	9.96E-38
<i>vpa0429</i>	conserved hypothetical protein	9.118	4.93E-51
<i>vp2872</i>	hypothetical protein	9.100	1.93E-32
<i>vpa0426</i>	TonB-like protein	8.806	3.98E-47
<i>vp2034</i>	hypothetical protein	8.637	1.47E-40
<i>vpa1656</i>	ferric vibrioferrin receptor	7.454	9.11E-42
<i>vp2036</i>	putative DNA polymerase III alpha chain	7.403	4.73E-39
<i>vp2585</i>	conserved hypothetical protein	7.259	8.75E-31

## Supplementary Materials

<i>vp2011</i>	tetrathionate reductase, subunit B	6.714	9.02E-18
<i>vpa1413</i>	hypothetical protein	6.607	3.26E-16
<i>vpa1657</i>	ferric siderophore receptor homolog	6.512	3.71E-38
<i>vpa1463</i>	hypothetical protein	6.098	4.32E-28
<i>vpa1412</i>	hypothetical polysaccharide biosynthesis related protein	5.953	2.85E-24
<i>vp2759</i>	N-acetyl-gamma-glutamyl- phosphate reductase	5.941	1.51E-20
<i>vp2161</i>	conserved hypothetical protein	5.924	7.33E-31
<i>vpa1464</i>	hypothetical protein	5.725	6.85E-33
<i>vp0595</i>	conserved hypothetical protein	5.625	6.36E-29
<i>vpa1466</i>	putative TonB system receptor	5.609	2.52E-34
<i>vpa0667</i>	hypothetical protein	5.343	4.40E-12
<i>vp0648</i>	DNA repair protein RecN	5.313	1.52E-29
<i>vp2603</i>	iron-regulated virulence regulatory protein homolog	5.211	1.53E-23
<i>vp0106</i>	hypothetical protein	5.192	2.98E-25
<i>vpa0358</i>	putative transcriptional regulator, LuxR family	5.176	7.31E-16
<i>vpa0777</i>	hypothetical protein	5.061	7.03E-26
<i>vpa1465</i>	hypothetical protein	4.983	1.22E-30
<i>vp2860</i>	superoxide dismutase, Mn	4.953	1.86E-25
<i>vp0018</i>	16 kDa heat shock protein A	4.820	1.04E-19
<i>vpa1467</i>	protease II	4.778	4.03E-30
<i>vpa1662</i>	putative diaminopimelate decarboxylase protein	4.756	8.68E-23
<i>vp1747</i>	putative amino acid transporter	4.686	2.86E-20
<i>vpa1341</i>	putative Spa29, component of the Mxi-Spa secretion machinery	4.672	1.01E-15
<i>vp2110</i>	hypothetical 16.4 kDa protein in moty 3'	4.590	2.53E-21
<i>vpa0535</i>	putative phosphomannomutase	4.583	3.51E-32
<i>vpa0980</i>	hypothetical protein	4.537	2.51E-23

<i>vpa1454</i>	conserved hypothetical protein	4.485	9.74E-29
<i>vp0596</i>	aminotransferase NifS, class V	4.467	3.44E-22
<i>vpa1443</i>	putative protein secretion protein	4.438	2.02E-18
<i>vp0628</i>	hypothetical protein	4.327	1.90E-20
<i>vp2779</i>	conserved hypothetical protein	4.322	3.86E-21
<i>vp2577</i>	$\sigma$ -E factor negative regulatory protein RseA	4.310	4.14E-22
<i>vp2602</i>	iron-regulated outer membrane virulence protein homolog	4.299	1.82E-16
<i>vpa0430</i>	hypothetical protein	4.226	4.09E-28
<i>vp0636</i>	putative outer membrane protein A	4.184	2.10E-10
<i>vp0295</i>	putative sodium/sulfate symporter	4.181	7.08E-17
<i>vpa1450</i>	MoxR-related protein	4.146	2.97E-27
<i>vpa1453</i>	hypothetical protein	4.095	1.07E-24
<i>vp2578</i>	RNA polymerase $\sigma$ -E factor	4.077	1.29E-20
<i>vp2012</i>	hypothetical protein	4.017	1.95E-04

**Table 18. Targets that were significantly downregulated in  $\Delta$ *pknT* swimmers when compared to wild type swimmers.** This table gives a list of all targets that were significantly downregulated in the swimmers of the  $\Delta$ *pknT* mutant strain when compared to wild type (Parameters:  $S_0$  of 0.1 and a False Discovery Rate (FDR) of 0.01). The targets were obtained through proteomics analyses. p-values were determined by Students t-test.

Gene	Annotation	Fold down-regulated in $\Delta$ <i>pknT</i> /WT (Swimmers)	p-value
<i>vp1214</i>	Helicase-related protein	6.202	1.12E-03
<i>vpA0878</i>	Uncharacterized protein	4.582	7.12E-05
<i>vpA0882</i>	Heme transport protein HutA	4.280	5.45E-06
<i>vp1481</i>	Uncharacterized protein VP1481	4.061	1.31E-03
<i>vp2174</i>	Putative regulatory protein	3.512	1.88E-03
<i>vp1008</i>	Putative outer membrane porin protein locus of qsr prophage	3.250	4.95E-05

## Supplementary Materials

<i>hmuV</i>	Hemin import ATP-binding protein HmuV (EC 3.6.3.-)	2.025	5.11E-04
<i>vpa0163</i>	Putative ATP-binding component of ABC transporter	1.736	1.45E-04
<i>vp2167</i>	Uncharacterized protein	1.232	5.61E-05
<i>vp1091</i>	Putative transmembrane protein affecting septum formation and cell membrane permeability	1.206	8.17E-07

**Table 19. Targets that were significantly upregulated in  $\Delta pknT$  swimmers when compared to wild type swimmers.** This table gives a list of all targets that were significantly upregulated in the swimmers of the  $\Delta pknT$  mutant strain when compared to wild type (Parameters:  $S_0$  of 0.1 and a False Discovery Rate (FDR) of 0.01). The targets were obtained through proteomics analyses. p-values were determined by Students t-test.

Gene	Annotation	Fold up-regulated in $\Delta pknT/WT$ (Swimmers)	p-value
<i>dusC</i>	tRNA-dihydrouridine(16) synthase (EC 1.3.1.-) (U16-specific dihydrouridine synthase) (U16-specific Dus) (tRNA-dihydrouridine synthase C)	8.732	1.07E-03
<i>lpxC</i>	UDP-3-O-acyl-N-acetylglucosamine deacetylase (UDP-3-O-acyl-GlcNAc deacetylase) (EC 3.5.1.108) (UDP-3-O-[R-3-hydroxymyristoyl]-N-acetylglucosamine deacetylase)	6.938	4.30E-03
VPA1286	Putative transcriptional regulator	4.541	2.83E-04
VPA1041	Uncharacterized protein	4.241	1.37E-03
VPA0808	Putative periplasmic linker protein	3.920	1.72E-05
VPA0809	Transporter, AcrB/D/F family	3.572	2.08E-08

metA	Homoserine O-succinyltransferase (EC 2.3.1.46) (Homoserine O-transsuccinylase) (HTS)	3.551	2.41E-04
VPA0474	Spermidine n1-acetyltransferase	3.423	1.33E-03
VP1266	Uncharacterized protein	3.226	1.50E-03
VPA0807	Putative multidrug resistance protein	3.063	1.91E-08
VP2294	Putative SAM-dependent methyltransferase	2.984	6.58E-06
VPA0215	Uncharacterized protein	2.979	1.71E-03
VP1875	Para-aminobenzoate synthase, component I	2.253	4.72E-04
VP0425	Outer membrane protein TolC	2.209	3.41E-08
VP2951	GlpG protein	2.132	4.87E-04
VPA1609	Proton/glutamate symporter	1.920	1.89E-04
VP0648	DNA repair protein RecN (Recombination protein N)	1.763	2.85E-04
VP0974	Uncharacterized protein	1.653	1.09E-05
topB	DNA topoisomerase 3 (EC 5.99.1.2) (DNA topoisomerase III)	1.516	2.86E-05
VPA1455	Uncharacterized protein	1.384	1.23E-04
VP2594	Uncharacterized protein	1.282	8.25E-05

**Table 20. List of strains used to calculate the frequency of Ser or Thr at the same position as T63 of EcFP.** This table provides a list of all organisms/ strains that were used to assess the frequency of occurrence of serine or threonine residues at the same position as that of the phosphorylatable T63 residue of EcFP (alongside the corresponding identifiers).

Organism/ strain used	Identifier
<i>Rhodanobacter</i> sp. 115	GCF_000264335.1
<i>Rhodopirellula islandica</i>	GCF_001027925.1
<i>Rudaea cellulolytica</i> DSM 22992	GCF_000378125.1
<i>Algoriphagus machipongonensis</i>	GCF_000166275.1
<i>Gimesia maris</i> DSM 8797	GCF_000181475.1
<i>Lysobacter enzymogenes</i>	GCF_001442515.1
<i>Hydrocarboniphaga effusa</i> AP103	GCF_000271305.1
<i>Stenotrophomonas maltophilia</i>	GCF_001499755.1
<i>Luteimonas</i> sp. J29	GCF_000472505.1

<i>Euryhalocaulis caribicus</i>	GCF_000412185.1
<i>Aquabacterium</i> sp. NJ1	GCF_000768065.1
<i>Marinomonas polaris</i> DSM 16579	GCF_900129155.1
<i>Rhodopirellula sallentina</i> SM41	GCF_000346505.1
<i>Sphingomonas</i> sp. Leaf412	GCF_001425405.1
<i>Brevundimonas aveniformis</i> DSM 17977	GCF_000428765.1
<i>Hahella chejuensis</i> KCTC 2396	GCF_000012985.1
<i>Luteimonas mephitis</i> DSM 12574	GCF_000422305.1
<i>Chloracidobacterium thermophilum</i> B	GCF_000226295.1
<i>Candidatus Koribacter versatilis</i> Ellin345	GCF_000014005.1
<i>Marinilabilia salmonicolor</i> JCM 21150	GCF_000259075.1
<i>Verrucomicrobiae bacterium</i> DG1235	GCF_000155695.1
<i>Vibrio fischeri</i> ES114	GCF_000011805.1
<i>Microbulbifer agarilyticus</i> S89	GCF_000220505.1
<i>Acidobacteriaceae bacterium</i> URHE0068	GCF_000620725.1
<i>Lysobacter antibioticus</i>	GCF_001442535.1
<i>Persicobacter</i> sp. JZB09	GCF_001308105.1
<i>Psychromonas arctica</i> DSM 14288	GCF_000482725.1
<i>Colwellia</i> sp. MT41	GCF_001444365.1
<i>Catenovulum maritimum</i>	GCF_001050375.1
<i>Pseudoxanthomonas mexicana</i>	GCF_001556105.1
<i>Pseudoxanthomonas suwonensis</i>	GCF_000972865.1
<i>Sphingopyxis terrae</i> NBRC 15098	GCF_001610975.1
<i>Teredinibacter</i> sp. 1162T.S.0a.05	GCF_000964245.1
<i>Hyphomonas beringensis</i>	GCF_000682755.1
<i>Luteimonas huabeiensis</i> HB2	GCF_000559025.1
<i>Bosea</i> sp. Root483D1	GCF_001429505.1
<i>Blastopirellula marina</i> DSM 3645	GCF_000153105.1
<i>Sphingopyxis</i> sp. Root1497	GCF_001427085.1
<i>Haloferula</i> sp. BvORR071	GCF_000739615.1
<i>Lysobacter concretions</i> Ko07 = DSM 16239	GCF_000768345.1
<i>Candidatus Solibacter usitatus</i> Ellin6076	GCF_000014905.1
<i>Salisaeta longa</i> DSM 21114	GCF_000419585.1
<i>Ideonella sakaiensis</i>	GCF_001293525.1
<i>Vibrio</i> genomsp. F6 str. FF-238	GCF_000272145.2
<i>Luteimonas</i> sp. FCS-9	GCF_001014645.1
<i>Paucibacter</i> sp. KCTC 42545	GCF_001477625.1
<i>Lysobacter</i> sp. URHA0019	GCF_000426005.1
<i>Vibrio scopthalmi</i>	GCF_001685465.1
<i>Vibrio</i> genomsp. F10 str. ZF-129	GCF_000287055.2
<i>Edaphobacter aggregans</i> DSM 19364	GCF_000745965.1

<i>Acidovorax radialis</i> N35	GCF_000204195.1
<i>Terriglobus</i> sp. TAA 43	GCF_000800015.1
<i>Photobacterium marinum</i>	GCF_000331515.1
<i>Stenotrophomonas daejeonensis</i>	GCF_001431505.1
<i>Archangium gephyra</i>	GCF_001027285.1
<i>Granulicella mallensis</i> MP5ACTX8	GCF_000178955.2
<i>Alteromonas stellipolaris</i>	GCF_001562115.1
<i>Lysobacter capsici</i>	GCF_001442785.1
<i>Lysobacter</i> sp. Root96	GCF_001429315.1
<i>Hyphomonas polymorpha</i> PS728	GCF_000685315.1
<i>Pelomonas</i> sp. Root662	GCF_001427705.1
<i>Stenotrophomonas rhizophila</i>	GCF_000661955.1
<i>Gloeobacter kilaueensis</i> JS1	GCF_000484535.1
<i>Arenimonas oryzae</i> DSM 21050 = YC6267	GCF_000420545.1
<i>Sphingomonas</i> sp. ERG5	GCF_000803065.1
<i>Nevskia ramosa</i> DSM 11499	GCF_000420645.1
<i>Silvibacterium bohemicum</i>	GCF_001006305.1
<i>Roseateles depolymerans</i>	GCF_001483865.1
<i>Vibrio vulnificus</i> YJ016	GCF_000009745.1
<i>Frateuria aurantia</i> DSM 6220	GCF_000242255.2
<i>Lysobacter</i> sp. A03	GCF_000855665.1
<i>Solimonas soli</i> DSM 21787	GCF_000474945.1
<i>Stenotrophomonas chelatiphaga</i>	GCF_001431535.1
<i>Hahella ganghwensis</i> DSM 17046	GCF_000376785.1
<i>Thermomonas fusca</i> DSM 15424	GCF_000423885.1
<i>Colwellia psychrerythraea</i> 34H	GCF_000012325.1
<i>Flammeovirga pacifica</i>	GCF_000807855.2
<i>Wenzhouxiangella marina</i>	GCF_001187785.1
<i>Frateuria</i> sp. Soil773	GCF_001428405.1
<i>Bryobacter aggregatus</i> MPL3	GCF_000702445.1
<i>Porphyrobacter cryptus</i> DSM 12079	GCF_000422985.1
<i>Singulisphaera acidiphila</i> DSM 18658	GCF_000242455.2
<i>Hyphomonas johnsonii</i> MHS-2	GCF_000685275.1
<i>Lysobacter daejeonensis</i> GH1-9	GCF_000768355.1
<i>Gemmatimonas phototrophica</i>	GCF_000695095.2
<i>Gemmatimonas aurantiaca</i> T-27	GCF_000010305.1
<i>[Polyangium] brachysporum</i>	GCF_001017435.1
<i>Pedosphaera parvula</i> Ellin514	GCF_000172555.1
<i>Chondromyces apiculatus</i> DSM 436	GCF_000601485.1
<i>Alteromonas australica</i>	GCF_000730385.1
<i>Thalassomonas actiniarum</i>	GCF_000948975.1

## Supplementary Materials

<i>Paraglaciecola polaris</i> LMG 21857	GCF_000315055.1
<i>Vibrio campbellii</i> ATCC BAA-1116	GCF_000017705.1
<i>Opitutus terrae</i> PB90-1	GCF_000019965.1
<i>Rubrivivax gelatinosus</i> IL144	GCF_000284255.1
<i>Marivirga tractuosa</i> DSM 4126	GCF_000183425.1
<i>Vibrio metschnikovii</i> CIP 69.14	GCF_000176155.1
<i>Vibrio parahaemolyticus</i> RIMD 2210633	GCF_000196095.1
<i>Rhodopirellula baltica</i> SH 1	GCF_000196115.1
<i>Verrucomicrobium spinosum</i> DSM 4136 = JCM 18804	GCF_000172155.1
<i>Arenimonas donghaensis</i> DSM 18148 = HO3-R19	GCF_000743535.1
<i>Pseudoalteromonas atlantica</i> T6c	GCF_000014225.1
<i>Pseudoxanthomonas spadix</i> BD-a59	GCF_000233915.3
<i>Lysobacter dokdonensis</i> DS-58	GCF_000770795.1
<i>Acidobacteriaceae bacterium</i> KBS 89	GCF_000381605.1
<i>Pseudoxanthomonas suwonensis</i> 11-1	GCF_000185965.1
<i>Lysobacter arseniciresistens</i> ZS79	GCF_000768335.1
<i>Pseudoxanthomonas suwonensis</i> J47	GCF_000513955.1
<i>Acidobacteriaceae bacterium</i> KBS 83	GCF_000381585.1
<i>Oleigrimonas soli</i>	GCF_000761445.1
<i>Gloeobacter violaceus</i> PCC 7421	GCF_000011385.1
<i>Arenimonas composti</i> TR7-09 = DSM 18010	GCF_000426365.1
bacterium L21-Spi-D4	GCF_001443605.1
<i>Psychromonas</i> sp. CNPT3	GCF_000153405.2
<i>Schlesneria paludicola</i> DSM 18645	GCF_000255655.1
<i>Rubinisphaera brasiliensis</i> DSM 5305	GCF_000165715.2
<i>Terriglobus saanensis</i> SP1PR4	GCF_000179915.2
<i>Pirellula staleyi</i> DSM 6068	GCF_000025185.1
beta proteobacterium AAP65	GCF_001295865.1
<i>Gemmata obscuriglobus</i> UQM 2246	GCF_000171775.1
<i>Stenotrophomonas panacihumi</i>	GCF_001431645.1
<i>Lysobacter</i> sp. Root494	GCF_001427225.1
<i>Pseudoxanthomonas dokdonensis</i>	GCF_001431405.1
<i>Paraglaciecola arctica</i> BSs20135	GCF_000314995.1
<i>Burkholderiales bacterium</i> JOSHI_001	GCF_000244995.1
<i>Photobacterium swingsii</i>	GCF_001077885.1
<i>Acidobacteriaceae bacterium</i> KBS 96	GCF_000381625.1
<i>Vibrio alginolyticus</i> NBRC 15630 = ATCC 17749	GCF_000354175.2
<i>Hyphomonas neptunium</i> ATCC 15444	GCF_000013025.1
<i>Isosphaera pallida</i> ATCC 43644	GCF_000186345.1
<i>Vibrio alginolyticus</i>	GCF_001525595.1
<i>Methylibium</i> sp. CF059	GCF_000799305.1



<i>Terracidiphilus gabretensis</i>	GCF_001449115.1
<i>Aliivibrio salmonicida</i> LFI1238	GCF_000196495.1
<i>Xanthomonas gardneri</i>	GCF_001908775.1
<i>Rheinheimera perlucida</i> DSM 18276	GCF_000382165.1
<i>Sorangium cellulosum</i> So ce56	GCF_000067165.1
<i>Dyella jiangningensis</i>	GCF_000632805.1
<i>Bacillus subtilis</i> subsp. <i>subtilis</i> str. 168	GCF_000009045.1



## Chapter 8: References



- Absalon, C., Obuchowski, M., Madec, E., Delattre, D., Holland, I. B., & S  r  r, S. J. (2009). CpgA, EF-Tu and the stressosome protein YezB are substrates of the Ser/Thr kinase/phosphatase couple, PrkC/PrpC, in *Bacillus subtilis*. *Microbiology*, 155(3), 932–943. <https://doi.org/10.1099/mic.0.022475-0>
- Ades, S. E., Connolly, L. E., Alba, B. M., & Gross, C. A. (1999). The *Escherichia coli*  $\sigma$ (E)-dependent extracytoplasmic stress response is controlled by the regulated proteolysis of an anti- $\sigma$  factor. *Genes and Development*, 13(18), 2449–2461. <https://doi.org/10.1101/gad.13.18.2449>
- Alberti, L., & Harshey, R. M. (1990). Differentiation of *Serratia marcescens* 274 into swimmer and swarmer cells. *Journal of Bacteriology*, 172(8), 4322–4328. <https://doi.org/10.1128/jb.172.8.4322-4328.1990>
- Alcalde-Rico, M., Hernando-Amado, S., Blanco, P., & Mart  nez, J. L. (2016). Multidrug Efflux Pumps at the Crossroad between Antibiotic Resistance and Bacterial Virulence. *Frontiers in Microbiology*. <https://doi.org/10.3389/fmicb.2016.01483>
- Alex, L. A., & Simon, M. I. (1994). Protein histidine kinases and signal transduction in prokaryotes and eukaryotes. *Trends in Genetics*. [https://doi.org/10.1016/0168-9525\(94\)90215-1](https://doi.org/10.1016/0168-9525(94)90215-1)
- Allison, C., Emody, L., Coleman, N., & Hughes, C. (1994). The role of swarm cell differentiation and multicellular migration in the uropathogenicity of *Proteus mirabilis*. *Journal of Infectious Diseases*, 169(5), 1155–1158. <https://doi.org/10.1093/infdis/169.5.1155>
- Allison, C., & Hughes, C. (1991). Bacterial swarming: an example of prokaryotic differentiation and multicellular behaviour. *Science Progress*, 75(298 Pt 3-4), 403–422.
- Allison, C., Lai, H. -C., Gygi, D., & Hughes, C. (1993). Cell differentiation of *Proteus mirabilis* is initiated by glutamine, a specific chemoattractant for swarming cells. *Molecular Microbiology*, 8(1), 53–60. <https://doi.org/10.1111/j.1365-2958.1993.tb01202.x>
- Allison, C., Lai, H. -C., & Hughes, C. (1992). Co-ordinate expression of virulence genes during swarm-cell differentiation and population migration of *Proteus mirabilis*. *Molecular Microbiology*. <https://doi.org/10.1111/j.1365-2958.1992.tb00883.x>
- Altschul, S. F., Gertz, E. M., Agarwala, R., Sch  ffer, A. A., & Yu, Y. K. (2009). PSI-BLAST pseudocounts and the minimum description length principle. *Nucleic Acids Research*. <https://doi.org/10.1093/nar/gkn981>
- Amstutz, P., Binz, H. K., Parizek, P., Stumpp, M. T., Kohl, A., Gr  tter, M. G., ... Pl  ckthun, A. (2005). Intracellular kinase inhibitors selected from combinatorial libraries of designed ankyrin repeat proteins. *Journal of Biological Chemistry*, 280(26), 24715–24722. <https://doi.org/10.1074/jbc.M501746200>
- Anaya-L  pez, J. L., L  pez-Meza, J. E., & Ochoa-Zarzosa, A. (2013). Bacterial resistance to cationic antimicrobial peptides. *Critical Reviews in Microbiology*. <https://doi.org/10.3109/1040841X.2012.699025>
- Anthony, J. R., Newman, J. D., & Donohue, T. J. (2004). Interactions between the *Rhodobacter sphaeroides* ECF sigma factor,  $\sigma$  E , and its anti-sigma factor, ChrR. *Journal of Molecular Biology*. <https://doi.org/10.1016/j.jmb.2004.06.018>
- Arbade, G. K. (2017). Extra Cytoplasmic Sigma Factors in *Staphylococcus aureus*; their Role and Significance in the Survival of Cocci. *Journal of Applied Biotechnology & Bioengineering*, 1(2), 53–57. <https://doi.org/10.15406/jabb.2016.01.00009>
- Ardito, F., Giuliani, M., Perrone, D., Troiano, G., & Muzio, L. Lo. (2017). The crucial role of protein phosphorylation in cell signaling and its use as targeted therapy (Review). *International Journal of Molecular Medicine*. <https://doi.org/10.3892/ijmm.2017.3036>
- Arnold, T. M., Forrest, G. N., & Messmer, K. J. (2007). Polymyxin antibiotics for gram-

## References

---

- negative infections. *American Journal of Health-System Pharmacy*.  
<https://doi.org/10.2146/ajhp060473>
- Arnosti, D. N., & Chamberlin, M. J. (1989). Secondary sigma factor controls transcription of flagellar and chemotaxis genes in *Escherichia coli*. *Proceedings of the National Academy of Sciences*. <https://doi.org/10.1073/pnas.86.3.830>
- Arora, G., Sajid, A., Arulanandh, M. D., Singhal, A., Mattoo, A. R., Pomerantsev, A. P., ... Singh, Y. (2012). Unveiling the novel dual specificity protein kinases in *Bacillus anthracis*: Identification of the first prokaryotic dual specificity tyrosine phosphorylation-regulated kinase (DYRK)-like kinase. *Journal of Biological Chemistry*. <https://doi.org/10.1074/jbc.M112.351304>
- Arthur, T. M., & Burgess, R. R. (1998). Localization of a  $\sigma 70$  binding site on the N terminus of the *Escherichia coli* RNA polymerase  $\beta'$  subunit. *Journal of Biological Chemistry*, 273(47), 31381–31387. <https://doi.org/10.1074/jbc.273.47.31381>
- Atsumi, T., McCarter, L., & Imae, Y. (1992). Polar and lateral flagellar motors of marine *Vibrio* are driven by different ion-motive forces. *Nature*, 355(6356), 182–184. <https://doi.org/10.1038/355182a0>
- Atsushi, M., Soon-Kwang, H., Hiroshi, I., Sueharu, H., & Teruhiko, B. (1994). Phosphorylation of the AfsR protein involved in secondary metabolism in *Streptomyces* species by a eukaryotic-type protein kinase. *Gene*, 146(1), 47–56. [https://doi.org/10.1016/0378-1119\(94\)90832-X](https://doi.org/10.1016/0378-1119(94)90832-X)
- Baer, C. E., Iavarone, A. T., Alber, T., & Sassetti, C. M. (2014). Biochemical and spatial coincidence in the provisional Ser/Thr protein kinase interaction network of *Mycobacterium tuberculosis*. *Journal of Biological Chemistry*. <https://doi.org/10.1074/jbc.M114.559054>
- Bamidele, A. I., & Babatunde, O. A. (2015). Swarming modulatory effects of some amino acids on *Proteus* strains from Lagos, Nigeria. *African Journal of Biotechnology*. <https://doi.org/10.5897/ajb2002.000-002>
- Barik, S., Sureka, K., Mukherjee, P., Basu, J., & Kundu, M. (2010). RseA, the SigE specific anti-sigma factor of *Mycobacterium tuberculosis*, is inactivated by phosphorylation-dependent ClpC1P2 proteolysis. *Molecular Microbiology*. <https://doi.org/10.1111/j.1365-2958.2009.07008.x>
- Barker H, W., & Gangarosa J, E. (1974). Food Poisoning Due To Staphylococci. *The Lancet*, 232(6009), 1010–1011. [https://doi.org/10.1016/s0140-6736\(00\)41532-1](https://doi.org/10.1016/s0140-6736(00)41532-1)
- Barne, K. A., Bown, J. A., Busby, S. J. W., & Minchin, S. D. (1997). Region 2.5 of the *Escherichia coli* RNA polymerase  $\sigma 70$  subunit is responsible for the recognition of the “extended -10” motif at promoters. *EMBO Journal*, 16(13), 4034–4040. <https://doi.org/10.1093/emboj/16.13.4034>
- Barthe, P., Mukamolova, G. V., Roumestand, C., & Cohen-Gonsaud, M. (2010). The structure of PknB extracellular PASTA domain from *Mycobacterium tuberculosis* suggests a ligand-dependent kinase activation. *Structure*, 18(5), 606–615. <https://doi.org/10.1016/j.str.2010.02.013>
- Barz, C., Abahji, T. N., Trülsch, K., & Heesemann, J. (2000). The *Yersinia* Ser/Thr protein kinase YpkA/YopO directly interacts with the small GTPases RhoA and Rac-1. *FEBS Letters*, 482(1–2), 139–143. [https://doi.org/10.1016/S0014-5793\(00\)02045-7](https://doi.org/10.1016/S0014-5793(00)02045-7)
- Bayer-Santos, E., Lima, L. dos P., Ceseti, L. de M., Ratagami, C. Y., de Santana, E. S., da Silva, A. M., ... Alvarez-Martinez, C. E. (2018). *Xanthomonas citri* T6SS mediates resistance to *Dictyostelium* predation and is regulated by an ECF  $\sigma$  factor and cognate Ser/Thr kinase. *Environmental Microbiology*, 20, 1562–1575. <https://doi.org/10.1111/1462-2920.14085>
- Beenstock, J., Mooshayef, N., & Engelberg, D. (2016). How Do Protein Kinases Take a Selfie (Autophosphorylate)? *Trends in Biochemical Sciences*, 41(11), 938–953. <https://doi.org/10.1016/j.tibs.2016.08.006>
- Belas, R., Erskine, D., & Flaherty, D. (1991). *Proteus mirabilis* mutants defective in swarmer cell differentiation and multicellular behavior. *Journal of Bacteriology*, 173(19), 6279–6288. <https://doi.org/10.1128/jb.173.19.6279-6288.1991>

- Belas, R., Schneider, R., & Melch, M. (1998). Characterization of *Proteus mirabilis* precocious swarming mutants: Identification of *rsbA*, encoding a regulator of swarming behavior. *Journal of Bacteriology*.
- Belas, R., Simon, M., & Silverman, M. (1986). Regulation of lateral flagella gene transcription in *Vibrio parahaemolyticus*. *Journal of Bacteriology*, 167(1), 210–218. <https://doi.org/10.1128/jb.167.1.210-218.1986>
- Beltrao, P., Bork, P., Krogan, N. J., & Van Noort, V. (2013). Evolution and functional cross-talk of protein post-translational modifications. *Molecular Systems Biology*. <https://doi.org/10.1002/msb.201304521>
- Ben-David, Y., Letwin, K., Tannock, L., Bernstein, A., & Pawson, T. (1991). A mammalian protein kinase with potential for serine/threonine and tyrosine phosphorylation is related to cell cycle regulators. *The EMBO Journal*, 10(2), 317–325.
- Bendt, A. K., Burkovski, A., Schaffer, S., Bott, M., Farwick, M., & Hermann, T. (2003). Towards a phosphoproteome map of *Corynebacterium glutamicum*. *Proteomics*, 3(8), 1637–1646. <https://doi.org/10.1002/pmic.200300494>
- Bibb, M. J., Molle, V., & Buttner, M. J. (2000).  $\sigma$ (BldN), an extracytoplasmic function RNA polymerase sigma factor required for aerial mycelium formation in *Streptomyces coelicolor* A3(2). *Journal of Bacteriology*, 182(16), 4606–4616. <https://doi.org/10.1128/JB.182.16.4606-4616.2000>
- Bidnenko, V., Shi, L., Kobir, A., Ventroux, M., Pigeonneau, N., Henry, C., ... Mijakovic, I. (2013). *Bacillus subtilis* serine/threonine protein kinase YabT is involved in spore development via phosphorylation of a bacterial recombinase. *Molecular Microbiology*, 88(5), 921–935. <https://doi.org/10.1111/mmi.12233>
- Boles, B. R., & McCarter, L. L. (2002). *Vibrio parahaemolyticus* *scrABC*, a novel operon affecting swarming and capsular polysaccharide regulation. *Journal of Bacteriology*, 184(21), 5946–5954. <https://doi.org/10.1128/JB.184.21.5946-5954.2002>
- Braun, V., Mahren, S., & Ogierman, M. (2003). Regulation of the FecI-type ECF sigma factor by transmembrane signalling. *Current Opinion in Microbiology*, 6(2), 173–180. [https://doi.org/10.1016/S1369-5274\(03\)00022-5](https://doi.org/10.1016/S1369-5274(03)00022-5)
- Brooks, B. E., & Buchanan, S. K. (2009). *Signaling Mechanisms for activation of ECF sigma factors*. 1778(9), 1930–1945. <https://doi.org/10.1016/j.bbamem.2007.06.005> Signaling
- Buck, M., & Cannon, W. (1992). Specific binding of the transcription factor sigma-54 to promoter DNA. *Nature*. <https://doi.org/10.1038/358422a0>
- Burbank, L., Mohammadi, M., & Roper, M. C. (2015). Siderophore-Mediated Iron Acquisition Influences Motility and Is Required for Full Virulence of the Xylem-Dwelling Bacterial Phytopathogen *Pantoea stewartii* subsp. *stewartii*. *Applied and Environmental Microbiology*. <https://doi.org/10.1128/aem.02503-14>
- Burchard, R. P. (1974). Studies on gliding motility in *Myxococcus xanthus*. *Archives of Microbiology*. <https://doi.org/10.1007/BF00696242>
- Burgess, R. R., Travers, A. A., Dunn, J. J., & Bautz, E. K. F. (1969). Factor stimulating transcription by RNA polymerase. *Nature*, 221(5175), 43–46. <https://doi.org/10.1038/221043a0>
- Burkart, M., Toguchi, A., & Harshey, R. M. (1998). The chemotaxis system, but not chemotaxis, is essential for swarming motility in *Escherichia coli*. *Proceedings of the National Academy of Sciences*, 95(5), 2568–2573. <https://doi.org/10.1073/pnas.95.5.2568>
- Burnett, G., & Kennedy, E. P. (1954). And eugene p. kennedy. *Cancer*, 969–980.
- Bush, M., & Dixon, R. (2012). The Role of Bacterial Enhancer Binding Proteins as Specialized Activators of 54-Dependent Transcription. *Microbiology and Molecular Biology Reviews*. <https://doi.org/10.1128/MMBR.00006-12>
- Butler, M. T., Wang, Q., & Harshey, R. M. (2010). Cell density and mobility protect swarming bacteria against antibiotics. *Proceedings of the National Academy of*

## References

---

- Sciences*, 107(8), 3776–3781. <https://doi.org/10.1073/pnas.0910934107>
- Buttner, M. J., Fearnley, I. M., Bibb, M. J., Lane, C., & Nr, N. (1987). *O/GG*. 3, 101–109.
- Buttner, M. J., Smith, A. M., & Bibb, M. J. (1988). At least three different RNA polymerase holoenzymes direct transcription of the agarase gene (*dagA*) of *Streptomyces coelicolor* A3(2). *Cell*, 52(4), 599–607. [https://doi.org/10.1016/0092-8674\(88\)90472-2](https://doi.org/10.1016/0092-8674(88)90472-2)
- Campagne, S., Damberger, F. F., Kaczmarczyk, A., Francez-Charlot, A., Allain, F. H.-T., & Vorholt, J. A. (2012a). Structural basis for sigma factor mimicry in the general stress response of Alphaproteobacteria. *Proceedings of the National Academy of Sciences*, 109(21), E1405–E1414. <https://doi.org/10.1073/pnas.1117003109>
- Campagne, S., Damberger, F. F., Kaczmarczyk, A., Francez-Charlot, A., Allain, F. H.-T., & Vorholt, J. A. (2012b). Structural basis for sigma factor mimicry in the general stress response of Alphaproteobacteria. *Proceedings of the National Academy of Sciences*, 109(21), E1405–E1414. <https://doi.org/10.1073/pnas.1117003109>
- Campagne, S., Marsh, M. E., Capitani, G., Vorholt, J. A., & Allain, F. H. T. (2014). Structural basis for -10 promoter element melting by environmentally induced sigma factors. *Nature Structural and Molecular Biology*, 21(3), 269–276. <https://doi.org/10.1038/nsmb.2777>
- Campbell, E. A., Greenwell, R., Anthony, J. R., Wang, S., Lim, L., Das, K., ... Darst, S. A. (2007). A Conserved Structural Module Regulates Transcriptional Responses to Diverse Stress Signals in Bacteria. *Molecular Cell*. <https://doi.org/10.1016/j.molcel.2007.07.009>
- Campbell, E. A., Muzzin, O., Chlenov, M., Sun, J. L., Olson, C. A., Weinman, O., ... Darst, S. A. (2002). Structure of the bacterial RNA polymerase promoter specificity  $\sigma$  subunit. *Molecular Cell*, 9(3), 527–539. [https://doi.org/10.1016/S1097-2765\(02\)00470-7](https://doi.org/10.1016/S1097-2765(02)00470-7)
- Campbell, E. A., Tupy, J. L., Gruber, T. M., Wang, S., Sharp, M. M., Gross, C. A., & Darst, S. A. (2003). Crystal structure of *Escherichia coli*  $\sigma$ E with the cytoplasmic domain of its anti- $\sigma$  RseA. *Molecular Cell*. [https://doi.org/10.1016/S1097-2765\(03\)00148-5](https://doi.org/10.1016/S1097-2765(03)00148-5)
- Cannon, W., Claverie-Martin, F., Austin, S., & Buck, M. (1993). Core RNA polymerase assists binding of the transcription factor  $\sigma$ ;54 to promoter DNA. *Molecular Microbiology*. <https://doi.org/10.1111/j.1365-2958.1993.tb01573.x>
- Cannon, W., Gallegos, M. T., Casaz, P., & Buck, M. (1999). Amino-terminal sequences of  $\sigma$ (N) ( $\sigma$ 54) inhibit RNA polymerase isomerization. *Genes and Development*. <https://doi.org/10.1101/gad.13.3.357>
- Canova, M. J., Baronian, G., Brelle, S., Cohen-Gonsaud, M., Bischoff, M., & Molle, V. (2014). A novel mode of regulation of the *Staphylococcus aureus* Vancomycin-resistance-associated response regulator VraR mediated by Stk1 protein phosphorylation. *Biochemical and Biophysical Research Communications*, 447(1), 165–171. <https://doi.org/10.1016/j.bbrc.2014.03.128>
- Canova, M. J., & Molle, V. (2014). Bacterial serine/threonine protein kinases in host-pathogen interactions. *Journal of Biological Chemistry*, 289(14), 9473–9479. <https://doi.org/10.1074/jbc.R113.529917>
- Cao, M., Bernat, B. A., Wang, Z., Armstrong, R. N., & Helmann, J. D. (2001). FosB, a cysteine-dependent fosfomycin resistance protein under the control of  $\sigma$ w, an extracytoplasmic-function  $\sigma$  factor in *Bacillus subtilis*. *Journal of Bacteriology*. <https://doi.org/10.1128/JB.183.7.2380-2383.2001>
- Cao, M., & Helmann, J. D. (2002). Regulation of the *Bacillus subtilis* *bcrC* bacitracin resistance gene by two extracytoplasmic function  $\sigma$  factors. *Journal of Bacteriology*, 184(22), 6123–6129. <https://doi.org/10.1128/JB.184.22.6123-6129.2002>
- Carrera, A. C., Alexandrov, K., & Roberts, T. M. (1993). The conserved lysine of the



- catalytic domain of protein kinases is actively involved in the phosphotransfer reaction and not required for anchoring ATP. *Proceedings of the National Academy of Sciences of the United States of America*.
- Chaba, R., Alba, B. M., Guo, M. S., Sohn, J., Ahuja, N., Sauer, R. T., & Gross, C. a. (2011). Signal integration by DegS and RseB governs the  $\sigma^E$ -mediated envelope stress response in *Escherichia coli*. *Proceedings of the National Academy of Sciences of the United States of America*, 108(5), 2106–2111. <https://doi.org/10.1073/pnas.1019277108/-/DCSupplemental.www.pnas.org/cgi/doi/10.1073/pnas.1019277108>
- Chaba, R., Grigorova, I. L., Flynn, J. M., Baker, T. a, & Gross, C. a. (2007). Design principles of the proteolytic cascade governing the SigmaE-mediated envelope stress response in *Escherichia coli*: keys to graded , buffered , and rapid signal transduction. *Genes and Development*, 21(1), 124–136. <https://doi.org/10.1101/gad.1496707>
- Chakraborti, P. K., Matange, N., Nandicoori, V. K., Singh, Y., Tyagi, J. S., & Visweswariah, S. S. (2011). Signalling mechanisms in Mycobacteria. *Tuberculosis*, 91(5), 432–440. <https://doi.org/10.1016/j.tube.2011.04.005>
- Chao, J. D., Papavinasasundaram, K. G., Zheng, X., Chávez-Steenbock, A., Wang, X., Lee, G. Q., & Av-Gay, Y. (2010). Convergence of Ser/Thr and two-component signaling to coordinate expression of the dormancy regulon in *Mycobacterium tuberculosis*. *Journal of Biological Chemistry*, 285(38), 29239–29246. <https://doi.org/10.1074/jbc.M110.132894>
- Chen, B. G., Turner, L., & Berg, H. C. (2007). The wetting agent required for swarming in *Salmonella enterica serovar typhimurium* is not a surfactant. *Journal of Bacteriology*. <https://doi.org/10.1128/JB.01109-07>
- Copeland, M. F., & Weibel, D. B. (2009). Bacterial swarming: A model system for studying dynamic self-assembly. *Soft Matter*, 5(6), 1174–1187. <https://doi.org/10.1039/b812146j>
- Cornelis, G. R., Boland, A., Boyd, A. P., Geuijen, C., Iriarte, M., Neyt, C., ... Stainier, I. (1998). The virulence plasmid of Yersinia, an antihost genome. *Microbiology and Molecular Biology Reviews : MMBR*.
- Corrales, R. M., Molle, V., Leiba, J., Mourey, L., de Chastellier, C., & Kremer, L. (2012). Phosphorylation of Mycobacterial PcaA Inhibits Mycolic Acid Cyclopropanation. *Journal of Biological Chemistry*, 287(31), 26187–26199. <https://doi.org/10.1074/jbc.m112.373209>
- Cousin, C., Derouiche, A., Shi, L., Pagot, Y., Poncet, S., & Mijakovic, I. (2013). Protein-serine/threonine/tyrosine kinases in bacterial signaling and regulation. *FEMS Microbiology Letters*, 346, 11–19. <https://doi.org/10.1111/1574-6968.12189>
- Cowley, S., Ko, M., Pick, N., Chow, R., Downing, K. J., Gordhan, B. G., ... Av-Gay, Y. (2004). The *Mycobacterium tuberculosis* protein serine/threonine kinase PknG is linked to cellular glutamate/glutamine levels and is important for growth in vivo. *Molecular Microbiology*, 52(6), 1691–1702. <https://doi.org/10.1111/j.1365-2958.2004.04085.x>
- Cox, J., & Mann, M. (2008). MaxQuant enables high peptide identification rates, individualized p.p.b.-range mass accuracies and proteome-wide protein quantification. *Nature Biotechnology*. <https://doi.org/10.1038/nbt.1511>
- Cozzone, A. J. (1993). ATP-dependent protein kinases in bacteria. *Journal of Cellular Biochemistry*, 51(1), 7–13. <https://doi.org/10.1002/jcb.240510103>
- Davis, M. C., Kesthely, C. A., Franklin, E. A., & MacLellan, S. R. (2016). The essential activities of the bacterial sigma factor. *Canadian Journal of Microbiology*, 63(2), 89–99. <https://doi.org/10.1139/cjm-2016-0576>
- de Hernández-Díaz, L. J., Leon-Sicairos, N., Velazquez-Roman, J., Flores-Villaseñor, H., Guadron-Llanos, A. M., Javier Martinez-Garcia, J., ... Canizalez-Roman, A. (2015). A pandemic *Vibrio parahaemolyticus* O3:K6 clone causing most associated diarrhea cases in the Pacific Northwest coast of Mexico. *Frontiers in*

## References

---

- Microbiology*. <https://doi.org/10.3389/fmicb.2015.00221>
- De Las Peñas, A., Connolly, L., & Gross, C. A. (1997). The  $\sigma(E)$ -mediated response to extracytoplasmic stress in *Escherichia coli* is transduced by RseA and RseB, two negative regulators of  $\sigma(E)$ . *Molecular Microbiology*, 24(2), 373–385. <https://doi.org/10.1046/j.1365-2958.1997.3611718.x>
- De, S. P., Banerjee, M., Deb, B. C., Sengupta, P. G., Sil, J., Sircar, B. K., ... Pal, S. C. (1977). Environmental Distribution of Vibrios in Calcutta India with Particular Reference to *Vibrio-Parahaemolyticus*. *Indian Journal Of Medical Research*.
- Deutscher, J., Saier, M. H., & Jr. (1983). ATP-dependent protein kinase-catalyzed phosphorylation of a seryl residue in HPr, a phosphate carrier protein of the phosphotransferase system in *Streptococcus pyogenes*. *Proceedings of the National Academy of Sciences of the United States of America*.
- Déziel, E., Comeau, Y., & Villemur, R. (2001). Initiation of biofilm formation by *Pseudomonas aeruginosa* 57RP correlates with emergence of hyperpilated and highly adherent phenotypic variants deficient in swimming, swarming, and twitching motilities. *Journal of Bacteriology*. <https://doi.org/10.1128/JB.183.4.1195-1204.2001>
- Didier, J. P., Cozzone, A. J., & Duclos, B. (2010). Phosphorylation of the virulence regulator SarA modulates its ability to bind DNA in *Staphylococcus aureus*. *FEMS Microbiology Letters*, 306(1), 30–36. <https://doi.org/10.1111/j.1574-6968.2010.01930.x>
- Dombroski, A. J., Walter, W. A., & Gross, C. A. (1993). Amino-terminal amino acids modulate  $\sigma$ -factor DNA-binding activity. *Genes and Development*, 7(12 A), 2446–2455. <https://doi.org/10.1101/gad.7.12a.2446>
- Domingues, M. M., Inácio, R. G., Raimundo, J. M., Martins, M., Castanho, M. A. R. B., & Santos, N. C. (2012). Biophysical characterization of polymyxin B interaction with LPS aggregates and membrane model systems. *Biopolymers*. <https://doi.org/10.1002/bip.22095>
- Donnenberg, M. S., & Kaper, J. B. (1991). Construction of an eae deletion mutant of enteropathogenic *Escherichia coli* by using a positive-selection suicide vector. *Infection and Immunity*.
- Dove, S. L., Darst, S. A., & Hochschild, A. (2003). Region 4 of  $\sigma$  as a target for transcription regulation. *Molecular Microbiology*. <https://doi.org/10.1046/j.1365-2958.2003.03467.x>
- Drake, S. L., Depaola, A., & Jaykus, L. A. (2007). An overview of *Vibrio vulnificus* and *Vibrio parahaemolyticus*. *Comprehensive Reviews in Food Science and Food Safety*. <https://doi.org/10.1111/j.1541-4337.2007.00022.x>
- Duan, G., & Walther, D. (2015). The Roles of Post-translational Modifications in the Context of Protein Interaction Networks. *PLoS Computational Biology*, 11(2), 1–23. <https://doi.org/10.1371/journal.pcbi.1004049>
- Dubrana, M. P., Guéguénat, J., Bertin, C., Duret, S., Arricau-Bouvery, N., Claverol, S., ... Béven, L. (2017). Proteolytic Post-Translational Processing of Adhesins in a Pathogenic Bacterium. *Journal of Molecular Biology*, 429(12), 1889–1902. <https://doi.org/10.1016/j.jmb.2017.05.004>
- Dufour, A., & Haldenwang, W. G. (1994). Interactions between a *Bacillus subtilis* anti-?? factor (RsbW) and its antagonist (RsbV). *Journal of Bacteriology*.
- Durocher, D., Henckel, J., Fersht, A. R., & Jackson, S. P. (1999). The FHA domain is a modular phosphopeptide recognition motif. *Molecular Cell*. [https://doi.org/10.1016/S1097-2765\(00\)80340-8](https://doi.org/10.1016/S1097-2765(00)80340-8)
- Dworkin, J. (2015a). Ser/Thr phosphorylation as a regulatory mechanism in bacteria. *Current Opinion in Microbiology*. <https://doi.org/10.1016/j.mib.2015.01.005>
- Dworkin, J. (2015b). Ser/Thr phosphorylation as a regulatory mechanism in bacteria. *Current Opinion in Microbiology*, 24, 47–52. <https://doi.org/10.1016/j.mib.2015.01.005>
- Eberl, L., Christlansen, G., Molin, S., & Givskov, M. (1996). Differentiation of *Serratia liquefaciens* into swarm cells is controlled by the expression of the *flhD* master

- operon. *Journal of Bacteriology*, 178(2), 554–559.  
<https://doi.org/10.1128/jb.178.2.554-559.1996>
- Eichmann, C., Tzitzilonis, C., Nakamura, T., Kwiatkowski, W., Maslennikov, I., Choe, S., ... Riek, R. (2016). S-Nitrosylation Induces Structural and Dynamical Changes in a Rhodanese Family Protein. *Journal of Molecular Biology*, 428(19), 3737–3751. <https://doi.org/10.1016/j.jmb.2016.07.010>
- Feklistov, A., & Darst, S. A. (2011). Structural basis for promoter -10 element recognition by the bacterial RNA polymerase  $\sigma$  subunit. *Cell*.  
<https://doi.org/10.1016/j.cell.2011.10.041>
- Feklistov, A., Sharon, B. D., Darst, S. A., & Gross, C. A. (2014). Bacterial Sigma Factors: A Historical, Structural, and Genomic Perspective. *Annual Review of Microbiology*, 68(1), 357–376. <https://doi.org/10.1146/annurev-micro-092412-155737>
- Fieulaine, S., Morera, S., Poncet, S., Monedero, V., Gueguen-Chaignon, V., Galinier, A., ... Nessler, S. (2001). X-ray structure of Hpr kinase: A bacterial protein kinase with a P-loop nucleotide-binding domain. *EMBO Journal*.  
<https://doi.org/10.1093/emboj/20.15.3917>
- Finn, R. D., Clements, J., & Eddy, S. R. (2011). HMMER web server: Interactive sequence similarity searching. *Nucleic Acids Research*.  
<https://doi.org/10.1093/nar/gkr367>
- FISCHER, E. H., & KREBS, E. G. (1955). Conversion of phosphorylase b to phosphorylase a in muscle extracts. *The Journal of Biological Chemistry*.
- Fleurie, A., Cluzel, C., Guiral, S., Freton, C., Galisson, F., Zanella-Cleon, I., ... Grangeasse, C. (2012). Mutational dissection of the S/T-kinase StkP reveals crucial roles in cell division of *Streptococcus pneumoniae*. *Molecular Microbiology*, 83(4), 746–758. <https://doi.org/10.1111/j.1365-2958.2011.07962.x>
- Forbes, A. J., Patrie, S. M., Taylor, G. K., Kim, Y.-B., Jiang, L., & Kelleher, N. L. (2004). Targeted analysis and discovery of posttranslational modifications in proteins from methanogenic archaea by top-down MS. *Proceedings of the National Academy of Sciences*, 101(9), 2678–2683. <https://doi.org/10.1073/pnas.0306575101>
- Francez-Charlot, A., Frunzke, J., Reichen, C., Ebnetter, J. Z., Gourion, B., & Vorholt, J. A. (2009). Sigma factor mimicry involved in regulation of general stress response. *Proceedings of the National Academy of Sciences*, 106(9), 3467–3472.  
<https://doi.org/10.1073/pnas.0810291106>
- Fridman, M., Williams, G. D., Muzamal, U., Hunter, H., Siu, K. W. M., & Golemi-Kotra, D. (2013). Two unique phosphorylation-driven signaling pathways crosstalk in *Staphylococcus aureus* to modulate the cell-wall charge: Stk1/Stp1 meets GraSR. *Biochemistry*, 52(45), 7975–7986. <https://doi.org/10.1021/bi401177n>
- Fuhrmann, J., Schmidt, A., Spiess, S., Lehner, A., Turgay, K., Mechtler, K., ... Clausen, T. (2009). McsB Is a Protein Arginine Kinase. *Science*, 1323(June), 1323–1328.  
<https://doi.org/10.1126/science.1170088>
- Fujino, T., Okuno, Y., Nakada, D., Aoyama, A., Fukai, K., Mukai, T., & Ueho, T. (1953). On the bacteriological examination of Shirasu-food poisoning. *Med Jour Osaka Univ*.
- Galibert, F., Finan, T. M., Long, S. R., Pühler, A., Abola, P., Ampe, F., ... Batut, J. (2001). The composite genome of the legume symbiont *Sinorhizobium meliloti*. *Science*. <https://doi.org/10.1126/science.1060966>
- Galyov, E. E., Håkansson, S., Forsberg, Å., & Wolf-Watz, H. (1993). A secreted protein kinase of *Yersinia pseudotuberculosis* is an indispensable virulence determinant. *Nature*. <https://doi.org/10.1038/361730a0>
- Garcia-Garcia, T., Poncet, S., Derouiche, A., Shi, L., Mijakovic, I., & Noirot-Gros, M. F. (2016). Role of protein phosphorylation in the regulation of cell cycle and DNA-related processes in bacteria. *Frontiers in Microbiology*, 7(FEB), 1–11.  
<https://doi.org/10.3389/fmicb.2016.00184>
- Garnak, M., & Reeves, H. C. (1979). Phosphorylation of Isocitrate dehydrogenase of

## References

---

- Escherichia coli*. *Science (New York, N.Y.)*, 203(4385), 1111–1112.  
<https://doi.org/10.1126/science.34215>
- Ge, J., Xu, H., Li, T., Zhou, Y., Zhang, Z., Li, S., ... Shao, F. (2009). A Legionella type IV effector activates the NF- $\kappa$ B pathway by phosphorylating the I $\kappa$ B family of inhibitors. *Proceedings of the National Academy of Sciences*.  
<https://doi.org/10.1073/pnas.0907200106>
- Geszvain, K., Gruber, T. M., Mooney, R. A., Gross, C. A., & Landick, R. (2004). A hydrophobic patch on the flap-tip helix of *E. coli* RNA polymerase mediates  $\sigma$  70 region 4 function. *Journal of Molecular Biology*, 343(3), 569–587.  
<https://doi.org/10.1016/j.jmb.2004.08.063>
- Gil, M., Graña, M., Schopfer, F. J., Wagner, T., Denicola, A., Freeman, B. A., ... Durán, R. (2013). Inhibition of *Mycobacterium tuberculosis* PknG by non-catalytic rubredoxin domain specific modification: Reaction of an electrophilic nitro-fatty acid with the Fe-S center. *Free Radical Biology and Medicine*, 65, 150–161.  
<https://doi.org/10.1016/j.freeradbiomed.2013.06.021>
- Gitt, M. A., Wang, L. F., & Doi, R. H. (1985). A strong sequence homology exists between the major RNA polymerase  $\sigma$  factors of *Bacillus subtilis* and *Escherichia coli*. *Journal of Biological Chemistry*.
- Gnad, F., Gunawardena, J., & Mann, M. (2011). PHOSIDA 2011: The posttranslational modification database. *Nucleic Acids Research*, 39(SUPPL. 1), 253–260.  
<https://doi.org/10.1093/nar/gkq1159>
- Gode-Potratz, C. J., Chodur, D. M., & McCarter, L. L. (2010). Calcium and iron regulate swarming and type III secretion in *Vibrio parahaemolyticus*. *Journal of Bacteriology*. <https://doi.org/10.1128/JB.00654-10>
- Gode-Potratz, C. J., & McCarter, L. L. (2011). Quorum sensing and silencing in *Vibrio parahaemolyticus*. *Journal of Bacteriology*, 193(16), 4224–4237.  
<https://doi.org/10.1128/JB.00432-11>
- Gómez-Santos, N., Pérez, J., Sánchez-Sutil, M. C., Moraleda-Muñoz, A., & Muñoz-Dorado, J. (2011). Core from *Myxococcus xanthus* is a Copper-Dependent RNA polymerase sigma factor. *PLoS Genetics*, 7(6).  
<https://doi.org/10.1371/journal.pgen.1002106>
- Grangeasse, C., Nessler, S., & Mijakovic, I. (2012). Bacterial tyrosine kinases: Evolution, biological function and structural insights. *Philosophical Transactions of the Royal Society B: Biological Sciences*. <https://doi.org/10.1098/rstb.2011.0424>
- Green, H. A., & Donohue, T. J. (2006). Activity of *Rhodobacter sphaeroides* RpoHII, a second member of the heat shock sigma factor family. *Journal of Bacteriology*.  
<https://doi.org/10.1128/JB.00405-06>
- Greenstein, A. E., Echols, N., Lombana, T. N., King, D. S., & Alber, T. (2007). Allosteric activation by dimerization of the PknD receptor Ser/Thr protein kinase from *Mycobacterium tuberculosis*. *Journal of Biological Chemistry*, 282(15), 11427–11435. <https://doi.org/10.1074/jbc.M610193200>
- Gronow, S., & Brade, H. (2001). Lipopolysaccharide biosynthesis: which steps do bacteria need to survive? *Journal of Endotoxin Research*.  
<https://doi.org/10.1179/096805101101532468>
- Gruber, T. M., & Gross, C. A. (2003). Multiple Sigma Subunits and the Partitioning of Bacterial Transcription Space. *Annual Review of Microbiology*.  
<https://doi.org/10.1146/annurev.micro.57.030502.090913>
- Gruber, T. M., Markov, D., Sharp, M. M., Young, B. A., Lu, C. Z., Zhong, H. J., ... Gross, C. A. (2001). Binding of the initiation factor  $\sigma$ 70 to core RNA polymerase is a multistep process. *Molecular Cell*, 8(1), 21–31. [https://doi.org/10.1016/S1097-2765\(01\)00292-1](https://doi.org/10.1016/S1097-2765(01)00292-1)
- Guzman, L. M., Belin, D., Carson, M. J., & Beckwith, J. (1995). Tight regulation, modulation, and high-level expression by vectors containing the arabinose PBAD promoter. *Journal of Bacteriology*.
- Haldenwang, W. G. (1995). The sigma factors of *Bacillus subtilis*. *Microbiological Reviews*.

- Han, G. (2002). On the origin of Ser/Thr kinases in a prokaryote. *FEMS Microbiology Letters*, 200(1), 79–84. [https://doi.org/10.1016/s0378-1097\(01\)00206-3](https://doi.org/10.1016/s0378-1097(01)00206-3)
- Hanks, S. K., & Hunter, T. (1995). Protein kinases 6. The eukaryotic protein kinase superfamily: kinase (catalytic) domain structure and classification. *FASEB Journal : Official Publication of the Federation of American Societies for Experimental Biology*, 9(8), 576–596. <https://doi.org/10.1096/fasebj.9.8.7768349>
- Hanks, S. K., Quinn, a M., & Hunter, T. (1988). The protein kinase family: conserved features and deduced phylogeny of the catalytic domains. *Science (New York, N.Y.)*, 241(1985), 42–52. <https://doi.org/10.1126/science.3291115>
- Harris, J. D., Heilig, J. S., Martinez, I. I., Calendar, R., & Isaksson, L. A. (1978). Temperature-sensitive *Escherichia coli* mutant producing a temperature-sensitive sigma subunit of DNA-dependent RNA polymerase. *Proceedings of the National Academy of Sciences*. <https://doi.org/10.1073/pnas.75.12.6177>
- Harshey, R. M., & Matsuyama, T. (1994). Dimorphic transition in *Escherichia coli* and *Salmonella typhimurium*: surface-induced differentiation into hyperflagellate swarmer cells. *Proceedings of the National Academy of Sciences*, 91(18), 8631–8635. <https://doi.org/10.1073/pnas.91.18.8631>
- Hatzios, S. K., Baer, C. E., Rustad, T. R., Siegrist, M. S., Pang, J. M., Ortega, C., ... Bertozzi, C. R. (2013). Osmosensory signaling in *Mycobacterium tuberculosis* mediated by a eukaryotic-like Ser/Thr protein kinase. *Proceedings of the National Academy of Sciences*, 110(52), E5069–E5077. <https://doi.org/10.1073/pnas.1321205110>
- Heinrich, J., & Wiegert, T. (2009). Regulated intramembrane proteolysis in the control of extracytoplasmic function sigma factors. *Research in Microbiology*, 160(9), 696–703. <https://doi.org/10.1016/j.resmic.2009.08.019>
- Helmann, J. D. (2002). The extracytoplasmic function (ECF) sigma factors. *Advances in Microbial Physiology*. [https://doi.org/10.1016/S0065-2911\(02\)46002-X](https://doi.org/10.1016/S0065-2911(02)46002-X)
- Helmann, J. D. (2016). *Bacillus subtilis* extracytoplasmic function (ECF) sigma factors and defense of the cell envelope. *Current Opinion in Microbiology*, 30, 122–132. <https://doi.org/10.1016/j.mib.2016.02.002>
- Helmann, J. D., & Chamberlin, M. J. (1988). STRUCTURE AND FUNCTION OF BACTERIAL SIGMA FACTORS. *Annual Review of Biochemistry*. <https://doi.org/10.1146/annurev.bi.57.070188.004203>
- Henrichsen, J. (1972). Bacterial surface translocation: a survey and a classification. *Bacteriological Reviews*, 36(4), 478–503.
- Hernandez, E., Ramisse, F., & Cavallo, J. D. (1999). Abolition of swarming of *Proteus* [5]. *Journal of Clinical Microbiology*.
- Hernández, F., & Rodríguez, E. (1993). The swarming phenomenon of *Clostridium tetani*. *Revista de Biología Tropical*.
- Herrou, J., Rotskoff, G., Luo, Y., Roux, B., & Crosson, S. (2012). Structural basis of a protein partner switch that regulates the general stress response of - proteobacteria. *Proceedings of the National Academy of Sciences*. <https://doi.org/10.1073/pnas.1116887109>
- Hisatsune, K., Kiuye, A., & Kondo, S. (1980). Sugar Composition of O-Antigenic Lipopolysaccharides Isolated from *Vibrio parahaemolyticus*. *MICROBIOLOGY and IMMUNOLOGY*. <https://doi.org/10.1111/j.1348-0421.1980.tb02870.x>
- Holub, M., Bezoušková, S., Kalachová, L., & Weiser, J. (2007). Protein synthesis elongation factor Tu present in spores of *Streptomyces coelicolor* can be phosphorylated in vitro by the spore protein kinase. *Folia Microbiologica*, 52(5), 471–478. <https://doi.org/10.1007/BF02932106>
- Hong, H. J., Paget, M. S. B., & Buttner, M. J. (2002). A signal transduction system in *Streptomyces coelicolor* that activates the expression of a putative cell wall glycan operon in response to vancomycin and other cell wall-specific antibiotics. *Molecular Microbiology*. <https://doi.org/10.1046/j.1365-2958.2002.02960.x>
- Horsburgh, M. J., Thackray, P. D., & Moir, A. (2001). Transcriptional responses during

## References

---

- outgrowth of *Bacillus subtilis* endospores. *Microbiology*.  
<https://doi.org/10.1099/00221287-147-11-2933>
- Howell, B. W., Afar, D. E., Lew, J., Douville, E. M., Icely, P. L., Gray, D. A., & Bell, J. C. (1991). STY, a tyrosine-phosphorylating enzyme with sequence homology to serine/threonine kinases. *Molecular and Cellular Biology*, 11(1), 568–572.  
<https://doi.org/10.1128/mcb.11.1.568>
- Huang, X., Decatur, A., Sorokin, A., & Helmann, J. D. (1997). The *Bacillus subtilis*  $\sigma(x)$  protein is an extracytoplasmic function  $\sigma$  factor contributing to survival at high temperature. *Journal of Bacteriology*, 179(9), 2915–2921.
- Huang, X., Fredrick, K. L., & Helmann, J. D. (1998). Promoter recognition by *Bacillus subtilis*  $\sigma(w)$ : Autoregulation and partial overlap with the  $\sigma(x)$  regulon. *Journal of Bacteriology*.
- Huang, X., Pinto, D., Fritz, G., & Mascher, T. (2015). Environmental Sensing in Actinobacteria: a Comprehensive Survey on the Signaling Capacity of This Phylum. *Journal of Bacteriology*. <https://doi.org/10.1128/jb.00176-15>
- Humphreys, S., Stevenson, A., Bacon, A., Weinhardt, A. B., & Roberts, M. (1999). The alternative sigma factor,  $\sigma(E)$ , is critically important for the virulence of *Salmonella typhimurium*. *Infection and Immunity*, 67(4), 1560–1568.
- Hunter, T. (2007). The Age of Crosstalk: Phosphorylation, Ubiquitination, and Beyond. *Molecular Cell*, 28(5), 730–738. <https://doi.org/10.1016/j.molcel.2007.11.019>
- Hunter, T., & Cooper, J. A. (1985). Protein-tyrosine kinases 1. *Annual Reviews Biochemistry*, 54, 897–930.
- Hunter, T., Sefton, B. M., & Holley, R. W. (1980). Transforming gene product of Rous sarcoma virus phosphorylates tyrosine (phosphotyrosine/protein kinase/src gene/phosphoproteins). *Biochemistry*, 77(3), 1311–1315.
- Jaques, S., & McCarter, L. L. (2006). Three new regulators of swarming in *Vibrio parahaemolyticus*. *Journal of Bacteriology*, 188(7), 2625–2635.  
<https://doi.org/10.1128/JB.188.7.2625-2635.2006>
- Jarick, M., Bertsche, U., Stahl, M., Schultz, D., Methling, K., Lalk, M., ... Ohlsen, K. (2018). The serine/threonine kinase Stk and the phosphatase Stp regulate cell wall synthesis in *Staphylococcus aureus*. *Scientific Reports*, 8(1), 1–13.  
<https://doi.org/10.1038/s41598-018-32109-7>
- Jensen, O. N. (2004). Modification-specific proteomics: Characterization of post-translational modifications by mass spectrometry. *Current Opinion in Chemical Biology*. <https://doi.org/10.1016/j.cbpa.2003.12.009>
- Jers, C., Kobir, A., Søndergaard, E. O., Jensen, P. R., & Mijakovic, I. (2011). *Bacillus subtilis* two-component system sensory kinase DegS is regulated by serine phosphorylation in its input domain. *PLoS ONE*.  
<https://doi.org/10.1371/journal.pone.0014653>
- Jiao, Q., Bi, L., Ren, Y., Song, S., Wang, Q., & Wang, Y. shan. (2018). Advances in studies of tyrosine kinase inhibitors and their acquired resistance. *Molecular Cancer*, 17(1), 1–12. <https://doi.org/10.1186/s12943-018-0801-5>
- Jogler, C., Waldmann, J., Huang, X., Jogler, M., Glöckner, F. O., Mascher, T., & Kolter, R. (2012). Identification of Proteins Likely To Be Involved in Morphogenesis, Cell Division, and Signal Transduction in Planctomycetes by Comparative Genomics. *Journal of Bacteriology*, 194(23), 6419–6430. <https://doi.org/10.1128/jb.01325-12>
- Johnson, D. L., & Mahony, J. B. (2007). *Chlamydophila pneumoniae* PknD exhibits dual amino acid specificity and phosphorylates Cpn0712, a putative type III secretion YscD homolog. *Journal of Bacteriology*, 189(21), 7549–7555.  
<https://doi.org/10.1128/JB.00893-07>
- Johnson, L. N., Noble, M. E. M., & Owen, D. J. (1996). Active and inactive protein kinases: Structural basis for regulation. *Cell*. [https://doi.org/10.1016/S0092-8674\(00\)81092-2](https://doi.org/10.1016/S0092-8674(00)81092-2)
- JONES, H. E., & PARK, R. W. A. (1967). The Influence of Medium Composition on the Growth and Swarming of *Proteus*. *Journal of General Microbiology*.  
<https://doi.org/10.1099/00221287-47-3-369>

- Joo, D. M., Ng, N., & Calendar, R. (1997). A sigma32 mutant with a single amino acid change in the highly conserved region 2.2 exhibits reduced core RNA polymerase affinity. *Proceedings of the National Academy of Sciences of the United States of America*.
- Juang, Y.-L., & Helmann, J. D. (2002). A Promoter Melting Region in the Primary  $\sigma$  Factor of *Bacillus subtilis*. *Journal of Molecular Biology*, Vol. 235, pp. 1470–1488. <https://doi.org/10.1006/jmbi.1994.1102>
- Julkowska, D., Obuchowski, M., Holland, I. B., & S  ror, S. J. (2005). Comparative analysis of the development of swarming communities of *Bacillus subtilis* 168 and a natural wild type: Critical effects of surfactin and the composition of the medium. *Journal of Bacteriology*. <https://doi.org/10.1128/JB.187.1.65-76.2005>
- Juris, S. J., Shah, K., Shokat, K., Dixon, J. E., & Vacratsis, P. O. (2006). Identification of otubain 1 as a novel substrate for the Yersinia protein kinase using chemical genetics and mass spectrometry. *FEBS Letters*. <https://doi.org/10.1016/j.febslet.2005.11.071>
- Kamei, A., Yuasa, T., Orikawa, K., Xiao Xing Geng, & Ikeuchi, M. (2001). A eukaryotic-type protein kinase, SpkA, is required for normal motility of the unicellular cyanobacterium *Synechocystis* sp. strain PCC 6803. *Journal of Bacteriology*. <https://doi.org/10.1128/JB.183.5.1505-1510.2001>
- Kaneko, T., & Colwell, R. R. (1973). Ecology of *Vibrio parahaemolyticus* in Chesapeake Bay. *Journal of Bacteriology*, 113(1), 24–32.
- Kaneko, T., & Colwell, R. R. (1975). Adsorption of *Vibrio parahaemolyticus* onto Chitin and Copepods. *Appl. Envir. Microbiol.*, 29(2), 269–274.
- Kang, C. M., Abbott, D. W., Sang, T. P., Dascher, C. C., Cantley, L. C., & Husson, R. N. (2005). The *Mycobacterium tuberculosis* serine/threonine kinases PknA and PknB: Substrate identification and regulation of cell shape. *Genes and Development*. <https://doi.org/10.1101/gad.1311105>
- Kang, C. M., Brody, M. S., Akbar, S., Yang, X., & Price, C. W. (1996). Homologous pairs of regulatory proteins control activity of *Bacillus subtilis* transcription factor  $\sigma$ (B) in response to environmental stress. *Journal of Bacteriology*.
- Kang, J. G., Paget, M. S. B., Seok, Y. J., Hahn, M. Y., Bae, J. B., Hahn, J. S., ... Roe, J. H. (1999). RsrA, an anti-sigma factor regulated by redox change. *EMBO Journal*, 18(15), 4292–4298. <https://doi.org/10.1093/emboj/18.15.4292>
- Karimova, G., Pidoux, J., Ullmann, A., & Ladant, D. (1998). A bacterial two-hybrid system based on a reconstituted signal transduction pathway. *Proceedings of the National Academy of Sciences of the United States of America*.
- Karimova, G., Robichon, C., & Ladant, D. (2009). Characterization of YmgF, a 72-residue inner membrane protein that associates with the *Escherichia coli* cell division machinery. *Journal of Bacteriology*. <https://doi.org/10.1128/JB.00331-08>
- Kazmierczak, M. J., Wiedmann, M., & Boor, K. J. (2005). Alternative Sigma Factors and Their Roles in Bacterial Virulence. *Microbiology and Molecular Biology Reviews*. <https://doi.org/10.1128/mmbr.69.4.527-543.2005>
- Kearns, D. B. (2011). A field guide to bacterial swarming motility Danielc Access. *Nat Rev Micro*, 8(9), 634–644. <https://doi.org/10.1038/nrmicro2405.A>
- Kearns, D. B., & Losick, R. (2003). Swarming motility in undomesticated *Bacillus subtilis*. *Molecular Microbiology*, 49(3), 581–590. <https://doi.org/10.1046/j.1365-2958.2003.03584.x>
- Khan, S. R., Gaines, J., Roop, R. M., & Farrand, S. K. (2008). Broad-host-range expression vectors with tightly regulated promoters and their use to examine the influence of TraR and TraM expression on Ti plasmid quorum sensing. *Applied and Environmental Microbiology*. <https://doi.org/10.1128/AEM.01098-08>
- Kibbe, W. A. (2007). OligoCalc: An online oligonucleotide properties calculator. *Nucleic Acids Research*. <https://doi.org/10.1093/nar/gkm234>
- Kim, C., Xuong, N. H., & Taylor, S. S. (2005). Crystal structure of a complex between the catalytic and regulatory (Rla) subunits of PKA. *Science*.

## References

---

- <https://doi.org/10.1126/science.1104607>
- Kim, D. W., Lenzen, G., Page, A.-L., Legrain, P., Sansonetti, P. J., & Parsot, C. (2005). The *Shigella flexneri* effector OspG interferes with innate immune responses by targeting ubiquitin-conjugating enzymes. *Proceedings of the National Academy of Sciences*. <https://doi.org/10.1073/pnas.0504466102>
- Kim, W., Killam, T., Sood, V., & Surette, M. G. (2003). Swarm-cell differentiation in *Salmonella enterica* serovar typhimurium results in elevated resistance to multiple antibiotics. *Journal of Bacteriology*, 185(10), 3111–3117. <https://doi.org/10.1128/JB.185.10.3111-3117.2003>
- Kim, Y. K., & McCarter, L. L. (2000). Analysis of the polar flagellar gene system of *Vibrio parahaemolyticus*. *Journal of Bacteriology*. <https://doi.org/10.1128/JB.182.13.3693-3704.2000>
- Kim, Y. K., & McCarter, L. L. (2004). Cross-regulation in *Vibrio parahaemolyticus*: Compensatory activation of polar flagellar genes by the lateral flagellar regulator LafK. *Journal of Bacteriology*. <https://doi.org/10.1128/JB.186.12.4014-4018.2004>
- Knighton, D. R., Xuong, N. H., Taylor, S. S., & Sowadski, J. M. (1991). Crystallization studies of cAMP-dependent protein kinase. Cocrystals of the catalytic subunit with a 20 amino acid residue peptide inhibitor and MgATP diffract to 3.0 Å resolution. *Journal of Molecular Biology*, 220(2), 217–220. [https://doi.org/10.1016/0022-2836\(91\)90005-Q](https://doi.org/10.1016/0022-2836(91)90005-Q)
- Kobir, A., Poncet, S., Bidnenko, V., Delumeau, O., Jers, C., Zouhir, S., ... Mijakovic, I. (2014). Phosphorylation of *Bacillus subtilis* gene regulator AbrB modulates its DNA-binding properties. *Molecular Microbiology*, 92(5), 1129–1141. <https://doi.org/10.1111/mmi.12617>
- Kohler, T., Curty, L. K., Barja, F., Van Delden, C., & Pechere, J. C. (2000). Swarming of *Pseudomonas aeruginosa* is dependent on cell-to-cell signaling and requires flagella and pili. *Journal of Bacteriology*. <https://doi.org/10.1128/JB.182.21.5990-5996.2000>
- Kojima, S., Yamamoto, K., Kawagishi, I., & Homma, M. (1999). The polar flagellar motor of *Vibrio cholerae* is driven by an Na<sup>+</sup> motive force. *Journal of Bacteriology*.
- Kourennaia, O. V., Tsujikawa, L., & DeHaseth, P. L. (2005). Mutational analysis of *Escherichia coli* heat shock transcription factor sigma 32 reveals similarities with sigma 70 in recognition of the -35 promoter element and differences in promoter DNA melting and -10 recognition. *Journal of Bacteriology*. <https://doi.org/10.1128/JB.187.19.6762-6769.2005>
- Kravanja, M., Engelmann, R., Dossonnet, V., Blüggel, M., Meyer, H. E., Frank, R., ... Hengstenberg, W. (1999). The hprK gene of *Enterococcus faecalis* encodes a novel bifunctional enzyme: The HPr kinase/phosphatase. *Molecular Microbiology*. <https://doi.org/10.1046/j.1365-2958.1999.01146.x>
- Kühn, M. J., Schmidt, F. K., Eckhardt, B., & Thormann, K. M. (2017). Bacteria exploit a polymorphic instability of the flagellar filament to escape from traps. *Proceedings of the National Academy of Sciences*. <https://doi.org/10.1073/pnas.1701644114>
- Kumar, D., Palaniyandi, K., Challu, V. K., Kumar, P., & Narayanan, S. (2013). PknE, a serine/threonine protein kinase from *Mycobacterium tuberculosis* has a role in adaptive responses. *Archives of Microbiology*, 195(1), 75–80. <https://doi.org/10.1007/s00203-012-0848-4>
- Kuznedelov, K., Minakhin, L., Niedziela-Majka, A., Dove, S. L., Rogulja, D., Nickels, B. E., ... Severinov, K. (2002). A role for interaction of the RNA polymerase flap domain with the  $\sigma$  subunit in promoter recognition. *Science*. <https://doi.org/10.1126/science.1066303>
- Laemmli, U. K. (1970). Cleavage of structural proteins during the assembly of the head of bacteriophage T4. *Nature*. <https://doi.org/10.1038/227680a0>
- Lai, H. C., Gygi, D., Fraser, G. M., & Hughes, C. (1998). A swarming-defective mutant of *Proteus mirabilis* lacking a putative cation-transporting membrane P-type ATPase. *Microbiology*. <https://doi.org/10.1099/00221287-144-7-1957>
- Lane, W. J., & Darst, S. A. (2010). Molecular Evolution of Multisubunit RNA



- Polymerases: Sequence Analysis. *Journal of Molecular Biology*.  
<https://doi.org/10.1016/j.jmb.2009.10.062>
- Langmead, B., & Salzberg, S. L. (2012). Fast gapped-read alignment with Bowtie 2. *Nature Methods*. <https://doi.org/10.1038/nmeth.1923>
- Laporte, D. C., & Koshland, D. E. (1982). A protein with kinase and phosphatase activities involved in regulation of tricarboxylic acid cycle. *Nature*.  
<https://doi.org/10.1038/300458a0>
- Le Jeune, A., Torelli, R., Sanguinetti, M., Giard, J. C., Hartke, A., Auffray, Y., & Benachour, A. (2010). The extracytoplasmic function sigma factor SigV plays a key role in the original model of lysozyme resistance and virulence of *Enterococcus faecalis*. *PLoS ONE*, 5(3), 1–12.  
<https://doi.org/10.1371/journal.pone.0009658>
- Lee, P.-C., Umeyama, T., & Horinouchi, S. (2002). *afsS* is a target of AfsR, a transcriptional factor with ATPase activity that globally controls secondary metabolism in *Streptomyces coelicolor* A3(2). *Molecular Microbiology*.
- Leiba, J., Carrère-Kremer, S., Blondiaux, N., Dimala, M. M., Wohlkönig, A., Baulard, A., ... Molle, V. (2014). The *Mycobacterium tuberculosis* transcriptional repressor EthR is negatively regulated by Serine/Threonine phosphorylation. *Biochemical and Biophysical Research Communications*, 446(4), 1132–1138.  
<https://doi.org/10.1016/j.bbrc.2014.03.074>
- Leiba, J., Hartmann, T., Cluzel, M. E., Cohen-Gonsaud, M., Delolme, F., Bischoff, M., & Molle, V. (2012). A novel mode of regulation of the *Staphylococcus aureus* catabolite control protein A (CcpA) mediated by Stk1 protein phosphorylation. *Journal of Biological Chemistry*, 287(52), 43607–43619.  
<https://doi.org/10.1074/jbc.M112.418913>
- Leonard, C. J., Arvind, L., & Koonin, E. V. (1998). Novel Families of Putative Protein Kinases in Bacteria and Archaea. *Genome Research*, 8(10), 1038–1047.
- Leonard, P. G., Golemi-Kotra, D., & Stock, A. M. (2013). Phosphorylation-dependent conformational changes and domain rearrangements in *Staphylococcus aureus* VraR activation. *Proceedings of the National Academy of Sciences*, 110(21), 8525–8530. <https://doi.org/10.1073/pnas.1302819110>
- Lesley, S. A., & Burgess, R. R. (1989). Characterization of the *Escherichia coli* Transcription Factor  $\sigma 70$ : Localization of a Region Involved in the Interaction with Core RNA Polymerase. *Biochemistry*. <https://doi.org/10.1021/bi00445a031>
- Letchumanan, V., Chan, K. G., & Lee, L. H. (2014). *Vibrio parahaemolyticus*: A review on the pathogenesis, prevalence, and advance molecular identification techniques. *Frontiers in Microbiology*. <https://doi.org/10.3389/fmicb.2014.00705>
- Letunic, I., & Bork, P. (2016). Interactive tree of life (iTOL) v3: an online tool for the display and annotation of phylogenetic and other trees. *Nucleic Acids Research*.  
<https://doi.org/10.1093/nar/gkw290>
- Levene, P. a, & Alsberg, C. L. (1906). the Cleavage Products of Vitellin. *J Biol Chem*.
- Li, H., Handsaker, B., Wysoker, A., Fennell, T., Ruan, J., Homer, N., ... Durbin, R. (2009). The Sequence Alignment/Map format and SAMtools. *Bioinformatics*.  
<https://doi.org/10.1093/bioinformatics/btp352>
- Li, L., Fang, C., Zhuang, N., Wang, T., & Zhang, Y. (2019). Structural basis for transcription initiation by bacterial ECF  $\sigma$  factors. *Nature Communications*, 10(1).  
<https://doi.org/10.1038/s41467-019-09096-y>
- Li, M., Moyle, H., & Susskind, M. M. (1994). Target of the transcriptional activation function of phage  $\lambda$  cl protein. *Science*. <https://doi.org/10.1126/science.8272867>
- Li, W., Bottrill, A. R., Bibb, M. J., Buttner, M. J., Paget, M. S. B., & Kleanthous, C. (2003). The role of zinc in the disulphide stress-regulated anti-sigma factor RsrA from *Streptomyces coelicolor*. *Journal of Molecular Biology*.  
<https://doi.org/10.1016/j.jmb.2003.08.038>
- Lima, A., Durán, R., Schujman, G. E., Marchissio, M. J., Portela, M. M., Obal, G., ... Cerveñansky, C. (2011). Serine/threonine protein kinase PrkA of the human

## References

---

- pathogen *Listeria monocytogenes*: Biochemical characterization and identification of interacting partners through proteomic approaches. *Journal of Proteomics*, 74(9), 1720–1734. <https://doi.org/10.1016/j.jprot.2011.03.005>
- Lin, W. J., Walthers, D., Connelly, J. E., Burnside, K., Jewell, K. A., Kenney, L. J., & Rajagopal, L. (2009). Threonine phosphorylation prevents promoter DNA binding of the Group B Streptococcus response regulator CovR. *Molecular Microbiology*, 71(6), 1477–1495. <https://doi.org/10.1111/j.1365-2958.2009.06616.x>
- Lin, W., Mandal, S., Degen, D., Cho, M. S., Feng, Y., Das, K., & Ebright, R. H. (2019). Structural basis of ECF- $\sigma$ -factor-dependent transcription initiation. *Nature Communications*, 10(1), 1–14. <https://doi.org/10.1038/s41467-019-08443-3>
- Lippmann, C., Lindschau, C., Vijgenboom, E., Schroder, W., Bosch, L., & Erdmann, V. A. (1993). Prokaryotic elongation factor Tu is phosphorylated in vivo. *Journal of Biological Chemistry*, 268(1), 601–607.
- Little, K., Austerman, J., Zheng, J., & Gibbs, K. (2018). Swarming bacteria respond to increasing barriers to motility by increasing cell length and modifying colony structure. *BioRxiv*.
- Liu, B., Hong, C., Huang, R. K., & Yu, Z. (2017). Transcription Activation. *Research*, 951(November), 947–951.
- Lizardi, P. M., Huang, X., Zhu, Z., Bray-Ward, P., Thomas, D. C., & Ward, D. C. (1998). Mutation detection and single-molecule counting using isothermal rolling-circle amplification. *Nature Genetics*. <https://doi.org/10.1038/898>
- Lonetto, M. A., Brown, K. L., Rudd, K. E., & Buttner, M. J. (1994). Analysis of the *Streptomyces coelicolor sigE* gene reveals the existence of a subfamily of eubacterial RNA polymerase sigma factors involved in the regulation of extracytoplasmic functions. *Proceedings of the National Academy of Sciences of the United States of America*, 91(16), 7573–7577.
- Lonetto, M., Gribskov, M., & Gross, C. A. (1992). The  $\sigma 70$  family: Sequence conservation and evolutionary relationships. *Journal of Bacteriology*. <https://doi.org/10.1128/jb.174.12.3843-3849.1992>
- Lu, C. T., Huang, K. Y., Su, M. G., Lee, T. Y., Bretaña, N. A., Chang, W. C., ... Huang, H. Da. (2013). DbPTM 3.0: An informative resource for investigating substrate site specificity and functional association of protein post-translational modifications. *Nucleic Acids Research*, 41(D1), 295–305. <https://doi.org/10.1093/nar/gks1229>
- Lukat, G. S., McCreary, W. R., Stockt, A. M., & Stock, J. B. (1992). Phosphorylation of bacterial response regulator proteins by low molecular weight phospho-donors (CheY/CheB/acetyl phosphate/carbamoyl phosphate/phosphoramidate). *Biochemistry*, 89(January), 718–722.
- Luo, Y., Asai, K., Sadaie, Y., & Helmann, J. D. (2010). Transcriptomic and phenotypic characterization of a *Bacillus subtilis* strain without extracytoplasmic function  $\sigma$  factors. *Journal of Bacteriology*, 192(21), 5736–5745. <https://doi.org/10.1128/JB.00826-10>
- Macek, B., Gnad, F., Soufi, B., Kumar, C., Olsen, J. V., Mijakovic, I., & Mann, M. (2007). Phosphoproteome Analysis of *E. coli* Reveals Evolutionary Conservation of Bacterial Ser/Thr/Tyr Phosphorylation. *Molecular & Cellular Proteomics*, 7(2), 299–307. <https://doi.org/10.1074/mcp.m700311-mcp200>
- Macek, B., Mijakovic, I., Olsen, J. V., Gnad, F., Kumar, C., Jensen, P. R., & Mann, M. (2007). The Serine/Threonine/Tyrosine Phosphoproteome of the Model Bacterium *Bacillus subtilis*. *Molecular & Cellular Proteomics*, 6(4), 697–707. <https://doi.org/10.1074/mcp.m600464-mcp200>
- Maillard, A. P., Girard, E., Ziani, W., Petit-Härtlein, I., Kahn, R., & Covès, J. (2014). The crystal structure of the anti- $\sigma$  factor CnrY in complex with the  $\sigma$  factor CnrH shows a new structural class of anti- $\sigma$  factors targeting extracytoplasmic function  $\sigma$  factors. *Journal of Molecular Biology*, 426(12), 2313–2327. <https://doi.org/10.1016/j.jmb.2014.04.003>
- Makino, K., Oshima, K., Kurokawa, K., Yokoyama, K., Uda, T., Tagomori, K., ... Iida, T. (2003). Genome sequence of *Vibrio parahaemolyticus*: A pathogenic mechanism

- distinct from that of *V. cholerae*. *Lancet*. [https://doi.org/10.1016/S0140-6736\(03\)12659-1](https://doi.org/10.1016/S0140-6736(03)12659-1)
- Malhotra, A., Severinova, E., & Darst, S. A. (1996). Crystal structure of a sigma 70 subunit fragment from *E. coli* {RNA} polymerase. *Cell*, 87, 127–136.
- Maluping, R. P., Ravelo, C., Lavilla-Pitogo, C. R., Krovacek, K., & Romalde, J. L. (2005). Molecular typing of *Vibrio parahaemolyticus* strains isolated from the Philippines by PCR-based methods. *Journal of Applied Microbiology*. <https://doi.org/10.1111/j.1365-2672.2005.02571.x>
- Manganelli, R., Voskuil, M. I., Schoolnik, G. K., Dubnau, E., Gomez, M., & Smith, I. (2002). Role of the extracytoplasmic-function  $\sigma$  factor  $\sigma^H$  in *Mycobacterium tuberculosis* global gene expression. *Molecular Microbiology*, 45(2), 365–374. <https://doi.org/10.1046/j.1365-2958.2002.03005.x>
- Manganelli, R., Voskuil, M. I., Schoolnik, G. K., & Smith, I. (2001). The *Mycobacterium tuberculosis* ECF sigma factor  $\sigma^S$ . *Molecular Microbiology*, 41(70), 423–437.
- Manson, M. D., Tedesco, P., Berg, H. C., Harold, F. M., & Van der Drift, C. (1977). A protonmotive force drives bacterial flagella. *Proceedings of the National Academy of Sciences*. <https://doi.org/10.1073/pnas.74.7.3060>
- Marcos-Torres, F. J., Perez, J., Gomez-Santos, N., Moraleda-Munoz, A., & Munoz-Dorado, J. (2016). In depth analysis of the mechanism of action of metal-dependent sigma factors: Characterization of CorE2 from *Myxococcus xanthus*. *Nucleic Acids Research*. <https://doi.org/10.1093/nar/gkw150>
- Martínez, A., Torello, S., & Kolter, R. (1999). Sliding motility in mycobacteria. *Journal of Bacteriology*.
- Mascher, T. (2013). Signaling diversity and evolution of extracytoplasmic function (ECF)  $\sigma$  factors. *Current Opinion in Microbiology*, 16(2), 148–155. <https://doi.org/10.1016/j.mib.2013.02.001>
- Masloboeva, N., Reutimann, L., Stiefel, P., Follador, R., Leimer, N., Hennecke, H., ... Fischer, H. M. (2012). Reactive oxygen species-inducible ecf  $\sigma$  factors of *Bradyrhizobium japonicum*. *PLoS ONE*, 7(8). <https://doi.org/10.1371/journal.pone.0043421>
- Mathew, R., & Chatterji, D. (2006). The evolving story of the omega subunit of bacterial RNA polymerase. *Trends in Microbiology*, 14(10), 450–455. <https://doi.org/10.1016/j.tim.2006.08.002>
- Mattick, J. S. (2002). Type IV Pili and Twitching Motility. *Annual Review of Microbiology*. <https://doi.org/10.1146/annurev.micro.56.012302.160938>
- McCarter, L. (1999). The multiple identities of *Vibrio parahaemolyticus*. *J Mol Microbiol Biotechnol*, 1(1), 51–57.
- McCarter, L., Hilmen, M., & Silverman, M. (1988). Flagellar dynamometer controls swarmer cell differentiation of *V. parahaemolyticus*. *Cell*, 54(3), 345–351. [https://doi.org/10.1016/0092-8674\(88\)90197-3](https://doi.org/10.1016/0092-8674(88)90197-3)
- McCarter, L. L. (1995). Genetic and molecular characterization of the polar flagellum of *Vibrio parahaemolyticus*. *Journal of Bacteriology*, 177(6), 1595–1609.
- McCarter, L. L., & Wright, M. E. (1993). Identification of genes encoding components of the swarmer cell flagellar motor and propeller and a sigma factor controlling differentiation of *Vibrio parahaemolyticus*. *Journal of Bacteriology*, 175(11), 3361–3371. <https://doi.org/10.1128/jb.175.11.3361-3371.1993>
- McCarter, L., & Silverman, M. (1989). Iron regulation of swarmer cell differentiation of *Vibrio parahaemolyticus*. *Journal of Bacteriology*, 171(2), 731–736. <https://doi.org/10.1128/jb.171.2.731-736.1989>
- McCarter, L., & Silverman, M. (1990). Surface-induced swarmer cell differentiation of *Vibrio parahaemolyticus*. *Molecular Microbiology*, 4(7), 1057–1062. <https://doi.org/10.1111/j.1365-2958.1990.tb00678.x>
- McClure, W. (1985). Mechanism and Control of Transcription Initiation in Prokaryotes. *Annual Review of Biochemistry*. <https://doi.org/10.1146/annurev.biochem.54.1.171>
- McInerney, M. P., Roberts, K. D., Thompson, P. E., Li, J., Nation, R. L., Velkov, T., &

## References

- Nicolazzo, J. A. (2016). Quantitation of Polymyxin-Lipopolysaccharide Interactions Using an Image-Based Fluorescent Probe. *Journal of Pharmaceutical Sciences*. <https://doi.org/10.1016/j.xphs.2015.10.028>
- Merino, S., Shaw, J. G., & Tomás, J. M. (2006). Bacterial lateral flagella: An inducible flagella system. *FEMS Microbiology Letters*. <https://doi.org/10.1111/j.1574-6968.2006.00403.x>
- Merrick, M. J. (1993). In a class of its own — the RNA polymerase sigma factor  $\sigma_{54}$  ( $\sigma_N$ ). *Molecular Microbiology*. <https://doi.org/10.1111/j.1365-2958.1993.tb00961.x>
- Mettrick, K. A., & Lamont, I. L. (2009). Different roles for anti-sigma factors in siderophore signalling pathways of *Pseudomonas aeruginosa*. *Molecular Microbiology*, 74(5), 1257–1271. <https://doi.org/10.1111/j.1365-2958.2009.06932.x>
- Mieczkowski, C., Iavarone, A. T., & Alber, T. (2008). Auto-activation mechanism of the *Mycobacterium tuberculosis* PknB receptor Ser/Thr kinase. *EMBO Journal*, 27(23), 3186–3197. <https://doi.org/10.1038/emboj.2008.236>
- Miller, H. K., Carroll, R. K., Burda, W. N., Krute, C. N., Davenport, J. E., & Shaw, L. N. (2012). The extracytoplasmic function sigma factor  $\sigma_s$  protects against both intracellular and extracytoplasmic stresses in *Staphylococcus aureus*. *Journal of Bacteriology*, 194(16), 4342–4354. <https://doi.org/10.1128/JB.00484-12>
- Miller, M. A., Byrne, B. A., Jang, S. S., Dodd, E. M., Dorfmeier, E., Harris, M. D., ... Miller, W. A. (2010). Enteric bacterial pathogen detection in southern sea otters (*Enhydra lutris nereis*) is associated with coastal urbanization and freshwater runoff. *Veterinary Research*. <https://doi.org/10.1051/vetres/2009049>
- Miller, M., Donat, S., Rackette, S., Stehle, T., Kouwen, T. R. H. M., Diks, S. H., ... Ohlsen, K. (2010). Staphylococcal PknB as the first prokaryotic representative of the proline-directed kinases. *PLoS ONE*, 5(2), 1–8. <https://doi.org/10.1371/journal.pone.0009057>
- Mir, M., Asong, J., Li, X., Cardot, J., Boons, G. J., & Husson, R. N. (2011). The extracytoplasmic domain of the *Mycobacterium tuberculosis* ser/thr kinase PknB binds specific muropeptides and is required for PknB localization. *PLoS Pathogens*, 7(7). <https://doi.org/10.1371/journal.ppat.1002182>
- Missiakas, D., Mayer, M. P., Lemaire, M., Georgopoulos, C., & Raina, S. (1997). Modulation of the *Escherichia coli*  $\sigma(E)$  (RpoE) heat-shock transcription-factor activity by the RseA, RseB and RseC proteins. *Molecular Microbiology*, 24(2), 355–371. <https://doi.org/10.1046/j.1365-2958.1997.3601713.x>
- Missiakas, D., & Raina, S. (1998). The extracytoplasmic function sigma factors: Role and regulation. *Molecular Microbiology*. <https://doi.org/10.1046/j.1365-2958.1998.00865.x>
- Miyazaki, H., Kato, H., Nakazawa, T., & Tsuda, M. (1995). A positive regulatory gene, pvdS, for expression of pyoverdinin biosynthetic genes in *Pseudomonas aeruginosa* PAO. *MGG Molecular & General Genetics*, 248(1), 17–24. <https://doi.org/10.1007/BF02456609>
- Moran, C. P., Johnson, W. C., & Losick, R. (1982). Close contacts between  $\sigma_{37}$ -RNA polymerase and a *Bacillus subtilis* chromosomal promoter. *Journal of Molecular Biology*. [https://doi.org/10.1016/0022-2836\(82\)90399-0](https://doi.org/10.1016/0022-2836(82)90399-0)
- Morrison, R. B., & Scott, A. (1966). Swarming of proteus - A solution to an old problem? *Nature*, 211(5046), 255–257. <https://doi.org/10.1038/211255a0>
- Mortazavi, A., Williams, B. A., McCue, K., Schaeffer, L., & Wold, B. (2008). Mapping and quantifying mammalian transcriptomes by RNA-Seq. *Nature Methods*. <https://doi.org/10.1038/nmeth.1226>
- Murakami, K. S. (2013). X-ray crystal structure of *Escherichia coli* RNA polymerase  $\sigma_{70}$  holoenzyme. *Journal of Biological Chemistry*, 288(13), 9126–9134. <https://doi.org/10.1074/jbc.M112.430900>
- Murakami, K. S. (2015). Structural biology of bacterial RNA polymerase. *Biomolecules*. <https://doi.org/10.3390/biom5020848>
- Murray, T. S., & Kazmierczak, B. I. (2008). *Pseudomonas aeruginosa* exhibits sliding

- motility in the absence of type IV pili and flagella. *Journal of Bacteriology*.  
<https://doi.org/10.1128/JB.01620-07>
- Muslin, A. J., Tanner, J. W., Allen, P. M., & Shaw, A. S. (1996). Interaction of 14-3-3 with signaling proteins is mediated by the recognition of phosphoserine. *Cell*.  
[https://doi.org/10.1016/S0092-8674\(00\)81067-3](https://doi.org/10.1016/S0092-8674(00)81067-3)
- Nagai, H., Shimamoto, N., & Ishihama, A. (1997). Regions of the *Escherichia coli* primary sigma factor  $\sigma 70$  that are involved in interaction with RNA polymerase core enzyme. *Genes to Cells*. <https://doi.org/10.1046/j.1365-2443.1997.1600357.x>
- NAKAYAMA, T., WILLIAMSON, V., BURTIS, K., & DOI, R. H. (1978). Purification and Properties of Two RNA Polymerases from Sporulating Cells of *Bacillus subtilis*. *European Journal of Biochemistry*. <https://doi.org/10.1111/j.1432-1033.1978.tb12433.x>
- Narberhaus, F., Krummenacher, P., Fischer, H. M., & Hennecke, H. (1997). Three disparately regulated genes for  $\sigma 32$ -like transcription factors in *Bradyrhizobium japonicum*. *Molecular Microbiology*. <https://doi.org/10.1046/j.1365-2958.1997.3141685.x>
- Nariya, H., & Inouye, S. (2006). A protein Ser/Thr kinase cascade negatively regulates the DNA-binding activity of MrpC, a smaller form of which may be necessary for the *Myxococcus xanthus* development. *Molecular Microbiology*, 60(5), 1205–1217. <https://doi.org/10.1111/j.1365-2958.2006.05178.x>
- Navarro, L., Koller, A., Nordfelth, R., Wolf-Watz, H., Taylor, S., & Dixon, J. E. (2007). Identification of a Molecular Target for the Yersinia Protein Kinase A. *Molecular Cell*. <https://doi.org/10.1016/j.molcel.2007.04.025>
- Nguyen, L. T., Schmidt, H. A., Von Haeseler, A., & Minh, B. Q. (2015). IQ-TREE: A fast and effective stochastic algorithm for estimating maximum-likelihood phylogenies. *Molecular Biology and Evolution*. <https://doi.org/10.1093/molbev/msu300>
- Nixon, B. T., Ronson, C. W., & Ausubel, F. M. (2006). Two-component regulatory systems responsive to environmental stimuli share strongly conserved domains with the nitrogen assimilation regulatory genes *ntrB* and *ntrC*. *Proceedings of the National Academy of Sciences*. <https://doi.org/10.1073/pnas.83.20.7850>
- Nolen, B., Taylor, S., & Ghosh, G. (2004). Regulation of protein kinases: Controlling activity through activation segment conformation. *Molecular Cell*, Vol. 15, pp. 661–675. <https://doi.org/10.1016/j.molcel.2004.08.024>
- Nováková, L., Sasková, L., Pallová, P., Janeček, J., Novotná, J., Ulrych, A., ... Branny, P. (2005). Characterization of a eukaryotic type serine/threonine protein kinase and protein phosphatase of *Streptococcus pneumoniae* and identification of kinase substrates. *FEBS Journal*, 272(5), 1243–1254. <https://doi.org/10.1111/j.1742-4658.2005.04560.x>
- Ochs, M., Veitinger, S., Kim, I., Weiz, D., Angerer, A., & Braun, V. (1995). Regulation of citrate-dependent iron transport of *Escherichia coli*: FecR is required for transcription activation by Fe<sup>2+</sup>. *Molecular Microbiology*, 15(1), 119–132. <https://doi.org/10.1111/j.1365-2958.1995.tb02226.x>
- Ochsner, U. A., Wilderman, P. J., Vasil, A. I., & Vasil, M. L. (2002). GeneChip expression analysis of the iron starvation response in *Pseudomonas aeruginosa*: identification of novel pyoverdine biosynthesis genes. *Molecular Microbiology*, 45(5), 1277–1287.
- Olaitan, A. O., Morand, S., & Rolain, J. M. (2014). Mechanisms of polymyxin resistance: Acquired and intrinsic resistance in bacteria. *Frontiers in Microbiology*. <https://doi.org/10.3389/fmicb.2014.00643>
- Oliveira, A. P., Ludwig, C., Picotti, P., Kogadeeva, M., Aebersold, R., & Sauer, U. (2012). Regulation of yeast central metabolism by enzyme phosphorylation. *Molecular Systems Biology*, 8(623). <https://doi.org/10.1038/msb.2012.55>
- Ortiz-Lombardía, M., Pompeo, F., Boitel, B., & Alzari, P. M. (2003). Crystal structure of the catalytic domain of the PknB serine/threonine kinase from *Mycobacterium tuberculosis*. *The Journal of Biological Chemistry*, 278(15), 13094–13100.

## References

---

- <https://doi.org/10.1074/jbc.M300660200>
- Ottemann, K. M., & Miller, J. F. (1997). Roles for motility in bacterial-host interactions. *Molecular Microbiology*, 24(6), 1109–1117. <https://doi.org/10.1046/j.1365-2958.1997.4281787.x>
- Overhage, J., Bains, M., Brazas, M. D., & Hancock, R. E. W. (2008). Swarming of *Pseudomonas aeruginosa* is a complex adaptation leading to increased production of virulence factors and antibiotic resistance. *Journal of Bacteriology*, 190(8), 2671–2679. <https://doi.org/10.1128/JB.01659-07>
- Page, C. A., & Krause, D. C. (2013). Protein kinase/phosphatase function correlates with gliding motility in *Mycoplasma pneumoniae*. *Journal of Bacteriology*. <https://doi.org/10.1128/JB.02277-12>
- Paget, M. S. (2015). Bacterial sigma factors and anti-sigma factors: Structure, function and distribution. *Biomolecules*. <https://doi.org/10.3390/biom5031245>
- Paget, M. S. B., Chamberlin, L., Atrih, A., Foster, S. J., & Buttner, M. J. (1999). Evidence that the extracytoplasmic function sigma factor  $\sigma^E$  is required for normal cell wall structure in *Streptomyces coelicolor* A3(2). *Journal of Bacteriology*, 181(1), 204–211.
- Paget, M. S. B., Hong, H., Bibb, M. J., & Buttner, M. J. (2002). The ECF sigma factors of *Streptomyces coelicolor* A3 ( 2 ). *Signals, Switches, Regulons, and Cascades Control of Bacterial Gene Expression*, 3(2), 105–125.
- Park, H.-D., Guinn, K. M., Harrell, M. I., Liao, R., Voskuil, M. I., Tompa, M., ... Sherman, D. R. (2003). Rv3133c/dosR is a transcription factor that mediates the hypoxic response of *Mycobacterium tuberculosis*. *Molecular Microbiology*, 48(3), 833–843.
- Park, S. T., Kang, C.-M., & Husson, R. N. (2008). Regulation of the SigH stress response regulon by an essential protein kinase in *Mycobacterium tuberculosis*. *Proceedings of the National Academy of Sciences*, 105(35), 13105–13110. <https://doi.org/10.1073/pnas.0801143105>
- Partridge, J. D., & Harshey, R. M. (2013). Swarming: Flexible roaming plans. *Journal of Bacteriology*. <https://doi.org/10.1128/JB.02063-12>
- Patrick, J. E., & Kearns, D. B. (2012). Swarming motility and the control of master regulators of flagellar biosynthesis. *Molecular Microbiology*. <https://doi.org/10.1111/j.1365-2958.2011.07917.x>
- Pawson, T., & Scott, J. D. (2005). Protein phosphorylation in signaling – 50 years and counting. *Trends in Biochemical Sciences*. <https://doi.org/10.1016/j.tibs.2005.04.013>
- Payankaulam, S., Li, L. M., & Arnosti, D. N. (2010). Transcriptional repression: Conserved and evolved features. *Current Biology*. <https://doi.org/10.1016/j.cub.2010.06.037>
- Pereira, S. F. F., Goss, L., & Dworkin, J. (2011a). Eukaryote-like serine/threonine kinases and phosphatases in bacteria. *Microbiology and Molecular Biology Reviews*, 75(1), 192–212. <https://doi.org/10.1128/MMBR.00042-10>
- Pereira, S. F. F., Goss, L., & Dworkin, J. (2011b). Eukaryote-Like Serine/Threonine Kinases and Phosphatases in Bacteria. *Microbiology and Molecular Biology Reviews*, 75(1), 192–212. <https://doi.org/10.1128/mmbr.00042-10>
- Pettersen, E. F., Goddard, T. D., Huang, C. C., Couch, G. S., Greenblatt, D. M., Meng, E. C., & Ferrin, T. E. (2004). UCSF Chimera--a visualization system for exploratory research and analysis. *Journal of Computational Chemistry*. <https://doi.org/10.1002/jcc.20084>
- Pompeo, F., Freton, C., Wicker-Planquart, C., Grangeasse, C., Jault, J. M., & Galinier, A. (2012). Phosphorylation of CpgA protein enhances both its GTPase activity and its affinity for ribosome and is crucial for *Bacillus subtilis* growth and morphology. *Journal of Biological Chemistry*, 287(25), 20830–20838. <https://doi.org/10.1074/jbc.M112.340331>
- Pruitt, K. D., Tatusova, T., & Maglott, D. R. (2007). NCBI reference sequences (RefSeq): A curated non-redundant sequence database of genomes, transcripts

- and proteins. *Nucleic Acids Research*. <https://doi.org/10.1093/nar/gkl842>
- Quinlan, A. R., & Hall, I. M. (2010). BEDTools: A flexible suite of utilities for comparing genomic features. *Bioinformatics*. <https://doi.org/10.1093/bioinformatics/btq033>
- Raivio, T. L., & Silhavy, T. J. (2002). Periplasmic Stress and ECF Sigma Factors. *Annual Review of Microbiology*. <https://doi.org/10.1146/annurev.micro.55.1.591>
- Rajagopal, L., Vo, A., Silvestroni, A., & Rubens, C. E. (2006). Regulation of cytotoxin expression by converging eukaryotic-type and two-component signalling mechanisms in *Streptococcus agalactiae*. *Molecular Microbiology*, 62(4), 941–957. <https://doi.org/10.1111/j.1365-2958.2006.05431.x>
- Rather, P. N. (2005). Swarmer cell differentiation in *Proteus mirabilis*. *Environmental Microbiology*, 7(8), 1065–1073. <https://doi.org/10.1111/j.1462-2920.2005.00806.x>
- Reizer, J., Romano, A. H., & Deutscher, J. (1993). The role of phosphorylation of HPr, a phosphocarrier protein of the phosphotransferase system, in the regulation of carbon metabolism in gram-positive bacteria. *Journal of Cellular Biochemistry*. <https://doi.org/10.1002/jcb.240510105>
- Reznikoff, W. S., Siegele, D. A., Deborah, W., & Gros, C. A. (1985). *TRANSCRIPTION INITIATION IN BACTERIA*.
- Rhodium, V. A., Suh, W. C., Nonaka, G., West, J., & Gross, C. A. (2006). Conserved and variable functions of the  $\sigma^E$  stress response in related genomes. *PLoS Biology*, 4(1), 0043–0059. <https://doi.org/10.1371/journal.pbio.0040002>
- Romano, P. R., Garcia-Barrio, M. T., Zhang, X., Wang, Q., Taylor, D. R., Zhang, F., ... Hinnebusch, A. G. (1998). Autophosphorylation in the activation loop is required for full kinase activity in vivo of human and yeast eukaryotic initiation factor 2alpha kinases PKR and GCN2. *Molecular and Cellular Biology*.
- Roychoudhury, S., Sakai, K., & Chakrabarty, A. M. (2006). AlgR2 is an ATP/GTP-dependent protein kinase involved in alginate synthesis by *Pseudomonas aeruginosa*. *Proceedings of the National Academy of Sciences*, 89(7), 2659–2663. <https://doi.org/10.1073/pnas.89.7.2659>
- Rutherford, S. T., & Bassler, B. L. (2012). Bacterial quorum sensing: Its role in virulence and possibilities for its control. *Cold Spring Harbor Perspectives in Medicine*. <https://doi.org/10.1101/cshperspect.a012427>
- Sadowski, I., Stone, J. C., & Pawson, T. (1986). A noncatalytic domain conserved among cytoplasmic protein-tyrosine kinases modifies the kinase function and transforming activity of Fujinami sarcoma virus P130gag-fps. *Molecular and Cellular Biology*, 6(12), 4396–4408.
- Sajid, A., Arora, G., Gupta, M., Singhal, A., Chakraborty, K., Nandicoori, V. K., & Singh, Y. (2011). Interaction of *Mycobacterium tuberculosis* elongation factor Tu with GTP is regulated by phosphorylation. *Journal of Bacteriology*, 193(19), 5347–5358. <https://doi.org/10.1128/JB.05469-11>
- Salveti, S., Faegri, K., Ghelardi, E., Kolstø, A.-B., & Senesi, S. (2011). Global Gene Expression Profile for Swarming *Bacillus cereus* Bacteria. *Applied and Environmental Microbiology*. <https://doi.org/10.1128/aem.00245-11>
- Santos, A. L., & Lindner, A. B. (2017). Protein Posttranslational Modifications: Roles in Aging and Age-Related Disease. *Oxidative Medicine and Cellular Longevity*, 2017, 1–19. <https://doi.org/10.1155/2017/5716409>
- Sar, N., McCarter, L., Simon, M., & Silverman, M. (1990). Chemotactic control of the two flagellar systems of *Vibrio parahaemolyticus*. *Journal of Bacteriology*, 172(1), 334–341. <https://doi.org/10.1128/jb.172.1.334-341.1990>
- Schindelin, J., Arganda-Carreras, I., Frise, E., Kaynig, V., Longair, M., Pietzsch, T., ... Cardona, A. (2012). Fiji: an open-source platform for biological-image analysis. *Nature Methods*. <https://doi.org/10.1038/nmeth.2019>
- Schmidl, S. R., Gronau, K., Pietack, N., Hecker, M., Becher, D., & Stülke, J. (2010). The Phosphoproteome of the Minimal Bacterium *Mycoplasma pneumoniae*. *Molecular & Cellular Proteomics*, 9(6), 1228–1242. <https://doi.org/10.1074/mcp.m900267-mcp200>

## References

---

- Schöbel, S., Zellmeier, S., Schumann, W., & Wiegert, T. (2004). The *Bacillus subtilis*  $\sigma^W$  anti-sigma factor RsiW is degraded by intramembrane proteolysis through YluC. *Molecular Microbiology*, 52(4), 1091–1105. <https://doi.org/10.1111/j.1365-2958.2004.04031.x>
- Senesi, S., Celandroni, F., Salvetti, S., Beecher, D. J., Wong, A. C. L., & Ghelardi, E. (2002). Swarming motility in *Bacillus cereus* and characterization of a *fliY* mutant impaired in swarm cell differentiation. *Microbiology*. <https://doi.org/10.1099/00221287-148-6-1785>
- Seth, D., Hausladen, A., Wang, Y. J., & Stamler, J. S. (2012). Endogenous protein S-nitrosylation in *E. coli*: Regulation by OxyR. *Science*. <https://doi.org/10.1126/science.1215643>
- Shah, I. M., & Dworkin, J. (2010). Induction and regulation of a secreted peptidoglycan hydrolase by a membrane Ser/Thr kinase that detects muropeptides. *Molecular Microbiology*, 75(5), 1232–1243. <https://doi.org/10.1111/j.1365-2958.2010.07046.x>
- Shah, I. M., Laaberki, M. H., Popham, D. L., & Dworkin, J. (2008). A Eukaryotic-like Ser/Thr Kinase Signals Bacteria to Exit Dormancy in Response to Peptidoglycan Fragments. *Cell*, 135(3), 486–496. <https://doi.org/10.1016/j.cell.2008.08.039>
- Sharma, K., Gupta, M., Pathak, M., Gupta, N., Koul, A., Sarangi, S., ... Singh, Y. (2006). Transcriptional Control of the Mycobacterial *embCAB* Operon by. *Journal of Bacteriology*, 188(8), 2936–2944. <https://doi.org/10.1128/JB.188.8.2936>
- Sharma, M., & Anand, S. K. (2002). Swarming: A coordinated bacterial activity. *Current Science*, 83(6), 707–715.
- Sharp, M. M., Chan, C. L., Lu, C. Z., Marr, M. T., Nechaev, S., Merritt, E. W., ... Gross, C. A. (1999). The interface of  $\sigma$  with core RNA polymerase is extensive, conserved, and functionally specialized. *Genes and Development*, 13(22), 3015–3026. <https://doi.org/10.1101/gad.13.22.3015>
- Shaw, L. N., Lindholm, C., Prajsnar, T. K., Miller, H. K., Brown, M. C., Golonka, E., ... Potempa, J. (2008). Identification and characterization of  $\sigma^S$ , a novel component of the *Staphylococcus aureus* stress and virulence responses. *PLoS ONE*, 3(12). <https://doi.org/10.1371/journal.pone.0003844>
- Shi, L., Potts, M., & Kennelly, P. J. (1998). The serine, threonine, and/or tyrosine-specific protein kinases and protein phosphatases of prokaryotic organisms: A family portrait. *FEMS Microbiology Reviews*. [https://doi.org/10.1016/S0168-6445\(98\)00015-1](https://doi.org/10.1016/S0168-6445(98)00015-1)
- Shinoda, S., & Okamoto, K. (1977). Formation and function of *Vibrio parahaemolyticus* lateral flagella. *Journal of Bacteriology*, 129(3), 1266–1271.
- Shoji, S., Titani, K., Demaille, J. G., & Fischer, E. H. (1979). Sequence of two phosphorylated sites in the catalytic subunit of bovine cardiac muscle adenosine 3':5'-monophosphate-dependent protein kinase. *Journal of Biological Chemistry*.
- Siegele, D. A., Hut, J. C., & Walter, W. A. (1989). *Altered Promoter Recognition by Mutant Forms of the 670 Subunit of*. 17, 591–603.
- Sievers, F., & Higgins, D. G. (2014). Clustal omega, accurate alignment of very large numbers of sequences. *Methods in Molecular Biology*. [https://doi.org/10.1007/978-1-62703-646-7\\_6](https://doi.org/10.1007/978-1-62703-646-7_6)
- Sineva, E., Savkina, M., & Ades, S. E. (2017). Themes and variations in gene regulation by extracytoplasmic function (ECF) sigma factors. *Current Opinion in Microbiology*. <https://doi.org/10.1016/j.mib.2017.05.004>
- Sircar, B., Deb, B., De, S., Ghosh, A., & Pal, S. C. (1976). Clinical and epidemiological studies on *V. parahaemolyticus* infection in Calcutta (1975). *Indian Journal Of Medical Research*, 64(11), 1576–1580.
- Skalhegg, B. S., & Tasken, K. (1997). Specificity in the cAMP/PKA signaling pathway. Differential expression, regulation, and subcellular localization of subunits of PKA. *Frontiers in Bioscience : A Journal and Virtual Library*.
- SKÓRKO, R. (1984). Protein phosphorylation in the Archaeobacterium *Sulfolobus acidocaldarius*. *European Journal of Biochemistry*, 145(3), 617–622.



- <https://doi.org/10.1111/j.1432-1033.1984.tb08601.x>
- Smith, D. G. (1972). The Proteus swarming phenomenon. *Science Progress*, 60(240), 487–506.
- Søberg, K., & Skålhegg, B. S. (2018). The Molecular Basis for Specificity at the Level of the Protein Kinase a Catalytic Subunit. *Frontiers in Endocrinology*, 9(September), 1–22. <https://doi.org/10.3389/fendo.2018.00538>
- Sohn, J., Grant, R. A., & Sauer, R. T. (2007). Allosteric activation of DegS, a stress sensor PDZ protease. *Cell*, 131(3), 572–583. <https://doi.org/10.1016/j.cell.2007.08.044>
- Spormann, A. M. (1999). Gliding motility in bacteria: insights from studies of *Myxococcus xanthus*. *Microbiology and Molecular Biology Reviews: MMBR*.
- Srinivas, P., & Rivard, K. (2017). Polymyxin resistance in Gram-negative pathogens. *Current Infectious Disease Reports*, 19(11), 38. <https://doi.org/10.1007/s11908-017-0596-3>
- Srinivasan, S., Kaplan, C. N., & Mahadevan, L. (2019). A multiphase theory for spreading microbial swarms and films. *ELife*. <https://doi.org/10.7554/elife.42697>
- Stancik, I. A., Šestak, M. S., Ji, B., Axelson-Fisk, M., Franjevic, D., Jers, C., ... Mijakovic, I. (2018). Serine/Threonine Protein Kinases from Bacteria, Archaea and Eukarya Share a Common Evolutionary Origin Deeply Rooted in the Tree of Life. *Journal of Molecular Biology*, 430(1), 27–32. <https://doi.org/10.1016/j.jmb.2017.11.004>
- Staroń, A., Sofia, H. J., Dietrich, S., Ulrich, L. E., Liesegang, H., & Mascher, T. (2009). The third pillar of bacterial signal transduction: Classification of the extracytoplasmic function (ECF)  $\sigma$  factor protein family. *Molecular Microbiology*, 74(3), 557–581. <https://doi.org/10.1111/j.1365-2958.2009.06870.x>
- Steichen, J. M., Iyer, G. H., Li, S., Saldanha, A., Deal, M. S., Woods, V. L., & Taylor, S. S. (2010). Global consequences of activation loop phosphorylation on protein kinase A. *Journal of Biological Chemistry*. <https://doi.org/10.1074/jbc.M109.061820>
- Steinberg, R. A., Cauthron, R. D., Symcox, M. M., & Shuntoh, H. (2015). Autoactivation of catalytic (C alpha) subunit of cyclic AMP-dependent protein kinase by phosphorylation of threonine 197. *Molecular and Cellular Biology*. <https://doi.org/10.1128/mcb.13.4.2332>
- Stewart, B. J., & McCarter, L. L. (2003). Lateral flagellar gene system of *Vibrio parahaemolyticus*. *Journal of Bacteriology*, 185(15), 4508–4518. <https://doi.org/10.1128/JB.185.15.4508-4518.2003>
- Stintzi, A., Johnson, Z., Stonehouse, M., Ochsner, U., Meyer, J. M., Vasil, M. L., & Poole, K. (1999). The pvc gene cluster of *Pseudomonas aeruginosa*: Role in synthesis of the pyoverdine chromophore and regulation by PtxR and PvdS. *Journal of Bacteriology*, 181(13), 4118–4124.
- Storey, J. D. (2002). A direct approach to false discovery rates. *Journal of the Royal Statistical Society. Series B: Statistical Methodology*. <https://doi.org/10.1111/1467-9868.00346>
- Su, Y., Dostmann, W. R. G., Herberg, F. W., Durick, K., Xuong, N. H., Ten Eyck, L., ... Varughese, K. I. (1995). Regulatory subunit of protein kinase A: Structure of deletion mutant with cAMP binding domains. *Science*. <https://doi.org/10.1126/science.7638597>
- Sun, F., Ding, Y., Ji, Q., Liang, Z., Deng, X., Wong, C. C. L., ... He, C. (2012). Protein cysteine phosphorylation of SarAMgrA family transcriptional regulators mediates bacterial virulence and antibiotic resistance. *Proceedings of the National Academy of Sciences*, 109(38), 15461–15466. <https://doi.org/10.1073/pnas.1205952109>
- Sun, J., Deng, Z., & Yan, A. (2014). Bacterial multidrug efflux pumps: Mechanisms, physiology and pharmacological exploitations. *Biochemical and Biophysical Research Communications*. <https://doi.org/10.1016/j.bbrc.2014.05.090>
- Sun, R., Converse, P. J., Ko, C., Tyagi, S., Morrison, N. E., & Bishai, W. R. (2004).

## References

- Mycobacterium tuberculosis* ECF sigma factor sigC is required for lethality in mice and for the conditional expression of a defined gene set. *Molecular Microbiology*, 52(1), 25–38. <https://doi.org/10.1111/j.1365-2958.2003.03958.x>
- Tanaka, K., Shiina, T., & Takahashi, H. (1988). Multiple principal sigma factor homologs in eubacteria: Identification of the “rpoD box.” *Science*. <https://doi.org/10.1126/science.3194753>
- Tare, P., Mallick, B., & Nagaraja, V. (2013). Co-evolution of specific amino acid in sigma 1.2 region and nucleotide base in the discriminator to act as sensors of small molecule effectors of transcription initiation in mycobacteria. *Molecular Microbiology*. <https://doi.org/10.1111/mmi.12384>
- Thackray, P. D., & Moir, A. (2003). SigM, an extracytoplasmic function sigma factor of *Bacillus subtilis*, is activated in response to cell wall antibiotics, ethanol, heat, acid, and superoxide stress. *Journal of Bacteriology*, 185(12), 3491–3498. <https://doi.org/10.1128/JB.185.12.3491-3498.2003>
- Thakur, M., & Chakraborti, P. K. (2006). GTPase activity of mycobacterial FtsZ is impaired due to its transphosphorylation by the eukaryotic-type Ser/Thr kinase, PknA. *Journal of Biological Chemistry*, 281(52), 40107–40113. <https://doi.org/10.1074/jbc.M607216200>
- Thakur, P. B., Vaughn-Diaz, V. L., Greenwald, J. W., & Gross, D. C. (2013). Characterization of Five ECF Sigma Factors in the Genome of *Pseudomonas syringae* pv. *syringae* B728a. *PLoS ONE*, 8(3). <https://doi.org/10.1371/journal.pone.0058846>
- Thongjun, J., Mittraparp-arthorn, P., Yingkajorn, M., Kongreung, J., Nishibuchi, M., & Vuddhakul, V. (2013). The Trend of *Vibrio parahaemolyticus* Infections in Southern Thailand from 2006 to 2010. *Tropical Medicine and Health*. <https://doi.org/10.2149/tmh.2013-06>
- Toguchi, A., Siano, M., Burkart, M., & Harshey, R. M. (2000). Genetics of swarming motility in *Salmonella enterica* serovar *Typhimurium*: Critical role for lipopolysaccharide. *Journal of Bacteriology*, 182(22), 6308–6321. <https://doi.org/10.1128/JB.182.22.6308-6321.2000>
- Travers, A. A., & Burgess, R. R. (1969). Cyclic Re-use of the RNA polymerase sigma factor. *Nature*. <https://doi.org/10.1038/222537a0>
- Tremblay, J., Richardson, A. P., Lépine, F., & Déziel, E. (2007). Self-produced extracellular stimuli modulate the *Pseudomonas aeruginosa* swarming motility behaviour. *Environmental Microbiology*, 9(10), 2622–2630. <https://doi.org/10.1111/j.1462-2920.2007.01396.x>
- Trepreau, J., De Rosny, E., Duboc, C., Sarret, G., Petit-Hartlein, I., Maillard, A. P., ... Covès, J. (2011). Spectroscopic characterization of the metal-binding sites in the periplasmic metal-sensor domain of CnrX from *Cupriavidus metallidurans* CH34. *Biochemistry*, 50(42), 9036–9045. <https://doi.org/10.1021/bi201031q>
- Trepreau, J., Girard, E., Maillard, A. P., De Rosny, E., Petit-Haertlein, I., Kahn, R., & Covès, J. (2011). Structural basis for metal sensing by CnrX. *Journal of Molecular Biology*, 408(4), 766–779. <https://doi.org/10.1016/j.jmb.2011.03.014>
- Treviño-Quintanilla, L., Freyre-González, J., & Martínez-Flores, I. (2013). Anti-Sigma Factors in *E. coli*: Common Regulatory Mechanisms Controlling Sigma Factors Availability. *Current Genomics*. <https://doi.org/10.2174/1389202911314060007>
- Trimble, M. J., & McCarter, L. L. (2011). Bis-(3'-5')-cyclic dimeric GMP-linked quorum sensing controls swarming in *Vibrio parahaemolyticus*. *Proceedings of the National Academy of Sciences*, 108(44), 18079–18084. <https://doi.org/10.1073/pnas.1113790108>
- Truong-Bolduc, Q. C., & Hooper, D. C. (2010). Phosphorylation of MgrA and its effect on expression of the NorA and NorB efflux pumps of *Staphylococcus aureus*. *Journal of Bacteriology*, 192(10), 2525–2534. <https://doi.org/10.1128/JB.00018-10>
- Turner, L., Zhang, R., Darnton, N. C., & Berg, H. C. (2010). Visualization of flagella during bacterial swarming. *Journal of Bacteriology*. <https://doi.org/10.1128/JB.00083-10>

- Tuson, H. H., Copeland, M. F., Carey, S., Sacotte, R., & Weibel, D. B. (2013). Flagellum density regulates *Proteus mirabilis* swarmer cell motility in viscous environments. *Journal of Bacteriology*, 195(2), 368–377. <https://doi.org/10.1128/JB.01537-12>
- Tyagi, N., Anamika, K., & Srinivasan, N. (2010). A framework for classification of prokaryotic protein kinases. *PLoS ONE*. <https://doi.org/10.1371/journal.pone.0010608>
- Tyanova, S., Temu, T., Sinitcyn, P., Carlson, A., Hein, M. Y., Geiger, T., ... Cox, J. (2016). The Perseus computational platform for comprehensive analysis of (prote)omics data. *Nature Methods*. <https://doi.org/10.1038/nmeth.3901>
- Ubersax, J. A., & Ferrell, J. E. (2007). Mechanisms of specificity in protein phosphorylation. *Nature Reviews Molecular Cell Biology*, 8(7), 530–541. <https://doi.org/10.1038/nrm2203>
- Ulijasz, A. T., Falk, S. P., & Weisblum, B. (2009). Phosphorylation of the RitR DNA-binding domain by a Ser-Thr phosphokinase: Implications for global gene regulation in the streptococci. *Molecular Microbiology*, 71(2), 382–390. <https://doi.org/10.1111/j.1365-2958.2008.06532.x>
- Ulitzur, S. (1974). Induction of swarming in *Vibrio parahaemolyticus*. *Archives of Microbiology*. <https://doi.org/10.1007/BF00455952>
- Umeyama, T., & Horinouchi, S. (2001). Autophosphorylation of a bacterial serine/threonine kinase, AfsK, is inhibited by KbpA, an AfsK-binding protein. *Journal of Bacteriology*, 183(19), 5506–5512. <https://doi.org/10.1128/JB.183.19.5506-5512.2001>
- Vassilyev, D. G., Sekine, S., Laptenko, O., Lee, J., Vassilyeva, M. N., & Borukhov, S. (2002). Crystal structure of a bacterial *Thermus thermophilus* RNA polymerase holoenzyme at 2.6 Å resolution. *Nature*, 417(June), 0–7.
- Voelker, U., Voelker, A., & Haldenwang, W. G. (1996). Reactivation of the *Bacillus subtilis* anti-σ(B) antagonist, RsbV, by stress- or starvation-induced phosphatase activities. *Journal of Bacteriology*.
- Vogel, F. C. W. (1885). Hauser, Ueber Fäulnisbakterien und deren Beziehungen zur Septicämie. Ein Beitrag zur Morphologie der Spaltpilze. Leipzig, Verlag. *Deutsche Medizinische Wochenschrift*. <https://doi.org/10.1055/s-0029-1208881>
- Walsh, C. T., Garneau-Tsodikova, S., & Gatto, G. J. (2005). Protein posttranslational modifications: The chemistry of proteome diversifications. *Angewandte Chemie - International Edition*, 44(45), 7342–7372. <https://doi.org/10.1002/anie.200501023>
- Walsh, D. A., Perkins, J. P., & Krebs, E. G. (1968). An adenosine 3',5'-monophosphate-dependant protein kinase from rabbit skeletal muscle. *Journal of Biological Chemistry*.
- Walter, G., Zillig, W., Palm, P., & Fuchs, E. (1967). Initiation of DNA-Dependent RNA Synthesis and the Effect of Heparin on RNA Polymerase. *European Journal of Biochemistry*. <https://doi.org/10.1111/j.1432-1033.1967.tb19515.x>
- Wang, Q., Zhang, Y., Yang, C., Xiong, H., Lin, Y., Yao, J., ... Zhao, G. P. (2010). Acetylation of metabolic enzymes coordinates carbon source utilization and metabolic flux. *Science*. <https://doi.org/10.1126/science.1179687>
- Wecke, T., Halang, P., Staroń, A., Dufour, Y. S., Donohue, T. J., & Mascher, T. (2012). Extracytoplasmic function σ factors of the widely distributed group ECF41 contain a fused regulatory domain. *MicrobiologyOpen*, 1(2), 194–213. <https://doi.org/10.1002/mbo3.22>
- Werner, F., & Grohmann, D. (2011a). Evolution of multisubunit RNA polymerases in the three domains of life. *Nature Reviews Microbiology*. <https://doi.org/10.1038/nrmicro2507>
- Werner, F., & Grohmann, D. (2011b). Evolution of multisubunit RNA polymerases in the three domains of life. *Nature Reviews Microbiology*, 9(2), 85–98. <https://doi.org/10.1038/nrmicro2507>
- Wertheimer, C., Siedlecki, J., Kook, D., Mayer, W. J., Wolf, A., Klingenstein, A., ... Eibl-

## References

---

- Lindner, K. (2015). EGFR inhibitor Gefitinib attenuates posterior capsule opacification in vitro and in the ex vivo human capsular bag model. *Graefes Archive for Clinical and Experimental Ophthalmology*, 253(3), 409–417. <https://doi.org/10.1007/s00417-014-2875-0>
- Wilken, C., Kitzing, K., Kurzbauer, R., Ehrmann, M., & Clausen, T. (2004). Crystal structure of the DegS stress sensor. *Cell*, 117(4), 483–494. [https://doi.org/10.1016/S0092-8674\(04\)00454-4](https://doi.org/10.1016/S0092-8674(04)00454-4)
- Wilson, M. J., & Lamont, I. L. (2006). Mutational analysis of an extracytoplasmic-function sigma factor to investigate its interactions with RNA polymerase and DNA. *Journal of Bacteriology*, 188(5), 1935–1942. <https://doi.org/10.1128/JB.188.5.1935-1942.2006>
- Wösten, M. M. S. M. (1998). Eubacterial sigma-factors. *FEMS Microbiology Reviews*. [https://doi.org/10.1016/S0168-6445\(98\)00011-4](https://doi.org/10.1016/S0168-6445(98)00011-4)
- Wright, D. P., & Ulijasz, A. T. (2014). Regulation of transcription by eukaryotic-like serine-threonine kinases and phosphatases in gram-positive bacterial pathogens. *Virulence*. <https://doi.org/10.4161/21505594.2014.983404>
- Wu, H., Liu, Q., Casas-Pastor, D., Dürr, F., Mascher, T., & Fritz, G. (2019). The role of C-terminal extensions in controlling ECF  $\sigma$  factor activity in the widely conserved groups ECF 41 and ECF 42. In *Molecular Microbiology*. <https://doi.org/10.1111/mmi.14261>
- Yaffe, M. B., Rittinger, K., Volinia, S., Caron, P. R., Aitken, A., Leffers, H., ... Cantley, L. C. (1997). The structural basis for 14-3-3:phosphopeptide binding specificity. *Cell*. [https://doi.org/10.1016/S0092-8674\(00\)80487-0](https://doi.org/10.1016/S0092-8674(00)80487-0)
- Yang, A., Tang, W. S., Si, T., & Tang, J. X. (2017). Influence of Physical Effects on the Swarming Motility of *Pseudomonas aeruginosa*. *Biophysical Journal*, 112(7), 1462–1471. <https://doi.org/10.1016/j.bpj.2017.02.019>
- Yang, J., Wu, J., Steichen, J. M., Kornev, A. P., Deal, M. S., Li, S., ... Taylor, S. S. (2012). A conserved Glu-Arg salt bridge connects coevolved motifs that define the eukaryotic protein kinase fold. *Journal of Molecular Biology*. <https://doi.org/10.1016/j.jmb.2011.11.035>
- Yang, J., Yan, R., Roy, A., Xu, D., Poisson, J., & Zhang, Y. (2014). The I-TASSER suite: Protein structure and function prediction. *Nature Methods*. <https://doi.org/10.1038/nmeth.3213>
- Yeats, C., Finn, R. D., & Bateman, A. (2002). The PASTA domain: A  $\beta$ -lactam-binding domain. *Trends in Biochemical Sciences*, 27(9), 438–440. [https://doi.org/10.1016/S0968-0004\(02\)02164-3](https://doi.org/10.1016/S0968-0004(02)02164-3)
- Yeh, H. Y., Chen, T. C., Liou, K. M., Hsu, H. T., Chung, K. M., Hsu, L. L., & Chang, B. Y. (2011). The core-independent promoter-specific interaction of primary sigma factor. *Nucleic Acids Research*, 39(3), 913–925. <https://doi.org/10.1093/nar/gkq911>
- Yin, J., Wang, J., & Koshland, D. E. (1978). *Kinase*. 7605–7609.
- Yoderian, P. (2004). Bacterial motility: Secretory secrets of gliding bacteria. *Current Biology*. [https://doi.org/10.1016/s0960-9822\(98\)70264-7](https://doi.org/10.1016/s0960-9822(98)70264-7)
- Young, B. A., Anthony, L. C., Gruber, T. M., Arthur, T. M., Heyduk, E., Lu, C. Z., ... Gross, C. A. (2001). A coiled-coil from the RNA polymerase  $\beta'$  subunit allosterically induces selective nontemplate strand binding by  $\sigma 70$ . *Cell*, 105(7), 935–944. [https://doi.org/10.1016/S0092-8674\(01\)00398-1](https://doi.org/10.1016/S0092-8674(01)00398-1)
- Young, T. A., Delagoutte, B., Endrizzi, J. A., Falick, A. M., & Alber, T. (2003). Structure of *Mycobacterium tuberculosis* PknB supports a universal activation mechanism for Ser/Thr protein kinases. *Nature Structural Biology*, 10(3), 168–174. <https://doi.org/10.1038/nsb897>
- Yuan, J., Jin, F., Glatter, T., & Sourjik, V. (2017). Osmosensing by the bacterial PhoQ/PhoP two-component system. *Proceedings of the National Academy of Sciences*. <https://doi.org/10.1073/pnas.1717272114>
- Zdanowski, K., Doughty, P., Jakimowicz, P., O'Hara, L., Buttner, M. J., Paget, M. S. B., & Kleanthous, C. (2006). Assignment of the zinc ligands in RsrA, a redox-sensing

- ZAS protein from *Streptomyces coelicolor*. *Biochemistry*, 45(27), 8294–8300.  
<https://doi.org/10.1021/bi060711v>
- ZHANG, G., CAMPBELL, E., MINAKHIN, L., RICHTER, C., SEVERINOV, K., & DARST, S. (1999). Crystal Structure of Core RNA Polymerase at 3.3 Å Resolution. *Cell*, 98(6), 811–824. [https://doi.org/10.1016/S0092-8674\(00\)81515-9](https://doi.org/10.1016/S0092-8674(00)81515-9)
- Zhang, G., & Darst, S. A. (1998). Structure of the *Escherichia coli* RNA polymerase  $\alpha$  subunit amino-terminal domain. *Science*.  
<https://doi.org/10.1126/science.281.5374.262>
- Zhang, W., Munoz-Dorado, J., Inouye, M., & Inouye, S. (1992). Identification of a putative eukaryotic-like protein kinase family in the developmental bacterium *Myxococcus xanthus*. *Journal of Bacteriology*, 174(16), 5450–5453.  
<https://doi.org/10.1128/jb.174.16.5450-5453.1992>
- Zhu, S., Kojima, S., & Homma, M. (2013). Structure, gene regulation and environmental response of flagella in *Vibrio*. *Frontiers in Microbiology*.  
<https://doi.org/10.3389/fmicb.2013.00410>
- Zschiedrich, C. P., Keidel, V., & Szurmant, H. (2016). Molecular Mechanisms of Two-Component Signal Transduction. *Journal of Molecular Biology*.  
<https://doi.org/10.1016/j.jmb.2016.08.003>
- Zuber, U., Drzewiecki, K., & Hecker, M. (2001). Putative sigma factor sigI (ykoZ) of *Bacillus subtilis* is induced by heat shock. *Journal of Bacteriology*, 183(4), 1472–1475. <https://doi.org/10.1128/JB.183.4.1472-1475.2001>



# Acknowledgments

The journey that this Ph.D has taken me on has been truly spectacular. It has been filled with mostly pleasant moments and I am grateful for that. I would like to thank the bacteria that I worked with who were cooperative and understanding most of the time. It was almost as if they empathized with me during times of stress.

“Behind every successful thesis is a bunch of people, both fictional and real”, is a saying that no one has ever heard of but here I am at exactly that juncture. First and foremost, I would like to thank my parents who provided me with a computer which enabled me to send out applications. I would like to thank them for the immense emotional support that they showed me throughout my doctoral studies. Despite the fact that most of my family is probably under the impression that I am most certainly going to find the cure for cholera, my kinase would not have been characterized (by me), had it not been for my parents’ collective encouragement.

Ah yes, and Friends. I would not have accomplished whatever I did during my Ph.D, had it not been for Monica, Rachel, Joey, Ross, Phoebe and particularly, Chandler.

In all seriousness, there are several people who hold a special place in my heart and each and every one of them has had an impact on me.

First and foremost, I owe a lot and then some more to my supervisor, Dr. Simon Ringgaard. Thank you so much for picking up someone who came with barely any knowledge of microbiology and giving him a space in your laboratory. Thank you for every single opportunity that you have provided along the way.

I would also like to thank my dear collaborators. Delia who has endured so many of my insipid questions and has become more of a friend; David who was sitting next to me on the bus and asked me casually to come over to his office so he can try and analyze my data; Dr. Georg Fritz for once again being at the right place at the right time at my IMPRS symposium and helping me understand why ECF  $\sigma$  factors are incredibly fascinating and Dr. Timo Glatter for making all the proteomics analyses feasible.

There are so many others who have helped me, aided me, motivated me and inspired me along the way. I would have to obviously start with my dear sweet polka-dot loving Carolina. From our little move down the corridor to having everything important scheduled together, I am absolutely grateful that I had someone who was with me every step of the way. I could not have asked for a better compatriot both within the lab and outside the lab. And then there is you, my QWERTEE loving ball-in-a-cup, Jan. For all those times at Chevy’s, for all those times at your backyard, for all those times you wish you could smack me at the back of my head, it was pretty awesome that eventually, you were literally just a tap away. My sweet Pringle, Alice. I think to find an underdog to lead the way, to find someone who understands you, who empathizes with you, is a marvel.

## Acknowledgments

---

Where do I even begin with you, Petra! Well, I will tell you this: there has never been and never will be a better technician. A sweeter technician. A cooler technician. A technician who lives for danger at the disco. Samada, you might be miles away and you might have forgotten about us lesser mortals but I will never forget your deathly stare, cautionary smile and breathtaking skills at team-building when it comes to making daal. This list would not be complete without at least a single mention of our very own zodiac-enthusiast. If he had a favorite beer, it might be a RuPaulaner. Erick, it has been truly spectacular getting to know you and I am hoping that by the time this is written, I would have convinced you to dress with me as the Bride Parade. And there is you, Barbaraptor, Barbie, Barbedwire, our personal little Quinoa, who is doing her own sweet thing and changing the face of the world as I type. Thank you for inspiring the inner millennial in me.

I would also thank every single person on my floor, especially Stephan “I miss sharing an office and making missile noises with you” Wimmi, Bailey “Bay leaves and Bailey’s” Davies for being patient with my puns and just for being downright supportive. I could not have asked for a better floor.

As my mind wanders through the Institute, several distinct faces stand out. They stand out almost as distinctly as the number of coffees or botherations that I have put them through. Maria: I used to live to disturb you in my first year and it was one of the best times of my year. I could not have dealt with any of the eventful things that transpired during my first year, had it not been for you. Long live the poop emoji. Anna, sweet Anna: My tea loving, horror comrade! I want you to know that every single person needs a sweet little rabbit to annoy with creepy music and you have a special place in my life. Luis: My other fellow horror comrade. One of these days, I will find a movie that you haven’t already watched and that day, you will know that balance is restored. As I dart elsewhere across the institute, a distinct face that reminded me of the horrors that await koalas stands out: Hanna. You can reach her at [Hanna.woulddjyourparty.alcohol](mailto:Hanna.woulddjyourparty.alcohol). And then there is the silver-haired Khaleesi herself: Nicole. I swear on Gloria bar and that sweet, sweet pomegranate-infused drink that I will still continue to discuss GoT with you fervently twenty years from now. Down the elevator, lo and behold, there she is! Izzy. I love you so much more than that kaya you gave me, so much more than that Nasi Lemak, so much more than that Teh Tarik you bought for me. From sober to slumber on the table, you are truly the best.

As I glide (dart, glide: fellow readers, I am referring to possible motilities) away from the institute, there are the usual suspects. The darlings. And she stands out: Joana: Our friendship goes beyond anything I can put on this page. All I can say is this: it’s maybe 3pm right now and I am already on my way somewhere to meet you for a drink. Maria: From the time that I met you at the selection symposium, I knew we understood each other’s language. You will always be the Amy Poehler to my Tina Fey. I am flying over to Berlin and there she is: Miss Malini Iyer. Even though you were far away, even though I hated the distance, I like the fact that you are and will always be a constant in my life. You will always be that sweet cherry in my wine. But I will drink it? This metaphor is taking a dark turn.



Then there are the non-microbiologists. From my pure chestnut Corey, my sushi cupcake Anja, the ever-smiling Laurita, the “Flower power” Natalia, my dumpling Shuai to my precious penguin/ ballet dancer/ A-dell Zozo, all of you have had a magical place in my hearts. Anna, my sister from another mister, our phone calls in the morning vitalized me, our relationship kept me going. Axel, I know I don’t say this much but Dunkelbruderling with you has been one of the best things ever to happen. Also, keep the memes coming please.

The joy of traveling that I have come to live for, the joy of tripping over thin air, the joy of Star Wars, the joy of cohabitating accidentally, the joy of the Cersei rap. Stu, the Cockatoo, you are hearted. Crossing the continent and there we go: my dear Magali and Bronwyn, my two beans. Thank you for your love, your rants, your engaging of my rants, your everything. Dear mum, Peg, I heart you. Thank you Leon “Shut up, Dad” for your continued randomness. Thank you, Brish for being there through it all. And to my dears in Chennai: Lakme, Saai, Vinod. You guys are truly phenomenal and will always hold a special place in my heart.

Just the thought of this next person, just the idea of typing these letters feels incredibly heavy. Kat, I am not going to tell you that I constantly feel your presence with me throughout the way because quite frankly, I could feel you roll your eyes. But I miss you every single second, every single day. That much is true. That much will always be true.

One quick trip back to Berlin and I see a face smiling at me, a face asking me, “Really”. A face that is probably preparing bircher muesli for the next day. Leandro, you are absolutely special and thank you so much for all the support and encouragement that you have given me every step of the doctoral thesis.

And that’s a wrap, ladies and gentlemen. Valar Morghulis.



# CURRICULUM VITAE

## SHANKAR CHANDRASHEKAR IYER

**Date of Birth:** 12.07.1991

**Nationality:** Indian

---

### EDUCATION

2015-present	<b>MPI for Terrestrial Microbiology</b> Ph.D (Dr.rer.nat) <b>Dissertation:</b> Transcriptional regulation by sigma factor phosphorylation controls polymyxin resistance and swarming behavior in <i>Vibrio parahaemolyticus</i> <b>Dissertation Advisor:</b> Dr. Simon Ringgaard, Department of Ecophysiology	<b>Marburg, Germany</b>
2008-2012	<b>Anna University</b> Bachelors of Technology (B.Tech) degree in Industrial Biotechnology Overall CGPA: 3.94/4 (Among the top 2% within the Department of Biotechnology) <b>Dissertation title:</b> Characterizing a zinc finger transcription factor in the fungal organism, <i>Candida albicans</i> <b>Dissertation advisor:</b> (Late) Dr. Parag Sadhale	<b>Chennai, India</b>

### WORK EXPERIENCE

June-Oct 2015	Analyst at TOWERS WATSON PVT. LTD	Singapore
Jan-June 2015	Healthcare Analyst at CXA Pvt. Ltd	Singapore
July-Nov 2014	Graduate Research Assistant	Singapore
Aug-June 2013	Internship at A-STAR	Singapore

### PUBLICATIONS

**Shankar Chandrashekar Iyer**, Delia Casas-Pastor, David Kraus, Petra Mann, Kathrin Schirner, Timo Glatter, Georg Fritz, and Simon Ringgaard. Transcriptional regulation by  $\sigma$  factor phosphorylation in bacteria. *Nature Microbiology*. In revision.



## ERKLÄRUNG

Hermit versichere ich, dass ich die vorliegende Dissertation mit dem **Titel „Transcriptional regulation by sigma factor phosphorylation controls polymyxin resistance and swarming behavior in *Vibrio parahaemolyticus*“** selbstständig verfasst, keine anderen als die Text angegebenen Hilfsmittel verwendet und sämtliche Stellen, die im Wortlaut oder dem Sinn nach anderen Werken entnommen sind, mit Quellenangaben kenntlich gemachth habe.

Die Dissertation wurde in der jetzigen oder einer ähnlichen Form noch bei keiner anderen Hochschule eingereicht und hat noch keinen sonstigen Prüfungswegen gedient.

---

Ort, Datum

---

Shankar Chandrashekar Iyer



# EINVERSTÄNDNISERKLÄRUNG

Ich erkläre mich dam einverstanden, dass die vorliegende Dissertation

**„Transcriptional regulation by sigma factor phosphorylation controls  
polymyxin resistance and swarming behavior in *Vibrio parahaemolyticus* “**

in Bibliotheken allgemein zugänglich gemacht wird. Dazu gehört, dass sie

- von der Bibliothek der Einrichtung, in der ich meine Arbeit anfertig habe, zur Benutzung in ihren Räumen bereitgehalten wird;
- in konventionellen und maschinenlesbaren Katalogen, Verzeichnissen und Datenbanken verzeichnet wird;
- im Rahmen der urheberrechtlichen Bestimmungen für Kopierzwecke genutzt werden kann.

Marburg, den 06.09.2019

---

Shankar Chandrashekar Iyer

---

Dr. Simon Ringgaard